THE UNIVERSITY OF CHICAGO

NON-INVERTIBLE SYMMETRY IN LOWER-DIMENSIONAL GAUGE THEORY

A DISSERTATION SUBMITTED TO
THE FACULTY OF THE DIVISION OF THE PHYSICAL SCIENCES
IN CANDIDACY FOR THE DEGREE OF
DOCTOR OF PHILOSOPHY

DEPARTMENT OF PHYSICS

BY
DIEGO GARCÍA SEPÚLVEDA

CHICAGO, ILLINOIS
JUNE 2025

CONTENTS

LIST OF FIGURES

LIST OF TABLES

ACKNOWLEDGMENTS

First, I would like to express my deepest gratitude to my Ph.D. advisor, Clay Córdova, for believing in my abilities as a theoretical physicist and letting me work under his guidance. I am grateful to his sense of camaraderie, fostering an environment where everyone has something to contribute. His breadth of knowledge and interests is also a constant source of inspiration that I can just hope to match someday.

I would also like to thank my seniors for the discussions and/or collaborations throughout the years. First, I would like to thank Jeff Harvey, whose sharp questions would often make me understand in better and new ways what I am working on and often lead to long emails explaining with more precision what I have in mind. I admire his particular ability to be "politely incisive," a style I look forward to reproducing myself in years to come. I have also had the wonderful opportunity to work with Kantaro Ohmori, whose extensive knowledge and willingness to share his ideas always seem to open up a path forward in the face of an apparent obstacle. I would also like to thank Sav Sethi, Michael Levin, and Lian Tao Wang for the many conversations during my Ph.D.

I am grateful to the many friends I have made in this period of my life. I would like to first express my gratitude to the friends of MCP 407: Anuj Apte, Harry Fosbinder-Elkins, Nicholas Holfester, Sihan Chen, and Murtaza Jafry, for fostering a collaborative atmosphere that encourages questions and promotes a spirit of intellectual openness, where every idea is open for discussion. And naturally, all while enjoying a good laugh. In general, my physics journey would not have been nearly as enjoyable and interesting without the many friends I have made along the way. I thank Davi Costa, Carolyn Zhang, Chin-Yi Tan, Matthew Yu, Justin Kulp, Ji Hoon Lee, Elliott Gesteau, Ruchira Mishra, Maxim Zelenko, Tai Wai Hu, Giovanni Rizi, Daine Danielson, Seth Koren, Xiaochuan Wu, Tzu-Chen (Jimmy) Huang, Bruno Balthasar, Anthony Ashmore, and Edward Mazenc for the friendship and the many discussions throughout the years. In general, I would like to thank all the students, professors

and University staff at Chicago, for providing such a welcoming and stimulating environment to pursue graduate studies.

I also had the fortunate opportunity to attend Perimeter Institute before arriving in Chicago, where I met many people for whom I am thankful to have been a part of my formation. In this regard, I would like to single out Alfredo Guevara and my PSI advisor Freddy Cachazo for teaching me by example a work ethic that I carry with me to this day. I would also like to thank P. Vieira and N. Berkovits for first believing in my talent years ago and for providing me with the opportunity to study outside my home country – an opportunity that has naturally developed and that finds a milestone in this thesis.

Finally, I would want to thank my family for their unwavering support throughout my physics journey and for fostering an intellectual environment early in my life.

ABSTRACT

This thesis explores several applications of anyon condensation as a mechanism to characterize and implement non-invertible symmetries in gauge theories in two and three spacetime dimensions. First, we propose that the concept of level-rank duality can be understood in full generality by considering non-invertible symmetries as gauge symmetries, leading to a broad generalization of examples and a unified understanding of previously known examples. We also study the relation between non-invertible symmetries and the coset construction of 2D CFT. In particular, we describe topological cosets – defined by the case where the coset CFT has a vanishing central charge – and apply the results to find non-invertible symmetries of 2D QCD. In particular, this is used to describe the low-energy regime of 2D QCD and to constrain the energy spectrum of gapped 2D QCD. Finally, we use anyon condensation to argue for the existence of non-invertible one-form symmetry at the transition point of certain Chern-Simons matter RG flows triggered by the Higgs mechanism.

CHAPTER 1

INTRODUCTION AND SUMMARY

In theoretical physics, the concept of symmetry –the idea that physical systems can remain invariant under particular changes– plays a foundational role in understanding the laws of nature. From classical mechanics to modern quantum field theory, symmetries have consistently guided the development of physical theories. In the early days of science, Newton's law of universal gravitation serves as a clear example of this. Without spherical symmetry, it would have been difficult to imagine that such a law would have emerged so clearly and so quickly. A less trivial example of the application of the notion of symmetry is how the symmetry of the hydrogen atom can explain the degeneracies in its energy levels. Fundamentally, symmetry principles form the foundation of many physical theories. The standard model of particle physics is a prominent case, grounded in symmetry from the outset.

While symmetry is intuitively recognizable in familiar settings, formalizing what we mean by a symmetry in physical theories is more subtle. Over the past century, this concept has been rigorously structured in terms of the mathematical framework of group theory. For instance, the Lorentz group encodes the symmetries of spacetime in special relativity, and the gauge group $U(1) \times SU(2) \times SU(3)$ underpins the standard model. Group theory thus provides a powerful language to describe symmetries across both classical and quantum regimes.

Significant developments have, however, occurred in our understanding of symmetry in quantum field theory (QFT) over the past few years, where new forms of symmetry have been identified that lie outside the mathematical framework of group theory. Instead, these new symmetries are defined by operators that are *topological* [6]. Importantly, under this definition, symmetries are not generically described by group theory, although it has been extensively investigated that they share and generalize many of the features that group-like symmetries present. Because of this departure, this new type of symmetry has been called

variously *Generalized Symmetry*, *Topological Symmetry*, or *Non-Invertible Symmetry*. The focus of this thesis is precisely on applications of generalized symmetries in quantum field theory. Specifically, this thesis focuses on gauge theories in two and three dimensions, where we have a comprehensive understanding of these symmetries.

The first subject explored in this thesis focuses on the relationship between generalized symmetries and the essential concepts that define a QFT. In the standard textbook formulation, QFTs are defined starting with a classical field theory, and then imposing over such classical theory the axioms of quantum mechanics. Strikingly, quantizing two different classical starting points can sometimes lead to a single underlying QFT. In this case, one has two different descriptions for the same underlying theory; a well-known phenomenon in physics known as *duality*. In particular, *Level-Rank dualities* stand out for being arguably the simplest type of duality, defined by the physical situation where certain three-dimensional topological QFTs describe the same physics, even when the *a priori* constructions of these QFTs are wildly different. Level-rank dualities are also useful in that they are the basic ingredient for more general forms of duality, and a good grasp of level-rank duality is also useful in constraining the low-energy dynamics of 3D gauge theories. See for instance [7–10].

In this context, in Chapter 3 we point out that the concept of level-rank duality can be broadened by understanding generalized symmetries as gauge symmetries, and we give several examples that are similar to those previously discussed in the literature, which only used standard group theory as gauge symmetries. This places level-rank duality in a unified framework, with generalized symmetries serving as the unifying element. The contents of this chapter are based on [3].

A general phenomenon in QFT is that the theory is well understood at weak coupling, where perturbative techniques are well understood. In the regime of strong interactions, however, QFT is well-known to become impractical. Fortunately, understanding aspects of QFT at strong coupling is still possible by exploiting symmetry considerations, and it

becomes natural to explore the consequences of non-invertible symmetries in the strongly coupled regime of gauge theories like the standard model.

We set out to explore this direction in Chapter 4 and Chapter 5. More precisely, we study theoretical analogs of QCD in two spacetime dimensions. In this case, the theory is under good technical control, and non-invertible symmetries are also well understood (see e.g. [11]). This setup provides a unique opportunity to peek into the mechanisms behind confinement and the mass gap of four-dimensional QCD and, even more generally, to understand general strongly coupled phenomena in QFT.

In this spirit, in Chapter 4 we apply a tool pioneered in condensed-matter physics known as non-abelian (non-invertible) anyon condensation, which may be understood as a gauging operation for non-invertible one-form symmetries in the context of 3D Topological Quantum Field Theories (3D TQFTs), to provide a computationally tractable construction of the infrared fixed point of gapped 2D QCD [12]. More generally, this description works for any 2D coset CFT with vanishing central charge, and thus provides a common paradigm for topological cosets and the more standard cosets of [2]. Furthermore, we also argue for the existence of chiral 2D QCD theories that are trivially gapped, in direct resemblance with the observations found in the standard model. The contents of this chapter are based on [12]

In Chapter 5 we import these tools to make precise statements regarding the finite energy spectrum of 2D QCD when the theory is gapped. In particular, we will see how to deduce precise degeneracies between particle and solitons states in these theories. The contents of this paper are based on [13].

Finally, in Chapter 6 we address the problem of finding non-invertible one-form symmetries in conformal field theories in three spacetime dimensions. More precisely, we study the existence of non-invertible one-form symmetries at a Chern-Simons matter fixed point transition between two topological phases determined at low energies by Higgsing of the Chern-Simons matter theory. Using anyon condensation and its relation to the coset con-

struction, we discuss a variety of concrete examples of non-invertible one-form symmetry in these fixed-point theories. For instance, $SU(k)_2$ Chern-Simons theory coupled to a scalar in the symmetric tensor representation produces a transition from an $SU(k)_2$ phase to an $SO(k)_4$ phase and has non-invertible one-form symmetry $PSU(2)_{-k}$ at the fixed point. In many of these examples, the non-invertible one-form symmetry is not a modular invariant TQFT, and thus does not decouple from the fixed-point dynamics. The contents of this paper are based on [14].

In Chapter 2 we provide a summary on the algebraic theory of anyons which is used prominently throughout this work, based mainly on Appendix A of [12].

CHAPTER 2

A SUMMARY ON THE ALGEBRAIC THEORY OF ANYONS

In this chapter we provide a summary of the main tools regarding Modular Tensor Categories (MTC) that will be used in the the rest of this thesis. For more references, see e.g. [15, 16]).

The main theory that we will be interested in is Chern-Simons theory [17]. This theory is defined by a gauge group G and a positive integer k called the level through the following action principle:

$$\frac{k}{4\pi}\int_M \mathrm{Tr}(A\wedge dA+\frac{2}{3}A\wedge A\wedge A). \tag{2.1}$$

Importantly, the theory does not depend on the metric of the three-manifold M and the theory is therefore *topological* (at least up to a few details that will be addressed in the following, and that were first pointed out in [18]). Thus, Chern-Simons theory is a prime example of a 3D TQFT.

In this work we will be furthermore interested in studying boundary conditions of Chern-Simons theories. Historically, the paper [4] studied the simplest possible form of this problem, and found that if we set boundary conditions such that $A_0 = 0$ at the boundary, we recover, remarkably, (the chiral half of) the Wess-Zumino-Witten (WZW) model, a conformal field theory in two spacetime dimensions defined by a Lie group G and a positive integer k, also called the level. The action principle is:

$$S_{WZW}=\frac{k}{16\pi}\int_\Sigma d^2x\,\mathrm{Tr}(\partial^\mu g^{-1}\partial_\mu g)-\frac{ik}{24\pi}\int_B d^3y\,\epsilon^{\alpha\beta\gamma}\,\mathrm{Tr}((g^{-1}\partial_\alpha g)(g^{-1}\partial_\beta g)(g^{-1}\partial_\gamma g)) \tag{2.2}$$

If we start with the WZW model, we can gauge a subgroup symmetry H of G such that the resulting theory is a gauged WZW model. A natural question to ask then, is what is the 3D TQFT that will have this gauged WZW model as boundary condition. This question was addressed by Moore and Seiberg in [2]. Schematically, in most cases the gauged WZW

model may be found at the boundary of the product Chern-Simons theory

$$\frac{G_k \times H_{-\tilde{k}}}{Z}, \tag{2.3}$$

with Z the common center of G and H, when we set boundary conditions such that the H gauge fields embed into the G gauge fields. There are, however, exceptions to this rule. A main goal of this thesis is to explore with more precision the interplay between bulk 3D Chern-Simons theories and the 2D theories supported at their boundaries –such as the WZW and gauged WZW models just introduced– and the consequences of this interplay. The main tool to understand this relationship in modern terms is going to be the formulation of 3D TQFTs in terms of a set of algebraic rules called *the algebraic formulation of anyons*, which we review next. In particular, Chern-Simons theory can be characterized in terms of these algebraic principles.

In the algebraic formulation of 3D TQFTs, one is interested in studying a set of topological line operators, called anyons, that are mathematically described by the objects of a MTC $\mathcal{C}$. An arbitrary anyon can always be expanded in a non-negative integer linear combination of a finite set of elementary anyons referred to as the *simple anyons* of the theory. These are the simple objects of the MTC $\mathcal{C}$. The simple anyons of $\mathcal{C}$ are denoted as $a, b, c,$ etc., while the set of all of the simple anyons in $\mathcal{C}$ is denoted by $\mathcal{I}$. The simple anyons in a MTC can fuse according to the fusion rules:

$$a \otimes b = b \otimes a = \bigoplus_{c \in \mathcal{I}} N_{ab}^{c}\, c \ , \tag{2.4}$$

where the N_{ab}^{c} are non-negative integers known as the fusion coefficients. The fusion product in an MTC is commutative and associative: $(a \otimes b) \otimes c = a \otimes (b \otimes c)$.

By definition, there exists a unique trivial anyon 0 (called variously the vacuum, the identity anyon, etc.) such that $a \otimes 0 = 0 \otimes a = a$ for any $a \in \mathcal{I}$. Furthermore, given this

identity anyon, for any simple $a \in \mathcal{I}$, there exists a unique simple $\bar{a}$ such that $a \otimes \bar{a} = 0 \oplus \cdots$ and thus we call $\bar{a}$ the conjugate of a. A simple anyon a is said to be *abelian* if and only if

$$\forall b \in \mathcal{I}, \quad a \otimes b = b \otimes a = c \tag{2.5}$$

for some $c \in \mathcal{I}$. That is, for any simple anyon b, fusion with a returns a single simple anyon c. Simple abelian anyons in a MTC always generate some abelian group, from which their name is derived. Otherwise, if there is more than one summand on the right-hand side for at least one simple b:

$$a \otimes b = b \otimes a = c_1 + c_2 + \cdots , \tag{2.6}$$

the simple anyon a is called *non-abelian*, or *non-invertible*.

Importantly, the abstract data of a MTC can be represented by well-known diagrammatic expressions, whereby anyons are represented by lines extending through time:

(2.7)

In terms of these diagrams, the fusion product just introduced corresponds to the parallel fusion of the lines. Fusion also allows us to construct splitting vector spaces V_c^{ab} and fusing vector spaces V_{ab}^c of dimension N_{ab}^c associated with trivalent junctions of the anyons. Equivalently, these are the vector spaces assigned to the two-sphere with three punctures in radial quantization. Choosing a basis in these vector spaces allows us to define the following vertex diagrams, from which we can construct more complex diagrams:

$\left(\frac{d_c}{d_a d_b}\right)^{1/4}$ 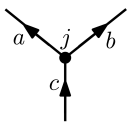

$=: |a, b, c; j\rangle \in V_c^{ab}$, $\left(\frac{d_c}{d_a d_b}\right)^{1/4}$ 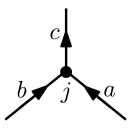

$=: \langle a, b, c; j| \in V_{ab}^c$. (2.8)

In these expressions, we have used the quantum dimension d_a of a simple anyon a, defined

as the largest eigenvalue of the matrix $\mathbf{N}_a$ with entries defined by the fusion coefficients $(\mathbf{N}_a)_{bc} \coloneqq N_{ab}^c$. The dimension of a non-simple anyon $\oplus_a a$ is then defined merely as the addition of the quantum dimensions of each component: $d_{\oplus_a a} = \sum_a d_a$. An important property of the quantum dimensions is that they satisfy the fusion algebra: $d_a d_b = \sum_{c\in\mathcal{I}} N_{ab}^c d_c$. It is also important to define the dimension of the MTC, which in turn is given by the quantum dimensions of the individual simple anyons as

$$\dim(\mathcal{C}) = \sum_{a\in\mathcal{I}} d_a^2 \,. \tag{2.9}$$

We may construct further diagrams using the trivalent vertices. An important one in the following is the bubble diagram:

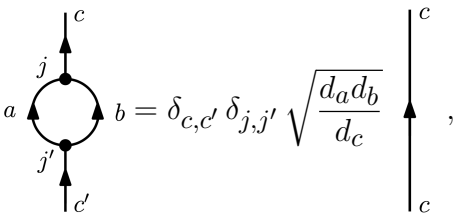

$$= \delta_{c,c'}\,\delta_{j,j'}\,\sqrt{\frac{d_a d_b}{d_c}} \,, \tag{2.10}$$

from which, taking $c = c' = 0, a = b$ we recover an expression for the quantum dimension d_a of a simple anyon a as the expectation value of an unknot of a:

$$d_a = \quad . \tag{2.11}$$

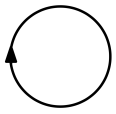

We can now compose trivalent junctions to draw a diagram splitting a simple anyon d into three a, b, c. There are two ways to do this: either fusing a with b first, or b with c first. As is well-known, the order is immaterial since it corresponds to the same splitting written in two different bases related by a unitary transformation. This unitary transformation is implemented by the F-symbols, which encode the associativity of splitting a single simple

anyon into three. Diagrammatically:

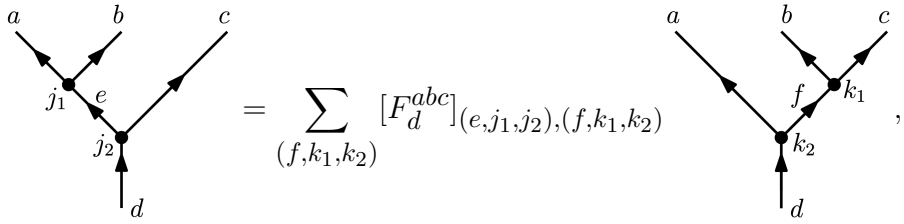

(2.12)

where the diagrams on the left and on the right are the different representations of the same splitting just mentioned. In a unitary theory, there always exists a basis where the matrices $[F_d^{abc}]$ are unitary (for a more in-depth discussion of unitarity in the context of ribbon categories, see [19]).

Rather than being arbitrary numbers, the F-symbols defining an MTC are constrained by the so-called pentagon equations, which guarantee consistency of the theory when applying F-symbols on higher-point diagrams. We will not need these equations in the following. See the original references [20, 21] for details.

Famously, anyons satisfy non-trivial braiding statistics. Algebraically, this fact is encoded in the R-symbols defining an MTC. In components, this is given by the diagrammatic expression

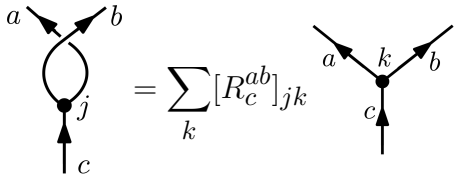

(2.13)

Similar to the F-symbols, the R-symbols are also constrained by analogous consistency conditions called hexagon equations. However, we will also not need these relations in the following. See [20, 21] for details.

Straightening a simple line a that "braids with itself" under a 2π rotation gives the

definition of a phase known as the topological spin θ_a:

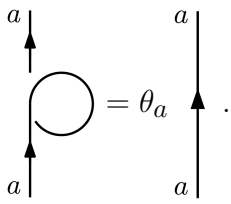

(2.14)

When meaningful, the topological spin is given by $\theta_a = e^{2\pi i h_a}$, with h_a the conformal weight of some 2D RCFT primary a related to the 3D TQFT by bulk-boundary correspondence. Often, h_a defined mod 1 is used to refer to the topological spin of a line instead of using θ_a directly. It is a result of [22, 23] that h_a is always a rational number. If $\theta_a = 1$, we say that the simple anyon a is a *boson*.

We define a matrix S with entries valued on the simple anyons of the MTC as:

$$\frac{S_{ab}}{S_{00}} = a$$ 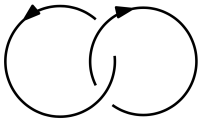 $$b,$$

(2.15)

where $S_{00} = 1/\sqrt{\dim(\mathcal{C})}$. This is the standard modular S-matrix. The statement that this matrix is non-degenerate provides the final requirement in the definition of a MTC. In passing, from the modular S-matrix we can define the braiding phase:

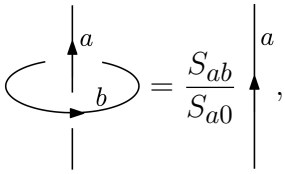

(2.16)

which allows us to unlink anyons circling around each other. Setting $a = 0$ we recover the well-known expression for the quantum dimension for the simple anyon b in terms of the modular S-matrix: $d_b = S_{0b}/S_{00}$.

Finally, given a 3D TQFT described by a MTC $\mathcal{C}$, we write $\bar{\mathcal{C}}$ for the orientation-reversal of $\mathcal{C}$. In practice, this amounts to a MTC with the same number of simple anyons and the

same fusion ring, but with all quantities defined above (e.g. topological spins, or F-symbols) differing by a complex conjugation. For instance, for simple $a \in \mathcal{C}$, call the associated anyon after orientation-reversal $a_{\text{rev}} \in \bar{\mathcal{C}}$, then $\theta_{a_{\text{rev}}} = \theta_a^*$ (for the precise mathematical definition of orientation-reversal, see Def. 6.13. in [24]). For a Chern-Simons theory G_k, this operation amounts to changing the sign of the level $G_k \to G_{-k}$. Below, unless we wish to emphasize the orientation-reversal, we will abuse language and repeat the notation for anyons in the original theory and the one obtained after orientation-reversal, as it will be clear from context with which theory we are working with.

CHAPTER 3

NON-INVERTIBLE ANYON CONDENSATION AND LEVEL-RANK DUALITIES

3.1 Introduction

In this chapter we derive new dualities of topological quantum field theories (TQFTs) in three spacetime dimensions. Our results generalize the celebrated level-rank dualities of Chern-Simons gauge theories, the most familiar of which are of the form:

$$SU(N)_K \leftrightarrow U(K)_{-N,-N}, \quad USp(N)_K \leftrightarrow USp(K)_{-N}, \quad SO(N)_K \leftrightarrow SO(K)_{-N}. \tag{3.1}$$

For unitary groups these dualities have been explored in [7, 25–30], the dualities for SO and USp were derived in [8], while those for more general orthogonal groups were discussed in [9]. Additionally, there are also dualities involving exceptional groups derived in [31]. Beyond their intrinsic conceptual interest, these dualities are important e.g. in that they provide non-trivial evidence for proposals of phase diagrams of 3D gauge theories [7, 10], and establish the existence of families of time-reversal invariant TQFTs [32].

Typically, the starting point to prove these dualities is to establish an equivalence of the associated chiral algebras that appear on the edge of the TQFT equipped with suitable boundary conditions [4, 18]. For connected, simple, and simply-connected gauge groups these are the familiar Kac-Moody current algebras (for an overview see e.g. [5]), while for other global forms of the gauge group, obtained by quotienting by central elements, they are instead extensions of the Kac-Moody algebras [2]. Often, the initial step in deriving these equivalences of chiral algebras is to find a larger chiral algebra that contains as a subalgebra the two chiral algebras of interest and then study how representations of the larger chiral algebra decompose under restriction to the subalgebras. Frequently, the larger algebra is

taken to be a Kac-Moody algebra at level one, with the same central charge as that of the two subalgebras combined, in which case such embeddings fall under the so-called *conformal embeddings*. In this technique, duality of chiral algebras is intimately related with conformal field theories (CFTs) that are derived from appropriate quotients of chiral algebras; namely, coset CFTs.

A well-known example illustrates the general procedure. Starting from the embedding:

$$SU(N)_K \times SU(K)_N \subset SU(NK)_1, \tag{3.2}$$

we learn that the chiral algebra $SU(N)_K$ can be presented as a coset:

$$SU(N)_K \cong \frac{SU(NK)_1}{SU(K)_N}. \tag{3.3}$$

Passing to the bulk TQFT one then obtains a duality of Chern-Simons theories:

$$SU(N)_K \cong \frac{SU(NK)_1 \times SU(K)_{-N}}{\mathbb{Z}_K}. \tag{3.4}$$

A particularly subtle point in the above is the appearance of the quotient by $\mathbb{Z}_K$, the common center of the gauge group. As we review in Section 3.2 this quotient necessarily appears so that the boundary CFT has a unique ground state without additional topological degrees of freedom. We can also directly interpret this quotient as a gauging operation on the theory $SU(NK)_1 \times SU(K)_{-N}$. Specifically this theory has abelian anyons, i.e. lines with abelian fusion rules, which are bosonic and hence may condense. In the language of higher symmetry [6, 33], these are one-form global symmetries and condensing them is equivalent to gauging this one-form symmetry. As an operation on the initial TQFT this condensation operation acts as a simple algorithm [2, 34]:

- We remove all lines that braid non-trivially with the condensing abelian anyons. Such

removed lines are often said to be *confined*.

- We identify any remaining lines that differ by fusion with the condensing abelian anyons. This is the step of forming gauge orbits.

- If a remaining line a is invariant under fusion with s condensing abelian anyons, then in the resulting theory the line a is split into s distinct lines.

This three-step gauging procedure allows us to treat many foundational examples of duality amongst TQFTs. However, as originally noted in [35, 36], there are certain cosets where this procedure of gauging by the common center to isolate a CFT with a unique vacuum fails. Traditionally such cosets were often referred to as *Maverick cosets* and in these cases, the construction of a standard CFT proceeds in an ad hoc manner. Two infinite series of such cosets are known:

$$\frac{SU(k)_2}{Spin(k)_4}, \quad c = \frac{2(k-1)}{k+2}, \quad \text{and} \quad \frac{Spin(2N)_2}{Spin(N)_2 \times Spin(N)_2}, \quad c = 1, \tag{3.5}$$

as well as a finite list of exceptional cases summarized in Section 3.3.2 below. One of the main results of this work is to provide a uniform analysis of these cosets, and their implications for duality in 3D TQFTs.

As we will exhibit, a key idea unifying these cosets is the appearance of *non-abelian* bosonic anyons in the associated TQFTs, as first explored in [24, 37]. To obtain boundary CFTs with unique vacua and no additional topological degrees of freedom we must condense such non-abelian bosons. This procedure unifies the treatment of Maverick and more familiar cosets, and in fact is even crucial for a complete understanding of the conformal embeddings behind more familiar level-rank dualities as we discuss in Section 3.5.

Non-abelian anyon condensation in 3D TQFTs can also be fruitfully described using the language of higher symmetry. Indeed, as already mentioned, abelian anyons are generators of one-form global symmetries i.e. they are line topological operators with abelian fusion

rules. Anyons with more general non-abelian fusion rules are therefore interpreted as non-invertible one-form symmetries. Such generalized symmetries have recently been investigated particularly in spacetime dimension greater than two. (See e.g. [38–40] for recent reviews and lectures).

Relatedly, on the boundary the bulk one-form symmetries restrict to ordinary, zero-form symmetries of the CFT. For abelian anyons, these boundary zero-form symmetries are group-like, but for non-abelian anyons, the boundary zero-form symmetries are a general fusion category. In this context, early foundational work on non-invertible symmetries and gauging was done in [41–46], and a rigorous mathematical treatment of condensing or gauging general symmetries was carried out in [47–52]. We briefly review this formalism in Section 3.6.1.

From a more physical point of view, a treatment of non-invertible topological lines in 2D theories as symmetries was pioneered in [11, 53, 54] and further discussed in [55, 56]. The relationship between the 3D bulk TQFT and 2D boundary CFT is a foundational example of the general paradigm of a bulk topological field theory controlling the generalized symmetry of the boundary theory [6,57–61]. The general idea of gauging and condensing non-invertible symmetries has been explored in [62–67] and the relationship between bulk and boundary non-invertible gauging has been utilized in [68–73]. Finally, recent discussions of gauging non-invertible symmetries in 2D CFTs, closely related to our analysis below, include in particular [74, 75]. Below we often make use of the language of generalized symmetries, interchangeably using non-abelian and non-invertible, as well as gauge and condense.

3.1.1 An Invitational Example with Fibonacci Anyons

As an illustrative example to show how non-abelian anyon condensation is in fact central to many dualities of TQFTs consider the exceptional conformal embedding [31, 76–79]:

$$SU(2)_1 \times SU(2)_3 \hookrightarrow (G_2)_1. \tag{3.6}$$

In CFT, the existence of this embedding can be interpreted in two ways:

- The branching functions of the coset $\frac{(G_2)_1}{SU(2)_1}$ give the characters of $SU(2)_3$.
- The branching functions of the coset $\frac{(G_2)_1}{SU(2)_3}$ give the characters of $SU(2)_1$.

Translating the first statement to 3D TQFTs following [2] gives the duality

$$SU(2)_3 \cong (G_2)_1 \times SU(2)_{-1}. \tag{3.7}$$

The simplicity of the TQFTs involved in this duality make it easy to verify explicitly. For instance, $SU(2)_k$ has $k+1$ anyons obeying (truncated) fusion rules of $SU(2)$ representations. Meanwhile $(G_2)_1$ is the theory of Fibonacci anyons, the simplest non-abelian TQFT consisting of two anyons 1 and ϕ obeying:

$$\phi \times \phi = 1 + \phi. \tag{3.8}$$

Thus, for example both sides of the duality (3.7) have four total anyons, and one may readily verify that their fusion rules and spins are identical.

The previous –seemingly simple– chain of ideas raises however an immediate puzzle. Suppose instead that we make use of the second implication of the embedding (3.6), then proceeding blindly along the same steps would have lead to the proposed duality:

$$SU(2)_1 \overset{?}{\cong} (G_2)_1 \times SU(2)_{-3}. \tag{3.9}$$

We note that, as in (3.7), there is no common center of the gauge groups on the right-hand side. However, (3.9) is obviously false, for instance the number of lines (2 vs. 8) does not match. The resolution of this puzzle is that while $(G_2)_1 \times SU(2)_{-3}$ does not have any condensable abelian anyons, there are non-abelian bosonic anyons which may condense, and doing so leads to a correct, and novel, duality.

To demonstrate this we begin with the correct duality (3.7). Reversing orientation (flipping the signs of all levels), and tensoring by $(G_2)_1$, we obtain

$$(G_2)_1 \times SU(2)_{-3} \cong (G_2)_1 \times (G_2)_{-1} \times SU(2)_1. \tag{3.10}$$

We now use that $(G_2)_1 \times (G_2)_{-1}$ is a Drinfeld double, i.e., it is of the form $G_k \times G_{-k}$. In particular for any such theory it is known that one can gauge/condense all the anyons and obtain a trivial theory [47, 50, 80]. The novelty here is that such condensation is necessarily non-abelian. Concretely then, we write

$$\mathcal{Z}(\mathbf{Fib}) \equiv (G_2)_1 \times (G_2)_{-1}, \tag{3.11}$$

where the notation above indicates that $\mathcal{Z}(\mathbf{Fib})$ is the Drinfeld center of the Fibonacci anyons (3.8). Condensing $\mathcal{Z}(\mathbf{Fib})$ in (3.10) then leads to a new duality:

$$SU(2)_1 \cong \frac{(G_2)_1 \times SU(2)_{-3}}{\mathcal{Z}(\mathbf{Fib})}. \tag{3.12}$$

In summary, $(G_2)_1 \times SU(2)_{-3}$ has non-abelian bosonic anyons, or in a different language, it has a non-anomalous non-invertible one-form symmetry, and gauging it, one finds an equivalence with the $SU(2)_1$ Chern-Simons gauge theory. These non-abelian condensable bosons thus play the role of the common center of the gauge group in more familiar examples. Compare for instance with the more familiar duality (3.4). In particular, this non-invertible one-form symmetry must be gauged to obtain the duality expected from the existence of the conformal embedding (3.6).

We study this example of non-abelian anyon condensation in more detail in Section 3.4.1 below, and review the condensation of $\mathcal{Z}(\mathbf{Fib})$ to the trivial theory in Section 3.6.2.

3.1.2 Summary of Selected Results

Having illustrated the ubiquitous nature of non-abelian anyon condensation let us summarize several key results derived using this formalism below.

Note that the central charges of the first infinite family of Maverick cosets in (3.5) match those of the parafermion CFTs [5, 81], so it is natural to suggest that this infinite Maverick family reproduces the parafermions. The parafermions also have two standard coset descriptions given by the $SU(2)_k/U(1)_{2k}$, or $(SU(k)_1 \times SU(k)_1)/SU(k)_2$ cosets [5]. We therefore conjecture the infinite series of dualities:

$$\frac{SU(k)_2 \times Spin(k)_{-4}}{\mathcal{A}_k} \cong \frac{SU(2)_k \times U(1)_{-2k}}{\mathbb{Z}_2} \cong \frac{SU(k)_1 \times SU(k)_1 \times SU(k)_{-2}}{\mathbb{Z}_k}, \tag{3.13}$$

for some suitable collection of condensable non-abelian anyons $\mathcal{A}_k$ on the left-hand side. Below in Section 3.5.2 we verify this result explicitly for the first non-trivial case $k = 3$. In this case the parafermion theory in question coincides with the three-state Potts model and the algebra of non-abelian anyons is generated by:

$$\mathcal{A}_3 = (\mathbf{1}, 0) + (\mathbf{1}, 8) + (\mathbf{8}, 4), \tag{3.14}$$

where we label $SU(3)$ representations by their dimension and $Spin(3) \cong SU(2)$ representations by their Dynkin index (i.e. their dimension is the label plus one.) In particular, the anyon $(\mathbf{8}, 4)$ is non-abelian with fusion rule:

$$(\mathbf{8}, 4) \times (\mathbf{8}, 4) = \sum_{i=0}^{4} (\mathbf{1}, 2i) + (\mathbf{8}, 2i) \to (\mathbf{1}, 0) + (\mathbf{1}, 8) + (\mathbf{8}, 4), \tag{3.15}$$

where the first equation denotes the fusion in the full TQFT, and the arrow indicates its projection back to $\mathcal{A}_3$.

We also analyze the second infinite sequence of Maverick cosets in (3.5). Since all of

these have $c = 1$ they must correspond to rational points in the moduli space of $c = 1$ CFTs. We conjecture that these cosets correspond to the orbifold points of $U(1)_{2N}$ modulo its $\mathbb{Z}_2$ reflection symmetry, which we denote as $U(1)^{\text{Orb}}_{2N}$. Lifting to TQFTs leads to the proposal

$$U(1)^{\text{Orb}}_{2N} \cong \frac{Spin(2N)_2 \times Spin(N)_{-2} \times Spin(N)_{-2}}{\mathcal{B}_N}. \tag{3.16}$$

For a suitable collection of condensable non-abelian anyons $\mathcal{B}_N$. In particular we verify this for the first non-trivial case $N = 3$ where:

$$\mathcal{B}_3 = (\mathbf{1}, 0, 0) + (\mathbf{1}, 4, 4) + (\mathbf{20'}, 0, 4) + (\mathbf{20'}, 4, 0) + (\mathbf{15}, 2, 2). \tag{3.17}$$

The fusion of the first four anyons above is abelian, but the last one is non-abelian with:

$$(\mathbf{15}, 2, 2) \times (\mathbf{15}, 2, 2) = \sum_{i,j=0}^{2} \left[(\mathbf{1}, 2i, 2j) + (\mathbf{15}, 2i, 2j) + (\mathbf{20'}, 2i, 2j)\right] \to \mathcal{B}_3, \tag{3.18}$$

where again the first equality is the fusion in the full TQFT and the arrow indicates the restriction to $\mathcal{B}_3$. We note that the Chern-Simons theory with the orbifold action is equivalent to changing the gauge group from $U(1)$ to $O(2)$. Level-rank dualities involving $O(N)$ were studied in [9] and we have the equivalence $U(1)^{\text{Orb}}_{2N} \cong O(2)^0_{2N,0}$ where the additional subscript and superscript on $O(2)$ indicate other possible levels. Because of this equivalence (3.16) can also be cast as a duality of orthogonal type Chern-Simons theories:

$$O(2)^0_{2N,0} \cong \frac{Spin(2N)_2 \times Spin(N)_{-2} \times Spin(N)_{-2}}{\mathcal{B}_N}. \tag{3.19}$$

Beyond analyzing these families of Maverick cosets we can also study many of the isolated examples in Section 3.3.2 and derive a variety of dualities. All of these examples have $c < 1$ and thus correspond to some (possibly non-diagonal) minimal model. For instance, the

simplest of these leads to the Ising TQFT:

$$\text{Ising TQFT} \cong \frac{SU(4)_1 \times SU(2)_{-10}}{\mathcal{A}}, \tag{3.20}$$

where

$$\mathcal{A} = (\mathbf{1}, 0) + (\mathbf{6}, 10) + (\mathbf{1}, 6) + (\mathbf{6}, 4), \tag{3.21}$$

and both $(\mathbf{1}, 6)$ and $(\mathbf{6}, 4)$ have non-abelian fusion.

Armed with our improved understanding of non-abelian anyon condensation, we also revisit the conformal embeddings generalizing the example of Section 3.1.1 to obtain other level-rank dualities involving non-abelian anyon condensation. For instance revisiting the embedding (3.2) of unitary groups allows us to derive:

$$SU(Nk)_1 \cong \frac{SU(N)_k \times SU(k)_N}{\mathcal{A}_{N,k}}, \tag{3.22}$$

where $\mathcal{A}_{N,k}$ is a suitable collection of non-abelian anyons. For instance for $N = 3$ and $k = 2$ this is the non-abelian anyon:

$$\mathcal{A}_{3,2} = (\mathbf{1}, 0) + (\mathbf{8}, 2). \tag{3.23}$$

Similarly, a less explored example arises from the conformal embedding

$$SO(N)_4 \times SU(2)_N \hookrightarrow USp(2N)_1. \tag{3.24}$$

This implies the level-rank duality:

$$SU(2)_N \cong \frac{USp(2N)_1 \times SO(N)_{-4}}{\mathcal{A}_N}, \tag{3.25}$$

where for instance in the case $N = 3$:

$$\mathcal{A} = (\mathbf{1}, 0) + (\mathbf{14}, 4_1), \tag{3.26}$$

with non-abelian fusion:

$$(\mathbf{14}, 4_1) \times (\mathbf{14}, 4_1) = (\mathbf{1}, 0) + (\mathbf{1}, 4_1) + (\mathbf{14}, 0) + (\mathbf{14}, 4_1) \to (\mathbf{1}, 0) + (\mathbf{14}, 4_1). \tag{3.27}$$

In general, many of the previous examples can be understood from the "principle of coset inversion," first derived mathematically in [24]. We explain this in Section 3.3.1 from a physics point of view and summarize it in mathematical form in Section 3.6.1. The principle may be summarized as follows: one may rearrange the numerator and denominator of any coset, provided we also allow for the possibility of non-abelian anyon condensation. This principle holds abstractly, independently of the description of the CFT in terms of WZW models. For instance we can even revisit the well-known TQFT associated to the unitary minimal models

$$M(k+3, k+2) \cong \frac{SU(2)_k \times SU(2)_1 \times SU(2)_{-k-1}}{\mathbb{Z}_2}, \tag{3.28}$$

where $M(k+3, k+2)$ denotes the k-th minimal model TQFT, with $k = 1$ the Ising model. Allowing for non-abelian anyon condensation implies that in general there is also an equivalence:

$$SU(2)_k \times SU(2)_1 \cong \frac{M(k+3, k+2) \times SU(2)_{k+1}}{\mathcal{A}_k}, \tag{3.29}$$

which we explicitly check for $k = 2$ in Section 3.4.2 (for $k = 1$ this expression may be checked by the three-step gauging rule). Finally, more examples of duality involving non-abelian anyon condensation may be found from the classification of RCFTs with a small number of primaries and a small central charge studied in [82, 83] and associated cosets of

holomorphic CFTs at $c = 24$ [84].[1]

3.2 Cosets, Interfaces, and Bulk-Boundary Correspondence

In this section we review the relationship between coset CFTs and associated boundary conditions in topological Chern-Simons theories. We pay particular attention to the interplay between gapless and gapped degrees of freedom at the boundary, whose understanding is important for determining dualities of the bulk topological theories.

Let us first recall the coset construction purely in the context of 2D CFT. Our starting point is a G_k WZW theory based on a group G and an integer level k. We take the group G to be compact and simply-connected. Let H be now a subgroup of G such that the Lie algebra of H embeds into the Lie algebra of G with embedding index ℓ. Then, there is an associated embedding of affine Lie algebras:

$$H_{\tilde{k}} \subseteq G_k \ , \quad \tilde{k} = \ell k \ . \tag{3.30}$$

Coset CFTs are constructed by expanding a chiral algebra with characters $\chi_\Lambda(q)$ in terms of the characters of a smaller algebra with characters $\chi_\lambda(q)$:

$$\chi_\Lambda(q) = \sum_\lambda b^\lambda_\Lambda(q)\chi_\lambda(q), \quad q = e^{2\pi i\tau}, \tag{3.31}$$

with τ the modular parameter. In our context, we assume the bigger chiral algebra is that of the G_k WZW theory, and the smaller chiral algebra is that of the $H_{\tilde{k}}$ WZW theory, with $H_{\tilde{k}}$ embedded in G_k. The quantities $b^\lambda_\Lambda(q)$ are called *branching functions*. The point of the previous expansion is to notice that, since the characters $\chi_\Lambda, \chi_\lambda$ are modular covariant, the branching functions inherit some form of modular covariance and can be thus thought of as

1. We thank B. Rayhaun for bringing this to our attention.

the characters of a new CFT with torus partition function

$$Z_{\text{Coset CFT}}\,(T^2) = \sum_{\Lambda,\lambda} |b^{\lambda}_{\Lambda}(q)|^2. \tag{3.32}$$

This is the so-called GKO coset construction [85,86], where for simplicity we have restricted ourselves to diagonal theories.

A subtlety in the construction above is the generic appearance of multiple copies of the vacuum and of many copies of the same chiral or Virasoro primary in the partition function. Relatedly, not all branching functions are non-zero, so the naive modular covariance of the branching functions in general requires further analysis.[2] In modern terms, we recognize the vacuum degeneracy as the presence of a topological sector coupled to gapless, CFT degrees of freedom. In some circumstances it is desirable to remove this degeneracy by, roughly speaking, "gauging away" this topological sector resulting in a CFT with a unique vacuum. In general, we should therefore differentiate between two possible notions of cosets:

- A coset CFT with degenerate vacua, where topological sectors are retained.
- A coset CFT with a unique vacuum state, where topological sectors have been removed.

The partition function (3.32) corresponds to the first notion above. The distinction between these possibilities is particularly important in the special case where the topological sector is all there is, as occurs for example in the case of conformal embeddings discussed below.

The phenomenon just described has been previously noticed and interpreted in terms of projection into universes and/or vacua (See [1,90]), and here we provide a further interpretation in the context of TQFTs with gapped and gapless boundaries, and lines ending or not perpendicularly at a topological junction.

2. Historically, these confusions led to the search for methods to remove such a degeneracy, such as the so-called "identification current method" or "fixed point resolutions" that made the final result into a CFT with a single vacuum, a non-degenerate modular S-matrix, etc. The result of such a procedure is what in some older literature is known as "the" coset CFT (See for instance [5,87–89]).

Turning now to the relationship between 3D TQFTs and 2D CFTs, a natural question to ask is what are the TQFTs associated to these two possible notions of cosets. As shown in [2] the TQFT that reproduces the coset CFT with a single vacuum at the boundary is given –often, but crucially not always– by the product Chern-Simons theory:

$$\frac{G_k \times H_{-\tilde{k}}}{Z} \ , \tag{3.33}$$

where Z is the common center of groups G and H. As in [2], Z is, for the time being, some abelian discrete group. Shortly, this assumption will be lifted. With an eye towards future generalizations let us deduce why (3.33) is correct. In particular, we would like to understand the difference between the boundary conditions in the Chern-Simons theories which differ by whether we gauge or not the common center. As we illustrate, this difference can be usefully phrased in terms of topological interfaces.

Consider first the case were we gauge the common center in the bulk as in (3.33). This situation is depicted in the left in Figure 3.1, where we denote the boundary condition as $(G_k/H_{\tilde{k}})_Z$ with a subindex to emphasize that the corresponding bulk has the center one-form symmetry gauged.[3] As mentioned above, this is the case where we have a theory with single vacuum on the boundary. Standard examples involving an abelian $\mathbb{Z}_2$ gauging that one could keep in mind are the minimal models $SU(2)_k \times SU(2)_1 \times SU(2)_{-k-1}/\mathbb{Z}_2$, or the parafermions $SU(2)_k \times U(1)_{-2k}/\mathbb{Z}_2$.

Separately, we note that in the Chern-Simons theory $G_k \times H_{-\tilde{k}}$, the common center indicates the presence of abelian anyons which define a gaugable one-form symmetry [2,34]. We can thus consider the topological interface generated by gauging the common center one-form symmetry on the right half of space, as depicted on the right in Figure 3.1. Placing this topological interface together with the coset boundary $(G_k/H_{\tilde{k}})_Z$ of Figure 3.1, we obtain

3. When discussing non-chiral 2D theories we should really picture the 3D theory with a left and right boundary component. In the following we illustrate one boundary component and we assume the same conditions on the left and right. This means that we consider diagonal theories.

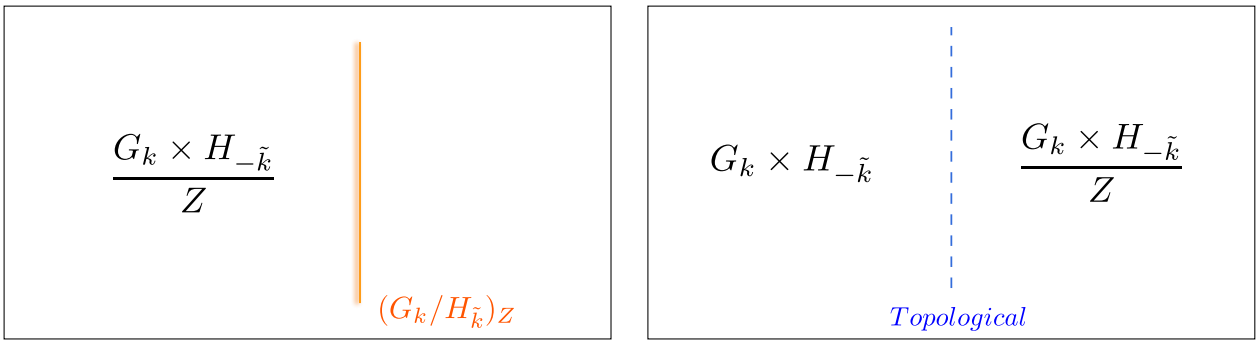

Figure 3.1: On the left: the theory $(G_k \times H_{-\tilde{k}})/Z$, where the common center Z of G_k and $H_{-\tilde{k}}$ has been gauged, in the presence of the CFT coset boundary condition which is denoted $(G_k/H_{\tilde{k}})_Z$. On the right: a topological interface connecting the product $G_k \times H_{-\tilde{k}}$ without the common center gauged and $(G_k \times H_{-\tilde{k}})/Z$.

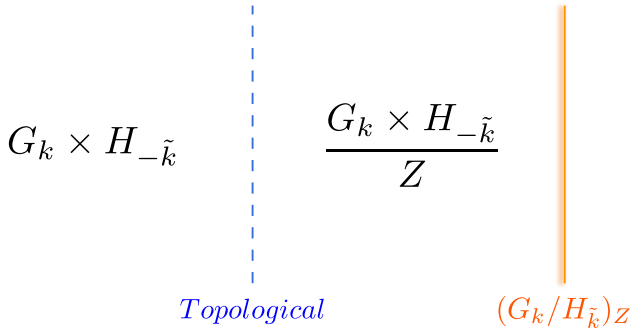

Figure 3.2: Coset boundary condition with single vacuum $(G_k/H_{\tilde{k}})_Z$ in the presence of the topological interface joining $G_k \times H_{-\tilde{k}}$ and $(G_k \times H_{-\tilde{k}})/Z$.

the construction depicted in Figure 3.2.

Since the interface is topological, we can move it towards the boundary to generate a new boundary condition for the theory without the common center one-form symmetry gauged. The latter boundary condition therefore differs from $(G_k/H_{\tilde{k}})_Z$ by some topological action, and so we call the new boundary condition $(G_k/H_{\tilde{k}})$ without a subindex to emphasize that the corresponding bulk has no one-form symmetry gauged. The result of all previous manipulations is depicted in Figure 3.3.

In summary, we see that the key difference between the coset boundary condition when

the bulk is given by $G_k \times H_{-\tilde{k}}$ and $(G_k \times H_{-\tilde{k}})/Z$ is determined by some topological degrees of freedom, here represented by the topological interface separating the product with and without the common center gauged. Notice the similarity with our comment above regarding the distinction between two notions of coset CFTs: one with and one without topological degrees of freedom removed.

Now that we understand how the boundary conditions $(G_k/H_{\tilde{k}})$ and $(G_k/H_{\tilde{k}})_Z$ are distinguished from each other we study how to setup the boundary condition $(G_k/H_{\tilde{k}})$ in $G_k \times H_{-\tilde{k}}$ recalling the well-known steps derived in [2,4]. The key point is that requiring the variation of the action to vanish implies the bulk equations of motion, but also the vanishing of a boundary term

$$\frac{k}{4\pi}\int_{\partial X} \mathrm{Tr}'_G(\delta A A) - \frac{\tilde{k}}{4\pi}\int_{\partial X} \mathrm{Tr}'_H(\delta B B), \tag{3.34}$$

where A and B are gauge fields based on the Lie algebras of G and H respectively, Tr'_G and Tr'_H are the respective representation-independent traces, and ∂X is the boundary of our bulk 3D spacetime X. Imposing $A_0 = 0$ and $B_0 = 0$ at the boundary gives the canonical

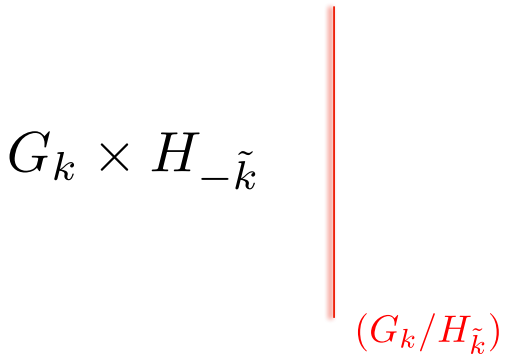

Figure 3.3: Pushing the topological interface towards the boundary and fusing it with the coset boundary condition $(G_k/H_{\tilde{k}})_Z$ generates a gapless boundary for the $G_k \times H_{-\tilde{k}}$ Chern-Simons theory (with no common center symmetry gauged). By the nature of the construction, the result is generically a gapless boundary intertwined with a topological sector (i.e., there are now many vacua/topological local operators at the boundary) that is denoted as $(G_k/H_{\tilde{k}})$ (with no Z subindex). The gapless boundary condition so generated corresponds to (the chiral version of) the associated gauged WZW model.

chiral WZW boundary [4]. However, since we have taken H to embed in G there is another boundary condition where we ask for the gauge field A projected onto the Lie algebra of H to equal the gauge field B, which also makes (3.34) vanish. The action then reduces, following the steps of [2, 4] to an expression involving WZW actions:

$$ikS_{WZW}(U) - i\tilde{k}S_{WZW}(V) + ik\int \mathrm{Tr}'_G\,\lambda(\partial_\phi U\,U^{-1} - \partial_\phi V\,V^{-1}), \tag{3.35}$$

where U and V are the Maurer-Cartan fields that arise when we integrate the time components of A and B respectively in the bulk, and λ is a Lagrange multiplier. As first described in [2], changing variables and using the Polyakov-Wiegmann formula gives the path integral of (the chiral version of) the gauged WZW model.[4] In summary, we see that what we have called above the $(G_k/H_{\tilde{k}})$ boundary condition corresponds to (the chiral version of) the gauged WZW action.

The path integral, clearly, takes into account contributions resulting from topological sectors. This can be illustrated for instance by taking $H_{\tilde{k}} = G_k$ so that we obtain the well-known G_k/G_k topological coset field theory [91–94] on the boundary, whose partition function over a Riemann surface Σ has been evaluated (see [93]) to be $Z_{G_k/G_k} = \dim(\mathcal{V})$, with $\dim(\mathcal{V})$ the number of conformal blocks of the corresponding G_k WZW model. On the torus, this evaluates to the number of chiral primaries of the underlying G_k WZW model. We can also view this G_k/G_k boundary condition as an instance of the universal gapped boundary for a bulk theory of the form $\mathcal{C}\times\overline{\mathcal{C}}$, with $\mathcal{C} = G_k$.[5]

Gauging the center one-form symmetry Z in the bulk implies that the gauge group on the boundary is no longer H, but a non-simply-connected version based on the same Lie algebra.

4. It is sometimes useful to express the trace in the algebra of H in the path integral in terms of that of G by noting that the embedding relates the normalization of the traces $\mathrm{Tr}'_H = \mathrm{Tr}'_G/\ell$ with ℓ the embedding index.

5. An easy way to see that the previous gapped boundary always exists is to notice that upon unfolding the interface is simply the identity interface between $\mathcal{C}$ and $\mathcal{C}$.

The corresponding summation over bundles/insertion of anyons generating Z descends into a corresponding summation on the gauged WZW model on the boundary. The corresponding model based on a non-simply-connected gauge group has a single vacuum and the so-called "identification current method" has been applied to remove multiple copies of the same chiral primary, as studied in [95] (see also [96] for recent related discussions). This corresponds to the boundary condition that we have called $(G_k/H_{\tilde{k}})_Z$ above.

Let us now interpret the prior story in terms of lines ending at the boundary. To do this consider first two extreme scenarios: that of the canonical (chiral) CFT boundary with no topological sectors other than the identity, illustrated in Figure 3.4, and that of a purely topological boundary, illustrated in Figure 3.5.

In the CFT boundary case all lines can end perpendicularly at the boundary on a non-topological junction, which generates the local operators of the RCFT [18]. Under parallel fusion with the boundary, the bulk lines becomes the Verlinde lines [97–100] of the RCFT [1]. In particular, this point of view is one way in which we can explain why the local operators and Verlinde lines of an RCFT follow the same fusion ring; namely, that of the bulk MTC [21], and why furthermore Verlinde lines in an RCFT generate a modular tensor category (MTC) instead of merely a fusion category. Importantly, because the bulk lines form a MTC, and all lines can end perpendicularly at the boundary with this choice of boundary condition, it trivially follows that the set of lines that can end perpendicularly at the boundary have non-trivial mutual braiding. That is, the braiding matrix projected to those lines that can end perpendicularly at the boundary is non-degenerate (i.e., the projected braiding matrix has maximal rank).

We can compare the discussion above with the case of a purely topological boundary. Since we are assuming Z to be abelian, only a square root of the total number of simple lines can end perpendicularly at the boundary [101–104], generating a topological junction

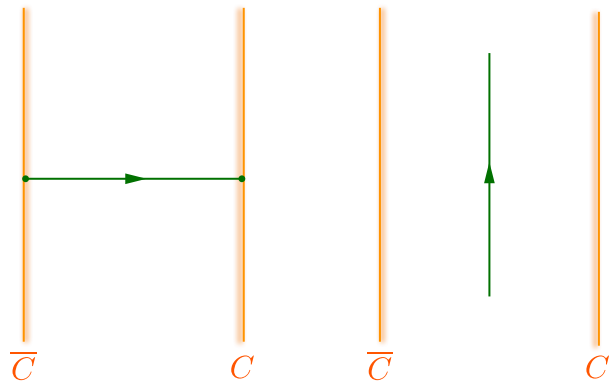

Figure 3.4: In the canonical CFT boundary condition (in orange), all lines of the bulk CS theory end perpendicularly at the boundary on a (non-topological) local operator of the WZW theory based on the same group and level. Relatedly, pushing a line to the boundary in parallel to it gives rise to a Verlinde line of the corresponding WZW theory.

in the process, and under parallel fusion with the boundary such lines becomes invisible[6] (See Figure 3.5). In particular, this set of lines has a size strictly smaller than that of the simple objects of the full bulk MTC, and in which all lines braid trivially with each other. That is, the braiding matrix projected to those lines that can end perpendicularly at the boundary is maximally degenerate (i.e., the projected braiding matrix has rank 1).

We now come back to the situation of the gauged WZW boundary condition $(G_k/H_{\tilde{k}})$. The general situation is complicated because of the variety of ways that the topological sector can intertwine with the CFT sector. However, we can get an idea of the general situation by considering the example $SU(2)_1 \times SU(2)_1 \times SU(2)_{-2}$ which is (up to the $\mathbb{Z}_2$ common center) the standard coset description of the Ising model. The branching rules of the characters are:

$$\chi_0^{SU(2)_1}\chi_0^{SU(2)_1} = \chi_0^I\,\chi_0^{SU(2)_2} + \chi_v^I\,\chi_2^{SU(2)_2}, \tag{3.36}$$

$$\chi_0^{SU(2)_1}\chi_1^{SU(2)_1} = \chi_\sigma^I\,\chi_1^{SU(2)_2}, \tag{3.37}$$

$$\chi_1^{SU(2)_1}\chi_0^{SU(2)_1} = \chi_\sigma^I\,\chi_1^{SU(2)_2} \tag{3.38}$$

6. Technically, one summarizes this statement saying that such lines participate in a Lagrangian subgroup.

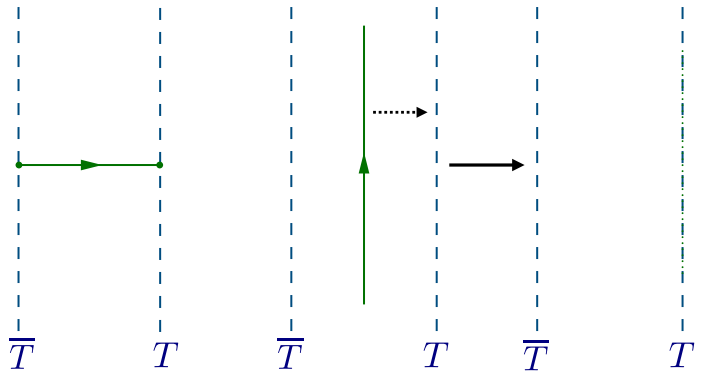

Figure 3.5: In a topological boundary condition not all lines of the bulk theory end perpendicularly to the boundary. Only those generating a Lagrangian algebra can end, resulting in a topological local operator at the junction. When Z is abelian as it is assumed in this section, the Lagrangian algebra is moreover a Lagrangian subgroup. Under parallel fusion, those lines in the Lagrangian subgroup become invisible at the boundary.

$$\chi_1^{SU(2)_1}\chi_1^{SU(2)_1} = \chi_0^I\,\chi_2^{SU(2)_2} + \chi_v^I\,\chi_0^{SU(2)_2}. \tag{3.39}$$

Comparing with (3.32), we obtain a total of six operators in the CFT, so not all lines of the bulk end at a non-trivial local operator of the boundary theory. Furthermore, every operator of the CFT sector appears twice, with a non-trivial topological operator appearing in the branching space associated to the $\mathbb{Z}_2$ generator in the bulk: the line $(1,1,2)$ in $SU(2)_1 \times SU(2)_1 \times SU(2)_{-2}$. The doubling of the spectrum can be then thought of as fusing this topological operator with the different CFT sectors.

We can also obtain the same conclusion by observing[7]

$$SU(2)_1 \times SU(2)_1 \times SU(2)_{-2} \cong \text{Ising} \times U(1)_2 \times U(1)_{-2}\ . \tag{3.40}$$

Then the gauged WZW boundary condition corresponds to setting the CFT boundary con-

7. This is a consequence of the fact that Ising $\cong (SU(2)_1 \times SU(2)_1 \times SU(2)_{-2})/\mathbb{Z}_2$. Ungauging the $\mathbb{Z}_2$ by gauging the quantum zero-form symmetry allows us to write $SU(2)_1 \times SU(2)_1 \times SU(2)_{-2}$ in terms of Ising and a twisted $\mathbb{Z}_2$ gauge theory. Comparing the spectrum of the lines on both sides we can convince ourselves that such twisted $\mathbb{Z}_2$ gauge theory is $U(1)_2 \times U(1)_{-2}$.

dition on the Ising factor, but the topological boundary condition on the $U(1)_2 \times U(1)_{-2}$ factor, which explains both why not all lines end perpendicularly at the boundary, and why the spectrum of Ising is doubled. Thus we see that the $(G_k/H_{\tilde{k}})$ boundary on the one hand is similar to the CFT boundary condition in that the boundary is non-topological and there exists a subset of the bulk lines ending perpendicularly at the boundary such that their mutual braiding is non-trivial and the junctions at the end of the lines are non-topological. On the other hand, there also exists lines that generate topological junctions which have trivial mutual braiding. The gauged WZW boundary condition $(G_k/H_{\tilde{k}})$ is like the topological boundary condition in that the braiding of those lines ending perpendicularly is degenerate, but unlike the purely topological boundary, not maximally so. That is, the braiding matrix projected to those lines that can end perpendicularly at the boundary is degenerate, but with neither minimal nor maximal rank.

In hindsight, this explains why historically the naive proposal (3.32) led to a degenerate CFT with multiple vacua – since there are multiple topological junctions from the bulk– and degenerate modular S-matrix –since the braiding of the bulk lines ending at the boundary is degenerate–. Upon gauging Z in the bulk to obtain $(G_k \times H_{-\tilde{k}})/Z$ what we are doing is making those lines generating topological junctions transparent and identified with each other, so in the boundary the corresponding degeneracy is removed, and we find a standard 2D RCFT: that which the methods in the older literature provided via the "field identification" and "fixed point resolution" methods.

Application to Level-Rank Dualities

A well-known and important application of coset CFTs is to level-rank dualities of 3d TQFTs [7–9, 25–31]. Consider for instance the conformal embedding

$$SU(N)_k \times SU(k)_N \hookrightarrow SU(Nk)_1. \tag{3.41}$$

At the level of the branching rules (3.31), the embedding (3.41) means that the characters of $SU(Nk)_1$ can be expanded in terms of products of those of $SU(N)_k$ and $SU(k)_N$. We can then construct the coset CFT with single vacuum $(SU(Nk)_1/SU(N)_k)_Z$, and by the previous conformal embedding the result must be equivalent to the $SU(k)_N$ WZW theory. We have then the equivalence of chiral algebras

$$SU(k)_N \longleftrightarrow \left(\frac{SU(Nk)_1}{SU(N)_k}\right)_Z, \tag{3.42}$$

Expressing now both sides in terms of their bulk TQFTs we obtain the duality

$$SU(k)_N \cong \frac{SU(NK)_1 \times SU(N)_{-k}}{\mathbb{Z}_N}. \tag{3.43}$$

More generally, the logic of the above example is simply that if we find two different descriptions of the same chiral algebra either in terms of a WZW theory on one side, and a coset description on the other, or by relating two different coset descriptions on either sides, we can use the relationship between bulk and boundary to find dual descriptions of the same bulk TQFT.

In particular, we must take care to ensure that the vacuum degeneracy on both sides matches. Often we implicitly assume that all such degeneracy is removed, as in (3.43) by a suitable gauging. In familiar examples this is achieved by gauging a one-form symmetry in the bulk (the common center group), but in the examples to follow the required gauging will be more subtle.

3.3 Dualities via Non-Invertible Anyon Condensation

In the previous section, we have outlined how to construct (bosonic) dualities of 3D TQFTs by making clever use of the boundary theory and a proper understanding of the coset construction of 2D RCFTs. However, most of our discussion relied on the standard assumption [2]

that gauging the common center Z of $G_k \times H_{-\tilde{k}}$ is sufficient to find a CFT with a single vacuum. However, already in [2] it was observed that there are exceptions to the idea that gauging by an abelian common center Z in $G_k \times H_{-\tilde{k}}$ is sufficient to remove all boundary topological degrees of freedom and obtain a standard boundary CFT with a unique vacuum, as in the case of the conformal embeddings.

In the context of the GKO coset construction, it is also known that there are exceptions to the methods mentioned in footnote 2 to construct CFTs with single vacuum from the "naive" partition function (3.32). In these exceptions there are additional selection rules (i.e. vanishing branching functions) and field identifications that are not a consequence of group-theoretical selection rules and thus cannot be submitted to the "field identification method" [88] mentioned above to find a CFT with single vacuum and non-degenerate S-matrix. Importantly, again the conformal embeddings appear as part of such exceptions (see [5, 105]). We stress that if the conformal embedding has two factors in the denominator we mean the full quotient appears as an exception, and not a standard coset based on just one of the factors. Furthermore, it is known that a handful of gapless cosets also share this feature. In the literature, these cosets have been referred to as "Maverick cosets," and the known examples have been constructed long ago in [35, 36, 87, 105]. In some sense, Maverick cosets are then a hybrid in between the standard cosets and the conformal embeddings. To the extent of the authors' knowledge, there is no known classification of Maverick cosets.

The previous observations suggest that in order to understand these exceptions we must relax the assumption that the bulk is given by $G_k \times H_{-\tilde{k}}$ gauged by an abelian one-form symmetry Z. Indeed, in the past few years it has been understood that the notion of gauging can be extended to the case where the symmetries are not necessarily group-like [37, 51, 55, 62–67, 74, 75, 106–108] , and it is natural to explore the consequences of such generalized gauging in the present context. In the following discussion we will not need a rigorous presentation of non-abelian anyon condensation, and content ourselves with a

physical presentation. In Section 3.6.1 we present a summary of the rigorous statements that we use, and outline them in a physics nomenclature in the next subsection. More extensive treatments of non-abelian anyon condensation from a physics perspective may be found in [37, 52, 106, 107]. See [109] for a review.

To begin, it is instructive to study the example of the exceptional conformal embedding discussed briefly in Section 3.1.1, which shows the inevitability of non-abelian anyon condensation in the general construction of coset CFTs, and in particular the conformal embeddings. The example is given by the embedding

$$SU(2)_1 \times SU(2)_3 \hookrightarrow (G_2)_1. \tag{3.44}$$

In 2D CFT terms, this conformal embedding is translated to the following branching rules:

$$\chi_{\mathbf{1}}^{(G_2)_1} = \chi_0^{SU(2)_1}\,\chi_0^{SU(2)_3} + \chi_1^{SU(2)_1}\,\chi_3^{SU(2)_3}, \tag{3.45}$$

$$\chi_{\mathbf{7}}^{(G_2)_1} = \chi_0^{SU(2)_1}\,\chi_2^{SU(2)_3} + \chi_1^{SU(2)_1}\,\chi_1^{SU(2)_3}, \tag{3.46}$$

where we have labeled the integrable representations of $(G_2)_1$ by the dimensionality of the representation $\mathbf{R}$, and those of $SU(2)_k$ as standard by an integer $i = 0, \ldots, k$. The notation is analogous whenever we consider negative levels in TQFT.

These branching rules can be regarded in many forms. In the simplest scenario, we can consider the coset $(G_2)_1/SU(2)_1$, and the branching rules above show that the branching functions are the characters of $SU(2)_3$. Specifically, using the torus partition function for coset CFTs (3.32), we find

$$Z_{T^2}\left[\frac{(G_2)_1}{SU(2)_1}\right] = \left|\chi_0^{SU(2)_3}\right|^2 + \left|\chi_1^{SU(2)_3}\right|^2 + \left|\chi_2^{SU(2)_3}\right|^2 + \left|\chi_3^{SU(2)_3}\right|^2 = Z_{T^2}[SU(2)_3]. \tag{3.47}$$

The result is already an ordinary 2D CFT, with no vacuum degeneracy and a non-degenerate

modular S-matrix. Clearly, this means that there are no topological sectors to consider, and the coset theory is simply

$$(G_2)_1/SU(2)_1 = SU(2)_3. \tag{3.48}$$

More interestingly, we can consider the coset $(G_2)_1/SU(2)_3$, and then the branching rules (3.45)-(3.46) tell us to regard the characters of the $SU(2)_1$ theory as the branching functions in the corresponding coset decomposition. More precisely, using (3.32) again:

$$Z_{T^2}\left[\frac{(G_2)_1}{SU(2)_3}\right] = 2\left|\chi_0^{SU(2)_1}\right|^2 + 2\left|\chi_1^{SU(2)_1}\right|^2 = 2Z_{T^2}[SU(2)_1], \tag{3.49}$$

from which it is clear that now we do obtain a topological sector. However, notice that the group G_2 has trivial center, so we cannot possibly interpret the previous degeneracy in terms of some $\mathbb{Z}_2$ common center as in more standard description of cosets. Even more concretely, if we translate the previous observation to the associated 3D TQFTs, it is straightforward to check that $(G_2)_1 \times SU(2)_{-3}$ simply does not have an abelian anyon in its spectrum.[8]

The resolution of this puzzle is that while $(G_2)_1 \times SU(2)_{-3}$ has no abelian boson in its spectrum, it does have a non-abelian one consisting of the product of the line $\mathbf{7} \in (G_2)_1$ and the line $2 \in SU(2)_{-3}$. Moreover, this is the exact combination giving the additional topological local operator in the branching rules (3.46). Therefore, if this boson were to end on the boundary, it would explain the degeneracy above, and noticing that both $\mathbf{7} \in (G_2)_1$ and $2 \in SU(2)_3$ follow Fibonacci fusion rules, provides us with a natural guess for the topological sector present on top of the CFT sector:

$$(G_2)_1/SU(2)_3 = \mathbf{Fib}^{\text{TQFT}} \times SU(2)_1^{\text{CFT}} = \frac{(G_2)_1}{(G_2)_1} \times SU(2)_1^{\text{CFT}}. \tag{3.50}$$

Shortly, we will give a more rigorous derivation of this topological sector using level-rank

8. See Tables 3.1 and 3.2 later in this work to check this statement.

duality and studying choices of boundary conditions. In passing, if we follow this proposal, it is clear that we can label the states in the coset $(G_2)_1/SU(2)_3$ as $(0,i)$ and (ϕ,i), with fusion rules

$$(0,i)\times(0,j)=(0,i+j), \tag{3.51}$$

$$(0,i)\times(\phi,j)=(\phi,i+j), \tag{3.52}$$

$$(\phi,i)\times(\phi,j)=(0,i+j)+(\phi,i+j), \tag{3.53}$$

where $i,j=0,1$ labels the integrable representations in the $SU(2)_1$ CFT factor.

Gauging by the non-abelian boson in the bulk would then remove the topological sector on the boundary, leaving us only with the non-degenerate CFT sector. This is clearly what we would have naively expected from the branching rules; that is, the $SU(2)_1$ WZW theory. Concretely:

$$SU(2)_1 \cong \frac{(G_2)_1\times SU(2)_{-3}}{\mathcal{Z}(\mathbf{Fib})}. \tag{3.54}$$

Below in Section 3.4.1 we will verify this statement by a direct computation using non-abelian anyon condensation. Therefore, this is a situation where the coset RCFT lives at the boundary of a bulk TQFT whose only non-trivial boson is non-abelian. Correspondingly, to find the RCFT with single vacuum on the boundary (in this example $SU(2)_1$) we have to identify fields in the branching rules that are not related by some abelian action as in e.g., the case of the Ising model at the end of Section 3.2. In other words, to find the RCFT with single vacuum in the boundary we would have to gauge/condense the non-abelian boson in the bulk.

Generically then, gauging non-abelian anyons in the bulk leads to some RCFT in the boundary, which may however also appear as a boundary condition in a different-looking bulk TQFT. Matching these different descriptions to one another is one way to guess dualities

of TQFTs, which we may then verify directly as a statement solely in the context of 3D TQFTs.

Finally, one can also consider the full coset $\frac{(G_2)_1}{SU(2)_1 \times SU(2)_3}$, which is topological since the central charge vanishes. Indeed, computing the coset torus partition function (3.32), one obtains:

$$Z_{T^2}\left[\frac{(G_2)_1}{SU(2)_1 \times SU(2)_3}\right] = 4. \tag{3.55}$$

Using similar steps as above the concrete proposal for the 2D TQFT is:

$$\frac{(G_2)_1}{SU(2)_1 \times SU(2)_3} = \mathbf{Fib}^{\mathrm{TQFT}} \otimes \mathbb{Z}_2^{\mathrm{TQFT}} = \frac{(G_2)_1}{(G_2)_1} \otimes \frac{SU(2)_1}{SU(2)_1} \tag{3.56}$$

The previous discussion can also be derived by examining choices of boundary conditions implied by the TQFT duality:

$$(G_2)_1 \times SU(2)_{-1} \cong SU(2)_3, \tag{3.57}$$

where it is straightforward to see that the spectrum of lines match on both sides. This shows that we can set the canonical $SU(2)_3$ RCFT boundary condition in the product $(G_2)_1 \times SU(2)_{-1}$, which gives the coset result (3.47). On the other hand, we can take the orientation reversal of the previous duality and tensor the resulting expression by $(G_2)_1$ which allows us to write

$$(G_2)_1 \times SU(2)_{-3} \cong (G_2)_1 \times (G_2)_{-1} \times SU(2)_1. \tag{3.58}$$

Then, by this duality, in the bulk theory $(G_2)_1 \times SU(2)_{-3}$ we are allowed to take as a boundary condition a canonical $SU(2)_1$ RCFT boundary condition for the $SU(2)_1$ factor, but the purely topological boundary condition for the factor $(G_2)_1 \times (G_2)_{-1}$ given by the diagonal Lagrangian algebra. Recall this type of topological boundary is given by the G_k/G_k

2D TQFT, which has as many topological local operators as the G_k WZW theory has chiral primaries, with the same fusion rules as the G_k WZW theory. The possibility of choosing this "combined CFT-Topological" boundary condition explains both the degeneracy of two in the torus partition function (3.49) as well as the precise Fibonacci TQFT factor in (3.50), since $(G_2)_1$ has Fibonacci fusion rules.

Finally, we can tensor (3.58) by a $SU(2)_{-1}$ factor to find

$$(G_2)_1 \times SU(2)_{-1} \times SU(2)_{-3} \cong (G_2)_1 \times (G_2)_{-1} \times SU(2)_1 \times SU(2)_{-1}, \tag{3.59}$$

which allows us to set a purely topological boundary condition for $(G_2)_1 \times SU(2)_{-1} \times SU(2)_{-3}$ by choosing the purely topological boundary in both the $(G_2)_1 \times (G_2)_{-1}$ and $SU(2)_1 \times SU(2)_{-1}$ factors given by the corresponding diagonal Lagrangian algebras. Similarly, the duality explains the resulting 2D TQFT (3.56) in the coset $(G_2)_1/(SU(2)_1 \times SU(2)_3)$, and the corresponding torus partition function (3.55).

Now that we have convinced ourselves of the a priori generic appearance of non-abelian anyon condensation in the context of level-rank dualities, we will explore more examples where this phenomenon occurs. One such instance will be in the case of the conformal embeddings, as hinted above. In [37] it was suggested that the failure of the "field identification method" in the case of the Maverick cosets could be explained in terms of non-abelian anyon condensation, and we use this observation to propose dualities by first inspecting the resulting CFT, checking directly via non-abelian anyon condensation as a statement in the bulk TQFT, and then comparing different coset descriptions with the same TQFT data. Finally, a proper physical interpretation of certain mathematical results outlined in the next subsection will make manifest that non-abelian anyon condensation already appears even in standard examples of the coset construction, such as in the well-known coset description of the minimal models. We summarize the precise mathematical statements in Section 3.6.1.

Below in this section, we will first discuss in generality the main setup that describes

the interplay between dualities and non-abelian anyon condensation, and then we consider the concrete case of Maverick cosets since the underlying CFT (with single vacuum) is non-trivial and it is most straightforward to repeat the arguments pertaining to the case of gauging by an abelian one-form symmetry based on the boundary CFT. The case of the conformal embeddings is slightly more complicated, so we discuss them later in Section 3.5. Since they have vanishing central charge, it seems like applying analogous arguments would lead to a rather trivial duality with the empty theory. This is indeed correct, but certain mathematical arguments will allow us to find non-trivial dualities nevertheless.

3.3.1 The General Picture

To proceed further, we need to formalize the statements about the coset construction that we have used to convince ourselves of the general necessity of non-abelian condensation. The mathematical framework that we use that addresses such general scenario, and that is behind the results discussed in this subsection, corresponds to the formalism of local modules of special symmetric commutative Frobenius algebras described in [24]. To avoid a heavy mathematical digression, we summarize the definitions and results in this language in Section 3.6.1, and in this subsection we approach such results from a physical point of view.

The main point is to unpack the results of [24] in the language of non-invertible one-form symmetry gauging. According to this result, starting from the decomposition of an affine Lie algebra, or more generally, a chiral algebra described by a MTC $\mathcal{M}$ in terms of a smaller one described by a MTC $\mathcal{M}'$ (as in (3.31)) we can write

$$\mathcal{M} \cong (\mathcal{C} \times \mathcal{M}')/\mathcal{A}, \tag{3.60}$$

where $\mathcal{C}$ is the MTC describing the coset theory and the quotient by $\mathcal{A}$ stands for some one-form gauging that is not necessarily abelian, and under rather general conditions over $\mathcal{A}$

(see Section 3.6.1 for the more precise statement) we can "solve" for $\mathcal{C}$ and obtain the coset MTC in terms of $\mathcal{M}$ and $\mathcal{M}'$ as:

$$\mathcal{C} \cong (\mathcal{M} \times \overline{\mathcal{M}'})/\mathcal{B}, \tag{3.61}$$

for some new one-form gauging $\mathcal{B}$. The latter is what in the work of Moore and Seiberg [2] was identified as the common center of the affine Lie algebras. However, notice that from the current point of view we have no reason to believe that this is generally the case. Indeed, the conformal embeddings and Maverick cosets are explicit counterexamples to the common center rule, but they are still comfortably described by (3.61) when we allow for non-invertible anyon condensation.

The previous is the situation found more often, but when the general conditions over $\mathcal{A}$ are not strictly fulfilled a mild variation of the previous theorem still holds. Namely, there exist (generically non-invertible) one-form symmetries $\mathcal{T}_1$ and $\mathcal{T}_2$ such that:

$$\mathcal{C}/\mathcal{T}_1 \cong (\mathcal{M} \times \overline{\mathcal{M}'})/\mathcal{T}_2. \tag{3.62}$$

Essentially, what the conditions over $\mathcal{A}$ do is to ensure that the chiral algebra described by $\mathcal{C}$ in (3.60) already appears "extended," as otherwise the latter form of the theorem will perform the extension in any case.

We may consider our previous $SU(2)_1 \times SU(2)_3 \hookrightarrow (G_2)_1$ example from this point of view. Taking $\mathcal{M} = (G_2)_1$, we can take $\mathcal{M}'$ to be $SU(2)_1$ or $SU(2)_3$, with $\mathcal{C}$ the remaining factor. When $\mathcal{M}' = SU(2)_1$, $\mathcal{B}$ is trivial, and (3.61) reproduces (3.7). When $\mathcal{M}' = SU(2)_3$, however, the previous formalism allows $\mathcal{B}$ to be non-trivial and non-invertible. As a result, (3.61) readily reproduces (3.12), which we previously reproduced by cleverly manipulating the factors. Equations (3.60) and (3.61) represent the abstract form of such manipulations, and hold for general MTCs.

An Interesting Corollary

Now, we notice the following rather interesting corollary of Eqs. (3.60) and (3.61). That is, from the CFT perspective, (3.60) may be interpreted as the existence of some branching rules (3.31) for $\mathcal{M}$ in terms of the $\mathcal{M}'$ data. But on the TQFT perspective by itself, it means that not only we can obtain $\mathcal{C}$ in terms of $\mathcal{M}$ and $\mathcal{M}'$ via (3.61) –which is the standard form of the coset construction– but that we can write $\mathcal{M}$ in terms of the coset $\mathcal{C}$ and $\mathcal{M}'$ after some one-form symmetry gauging. The gauging is generically by a non-invertible symmetry, even if the gauging by $\mathcal{B}$ in (3.61) is abelian and given by the common center. Because of this inversion property between (3.60) and (3.61), we refer to such expressions as the "coset inversion formulas" or "coset inversion theorem" in the following.

To illustrate this coset inversion theorem, we may consider the standard coset description for minimal models $(SU(2)_k \times SU(2)_1 \times SU(2)_{-k-1})/\mathbb{Z}_2$. By the formulas above, we expect that $SU(2)_k \times SU(2)_1$ can be written in terms of the k-th minimal model as

$$SU(2)_k \times SU(2)_1 \cong \frac{M(k+3,k+2) \times SU(2)_{k+1}}{\mathcal{A}_k}, \tag{3.63}$$

for some generically non-invertible gauging $\mathcal{A}_k$, where $M(k+3,k+2)$ stands for the k-th minimal model with $k=1$ the Ising model. As a check, it is readily shown that the combination of the $(1,3)$ primary[9] in the $M(k+3,k+2)$ minimal model and the line in the adjoint representation in $SU(2)_{k+1}$ are such that $h_{1,3}^{M(k+3,k+2)} + h_2^{SU(2)_{k+1}} = k+1/(k+3)+2/(k+3) = 1$, so the product line for any k is a boson that is generically non-abelian. For $k=1$ the gauging on the right-hand side by this combination is a standard abelian $\mathbb{Z}_2$ gauging. However, already at $k=2$ it can be seen that the gauging generically involves a non-invertible boson. It is amusing to check that this is indeed the case –so that (3.63) holds– which we verify in Section 3.4.2 below by a direct computation on non-abelian anyon

9. As usual, we have denoted primaries in minimal models as pairs (r,s) in the Kac table [5].

condensation.

3.3.2 Maverick Cosets and Dualities

In this section we provide some explicit proposal of dualities involving non-abelian anyon condensation based on the many observations that we have made previously in this work. The case of the conformal embeddings is treated separately in Section 3.5.

In the following we will need the explicit expression for the Maverick cosets. The list of Maverick cosets known to date [35, 36, 87, 105] and their central charges is:

$$\frac{SU(k)_2}{Spin(k)_4}, \qquad c = \frac{2(k-1)}{k+2}, \tag{3.64}$$

$$\frac{Spin(2N)_2}{Spin(N)_2 \times Spin(N)_2}, \qquad c = 1, \tag{3.65}$$

$$\frac{(E_6)_2}{USp(16)_2}, \qquad c = 6/7, \tag{3.66}$$

$$\frac{(E_7)_2}{SU(8)_2}, \qquad c = 7/10, \tag{3.67}$$

$$\frac{(E_8)_2}{Spin(16)_2}, \qquad c = 1/2, \tag{3.68}$$

$$\frac{(E_8)_2}{SU(2)_2 \times (E_7)_2}, \qquad c = 7/10, \tag{3.69}$$

$$\frac{(E_7)_2}{SU(2)_2 \times Spin(12)_2}, \qquad c = 8/10, \tag{3.70}$$

$$\frac{SU(4)_1}{SU(2)_{10}}, \qquad c = 1/2, \tag{3.71}$$

$$\frac{Spin(7)_1}{SU(2)_{28}}, \qquad c = 7/10. \tag{3.72}$$

It is straightforward to check that for the Maverick cosets $G_k/H_{\tilde{k}}$ above there is indeed a

non-abelian boson in the spectrum of the associated $G_k \times H_{-\tilde{k}}$ TQFT.

First Family of Maverick Dualities

As a warm-up, let us start considering the simplest example of a Maverick coset corresponding to the $k = 3$ case in the first infinite family of Maverick cosets (3.48):

$$SU(3)_2/SU(2)_8, \tag{3.73}$$

where we have used the exceptional isomorphism of chiral algebras $Spin(3)_k = SU(2)_{2k}$ [8]. The central charge of such coset is $c = 4/5$ meaning it could in principle be the Tetracritical Ising Model or the three-state Potts model (TSPM). Fortunately, already in [35, 36] from an analysis of the branching rules it was noticed that the result actually corresponds to the TSPM, which is known to allow for other coset descriptions. For instance, $SU(2)_3/U(1)_6$, or $(SU(3)_1 \times SU(3)_1)/SU(3)_2$ are coset description that reproduce the TSPM [5].

Translating to TQFT then by the rules of [2], we observe that both of the standard cosets $SU(2)_3/U(1)_6$, or $(SU(3)_1 \times SU(3)_1)/SU(3)_2$ translate to the TQFTs

$$\frac{SU(2)_3 \times U(1)_{-6}}{\mathbb{Z}_2}, \quad \text{or} \quad \frac{SU(3)_1 \times SU(3)_1 \times SU(3)_{-2}}{\mathbb{Z}_3} \tag{3.74}$$

respectively, both of which are readily seen to match the spectrum of the TSPM after applying the three-step gauging procedure [2]. However, translating the Maverick coset version of the TSPM to TQFTs is not so straightforward. Obviously, $SU(3)_2 \times SU(2)_{-8}$ has too many lines to identify it by itself with the TSPM, so we must gauge some lines away in order to make them coincide. However, $SU(2)$ and $SU(3)$ have a trivial common center, so it does not seem possible to use the standard gauging procedure of [2] to do so. Notice that $SU(3)_2 \times SU(2)_{-8}$ does have a non-trivial abelian boson in its spectrum; namely $(\mathbf{1}, 8)$, [10]

10. Here and below we have used our notation of denoting a line in $SU(3)_2$ by the dimension of its

but gauging it gives $SU(3)_2 \times SO(3)_{-4}$, which is also does not match the spectrum of the TSPM.

The solution to this conundrum, of course, is that $SU(3)_2 \times SU(2)_{-8}$ has yet another non-trivial boson in its spectrum: $(\mathbf{8}, 4)$, and it is a non-abelian one! Clearly, we can now attempt to condense it in order to reproduce the spectrum of the TSPM. It goes without saying, the non-abelian anyon condensation calculation indeed reproduces the spectrum of the TSPM. The prior calculation was done in [37] as a test example of the formalism of non-abelian anyon condensation. Instead, later in Section 3.5.2 we will provide an alternative argument based on exceptional conformal embeddings that simplifies the calculation considerably, on top of relating quite directly this Maverick coset with conformal embeddings and the standard arguments for level-rank duality.

In summary, (3.73) and (3.74) are three different coset descriptions for the same underlying 3D TQFT (i.e., we have found three different Chern-Simons-like descriptions of the same underlying MTC data), two of which are rather standard and one which involves non-abelian anyon condensation. Since all of these descriptions describe the same underlying theory, we can now relate all the previous Chern-Simons-like descriptions of the TSPM to one another, obtaining the dualities:

$$\frac{SU(3)_2 \times SU(2)_{-8}}{\mathcal{A}_3} \cong \frac{SU(2)_3 \times U(1)_{-6}}{\mathbb{Z}_2} \cong \frac{SU(3)_1 \times SU(3)_1 \times SU(3)_{-2}}{\mathbb{Z}_3}, \tag{3.75}$$

where the first of these involves non-abelian anyon condensation by the algebra object $\mathcal{A}_3 = (\mathbf{1}, 0) + (\mathbf{1}, 8) + (\mathbf{8}, 4)$. Of course, starting with these expressions we can now attempt to "make the dualities proliferate" by gauging zero-form or one-form symmetries on either side, turning-on background fields possibly with discrete torsion, coupling to spin structure or combining these dualities with previously known ones, etc. We do not attempt this here, and we set it aside for future work.

representation in bold letters, and a line in $SU(2)_k$ by the standard integer $i = 0, 1, \ldots k$.

This example can be generalized to the complete first infinite family of Maverick cosets (3.64) noticing that the central charges match those of the parafermion CFTs [5, 81], so it is natural to suggest that this infinite Maverick family reproduces the parafermions. Indeed, the three-state Potts model corresponds to the $\mathbb{Z}_3$ parafermion, so we could have foreseen the previous results by merely matching the central charges to that of the parafermions.

The parafermions also have two standard coset descriptions given by the $SU(2)_k/U(1)_{2k}$, or $(SU(k)_1 \times SU(k)_1)/SU(k)_2$ cosets [5], which generalize the cosets of the TSPM above. Using the same arguments (although now with lack of a general calculation valid for any k), we expect the infinite family of dualities

$$\boxed{\frac{SU(k)_2 \times Spin(k)_{-4}}{\mathcal{A}_k} \cong \frac{SU(2)_k \times U(1)_{-2k}}{\mathbb{Z}_2} \cong \frac{SU(k)_1 \times SU(k)_1 \times SU(k)_{-2}}{\mathbb{Z}_k}}, \tag{3.76}$$

for some suitable algebra object $\mathcal{A}_k$ on the left-hand side. For $k = 3$ this reproduces the result for the TSPM above.

Second Family of Maverick Dualities

We study now the second infinite family of Maverick cosets (3.65). Since the value of the central charge is one there are now two natural possibilities for such infinite family: either an infinite family corresponding to the free boson branch of $c = 1$ RCFTs, or an infinite family corresponding to the orbifold branch of $c = 1$ RCFTs.

To decide for one of these families, we will have to perform an explicit calculation in the simplest case of the second infinite family of Maverick cosets (3.65), corresponding to $N = 3$. For the sake of presentation, we do not perform this calculation here but show this computation in Section 3.4.3 below. The calculation shows that for $N = 3$, the result of the non-abelian anyon condensation is actually the orbifold of $U(1)_6$, which we denote $U(1)_6^{\mathrm{Orb}}$. Based on this result, we conjecture that after some condensation of non-abelian

bosons, the first infinite family of Maverick cosets leads to the orbifold branch of $c = 1$ RCFTs. This suggests the following dualities between theories at the orbifold branch and Chern-Simons-like theories based on Spin groups:

$$\boxed{U(1)^{\text{Orb}}_{2N} \cong \frac{Spin(2N)_2 \times Spin(N)_{-2} \times Spin(N)_{-2}}{\mathcal{B}_N}} \tag{3.77}$$

for some suitable algebras $\mathcal{B}_N$. The case we will verify explicitly below corresponds to $N = 3$, and it is straightforward to check that in the cases $N = 1$ and $N = 2$ the formula still holds.

A quick argument in support of the previous proposal that does not rely on going through the whole computation in Section 3.4.3 is given as follows. We can use the exceptional isomorphisms of chiral algebras

$$Spin(3)_k \cong SU(2)_{2k}\,, \tag{3.78}$$

$$Spin(4)_k \cong SU(2)_k \times SU(2)_k\,, \tag{3.79}$$

$$Spin(6)_k \cong SU(4)_k, \tag{3.80}$$

to massage the expression for the Maverick coset (3.65) at $N = 3$ in the following way:

$$Spin(6)_2 \times Spin(3)_{-2} \times Spin(3)_{-2} \cong SU(4)_2 \times SU(2)_{-4} \times SU(2)_{-4} \tag{3.81}$$

$$\cong SU(4)_2 \times Spin(4)_{-4}. \tag{3.82}$$

That is, using the exceptional isomorphisms of chiral algebras we have written the Maverick coset (3.65) at $N = 3$ as the Maverick coset in the first infinite Maverick family (3.64) at $k = 4$. This is the next example in such family after the TSPM at $k = 3$ studied above.

Let us assume now that the first infinite family of Maverick cosets (3.64) is given by the parafermion CFTs, as pointed out above. Then, the $\mathbb{Z}_4$ parafermion can actually be

identified with the $U(1)_6^{\text{Orb}}$ orbifold CFT [5], and we have the explicit result

$$U(1)_6^{\text{Orb}} \cong \frac{SU(4)_2 \times Spin(4)_{-4}}{\mathcal{A}_4} \cong \frac{Spin(6)_2 \times Spin(3)_{-2} \times Spin(3)_{-2}}{\mathcal{B}_3}, \tag{3.83}$$

for some appropriate algebra objects $\mathcal{A}_4 \cong \mathcal{B}_3$. In Section 3.4.3 below we will verify this statement by a direct computation on non-abelian anyon condensation. Naturally, since this specific case turns out to be a parafermion, we can actually further identify (3.83) with the other Chern-Simons-like expressions on Eqn. (3.76) for $k = 4$.

Isolated Maverick Dualities

We now study a few of the isolated Maverick cosets (3.66)-(3.72), all of which have $c < 1$ and thus correspond to some (possibly non-diagonal) minimal model. The simplest of these is an interesting example leading to the Ising TQFT:

$$\text{Ising TQFT} \cong \frac{SU(4)_1 \times SU(2)_{-10}}{\mathcal{A}}, \tag{3.84}$$

for some appropriate algebra object $\mathcal{A}$. We verify this example by a direct computation in Section 3.6.2. The Maverick coset (3.68) similarly leads to the Ising model and can also be checked by an explicit calculation.

Minimal models, and in particular the Ising model, have many (standard) coset descriptions. Using these many descriptions, and equating them to the Maverick result above we obtain many instances of dualities involving a gauging by a non-invertible symmetry. Explicitly, for instance:

$$\begin{aligned}\frac{SU(4)_1 \times SU(2)_{-10}}{\mathcal{A}} &\cong \frac{(E_8)_2 \times Spin(16)_{-2}}{\mathcal{A}'} \cong \frac{SU(2)_1 \times SU(2)_1 \times SU(2)_{-2}}{\mathbb{Z}_2} \\ \cong &\frac{SU(2)_2 \times U(1)_{-4}}{\mathbb{Z}_2} \cong (E_8)_1 \times (E_8)_1 \times (E_8)_{-2} \cong \frac{USp(4)_1 \times SU(2)_{-1} \times SU(2)_{-1}}{\mathbb{Z}_2},\end{aligned} \tag{3.85}$$

for some appropriate algebra objects $\mathcal{A}$ and $\mathcal{A}'$.

We can play a similar strategy with the Tricritical Ising TQFT, which also has many (standard) coset descriptions as well as three Maverick descriptions, (3.67), (3.69), and (3.72). Following the same steps, we obtain:

$$\begin{aligned}
&\frac{Spin(7)_1 \times SU(2)_{-28}}{\mathcal{A}} \cong \frac{(E_8)_2 \times SU(2)_{-2} \times (E_7)_{-2}}{\mathcal{A}'} \cong \frac{(E_7)_2 \times SU(8)_{-2}}{\mathcal{A}''} \\
\cong &\frac{SU(2)_2 \times SU(2)_1 \times SU(2)_{-3}}{\mathbb{Z}_2} \cong \frac{(E_7)_1 \times (E_7)_1 \times (E_7)_{-2}}{\mathbb{Z}_2} \cong (F_4)_1 \times Spin(9)_{-1}, \\
\cong &\frac{USp(6)_1 \times USp(4)_{-1} \times SU(2)_{-1}}{\mathbb{Z}_2} \cong \frac{SU(3)_2 \times SU(2)_{-2} \times U(1)_{-12}}{\mathbb{Z}_6},
\end{aligned} \tag{3.86}$$

for some appropriate algebra objects $\mathcal{A}$, $\mathcal{A}'$, $\mathcal{A}''$. The last case is notable since the gauging is by an abelian anyon, but it cannot be interpreted as a common center. Rather it is a quantum one-form symmetry present due to the specific Chern-Simons levels.

3.4 Explicit Checks via Non-Abelian Anyon Condensation

In this section, we present a detailed description of some computations involving non-abelian anyon condensation, specifically with the aim of providing a non-trivial check of the dualities claimed above.

First, we summarize some consistency conditions that will allow us to pin down the resulting theory after non-abelian anyon condensation. We follow the heuristic rules of [37] for this purpose. Non-abelian anyon condensation was formalized in [52], but the rules of [37] are more useful for practical calculations. Following the logic of the three-step gauging procedure reviewed in Section 3.1, we aim to obtain the spectrum and topological spins of the anyons in the gauged theory without working out the full MTC data. The rules of [37] enable this approach. In successive subsections, we consider many explicit examples of interest. In the following, we refer as *parent theory* to the original theory before condensation/gauging,

and as *child theory* to the one obtained after condensation/gauging. For obvious reasons, we also refer to the parent and child as uncondensed and condensed theories, respectively. As in the case of standard gaugings of abelian anyons (one-form global symmetries) only bosons can condense, paralleling the fact that for abelian anyons the topological spins capture the 't Hooft anomalies [6, 10, 34].[11]

When we perform anyon condensation, the simple anyons of the parent theory are generically split into many terms associated with excitations in the child theory:

$$a \longrightarrow \sum_i n_i^a a_i, \quad {n_i}^c \in \mathbb{N}. \tag{3.87}$$

It is useful at this intermediate stage to distinguish between genuine line operators, and non-genuine line operators which necessarily arise at the end of topological surface operators [110]. Below we often refer to genuine line operators as unconfined excitations, and non-genuine line operators as confined. Shortly we will see how to differentiate between confined excitations and unconfined ones on the right-hand side of a restriction.

The labels a_i on the right-hand side of (3.87) do not necessarily correspond to genuine line operators in the child, and furthermore, many labels a_i corresponding to different anyons a in the parent theory do not necessarily correspond to different excitations in the child theory. Below we will write certain consistency conditions for non-abelian anyon condensation, and imposing such conditions may imply identifications between these many labels. In the following, we will refer to the decomposition (3.87) as *the restriction of the anyon* a.[12]

We call the different elements a_i on the right-hand side of the restriction (3.87) the

11. Relatedly, commutative algebras in a MTC decompose necessarily in terms of simple anyons with trivial topological spin. In particular then, special symmetric commutative Frobenius algebras decompose in terms of simple anyons with trivial topological spin.

12. In this context, some references refer to the splitting $a \to \sum_i {n_i}^a a_i$ as "branching". We avoid this terminology to prevent confusion with the *a priori* different concept of branching rules of affine Lie algebras.

components of the anyon a in the parent theory. When an anyon a restricts to a single label with unit multiplicity on the right-hand side (i.e., it does not "split"), we abuse notation and call the corresponding component on the right-hand side a as well. When the latter happens, the corresponding (non-necessarily genuine) line operator in some sense "descends trivially" from the parent theory. We adopt the previous nomenclature in the next subsections.

We assume that when we condense non-abelian anyons, the resulting theory has fusion rules fulfilling the following standard requirements: associativity, existence of a unique vacuum, and existence of unique conjugate representations with a unique way to annihilate to the vacuum. Additionally, condensation is subject to the following rules [37]:

1) A sector that condenses has a component that is indistinguishable from the vacuum sector in the condensed phase. Specifically:

$$c \longrightarrow (c_1 \equiv 0) + \sum_{i>1} {n_i}^c c_i, \quad {n_i}^c \in \mathbb{N}, \tag{3.88}$$

where we assume the vacuum component to have multiplicity one.

2) We require fusion of the old and new labels to be compatible with the restriction, i.e., restricting to the resulting theory and fusion must commute:

$$a \times b = \sum_c N_{ab}^c c \Longrightarrow \Big(\sum_i {n_i}^a a_i\Big) \times \Big(\sum_j {n_j}^b b_j\Big) = \sum_{c,k} N_{ab}^c {n_k}^c c_k. \tag{3.89}$$

Additionally, if a and $\bar{a}$ are conjugates to each other in the parent:

$$a \longrightarrow \sum_i {n_i}^a a_i \Longrightarrow \bar{a} \longrightarrow \sum_i {n_i}^a \bar{a}_i. \tag{3.90}$$

In order for these compatibility conditions to hold, it may be necessary to identify two different labels a_i and b_j on the right sides of the restrictions of two anyons a and b in the parent.

As a consequence of these assumptions the quantum dimensions are preserved under restriction:

$$a \longrightarrow \sum_b n_b{}^a b \Longrightarrow d_a = \sum_b n^a{}_b d_b, \tag{3.91}$$

which will be a crucial tool below when doing explicit computations.

3) Confined and deconfined excitations c_i are distinguished by their lift to anyons c in the parent theory. If the set of all the components that we identify to a certain c_i lift to anyons in the parent theory that do not all have the same topological spin, the corresponding c_i confines and thus it does not correspond to a simple object in the MTC data describing the condensed theory.

3.4.1 Checking the $SU(2)_1 \cong \big((G_2)_1 \times SU(2)_{-3}\big)/\mathcal{Z}(\mathbf{Fib})$ *Duality*

In this first check we analyze the straightforward example described in Section 3.1.1 and Section 3.3 through direct, in-depth computation of non-abelian anyon condensation.

The spectra of $(G_2)_1$ and $SU(2)_3$ are given in Tables 3.1 and 3.2 respectively. We call ϕ the only non-trivial anyon of $(G_2)_1$, which obeys Fibonacci fusion rules. $SU(2)_k$ for general k consists of $k+1$ lines labeled from 0 to k, and with fusion rules given by

$$\Lambda_1 \times \Lambda_2 = \sum_{\Lambda=|\Lambda_1-\Lambda_2|}^{\min(\Lambda_1+\Lambda_2,2k-\Lambda_1-\Lambda_2)} \Lambda, \tag{3.92}$$

where the sum is restricted such that $\Lambda_1 + \Lambda_2 - \Lambda$ is even. We denote the lines in $(G_2)_1 \times SU(2)_{-3}$ in the obvious way: $(0,i)$ and (ϕ,i) with $i = 0,1,2,3$.

It is easy to check that there is only one non-trivial boson $(\phi,2)$ in the spectrum of $(G_2)_1 \times SU(2)_{-3}$, and it is non-abelian. Let us assume that such anyon can condense, which is the statement that

$$(\phi,2) \longrightarrow 0 + (\phi,2)_2, \quad d_{(\phi,2)_2} = \frac{1+\sqrt{5}}{2}. \tag{3.93}$$

$(G_2)_1$		
Line label	Quantum Dimension	Conformal Weight
0	$d_0 = 1$	$h_0 = 0$
ϕ	$d_\phi = \frac{1+\sqrt{5}}{2}$	$h_\phi = 2/5$

Table 3.1: $(G_2)_1$ data. In the table and in the text ϕ denotes the unique non-trivial line of $(G_2)_1$ with Fibonacci fusion rule $\phi \times \phi = 0 + \phi$.

The simplest way to see that on top of 0 there must be a single further label on the right-hand side of (3.93) is to check the conservation of the quantum dimension. Since $d_0 = 1$, the remaining quantum dimension is $\frac{1+\sqrt{5}}{2}$, which is too small to allow a splitting. For future reference, another method to check that only a single line is allowed on top of 0 in (3.93) is to inspect the fusion of $(\phi, 2)$ with itself:

$$(\phi, 2) \times (\phi, 2) = (0, 0) + (0, 2) + (\phi, 0) + (\phi, 2) \longrightarrow 0 + 0 + \ldots, \tag{3.94}$$

where the arrow means that we have taken the restriction of the anyons on the right-hand side of the equality, and since $(\phi, 2)$ condenses, a vacuum arises on the right-hand side. This means that we need $(\phi, 2)$ to split into two components on the left-hand side. Since one of them is the vacuum 0 by assumption, the other one must be a single line with quantum dimension $\frac{1+\sqrt{5}}{2}$. Furthermore, since the vacuum 0 is self-conjugate, we deduce that $(\phi, 2)_2$ must also be self-conjugate.

We also observe that all anyons of the form $(0, i)$ cannot split, since they do not have large enough quantum dimension. Similarly, the anyons $(\phi, 0)$ and $(\phi, 3)$ cannot split.

$SU(2)_3$		
Line label	Quantum Dimension	Conformal Weight
0	$d_0 = 1$	$h_0 = 0$
1	$d_1 = \frac{1+\sqrt{5}}{2}$	$h_1 = 3/20$
2	$d_2 = \frac{1+\sqrt{5}}{2}$	$h_2 = 2/5$
3	$d_3 = 1$	$h_3 = 3/4$

Table 3.2: $SU(2)_3$ data.

We can deduce the fate of $(\phi, 2)_2$ upon condensation by studying its fusion with $(0, 2)$:

$$(0, 2) \times (\phi, 2) = (\phi, 0) + (\phi, 2) \longrightarrow 0 + \ldots \tag{3.95}$$

This implies that $(0, 2)$, which we already deduced does not split, is conjugate with one component of $(\phi, 2)$. But $(0, 2)$ is self-conjugate and it cannot be identified with the vacuum, since it has neither the appropriate quantum dimension, nor the spin to condense. Therefore, we must identify $(0, 2) \cong (\phi, 2)_2$. Now, note that $(\phi, 2)_2$ lifts to $(\phi, 2)$ while $(0, 2)$ in the child theory lifts to $(0, 2)$ in the parent theory, but $(0, 2)$ and $(\phi, 2)$ have different topological spins, so it follows that $(0, 2) \cong (\phi, 2)_2$ confine. A completely analogous argument shows that $(\phi, 0)$ belongs in the restriction of $(\phi, 2)$ and we have the identification $(\phi, 0) \cong (\phi, 2)_2 \cong (0, 2)$.

Since $(\phi, 1)$ has sufficient quantum dimension to split we must check if it does. Computing its self-fusion:

$$(\phi, 1) \times (\phi, 1) = (0, 0) + (0, 2) + (\phi, 0) + (\phi, 2) \longrightarrow 0 + 0 + \ldots, \tag{3.96}$$

we deduce that it splits into two components $(\phi, 1) \to (\phi, 1)_1 + (\phi, 1)_2$.

Now that we know the splitting pattern we have to assign quantum dimensions. It is straightforward to check that

$$(\phi, 3) \times (\phi, 1) = (0, 2) + (\phi, 2) \longrightarrow 0 + \ldots, \tag{3.97}$$

implies that $(\phi, 3)$ belongs in the restriction of $(\phi, 1)$ since $(\phi, 3)$ is self-conjugate, and since $d_{(\phi,3)} = (1 + \sqrt{5})/2$, by conservation of the quantum dimension it must be that the other component of $(\phi, 1)$ has unit quantum dimension. That is, $d_{(\phi,1)_1} = (1+\sqrt{5})/2$ and $d_{(\phi,1)_2} = 1$.

From the fusions

$$(0,1)\times(\phi,1)=(\phi,0)+(\phi,2)\longrightarrow 0+\ldots, \tag{3.98}$$

$$(0,3)\times(\phi,1)=(\phi,2)\longrightarrow 0+\ldots, \tag{3.99}$$

we deduce by similar arguments as above that $(0,1),(0,3)\in(\phi,1)$. From the quantum dimensions $d_{(0,1)}=(1+\sqrt{5})/2$ and $d_{(0,3)}=1$ we obtain that there is a single way to fit $(0,1)$ and $(0,3)$ in the restriction of $(\phi,1)$, implying the identifications $(\phi,3)\cong(\phi,1)_1\cong(0,1)$ and $(\phi,1)_2\cong(0,3)$.

All in all, we obtain the condensation pattern:

$$(0,0)\to(0,0),\quad (0,1)\to(0,1),\quad (0,2)\to(0,2),\quad (0,3)\to(0,3),$$

$$(\phi,0)\to(0,2),\quad (\phi,1)\to(0,1)+(0,3),\quad (\phi,2)\to 0+(0,2),\quad (\phi,3)\to(0,1),$$

from which it is straightforward to check that only $(0,0)$ and $(0,3)$ lift to anyons in the parent that have common topological spin and thus do not confine. They also have the correct fusion rules, spins and quantum dimensions to match those of $SU(2)_1$, as expected.

3.4.2 Checking the $SU(2)_1\times SU(2)_2\cong\big(M(5,4)\times SU(2)_3\big)/\mathcal{A}$ Duality

In this subsection we check the coset inversion formulas (3.60)-(3.61) observed on mathematical grounds in Section 3.3.1. Specifically we consider the example given in Eqn. (3.63), and check that

$$SU(2)_k\times SU(2)_1\cong\frac{M(k+3,k+2)\times SU(2)_{k+1}}{\mathcal{A}},\quad k\geq 1, \tag{3.100}$$

Tricritical Ising Model $M(5,4)$		
Line label	Quantum Dimension	Conformal Weight
0	$d_0 = 1$	$h_0 = 0$
ε	$d_\varepsilon = \frac{1+\sqrt{5}}{2}$	$h_\varepsilon = 1/10$
ε'	$d_{\varepsilon'} = \frac{1+\sqrt{5}}{2}$	$h_{\varepsilon'} = 3/5$
ε''	$d_{\varepsilon''} = 1$	$h_{\varepsilon''} = 3/2$
σ	$d_\sigma = \sqrt{2}\left(\frac{1+\sqrt{5}}{2}\right)$	$h_\sigma = 3/80$
σ'	$d_{\sigma'} = \sqrt{2}$	$h_{\sigma'} = 7/16$

Table 3.3: Data of the Tricritical Ising Model.

in the case $k = 2$. When $k = 1$ the gauging is abelian and the expression is easily checked by the three-step gauging rule [2, 34]. The case $k = 2$ is more interesting, since the gauging is by a non-invertible one-form symmetry.

When $k = 2$, $M(5, 4)$ corresponds to the Tricritical Ising Model, whose spectrum can be found in Table 3.3. Its non-trivial fusion rules are

$$\varepsilon'' \times \varepsilon'' = 0, \qquad \varepsilon'' \times \varepsilon' = \varepsilon, \qquad \varepsilon'' \times \varepsilon = \varepsilon', \quad \varepsilon'' \times \sigma = \sigma, \quad \varepsilon'' \times \sigma' = \sigma', \tag{3.101}$$

$$\varepsilon' \times \varepsilon' = 0 + \varepsilon', \qquad \varepsilon' \times \varepsilon = \varepsilon + \varepsilon'', \quad \varepsilon' \times \sigma = \sigma + \sigma', \quad \varepsilon' \times \sigma' = \sigma, \tag{3.102}$$

$$\varepsilon \times \varepsilon = 0 + \varepsilon', \qquad \varepsilon' \times \sigma = \sigma + \sigma', \quad \varepsilon \times \sigma' = \sigma, \tag{3.103}$$

$$\sigma \times \sigma = 0 + \varepsilon + \varepsilon' + \varepsilon'', \quad \sigma \times \sigma' = \varepsilon + \varepsilon', \quad \sigma' \times \sigma' = 0 + \varepsilon''. \tag{3.104}$$

Meanwhile, the spectrum of $SU(2)_3$ and that of the expected result $SU(2)_1 \times SU(2)_2$ are shown in tables 3.2 and 3.4 respectively. Their fusion rules are easily derived from Eqn. (3.92). In the following we denote the anyons in the obvious way as in the product $M(5, 4) \times SU(2)_3$.

We start noticing that in the product $M(5, 4) \times SU(2)_3$ there is a single boson $(\varepsilon', 2)$,

and it is non-abelian. Then, condensing $(\varepsilon', 2)$ is the statement that we have the splitting

$$(\varepsilon', 2) \to 0 + (\varepsilon', 2)_2, \tag{3.105}$$

with $d_{(\varepsilon',2)_2} = (1+\sqrt{5})/2$ by conservation of the quantum dimension, so $(\varepsilon', 2)$ cannot split further.

Now notice that the following pairs of anyons

$$\begin{aligned} &\{(0,0),(\varepsilon',2)\}, \quad \{(\varepsilon'',3),(\varepsilon,1)\}, \quad \{(\sigma',3),(\sigma,1)\}, \\ &\{(\sigma',0),(\sigma,2)\}, \quad \{(\varepsilon'',0),(\varepsilon,2)\}, \quad \{(0,3),(\varepsilon',1)\} \end{aligned} \tag{3.106}$$

share the same topological spins as the anyons in $SU(2)_1 \times SU(2)_2$, respectively in the same order as shown in Table 3.4. Based on this observation, consider the second pair $\{(\varepsilon'', 3), (\varepsilon, 1)\}$ (since the first pair is basically the condensing boson), and study the fusion rules in this pair:

$$(\varepsilon, 1) \times (\varepsilon, 1) = (0,0) + (0,2) + (\varepsilon', 0) + (\varepsilon', 2) \longrightarrow 0 + 0 + \ldots \tag{3.107}$$

$$(\varepsilon'', 3) \times (\varepsilon, 1) = (\varepsilon', 2) \longrightarrow 0. \tag{3.108}$$

$SU(2)_2 \times SU(2)_1$		
Line label	Quantum Dimension	Conformal Weight
(0,0)	$d_{(0,0)} = 1$	$h_{(0,0)} = 0$
(0,1)	$d_{(0,1)} = 1$	$h_{(0,1)} = 1/4$
(1,0)	$d_{(1,0)} = \sqrt{2}$	$h_{(1,0)} = 3/16$
(1,1)	$d_{(1,1)} = \sqrt{2}$	$h_{(1,1)} = 7/16$
(2,0)	$d_{(2,0)} = 1$	$h_{(2,0)} = 1/2$
(2,1)	$d_{(2,1)} = 1$	$h_{(2,1)} = 3/4$

Table 3.4: $SU(2)_2 \times SU(2)_1$ Data

The first fusion rule tells us that $(\varepsilon, 1)$ splits in two, while the second one implies that $(\varepsilon'', 3) \in (\varepsilon, 1)$. So, we have the splitting

$$(\varepsilon, 1) \to (\varepsilon'', 3) + (\varepsilon, 1)_2. \tag{3.109}$$

Using the same arguments, same conclusions follow for each of the pairs mentioned above; namely, the second anyon in a pair splits in two, and one of its components corresponds to the first anyon in the same pair.

Checking for confinement given this structure is now easy. Take for example the anyons $(\varepsilon', 0)$ and $(0, 2)$ and consider their fusion with $(\varepsilon', 2)$:

$$(\varepsilon', 0) \times (\varepsilon', 2) = (0, 2) + (\varepsilon', 2) \longrightarrow 0 + \ldots, \tag{3.110}$$

$$(0, 2) \times (\varepsilon', 2) = (\varepsilon', 0) + (\varepsilon', 2) \longrightarrow 0 + \ldots. \tag{3.111}$$

This means that $(\varepsilon', 0), (0, 2) \in (\varepsilon', 2)$, and it is easy to see that there is only one way to match quantum dimensions with the restriction (3.105). We must have the identification

$$(0, 2) \cong (\varepsilon', 0) \cong (\varepsilon', 2)_2. \tag{3.112}$$

Clearly, all these excitations lift to anyons of different topological spin in the parent theory, so we deduce their confinement in the child theory.

A similar argument runs for the remaining excitations. That is, for any anyon not listed in (3.106) we can find an anyon that appears second in a pair of (3.106) such that from their fusion we can deduce that the former anyon belongs in the restriction of the latter anyon. This implies the confinement of all excitations, except for those that appear in the first entry of the pairs in (3.106), which exactly matches the spectra of $SU(2)_2 \times SU(2)_1$ shown in Table 3.4, as desired.

$SU(4)_2$		
Line label	Quantum Dimension	Conformal Weight
$\mathbf{1}$	$d_{\mathbf{1}} = 1$	$h_{\mathbf{1}} = 0$
$\overline{\mathbf{10}}$	$d_{\overline{\mathbf{10}}} = 1$	$h_{\overline{\mathbf{10}}} = 3/4$
$\mathbf{20'}$	$d_{\mathbf{20'}} = 1$	$h_{\mathbf{20'}} = 1$
$\mathbf{10}$	$d_{\mathbf{10}} = 1$	$h_{\mathbf{10}} = 3/4$
$\overline{\mathbf{4}}$	$d_{\overline{\mathbf{4}}} = \sqrt{3}$	$h_{\overline{\mathbf{4}}} = 5/16$
$\mathbf{20}$	$d_{\mathbf{20}} = \sqrt{3}$	$h_{\mathbf{20}} = 13/16$
$\overline{\mathbf{20}}$	$d_{\overline{\mathbf{20}}} = \sqrt{3}$	$h_{\overline{\mathbf{20}}} = 13/16$
$\mathbf{4}$	$d_{\mathbf{4}} = \sqrt{3}$	$h_{\mathbf{4}} = 5/16$
$\mathbf{15}$	$d_{\mathbf{15}} = 2$	$h_{\mathbf{15}} = 2/3$
$\mathbf{6}$	$d_{\mathbf{6}} = 2$	$h_{\mathbf{6}} = 5/12$

Table 3.5: $SU(4)_2$ data.

3.4.3 Checking the $U(1)_6^{\mathrm{Orb}} \cong (SU(4)_2 \times Spin(4)_{-4})/\mathcal{A}$ Duality

This is an important example of a Maverick coset which we will verify upon non-invertible anyon condensation gives a theory on the orbifold branch of $c = 1$ theories; namely, the orbifold of the $U(1)_6$ free boson, which we denote $U(1)_6^{\mathrm{Orb}}$. This allows us to write the following Maverick duality of Chern-Simons-like theories:

$$U(1)_6^{\mathrm{Orb}} \cong \frac{SU(4)_2 \times Spin(4)_{-4}}{\mathcal{B}_3}, \tag{3.113}$$

for some appropriate gauging by an algebra object $\mathcal{B}_3$ that we write below. This example was studied in Section 3.3.2 above, as the first example in the second infinite family (3.65) of Maverick cosets.

To check this example, we follow similar manipulations as in previous examples. The spectrum of $SU(4)_2$ is shown in Table 3.5, and the subset of the fusion rules that we will use below can be described as follows. The line $\mathbf{10}$ generates a $\mathbf{Z}_4$ symmetry such that we have the orbits

$$\mathbf{10}^2 = \mathbf{20'}, \quad \mathbf{10}^3 = \overline{\mathbf{10}}, \quad \mathbf{10} \times \mathbf{15} = \mathbf{6}, \quad \mathbf{10} \times \mathbf{6} = \mathbf{15}, \tag{3.114}$$

$$\mathbf{10} \times \mathbf{4} = \overline{\mathbf{20}}, \quad \mathbf{10} \times \overline{\mathbf{20}} = \mathbf{20}, \quad \mathbf{10} \times \mathbf{20} = \overline{\mathbf{4}}, \quad \mathbf{10} \times \overline{\mathbf{4}} = \mathbf{4}. \tag{3.115}$$

The line **15** will be important and is such that

$$\mathbf{15} \times \mathbf{15} = \mathbf{1} + \mathbf{15} + \mathbf{20'}. \tag{3.116}$$

Finally, we will also need the fusion

$$\mathbf{4} \times \overline{\mathbf{4}} = \mathbf{1} + \mathbf{15}. \tag{3.117}$$

Other fusion rules may be found using the Kac software program [111]. The spectrum of $SU(2)_4$ is shown in Table 3.6, whose fusion rules can be read-off from Eqn. (3.92). In this subsection we write $(\mathbf{R}, i, j)$ where $\mathbf{R}$ labels the line in representation $\mathbf{R}$ of $SU(4)$, and the $i, j = 0, \ldots, 4$ labels the corresponding line in the $SU(2)_{-4}$ factor. The **10**, **20′**, and $\overline{\mathbf{10}}$ act as simple currents, so if we understand the fate of $(\mathbf{1}, i, j)$, $(\mathbf{15}, i, j)$, and $(\mathbf{4}, i, j)$ upon gauging/condensation we can deduce the rest by acting with such simple currents. For future reference, the spectrum of $U(1)_6^{\text{Orb}}$ is presented in Table 3.7.

In the product $SU(4)_2 \times SU(2)_{-4} \times SU(2)_{-4}$ we have a set of eight abelian bosons

$$(\mathbf{1}, 0, 0), \qquad (\mathbf{1}, 0, 4), \qquad (\mathbf{1}, 4, 0), \qquad (\mathbf{1}, 4, 4),$$

$SU(2)_4$		
Line label	Quantum Dimension	Conformal Weight
0	$d_0 = 1$	$h_0 = 0$
1	$d_1 = \sqrt{3}$	$h_1 = 1/8$
2	$d_2 = 2$	$h_2 = 1/3$
3	$d_3 = \sqrt{3}$	$h_3 = 5/8$
4	$d_4 = 1$	$h_4 = 1$

Table 3.6: $SU(2)_4$ data.

$U(1)_6^{\mathrm{Orb}}$		
Line label	Quantum Dimension	Conformal Weight
0	$d_0 = 1$	$h_0 = 0$
1	$d_1 = 1$	$h_1 = 3/4$
2	$d_2 = 1$	$h_2 = 1$
3	$d_3 = 1$	$h_3 = 3/4$
4	$d_4 = 2$	$h_4 = 1/12$
5	$d_5 = 2$	$h_5 = 1/3$
6	$d_6 = \sqrt{3}$	$h_6 = 1/16$
7	$d_7 = \sqrt{3}$	$h_7 = 9/16$
8	$d_8 = \sqrt{3}$	$h_8 = 9/16$
9	$d_9 = \sqrt{3}$	$h_9 = 1/16$

Table 3.7: $U(1)_6^{\mathrm{Orb}}$ data.

$$(\mathbf{20'}, 0, 0), \qquad (\mathbf{20'}, 0, 4), \qquad (\mathbf{20'}, 4, 0), \qquad (\mathbf{20'}, 4, 4),$$

and a set of five non-abelian bosons

$$(\mathbf{10}, 1, 3), \quad (\mathbf{10}, 3, 1), \quad (\bar{\mathbf{10}}, 1, 3), \quad (\bar{\mathbf{10}}, 3, 1), \quad (\mathbf{15}, 2, 2). \tag{3.118}$$

We first show that $(\mathbf{10}, 1, 3)$ cannot condense. To show this let us assume it does and find an inconsistency. Consider the fusion

$$(\mathbf{10}, 1, 3) \times (\bar{\mathbf{10}}, 1, 3) = (\mathbf{1}, 0, 0) + (\mathbf{1}, 0, 2) + (\mathbf{1}, 2, 0) + (\mathbf{1}, 2, 2), \tag{3.119}$$

which shows that $(\mathbf{10}, 1, 3)$ and $(\bar{\mathbf{10}}, 1, 3)$ are conjugates in the parent theory, so if one condenses and splits so does the other. If $(\mathbf{10}, 1, 3)$ condenses it necessarily splits since $d_{(\mathbf{10},1,3)} = 3$, but this is inconsistent with (3.119) since there are no non-trivial bosons in the right-hand side. It follows that $(\mathbf{10}, 1, 3)$ cannot condense. By a similar argument $(\bar{\mathbf{10}}, 1, 3)$, $(\mathbf{10}, 3, 1)$, and $(\bar{\mathbf{10}}, 3, 1)$ do not condense.

The only non-abelian boson that we can potentially condense is therefore $(\mathbf{15}, 2, 2)$. But

notice that we cannot condense all abelian bosons on top of this non-abelian one, since

$$(\mathbf{15},2,2)\times(\mathbf{15},2,2)=\text{All abelian bosons}+(\mathbf{15},2,2)+\ldots, \tag{3.120}$$

and the quantum dimension of $(\mathbf{15},2,2)$ is $d_{(\mathbf{15},2,2)}=8$, meaning that it can split into at most eight labels. However, we have eight abelian bosons, so if all abelian bosons condense on top of $(\mathbf{15},2,2)$ we find nine vacua on the right-hand side of the previous fusion, leading to an inconsistency.

For the sake of presentation let us first take as condensing bosons

$$(\mathbf{1},4,4)\to 0,\quad (\mathbf{20'},0,4)\to 0,\quad (\mathbf{20'},4,0)\to 0,\quad (\mathbf{15},2,2)\to 0+\ldots, \tag{3.121}$$

or mathematically, the algebra object $\mathcal{B}_3$ given by the non-simple anyon

$$\mathcal{B}_3=(\mathbf{1},0,0)+(\mathbf{1},4,4)+(\mathbf{20'},0,4)+(\mathbf{20'},4,0)+(\mathbf{15},2,2), \tag{3.122}$$

and check that gauging gives rise to the spectrum of the $U(1)_6^{\text{Orb}}$. After that we will see that other options are not consistent.

Notice that since $(\mathbf{1},4,4)\to 0$ condenses, the lines of the form $(\mathbf{1},a,b)$ arrange according

$SO(4)_4$		
Line label	Quantum Dimension	Conformal Weight
(0,0)	$d_{(0,0)}=1$	$h_{(0,0)}=0$
(0,4) $\cong$ (4,0)	$d_{(0,4)}=1$	$h_{(0,4)}=1$
(2,0) $\cong$ (2,4)	$d_{(2,0)}=2$	$h_{(2,0)}=1/3$
(1,1) $\cong$ (3,3)	$d_{(1,1)}=3$	$h_{(1,1)}=1/4$
(1,3) $\cong$ (3,1)	$d_{(1,3)}=3$	$h_{(1,3)}=3/4$
(0,2) $\cong$ (4,2)	$d_{(0,2)}=2$	$h_{(0,2))}=1/3$
$(2,2)_1$	$d_{(2,2)_1}=2$	$h_{(2,2)_1}=2/3$
$(2,2)_2$	$d_{(2,2)_2}=2$	$h_{(2,2)_2}=2/3$

Table 3.8: $SO(4)_4$ data.

to the gauging of $Spin(4)_4$ down to $SO(4)_4$. We will use this fact repeatedly later, so for the reader's convenience, we have summarized the spectrum of $SO(4)_4$ in terms of the lines of the parent in Table 3.8. Entries that do not appear there confine, in accordance with the gauging of $Spin(4)_4$ to $SO(4)_4$. The theory $SO(4)_4$ can be understood easily from the three-step gauging rule [2, 34], so we do not reproduce such details here. Notice that although the lists of anyons in Table 3.8 do not confine in $SO(4)_4$, their associated lines of the form $(\mathbf{1}, a, b)$ in the current example may still confine because there could be additional identifications that imply their confinement.

To study how $(\mathbf{15}, 2, 2)$ restricts we study the fusion with anyons of the form $(\mathbf{1}, a, b)$ with a and b even:

$$(\mathbf{15}, 2, 2) \times (\mathbf{1}, 0, 2) = (\mathbf{15}, 2, 0) + (\mathbf{15}, 2, 2) + (\mathbf{15}, 2, 4) \tag{3.123}$$

$$(\mathbf{15}, 2, 2) \times (\mathbf{1}, 2, 0) = (\mathbf{15}, 0, 2) + (\mathbf{15}, 2, 2) + (\mathbf{15}, 4, 2) \tag{3.124}$$

$$(\mathbf{15}, 2, 2) \times (\mathbf{1}, 0, 4) = (\mathbf{15}, 2, 2) \tag{3.125}$$

$$\begin{aligned}(\mathbf{15}, 2, 2) \times (\mathbf{1}, 2, 2) = {} & (\mathbf{15}, 0, 0) + (\mathbf{15}, 0, 2) + (\mathbf{15}, 0, 4) \\ & + (\mathbf{15}, 2, 0) + (\mathbf{15}, 2, 2) + (\mathbf{15}, 2, 4) \\ & + (\mathbf{15}, 4, 0) + (\mathbf{15}, 4, 2) + (\mathbf{15}, 4, 4).\end{aligned} \tag{3.126}$$

From the condensation of $Spin(4)_4$ to obtain $SO(4)_4$ we know that $(\mathbf{1}, 2, 0)$, $(\mathbf{1}, 0, 2)$ and $(\mathbf{1}, 2, 2)_1$ are not identified with each other. For instance, if we assume $(\mathbf{1}, 0, 2)$ and $(\mathbf{1}, 2, 0)$ identify, we obtain that

$$(\mathbf{1}, 0, 2) \times (\mathbf{1}, 0, 2) = (\mathbf{1}, 0, 0) + (\mathbf{1}, 0, 2) + (\mathbf{1}, 0, 4), \tag{3.127}$$

and

$$(\mathbf{1},0,2)\times(\mathbf{1},2,0)=(\mathbf{1},2,2) \tag{3.128}$$

would imply that $(\mathbf{1},2,2)$ condenses, which is not possible since $(\mathbf{1},2,2)$ does not have the correct topological spin to do so.

The set of fusions (3.123)-(3.126) upon restricting $(\mathbf{15},2,2)$ on the right-hand side imply that $(\mathbf{1},0,2)$, $(\mathbf{1},2,0)$, $(\mathbf{1},0,4)$, and one component of $(\mathbf{1},2,2)$ must belong to the restriction of $(\mathbf{15},2,2)$.[13] Using also the previous argument that $(\mathbf{1},0,2)$, $(\mathbf{1},2,0)$, and $(\mathbf{1},2,2)$ cannot identify with each other, we obtain that the restriction of $(\mathbf{15},2,2)$ takes the form

$$(\mathbf{15},2,2)\longrightarrow 0+(\mathbf{15},2,2)_2+(\mathbf{15},2,2)_3+(\mathbf{15},2,2)_4+(\mathbf{15},2,2)_4, \tag{3.129}$$

with

$$(\mathbf{15},2,2)_2\cong(\mathbf{1},0,4)\cong(\mathbf{1},4,0),\quad d_{(\mathbf{1},0,4)}=1, \tag{3.130}$$

$$(\mathbf{15},2,2)_3\cong(\mathbf{1},0,2)\cong(\mathbf{1},4,2),\quad d_{(\mathbf{1},0,2)}=2, \tag{3.131}$$

$$(\mathbf{15},2,2)_4\cong(\mathbf{1},2,0)\cong(\mathbf{1},2,4),\quad d_{(\mathbf{1},2,0)}=2, \tag{3.132}$$

$$(\mathbf{15},2,2)_5\cong(\mathbf{1},2,2)_1,\qquad\qquad d_{(\mathbf{1},2,2)_1}=2, \tag{3.133}$$

with no further splittings since we have saturated the conservation of quantum dimension. In the restriction above we had to make a choice between $(\mathbf{1},2,2)_1$ or $(\mathbf{1},2,2)_2$ to appear in the restriction of $(\mathbf{15},2,2)$. Since in $SO(4)_4$ the lines $(2,2)_1$ and $(2,2)_2$ are symmetric between each other, the choice is actually immaterial, and by definition we have chosen $(\mathbf{1},2,2)_1$ to be the one appearing in the restriction of $(\mathbf{15},2,2)$.

In passing, let us note that now $(\mathbf{1},0,2)$, $(\mathbf{1},2,0)$, and $(\mathbf{1},2,2)_1$ have an additional lift

13. It is straightforward to check by computing self-fusions that $(\mathbf{1},0,2)$, $(\mathbf{1},2,0)$, $(\mathbf{1},0,4)$ do not split.

to $(\mathbf{15}, 2, 2)$, which implies that while $(\mathbf{1}, 0, 2)$, $(\mathbf{1}, 2, 0)$, and $(\mathbf{1}, 2, 2)_1$ were unconfined in the $SO(4)_4$ theory, in the current example they confine.

Next let us show that $(\mathbf{10}, 3, 1)$ confines. This is easily seen by acting with our condensing abelian bosons:

$$(\mathbf{1}, 4, 4) \times (\mathbf{10}, 3, 1) = (\mathbf{10}, 1, 3) \tag{3.134}$$

$$(\mathbf{20'}, 0, 4) \times (\mathbf{10}, 3, 1) = (\overline{\mathbf{10}}, 3, 3) \tag{3.135}$$

$$(\mathbf{20'}, 4, 0) \times (\mathbf{10}, 3, 1) = (\overline{\mathbf{10}}, 1, 1). \tag{3.136}$$

Using that the abelian bosons condense, we deduce the identifications $(\mathbf{10}, 3, 1) \cong (\mathbf{10}, 1, 3) \cong (\overline{\mathbf{10}}, 1, 1) \cong (\overline{\mathbf{10}}, 3, 3)$. From this is easy to see that $(\mathbf{10}, 3, 1)$ and the rest of the labels on the list confine. A completely analogous argument allows us to deduce the identifications

$$(\mathbf{10}, 1, 1) \cong (\mathbf{10}, 3, 3) \cong (\overline{\mathbf{10}}, 1, 3) \cong (\overline{\mathbf{10}}, 3, 1), \tag{3.137}$$

$$(\mathbf{1}, 1, 1) \cong (\mathbf{1}, 3, 3) \cong (\mathbf{20'}, 1, 3) \cong (\mathbf{20'}, 3, 1), \tag{3.138}$$

$$(\mathbf{1}, 1, 3) \cong (\mathbf{1}, 3, 1) \cong (\mathbf{20'}, 1, 1) \cong (\mathbf{20'}, 3, 3), \tag{3.139}$$

from which in turn we can deduce the corresponding confinement of all the labels in the lists above. The remaining anyons of the form $(\mathbf{1}, i, j)$ that we have not treated here all confine, as they already confined as (i, j) in $SO(4)_4$.

In summary, the anyons of the form $(\mathbf{1}, i, j)$ that do not confine are $(\mathbf{1}, 0, 0)$, $(\mathbf{1}, 0, 4)$, and $(\mathbf{1}, 2, 2)_2$. It is straightforward to see that they match the anyons labelled by 0, 2 and 5 respectively in Table 3.7 showing the spectrum of the $U(1)_6^{\mathrm{Orb}}$ theory, both in their conformal weight as in their quantum dimensions. As another check, the fusion rules for these lines in the orbifold theory are indeed the same as those of the corresponding lines in the $SO(4)_4$

theory.

We now move to work out lines of the form $(\mathbf{15}, a, b)$. Notice that the condensing abelian bosons relate $(\mathbf{15}, a, b)$ and $(\mathbf{6}, a, b)$, so studying the former fixes the latter. Start by analyzing $(\mathbf{15}, 0, 0)$:

$$(\mathbf{15}, 0, 0) \times (\mathbf{15}, 0, 0) = (\mathbf{1}, 0, 0) + (\mathbf{15}, 0, 0) + (\mathbf{20'}, 0, 0). \tag{3.140}$$

Thus $(\mathbf{15}, 0, 0)$ does not split since $(\mathbf{20'}, 0, 0)$ does not condense. From

$$(\mathbf{15}, 0, 0) \times (\mathbf{15}, 2, 2) = (\mathbf{15}, 2, 2) + \dots \tag{3.141}$$

we deduce that upon restricting $(\mathbf{15}, 2, 2)$ on the right-hand side, since $(\mathbf{15}, 0, 0)$ is self-conjugate, it belongs to the restriction of $(\mathbf{15}, 2, 2)$. In particular, it must be identified with one of the quantum dimension two components of $(\mathbf{15}, 2, 2)$. As such, it follows that $(\mathbf{15}, 0, 0)$ confines.

To figure out what component we have to identify $(\mathbf{15}, 0, 0)$ with precisely, consider

$$\begin{aligned}(\mathbf{15}, 2, 2) = (\mathbf{15}, 0, 0) \times (\mathbf{1}, 2, 2) &\longrightarrow (\mathbf{15}, 0, 0) \times (\mathbf{1}, 2, 2)_1 + (\mathbf{15}, 0, 0) \times (\mathbf{1}, 2, 2)_2 \\ &\longrightarrow 0 \dots,\end{aligned} \tag{3.142}$$

where in the upper arrow we have restricted the right-hand side, while in the lower arrow we have restricted the left-hand side. Since $(\mathbf{1}, 2, 2)_1$ and $(\mathbf{1}, 2, 2)_2$ are self-conjugate, and $(\mathbf{1}, 2, 2)_1 \in (\mathbf{15}, 2, 2)$ but $(\mathbf{1}, 2, 2)_2 \notin (\mathbf{15}, 2, 2)$ it must be that

$$(\mathbf{15}, 0, 0) \cong (\mathbf{1}, 2, 2)_1. \tag{3.143}$$

In passing, acting with the condensing abelian bosons as in (3.134)-(3.136) and (3.137)-

(3.139), we obtain the additional identifications

$$(\mathbf{15},0,0) \cong (\mathbf{1},2,2)_1 \cong (\mathbf{15},4,4) \cong (\mathbf{15},0,4) \cong (\mathbf{15},4,0). \tag{3.144}$$

With the result (3.139) is straightforward to extract the content of the lines of the form $(\mathbf{15},a,b)$, since we can do

$$(\mathbf{15},a,b) = (\mathbf{15},0,0) \times (\mathbf{1},a,b) \cong (\mathbf{1},2,2)_1 \times (\mathbf{1},a,b), \tag{3.145}$$

and then we can proceed to use the fusion rules of $SO(4)_4$ to derive the splitting of $(\mathbf{15},a,b)$ in terms of $(\mathbf{1},a,b)$'s which we already know. Of course, this means that $(\mathbf{15},a,b)$ will not give us any new lines in the spectrum of the child theory, since all of them can be identified in terms of lines that we have already considered. To check that none of the unconfined lines already obtained confine upon lifting them to $(\mathbf{15},a,b)$'s it is useful to know the explicit results

$$(\mathbf{15},0,2) \longrightarrow (\mathbf{1},2,0) + (\mathbf{1},2,2)_2, \tag{3.146}$$

$$(\mathbf{15},2,0) \longrightarrow (\mathbf{1},0,2) + (\mathbf{1},2,2)_2, \tag{3.147}$$

$$(\mathbf{15},4,2) \longrightarrow (\mathbf{1},2,0) + (\mathbf{1},2,2)_2, \tag{3.148}$$

$$(\mathbf{15},2,4) \longrightarrow (\mathbf{1},0,2) + (\mathbf{1},2,2)_2, \tag{3.149}$$

$$(\mathbf{1},2,2) \longrightarrow (\mathbf{1},2,2)_1 + (\mathbf{1},2,2)_2, \tag{3.150}$$

$$(\mathbf{20'},2,2) \longrightarrow (\mathbf{1},2,2)_1 + (\mathbf{1},2,2)_2. \tag{3.151}$$

Thus, the unconfined lines on the right-hand-side of $(\mathbf{15},0,2)$, $(\mathbf{15},2,0)$, $(\mathbf{15},2,4)$, $(\mathbf{15},4,2)$, $(\mathbf{1},2,2)$, and $(\mathbf{20'},2,2)$ are all the same; namely $(\mathbf{1},2,2)_2$, which is easy to see that it does

not confine when considering the new splittings above, as all left-hand sides share the same topological spin. Similarly, from the fusion rules of $SU(2)_4 \times SU(2)_4$ it is straightforward to check that $(\mathbf{1}, 0, 4)$, $(\mathbf{1}, 4, 0)$ are never contained in $(\mathbf{1}, 2, 2) \times (\mathbf{1}, a, b)$, for any a, b other than $a = b = 2$, and thus also not contained in $(\mathbf{15}, a, b) = (\mathbf{1}, 2, 2)_1 \times (\mathbf{1}, a, b)$, so there are no new liftings that could confine $(\mathbf{1}, 0, 4)$.

Before working-out the lines of the form $(\mathbf{4}, a, b)$, let us apply the simple currents $(\overline{\mathbf{10}}, 0, 0)$ to the unconfined spectra found thus far consisting of $(\mathbf{1}, 0, 0)$, $(\mathbf{1}, 0, 4)$ and $(\mathbf{1}, 2, 2)_1$. We find

$$(\overline{\mathbf{10}}, 0, 0) \times (\mathbf{1}, 0, 0) = (\overline{\mathbf{10}}, 0, 0), \tag{3.152}$$

$$(\overline{\mathbf{10}}, 0, 0) \times (\mathbf{1}, 0, 4) = (\overline{\mathbf{10}}, 0, 4), \tag{3.153}$$

$$(\overline{\mathbf{10}}, 0, 0) \times (\mathbf{1}, 2, 2)_2 = (\overline{\mathbf{10}}, 2, 2)_2. \tag{3.154}$$

It is straightforward to see that further actions of the simple current will just permute the four lines on the right-hand sides above. Of course, we can apply $(\overline{\mathbf{10}}, 0, 0)$ to all the rest of the lines we have found before, but this would either give confined sectors, or unconfined ones that are related to the lines on the right-hand side above by identifications already obtained at the level of $(\mathbf{1}, a, b)$'s and $(\mathbf{15}, a, b)$'s. Thus the action of the simple currents provide us with three new unconfined excitations in the child theory: $(\overline{\mathbf{10}}, 0, 0)$, $(\overline{\mathbf{10}}, 0, 4)$, and $(\overline{\mathbf{10}}, 2, 2)_2$. We can easily check that they match, both in topological spin and quantum dimension to the lines labelled as 1, 3 and 4 in Table 3.7 outlining the spectrum of $U(1)_6^{\mathrm{Orb}}$.

We move now to study the restriction of lines of the form $(\mathbf{4}, a, b)$. First, notice that using our condensing abelian bosons as in (3.134)-(3.136), (3.137)-(3.139), or as in Eqn. (3.144) we can derive the identifications

$$(\mathbf{4}, 1, 1) \cong (\mathbf{4}, 3, 3) \cong (\mathbf{20}, 1, 3) \cong (\mathbf{20}, 3, 1), \tag{3.155}$$

$$(\mathbf{4},1,3) \cong (\mathbf{4},3,1) \cong (\mathbf{20},1,1) \cong (\mathbf{20},3,3), \tag{3.156}$$

$$(\bar{\mathbf{4}},1,1) \cong (\bar{\mathbf{4}},3,3) \cong (\overline{\mathbf{20}},1,3) \cong (\overline{\mathbf{20}},3,1), \tag{3.157}$$

$$(\bar{\mathbf{4}},1,3) \cong (\bar{\mathbf{4}},3,1) \cong (\overline{\mathbf{20}},1,1) \cong (\overline{\mathbf{20}},3,3). \tag{3.158}$$

The identifications imply that we can concentrate our attention to the leftmost anyons in each line. It is easy to check that these identification do not lead to the confinement of any of the anyons involved.

Consider now the fusion rule

$$\begin{aligned}(\mathbf{4},1,3) \times (\bar{\mathbf{4}},1,3) = (\mathbf{1},0,0) + (\mathbf{1},0,2) + (\mathbf{1},2,0) + (\mathbf{1},2,2) \\ + (\mathbf{15},0,0) + (\mathbf{15},0,2) + (\mathbf{15},2,0) + (\mathbf{15},2,2),\end{aligned} \tag{3.159}$$

which upon restriction implies the splittings

$$(\mathbf{4},1,3) \longrightarrow (\mathbf{4},1,3)_1 + (\mathbf{4},1,3)_2, \tag{3.160}$$

$$(\bar{\mathbf{4}},1,3) \longrightarrow \overline{(\mathbf{4},1,3)_1} + \overline{(\mathbf{4},1,3)_2}, \tag{3.161}$$

and a similar fusion implies the splittings $(\mathbf{4},1,1) \rightarrow (\mathbf{4},1,1)_1 + (\mathbf{4},1,1)_2$, $(\bar{\mathbf{4}},1,1) \rightarrow \overline{(\mathbf{4},1,1)_1} + \overline{(\mathbf{4},1,1)_2}$. We can now consider the crossed fusion rule

$$(\mathbf{4},1,3) \times (\bar{\mathbf{4}},1,1) = (\mathbf{15},2,2) + \ldots \longrightarrow 0 + \ldots, \tag{3.162}$$

which implies that one component of $(\mathbf{4},1,3)$ identifies with one component of $(\bar{\mathbf{4}},1,1)$. Let us define the subindex 2 in the previous splitting to be such that this holds. We find then

$$(\mathbf{4},1,1) \longrightarrow (\mathbf{4},1,1)_1 + (\mathbf{4},1,1)_2, \tag{3.163}$$

$$(\mathbf{4},1,3) \longrightarrow (\mathbf{4},1,3)_1 + (\mathbf{4},1,1)_2, \tag{3.164}$$

$$(\bar{\mathbf{4}},1,1) \longrightarrow \overline{(\mathbf{4},1,1)_1} + \overline{(\mathbf{4},1,1)_2}, \tag{3.165}$$

$$(\bar{\mathbf{4}},1,3) \longrightarrow \overline{(\mathbf{4},1,3)_1} + \overline{(\mathbf{4},1,1)_2}, \tag{3.166}$$

from which it is easy to see that $(\mathbf{4},1,1)_2$ confines. Because of this, the lines with subindex 1 in the previous restrictions share the same quantum dimension.

Next we must determine the assignment of quantum dimensions. The easiest way to do this at this point is to use the formula relating the central charge with topological spins and quantum dimensions:

$$e^{i\frac{\pi}{4}c} = \frac{1}{\sqrt{\sum_i d_i^2}} \sum_i d_i^2 \theta_i, \tag{3.167}$$

and plugging in $c = 1$ and the values for the unconfined excitations, whose topological spins and quantum dimensions we know (except of course for the quantum dimension that we want to determine). The equation can then be solved for the remaining unknown quantum dimension, which we assign to the unconfined excitations above. The result is that the assignments must be $d_{(\mathbf{4},1,1)_1} = \sqrt{3}$ and $d_{(\mathbf{4},1,1)_2} = 2\sqrt{3}$.

A slickly argument that does not involve using an additional formula nor using the central charge or other quantities as input, but that uses the same manipulations with fusions and quantum dimensions that we have used until now is given as follows. Split the quantum dimensions as:

$$3\sqrt{3} = \frac{3\sqrt{3}}{a} + \frac{3\sqrt{3}}{a}(a-1), \quad a > 1, \tag{3.168}$$

and recall that quantum dimensions satisfy the fusion algebra, meaning that the assignments of quantum dimensions must be consistent with the fusion (3.159).[14] However, we have already determined the quantum dimensions on the right-hand side of (3.159), and they are

14. In (3.159) we have written the fusion of $(\mathbf{4},1,3)$ and its conjugate, but an analog fusion holds for $(\mathbf{4},1,1)$ and its conjugate.

given by 1s and 2s. It is actually sufficient to know that the right-hand side of (3.159) gives an integer quantum dimension for any fusion product on the left-hand side.

Thus, we must have that $27/a^2 \in \mathbb{N}_{>0}$, and $(a-1)27/a^2 \in \mathbb{N}_{>0}$, where we may think of these two conditions as arising from the $(\mathbf{4},1,1)_1 \times (\mathbf{4},1,1)_1$ and $(\mathbf{4},1,1)_1 \times (\mathbf{4},1,1)_2$ fusion products, respectively. The first condition gives that $a = 3\sqrt{3}/\sqrt{n}$ for some positive integer n, and on the second condition this gives $(3\sqrt{3n} - n) \in \mathbb{N}_{>0}$. It is now direct to see that the only possible solutions are $n = 3, 12$, which lead however to the same splitting of the quantum dimension:

$$3\sqrt{3} = \sqrt{3} + 2\sqrt{3}. \tag{3.169}$$

To decide which quantum dimension to assign to $(\mathbf{4},1,1)_1$, notice that the fusion product of two genuine line operators must be genuine line operators. This means that in (3.159), the product of the quantum dimensions in the fusion $(\mathbf{4},1,1)_1 \times (\mathbf{4},1,1)_1$ is bounded by the sum of the quantum dimensions of the unconfined excitations on the right-hand side. It is straightforward to check that the latter sums to nine, so the only consistent assignment is the one we found above: $d_{(\mathbf{4},1,1)_1} = \sqrt{3}$ and $d_{(\mathbf{4},1,1)_2} = 2\sqrt{3}$.

In summary, the unconfined excitations that we have found in the $(\mathbf{4},i,j)$ sector are $(\mathbf{4},1,1)_1$, $(\mathbf{4},1,3)_1$, and their conjugates. All of them have the same quantum dimension $d_{(\mathbf{4},1,1)_1} = \sqrt{3}$. We can check now that this matches with the lines 6,7,8,9 in the $U(1)_6^{\mathrm{Orb}}$ spectrum shown in Table 3.7.

Using the condensing abelian bosons as above is easy to show that the remaining anyons of the form $(\mathbf{4},i,j)$ confine. For example, $(\mathbf{4},0,0) \times (\mathbf{20'},0,4) = (\mathbf{20},0,4)$ and $(\mathbf{20'},0,4) \to 0$, but $(\mathbf{4},0,0)$ has topological spin $e^{2\pi i 5/16}$ while $(\mathbf{20},0,4)$ has topological spin $e^{2\pi i 13/16}$, implying that $(\mathbf{4},0,0)$ confines.

Inconsistency of Condensing Different Abelian Bosons

We conclude this subsection indicating how making a putative different choice of condensing bosons (including the non-abelian one) other than (3.121) leads to an inconsistency.

We have already shown that condensing all abelian bosons leads to an inconsistency, so we need to take a subset of them closed under fusion. First suppose we were to take $(\mathbf{1}, 4, 4)$, $(\mathbf{20'}, 0, 0)$, $(\mathbf{20'}, 4, 4)$ to condense on top of the non-abelian boson $(\mathbf{15}, 2, 2)$. Since $(\mathbf{20'}, 0, 0)$ condenses:

$$(\mathbf{15}, 0, 0) \times (\mathbf{15}, 0, 0) = (\mathbf{1}, 0, 0) + (\mathbf{20'}, 0, 0) + (\mathbf{15}, 0, 0) \longrightarrow 0 + 0 + \ldots, \tag{3.170}$$

so $(\mathbf{15}, 0, 0)$ must split into two components each with unit quantum dimension. However, because $(\mathbf{1}, 4, 4) \to 0$, $(\mathbf{1}, 2, 2) \to (\mathbf{1}, 2, 2)_1 + (\mathbf{1}, 2, 2)_2$ each with quantum dimension 2, since this follows from the gauging of $Spin(4)_4$ to $SO(4)_4$. This is inconsistent since the left-hand side of

$$(\mathbf{15}, 2, 2) = (\mathbf{15}, 0, 0) \times (\mathbf{1}, 2, 2). \tag{3.171}$$

condenses, but the right hand side decomposes into fusions of components of quantum dimensions one and two. Since conjugates need to have the same quantum dimension, there is no way to accommodate a pair of conjugates that fuse to a vacuum.

Now suppose we were to take $(\mathbf{1}, 4, 4)$, $(\mathbf{1}, 0, 4)$, $(\mathbf{1}, 4, 0)$ as condensing abelian bosons. From (3.170) we see that $(\mathbf{15}, 0, 0)$ does not split in this case. However now

$$(\mathbf{1}, 2, 2) \times (\mathbf{1}, 2, 2) = (\mathbf{1}, 0, 0) + (\mathbf{1}, 0, 4) + (\mathbf{1}, 4, 0) + (\mathbf{1}, 4, 4) + \ldots \longrightarrow 0 + 0 + 0 + 0 + \ldots, \tag{3.172}$$

implies $(\mathbf{1}, 2, 2)$ splits into four unit quantum dimension components. The same argument as before using (3.171) implies an inconsistency.

The case when we try to condense $(\mathbf{1}, 0, 4)$, $(\mathbf{20'}, 4, 0)$ and $(\mathbf{20'}, 4, 4)$ is a bit different.

First, notice that if we take $(\mathbf{1}, 0, 4)$ to condense then the right $SU(2)_4$ factor condenses to $SU(3)_1$, and $(\mathbf{1}, i, 2) \to (\mathbf{1}, i, 2_1) + (\mathbf{1}, i, 2_2)$, for any $i = 0, \ldots, 4$. We now observe that the fusion products of $(\mathbf{15}, 2, 2)$ with $(\mathbf{1}, 2, 0)$, $(\mathbf{1}, 4, 0)$, $(\mathbf{1}, 0, 2)$, $(\mathbf{1}, 2, 2)$ and $(\mathbf{1}, 4, 2)$ all will have a $(\mathbf{15}, 2, 2)$ on the right-hand side and thus will have a vacuum after restriction. In particular it follows that $(\mathbf{1}, 4, 0), (\mathbf{1}, 4, 2_1), (\mathbf{1}, 2, 0) \in (\mathbf{15}, 2, 2)$. [15] It is easy to check that $(\mathbf{1}, 2, 0)$ splits, and notice that $(\mathbf{1}, 4, 0)$ cannot possibly be identified with $(\mathbf{1}, 4, 2_1)$, as if this was the case we could fuse both sides with $(\mathbf{1}, 4, 0)$ obtaining an identification of $(\mathbf{1}, 4, 2_1)$ with $(\mathbf{1}, 0, 0)$ which is not possible since $(\mathbf{1}, 4, 2_1)$ does not have the topological spin to condense. It follows that the restriction of $(\mathbf{15}, 2, 2)$ must be of the form

$$(\mathbf{15}, 2, 2) \longrightarrow 0 + (\mathbf{1}, 4, 0) + (\mathbf{1}, 4, 2_1) + (\mathbf{1}, 2, 0) + b, \tag{3.173}$$

for some b with quantum dimension $d_b = 3$. However we now take that $(\mathbf{1}, 2, 2_1)$ must also be in the restriction $(\mathbf{15}, 2, 2)$, and the only candidate that matches the quantum dimension above is $(\mathbf{1}, 2, 0)$, which is however inconsistent since identifying $(\mathbf{1}, 2, 0)$ with $(\mathbf{1}, 2, 2_1)$ implies upon fusing with $(\mathbf{1}, 2, 0)$ that $(\mathbf{1}, 0, 0) + (\mathbf{1}, 2, 0) + (\mathbf{1}, 4, 0)$ is identified with $(\mathbf{1}, 0, 2_1) + (\mathbf{1}, 2, 2_1) + (\mathbf{1}, 4, 2_1)$, but none of these last anyons can condense, thus finding an inconsistency.

Finally, had we taken a single abelian boson to condense on top of the non-abelian one, $(\mathbf{15}, 2, 2)$ would have split into just three components. Either $(\mathbf{1}, 4, 0)$ or $(\mathbf{1}, 0, 4)$ would not condense and it would belong in the restriction of $(\mathbf{15}, 2, 2)$. So, the third anyon in the restriction would have quantum dimension 6. It is then easily seen that either $(\mathbf{1}, 2, 0)$ or $(\mathbf{1}, 0, 2)$ do not split and belong to $(\mathbf{15}, 2, 2)$, but there is no component in the decomposition that matches the quantum dimension, leading to an inconsistency.

15. Since the fusion rules in $SU(3)_1$ are symmetric between 2_1 and 2_2 we could have chosen $(\mathbf{1}, 4, 2_2)$ here instead. It is easy to see that the same conclusions follow.

3.5 Revisiting Conformal Embeddings and Level-Rank Dualities

In this section we revisit the conformal embeddings of [7–9, 31] and their relation to gauging of non-invertible symmetries. We have already touched upon this matter in Section 3.3, and here we will generalize that discussion to other conformal embeddings. In particular, in the case of the exceptional conformal embeddings of [31], we will see that running an analogous argument to that of the classical embeddings of [7–9] will already lead us to the consideration of non-abelian anyon condensation to make the dualities work.

3.5.1 Revisiting Classical Conformal Embeddings

Let us start motivating our discussion with the simple case of that of the unitary series of conformal embeddings

$$SU(N)_k \times SU(k)_N \hookrightarrow SU(Nk)_1, \quad N, k \in \mathbb{N}_{\geq 2}, \tag{3.174}$$

whose standard 3D TQFT duality interpretation, as reviewed at the end of Section 3.2, is [7]:

$$SU(k)_N \cong \frac{SU(Nk)_1 \times SU(N)_{-k}}{\mathbb{Z}_N}. \tag{3.175}$$

To relate conformal embeddings to the gauging of non-invertible symmetries, we point out that the following alternative results also applies:

$$\boxed{SU(Nk)_1 \cong \frac{SU(N)_k \times SU(k)_N}{\mathcal{A}_{N,k}}} \tag{3.176}$$

where $\mathcal{A}_{N,k}$ is some gaugable algebra object (for brevity, on the rest of this section when we write a letter in calligraphic font we always mean some appropriate algebra object that we can use to gauge, and from now on we will not remark on what such objects stand for). The previous statement has been discussed in many mathematical references [24, 50, 52, 80,

112, 113], but in our context it is most quickly understood from the coset inversion formula (3.60) with $\mathcal{M} = SU(Nk)_1$, $\mathcal{C} = SU(k)_N$ and $\mathcal{M}' = SU(N)_k$. In this sense, (3.175) is nothing but the standard form of cosets, Eqn. (3.61) of the coset inversion formulas, while (3.176) is "the parent statement" Eqn. (3.60) translated to a form more akin to physics, and for the particular example at hand. Clearly, the unitary groups play no role in the previous argument, and as such the same would hold for any other conformal embeddings. We explore this in the next sections below.

As we will see shortly, in the form (3.176) the algebra object that we need to gauge is generically that of a non-invertible symmetry, although in particular cases it may simplify to some abelian gauging. For instance, it is easy to see that if we apply this form of the conformal embedding of unitary groups for $N = k = 2$ we obtain

$$SU(4)_1 \cong \frac{SU(2)_2 \times SU(2)_2}{\mathbb{Z}_2}, \tag{3.177}$$

where the $\mathbb{Z}_2$ algebra is given by $\mathcal{A} = (0,0) + (2,2)$, where (i,j) stands for the spin $i/2$ and $j/2$ representations of each $SU(2)_2$ factor. Eqn. (3.177) can be verified by a simple use of the three-step gauging procedure [2].

The simplest instance where we need to consider gauging by a non-invertible one-form symmetry to make (3.176) valid occurs at $N = 3$ and $k = 2$, which we verify by a direct non-abelian anyon condensation computation on the following example. Further conformal embeddings will be studied in Section 3.5.1 and Section 3.5.2 below once we finish illustrating this example.

Checking the $SU(6)_1 \cong (SU(3)_2 \times SU(2)_3)/\mathcal{A}$ Duality

In this subsection we check by direct computation that $SU(6)_1$ can be found as a non-abelian anyon condensation of $SU(3)_2 \times SU(2)_3$. This is the simplest example in the infinite tower

of conformal embeddings

$$SU(N)_k \times SU(k)_N \hookrightarrow SU(Nk)_1, \quad N, k \in \mathbb{N}_{\geq 2}, \tag{3.178}$$

where we can think of $SU(Nk)_1$ as a non-abelian anyon condensation of $SU(N)_k \times SU(k)_N$. Such conformal embeddings are particularly interesting because of their intimate relation to level-rank dualities [7].

We follow the same procedure as in Section 3.4, so the reader may find useful to read that section first before going through this example. The spectrum of $SU(2)_3$ is given in Table 3.2, while the spectrum of $SU(3)_2$ is given in Table 3.9. In the following, we write $(\mathbf{R}, i)$ for a line in $SU(3)_2 \times SU(2)_3$, where $\mathbf{R}$ labels a line in representation $\mathbf{R}$ of $SU(3)$ and $i = 0, 1, 2, 3$ labels the corresponding line in $SU(2)_3$. We will need the fusion rules for $SU(2)_k$ which can be found above in Eqn. (3.92), and the fusion rules for $SU(3)_2$:

$$\mathbf{3} \times \mathbf{3} = \bar{\mathbf{3}} + \mathbf{6}, \quad \mathbf{3} \times \bar{\mathbf{3}} = \mathbf{1} + \mathbf{8}, \quad \mathbf{3} \times \mathbf{8} = \mathbf{3} + \bar{\mathbf{6}}, \quad \mathbf{3} \times \mathbf{6} = \bar{\mathbf{3}}, \quad \mathbf{3} \times \bar{\mathbf{6}} = \mathbf{8}$$

$$\bar{\mathbf{3}} \times \bar{\mathbf{3}} = \mathbf{3} + \bar{\mathbf{6}}, \quad \bar{\mathbf{3}} \times \mathbf{8} = \bar{\mathbf{3}} + \mathbf{6}, \quad \bar{\mathbf{3}} \times \mathbf{6} = \mathbf{3}, \quad \bar{\mathbf{3}} \times \bar{\mathbf{6}} = \mathbf{8},$$

$$\mathbf{8} \times \mathbf{8} = \mathbf{1} + \mathbf{8}, \quad \mathbf{8} \times \mathbf{6} = \bar{\mathbf{3}}, \quad \mathbf{8} \times \bar{\mathbf{6}} = \mathbf{3},$$

$$\mathbf{6} \times \mathbf{6} = \bar{\mathbf{6}}, \quad \mathbf{6} \times \bar{\mathbf{6}} = \mathbf{1}, \quad \bar{\mathbf{6}} \times \bar{\mathbf{6}} = \mathbf{6}.$$

Notice that in the spectrum of $SU(3)_2$ the lines $\mathbf{6}$ and $\bar{\mathbf{6}}$ act as $\mathbb{Z}_3$ simple currents, meaning that if we know the fate of $(\mathbf{1}, i)$ and $(\mathbf{8}, i)$ upon gauging/condensation, we can deduce that of $(\mathbf{6}, i)$, $(\mathbf{3}, i)$, and their conjugates by acting with $(\mathbf{6}, 0)$ and $(\bar{\mathbf{6}}, 0)$. Thus, we concentrate on $(\mathbf{1}, i)$ and $(\mathbf{8}, i)$.

To begin, observe that there is only one non-trivial boson in the product theory $SU(3)_2 \times SU(2)_3$; namely, the boson $(\mathbf{8}, 2)$, with quantum dimension $d_{(\mathbf{8},2)} = \frac{3+\sqrt{5}}{2}$. Let us assume this boson condenses, which has to be the case since it would be the only way to obtain

$SU(3)_2$		
Line label	Quantum Dimension	Conformal Weight
$\mathbf{1}$	$d_{\mathbf{1}} = 1$	$h_{\mathbf{1}} = 0$
$\mathbf{3}$	$d_{\mathbf{3}} = \frac{1+\sqrt{5}}{2}$	$h_{\mathbf{3}} = 4/15$
$\bar{\mathbf{3}}$	$d_{\bar{\mathbf{3}}} = \frac{1+\sqrt{5}}{2}$	$h_{\bar{\mathbf{3}}} = 4/15$
$\mathbf{8}$	$d_{\mathbf{8}} = \frac{1+\sqrt{5}}{2}$	$h_{\mathbf{8}} = 3/5$
$\mathbf{6}$	$d_{\mathbf{6}} = 1$	$h_{\mathbf{6}} = 2/3$
$\bar{\mathbf{6}}$	$d_{\bar{\mathbf{6}}} = 1$	$h_{\bar{\mathbf{6}}} = 2/3$

Table 3.9: $SU(3)_2$ data.

$SU(6)_1$ from a condensation of $SU(3)_2 \times SU(2)_3$.

Assuming that $(\mathbf{8}, 2)$ condenses is the statement that $(\mathbf{8}, 2)$ restricts as

$$(\mathbf{8}, 2) \to 0 + (\mathbf{8}, 2)_2 \,, \tag{3.179}$$

where by conservation of the quantum dimension, $d_{(\mathbf{8},2)_2} = \frac{1+\sqrt{5}}{2}$. This is too small to allow a further splitting, so $(\mathbf{8}, 2)$ must restrict to just two components.

Let us now notice that the line $(\mathbf{1}, 2)$ cannot split as it does not have large enough quantum dimension to do so. With this observation, consider

$$(\mathbf{8}, 2) \times (\mathbf{1}, 2) = (\mathbf{8}, 0) + (\mathbf{8}, 2) \longrightarrow 0 + \ldots, \tag{3.180}$$

which shows that $(\mathbf{1}, 2) \in (\mathbf{8}, 2)$ since $(\mathbf{1}, 2)$ is self-conjugate. Matching quantum dimensions the only possibility is to have the identification $(\mathbf{1}, 2) \cong (\mathbf{8}, 2)_2$, which in turn implies the confinement of these components since they lift to anyons in the parent theory with different topological spins.

To study the result of $(\mathbf{1}, 1)$ and $(\mathbf{1}, 3)$ after condensation, notice that these lines cannot split since they do not have large enough quantum dimension, and consider the fusion rules

$$(\mathbf{8}, 2) \times (\mathbf{1}, 1) = (\mathbf{8}, 1) + (\mathbf{8}, 3), \tag{3.181}$$

and

$$(\mathbf{8},2)\times(\mathbf{1},3)=(\mathbf{8},1) \tag{3.182}$$

$$=(\mathbf{1},3)+(\mathbf{1},2)\times(\mathbf{1},3)=(\mathbf{1},3)+(\mathbf{1},1), \tag{3.183}$$

where in the last expression the first equality comes from doing the standard fusion on the parent theory and the second line comes from first restricting $(\mathbf{8},2)\to 0+(\mathbf{1},2)$ on the left-hand side, and then performing the fusion of these components with $(\mathbf{1},3)$. Comparing both expressions, we obtain the restriction of $(\mathbf{8},1)$ into an abelian anyon $(\mathbf{1},3)$ and a non-abelian anyon $(\mathbf{1},1)$:

$$(\mathbf{8},1)\longrightarrow(\mathbf{1},1)+(\mathbf{1},3). \tag{3.184}$$

It is easy to check now that the topological spin of $(\mathbf{1},1)$ is not equal to that of $(\mathbf{8},1)$ in the parent theory, and thus it follows that $(\mathbf{1},1)$ confines. Meanwhile, the topological spins of $(\mathbf{8},1)$ and $(\mathbf{1},3)$ match.

Using this information in the first fusion rule (3.181) we obtain

$$(\mathbf{8},2)\times(\mathbf{1},1)=(\mathbf{1},1)+(\mathbf{1},3)+(\mathbf{8},3) \tag{3.185}$$

$$=(\mathbf{1},1)+(\mathbf{1},1)+(\mathbf{1},3), \tag{3.186}$$

where in the first equality we have used that $(\mathbf{8},1)\to(\mathbf{1},1)+(\mathbf{1},3)$ on the right side of (3.181), and in the second equality we have instead first restricted $(\mathbf{8},2)\to 0+(\mathbf{1},2)$. We must therefore identify $(\mathbf{1},1)\cong(\mathbf{8},3)$.

It remains to study $(\mathbf{8},0)$, which does not split since it does not have large enough quantum dimension. Now, inspect the fusion

$$(\mathbf{8},2)\times(\mathbf{8},0)=(\mathbf{1},2)+(\mathbf{8},2)=(\mathbf{1},2)+0+(\mathbf{1},2) \tag{3.187}$$

$SU(6)_1$		
Line label	Quantum Dimension	Conformal Weight
0	$d_1 = 1$	$h_1 = 0$
1	$d_2 = 1$	$h_2 = 5/12$
2	$d_3 = 1$	$h_3 = 2/3$
3	$d_4 = 1$	$h_4 = 3/4$
4	$d_5 = 1$	$h_5 = 2/3$
5	$d_6 = 1$	$h_6 = 5/12$

Table 3.10: $SU(6)_1$ data. The label n on the left column labels the fully antisymmetric representation with a single column with n boxes in the Young tableux.

$$= (\mathbf{8}, 0) + (\mathbf{8}, 2) = (\mathbf{8}, 0) + 0 + (\mathbf{1}, 2), \tag{3.188}$$

where in the first line we have performed the fusion on the parent theory and then used the restriction $(\mathbf{8}, 2) \to 0 + (\mathbf{1}, 2)$, while in the second line we have first restricted on the left-hand side and later computed the corresponding fusions, after which we used the $(\mathbf{8}, 2)$ restriction again. It follows that we must identify $(\mathbf{8}, 0) \cong (\mathbf{1}, 2)$.

Clearly, the only unconfined lines in the $(\mathbf{1}, i)$ and $(\mathbf{8}, i)$ sectors are $(\mathbf{1}, 0)$ and $(\mathbf{1}, 3)$ (up to identifications). Following our comments above, we can now consider the action of the simple currents of $SU(3)_2$ in the form $(\mathbf{6}, 0)$ and $(\bar{\mathbf{6}}, 0)$ over the confined and unconfined excitations already found, which generates the rest of the sectors not considered up to this point. The spectrum of unconfined excitations is seen to match that of the expected $SU(6)_1$ theory, whose spectrum is summarized in Table 3.10. Furthermore, since in this example the lines in the child theory descend trivially from those of the parent, we can easily check the $\mathbb{Z}_6$ fusion rules expected of $SU(6)_1$ by computing them directly in the parent:

$$(\mathbf{6}, 3)^2 = (\bar{\mathbf{6}}, 0), \quad (\mathbf{6}, 3)^3 = (\mathbf{1}, 3), \quad (\mathbf{6}, 3)^6 = (\mathbf{1}, 0). \tag{3.189}$$

The condensation computation thus points that indeed[16]

$$\boxed{SU(6)_1 \cong \frac{SU(3)_2 \times SU(2)_3}{\mathcal{A}_{3,2}}} \tag{3.190}$$

with the algebra element $\mathcal{A}_{3,2} = (\mathbf{1}, 0) + (\mathbf{8}, 2)$.

Continuing Classical Embeddings

In the same way that we obtained the main duality for unitary groups via non-abelian anyon condensation; namely, Eqn. (3.176) in the last section, we can find additional dualities based on other groups as long as they participate in some conformal embedding. The list of conformal embeddings can be found in [50], which we use in the following.

Let us start this discussion by recalling the conformal embeddings based on Spin groups studied in [8, 9] which are the next natural examples to consider:

$$SO(N)_K \times SO(K)_N \hookrightarrow Spin(NK)_1, \quad N \text{ even, } K \text{ even}, \tag{3.191}$$

$$Spin(N)_K \times SO(K)_N \hookrightarrow Spin(NK)_1, \quad N \text{ even, } K \text{ odd}, \tag{3.192}$$

$$Spin(N)_K \times Spin(K)_N \hookrightarrow Spin(NK)_1, \quad N \text{ odd, } K \text{ odd}. \tag{3.193}$$

These conformal embeddings yield the following standard 3D TQFT duality interpretation, obtained by the common center argument in accordance with [8, 9]:

$$Spin(N)_K \cong \frac{Spin(NK)_1 \times Spin(K)_{-N}}{\mathbb{Z}_2}, \quad N \text{ odd, } K \text{ odd} \tag{3.194}$$

$$Spin(N)_K \cong Spin(NK)_1 \times SO(K)_{-N}, \quad N \text{ even, } K \text{ odd} \tag{3.195}$$

16. To make this precise we would have to check the modular S-matrix, F-symbols and R-symbols, but the previous consistency conditions do not provide us with these, and we need external sources to point us to what the result should be.

$$SO(N)_K \cong \frac{Spin(NK)_1 \times Spin(K)_{-N}}{B}, \quad N \text{ odd, } K \text{ even} \tag{3.196}$$

$$SO(N)_K \cong \frac{Spin(NK)_1 \times SO(K)_{-N}}{\mathbb{Z}_2}, \quad N \text{ even, } K \text{ even,} \tag{3.197}$$

where B above is such that $B = \mathbb{Z}_2 \times \mathbb{Z}_2$ for $k = 0 \mod 4$ and $B = \mathbb{Z}_4$ for $k = 2 \mod 4$. These dualities (derived in [8]) may be interpreted as solving for the cosets as in Eqn. (3.61). If we invert these expressions into the initial ones (3.60), which exhibit the embeddings of the two factors into the bigger algebra as we did in the unitary case, we add the dualities

$$Spin(NK)_1 = \frac{SO(N)_k \times SO(k)_N}{\mathcal{A}_{N,k}}, \quad N \text{ even, } K \text{ even,} \tag{3.198}$$

$$Spin(NK)_1 = \frac{Spin(N)_k \times SO(k)_N}{\mathcal{A}_{N,k}}, \quad N \text{ even, } K \text{ odd,} \tag{3.199}$$

$$Spin(NK)_1 = \frac{Spin(N)_k \times Spin(k)_N}{\mathcal{A}_{N,k}}, \quad N \text{ odd, } K \text{ odd,} \tag{3.200}$$

which generically involve gauging by a non-invertible symmetry. We verify this in Section 3.6.2 in the $N = k = 3$ case, which is the simplest example of the above dualities that involve non-invertible anyon condensation.

A similar story holds for the dualities and embeddings associated with symplectic groups [8]:

$$USp(2N)_k \times USp(2k)_N \hookrightarrow Spin(4Nk)_1, \tag{3.201}$$

which have the 3D TQFT duality interpretation

$$USp(2N)_k \cong \frac{Spin(4Nk)_1 \times USp(2k)_{-N}}{\mathbb{Z}_2} \longleftrightarrow Spin(4NK)_1 \cong \frac{USp(2N)_k \times USp(2k)_N}{\mathcal{A}_{N,k}}, \tag{3.202}$$

where the left duality can be obtained by the common-center argument, as in [8]. The right duality is obtained following the arguments outlined above both in the unitary and Spin

cases, and it can be readily verified in the case $N = 2$, $k = 1$ where both sides are related by abelian anyon condensation. The gauging on the right duality is generically by a non-invertible symmetry, however, as the next simplest case $N = k = 2$ already shows. In the product $USp(4)_2 \times USp(4)_2$ there are both abelian and non-abelian bosons, but it can be checked that no abelian gauging is sufficient to give $Spin(16)_1$ back.

In the previous examples the standard form of the cosets (3.175), (3.194)-(3.197) and the left duality on (3.202) studied in [7–9] all involve gauging by an abelian symmetry. However, it is well-known that there is yet an additional infinite series of conformal embeddings with a tensoring of two affine lie algebras embedding into a bigger algebra [50]. Namely:

$$SO(N)_4 \times SU(2)_N \hookrightarrow USp(2N)_1. \tag{3.203}$$

This is an interesting example, as suppose we tried to follow the same logic as in the aforementioned "standard coset dualities" and try to isolate $SU(2)_N$ in terms of $USp(2N)_1$ and $SO(N)_{-4}$, and running the common center procedure. For $N = 2$ there are no novelties and we find $SU(2)_2 \cong USp(4)_1 \times U(1)_{-4}/\mathbb{Z}_2$.[17] However, already at $N = 3$ we observe that there is no abelian boson in the spectrum of $USp(6)_1 \times SO(3)_{-4}$, so the common center procedure manifestly does not work for this value of N.

The cure to the puzzle just mentioned is clear based on what we have studied so far in this work, and it is to extend the common center procedure and allow for gauging by non-invertible symmetries. Indeed, $USp(6)_1 \times SO(3)_{-4}$ has two non-abelian bosons in its spectrum, and we can condense them and find $SU(2)_3$ correspondingly. We study the details of this procedure in Section 3.6.2. In general then, we have the duality

$$SU(2)_N \cong \frac{USp(2N)_1 \times SO(N)_{-4}}{\mathcal{A}_N}, \tag{3.204}$$

17. Here we have used that $SO(2)_k \cong U(1)_k$.

where as the prior example shows, we must allow for the gauging of a non-invertible one-form symmetry on the right-hand side.

Of course, as we did previously for the other conformal embeddings, we can still apply the coset inversion theorem and write the duality implied by (3.60). This gives:

$$USp(2N)_1 \cong \frac{SU(2)_N \times SO(N)_4}{\mathcal{A}_N}, \tag{3.205}$$

and as above, for $N = 2$ the gauging is by an abelian symmetry, but at $N = 3$ we already need non-abelian anyon condensation to make the duality valid.

3.5.2 Further Conformal Embeddings

Now we move to discuss the rest of the conformal embeddings, with a focus on those that involve non-invertible symmetries. A list of the conformal embeddings can be found in [50]. We begin considering conformal embeddings with a product of two affine lie algebras in the denominator, as in the previous subsection, but we study those associated to exceptional Lie algebras. These embeddings have been previously studied in [31], and here we extend and understand the associated dualities in terms of non-invertible symmetries. The subset of these embeddings for which non-abelian anyon condensation is necessary to understand the dualities are

$$\begin{aligned}
&SU(2)_1 \times SU(2)_3 \hookrightarrow (G_2)_1, \qquad SU(2)_1 \times USp(6)_1 \hookrightarrow (F_4)_1, \qquad SU(3)_1 \times SU(3)_2 \hookrightarrow (F_4)_1,\\
&SO(3)_4 \times (G_2)_1 \hookrightarrow (F_4)_1, \qquad SU(2)_3 \times (F_4)_1 \hookrightarrow (E_7)_1, \qquad USp(6)_1 \times (G_2)_1 \hookrightarrow (E_7)_1,\\
&SU(2)_7 \times (G_2)_2 \hookrightarrow (E_7)_1, \qquad SU(3)_2 \times (G_2)_1 \hookrightarrow (E_6)_1,
\end{aligned} \tag{3.206}$$

Here we recognize the example $SU(2)_1 \times SU(2)_3 \hookrightarrow (G_2)_1$ we elaborated upon in Section 3.1.1 and in Section 3.3. Basically the same argument follows through in all of

these embeddings. Let us quickly recall this argument in an alternative example. For instance, if we take the third example in the first line and try to isolate $SU(3)_2$ we obtain $SU(3)_2 \cong (F_4)_1 \times SU(3)_{-1}$, with no further gauging on the right-hand side and everything is in order. If we instead try to isolate $SU(3)_1$, as explained previously there is no abelian common center to gauge by, but we still have to take into account non-abelian anyon condensation, and we obtain

$$SU(3)_1 \cong \frac{(F_4)_1 \times SU(3)_{-2}}{\mathcal{Z}(\mathbf{Fib})}, \tag{3.207}$$

where by $\mathcal{Z}(\mathbf{Fib})$ we mean an algebra object that can be traced back to a Lagrangian algebra responsible for gauging away $(G_2)_1 \times (G_2)_{-1}$ or $(F_4)_1 \times (F_4)_{-1}$ down to the trivial theory as in Section 3.1.1, for which reason we interpret it as gauging by a Drinfeld center of a Fibonacci fusion category. An analogous example of this same form was verified in detail by a direct non-abelian anyon condensation computation in Section 3.4.1.

All of the conformal embeddings in (3.206) yield dualities that can be obtained by the same arguments, and with one exception, in all of them we gauge by some Fibonacci Drinfeld center. The only exception is the first example in the third line, where

$$(E_7)_1 \cong \frac{SU(2)_7 \times (G_2)_2}{\mathcal{Z}\big((G_2)_2\big)}, \tag{3.208}$$

which is however obtained by the same arguments.

We discuss now those conformal embeddings with a simple group, or single affine Lie algebra in the denominator of the conformal embedding, such as in the $SU(3)_1/SU(2)_4$ example. We clearly cannot use the same arguments that were used to obtain the "standard coset form" of the dualities, since now we do not have two factors in the denominator. That is, we will not have an analog of expressions such as (3.175) or their counterparts for algebras other than unitary. However, we still have an analog of the dualities in the form outlined in

this work, Eqn. (3.176). Indeed, this is tantamount to using (3.60) with $\mathcal{C}$ describing the trivial theory. In the example $SU(3)_1/SU(2)_4$ this is nothing but the statement that we can gauge $SU(2)_4$ by some algebra to obtain $SU(3)_1$. Indeed, it is well-known that

$$SU(3)_1 \cong SU(2)_4/\mathbb{Z}_2. \tag{3.209}$$

Clearly, the general story for an arbitrary conformal embedding will be essentially the same, but where we allow to gauge by a non-invertible symmetry as per (3.60).

With the previous remarks in mind let us summarize a few results. Exploring the conformal embeddings, we find the following infinite families of dualities

$$Spin(N^2-1)_1 \cong \frac{SU(N)_N}{\mathcal{A}_N} \tag{3.210}$$

$$SU\big(N(N\pm 1)/2\big)_1 \cong \frac{SU(N)_{N\pm 2}}{\mathcal{A}_N} \tag{3.211}$$

$$Spin\big(N(N-1)/2\big)_1 \cong \frac{Spin(N)_{N-2}}{\mathcal{A}_N} \tag{3.212}$$

$$Spin\big((N^2+N-2)/2\big)_1 \cong \frac{Spin(N)_{N+2}}{\mathcal{A}_N}, \tag{3.213}$$

Notice that the first of these corresponds to the conformal embedding used in [1] in the context of 2D CFT to propose the IR phases of 2D Adjoint QCD. Here we use the conformal embedding to establish a duality of 3D TQFTs. There are various checks that can be performed in the series above. The case $N = 4$ in (3.213) gives $Spin(9)_1 \cong Spin(4)_6$, which we verify by a explicit computation in Section 3.6.2 and is actually equivalent to the duality (3.200) for $N = 3$.

We finish mentioning the isolated cases (i.e., no infinite family) of the conformal embeddings where there is a single affine Lie algebra in the denominator. The complete list of

these cases can be obtained by reading [50], and yields the following list of dualities:

$$SU(16)_1 \cong Spin(10)_4/\mathcal{A}, \quad SU(27)_1 \cong (E_6)_6/\mathcal{A}, \quad Spin(70)_1 \cong SU(8)_{10}/\mathcal{A}, \tag{3.214}$$

$$USp(4)_1 \cong SU(2)_{10}/\mathcal{A}, \quad USp(20)_1 \cong SU(6)_6/\mathcal{A}, \quad (E_6)_1 \cong SU(3)_9/\mathcal{A}, \tag{3.215}$$

$$(E_7)_1 \cong SU(3)_{21}/\mathcal{A}, \quad (G_2)_1 \cong SU(2)_{28}/\mathcal{A}, \quad Spin(16)_1 \cong Spin(9)_2/\mathcal{A}, \tag{3.216}$$

$$Spin(128)_1 \cong Spin(16)_{16}/\mathcal{A}, \quad Spin(42)_1 \cong USp(8)_7/\mathcal{A}, \quad USp(32)_1 \cong Spin(12)_8/\mathcal{A}, \tag{3.217}$$

$$Spin(78)_1 \cong (E_6)_{12}/\mathcal{A}, \quad Spin(133)_1 \cong (E_7)_{18}/\mathcal{A} \quad Spin(248)_1 \cong (E_8)_{30}/\mathcal{A}, \tag{3.218}$$

$$USp(14)_1 \cong USp(6)_5/\mathcal{A}, \quad USp(56)_1 \cong (E_7)_{12}/\mathcal{A}, \quad (E_8)_1 \cong USp(4)_{12}/\mathcal{A}, \tag{3.219}$$

$$Spin(26)_1 \cong (F_4)_3/\mathcal{A}, \quad Spin(52)_1 \cong (F_4)_9/\mathcal{A}, \quad Spin(14)_1 \cong (G_2)_4/\mathcal{A}, \tag{3.220}$$

$$(E_6)_1 \cong (G_2)_3/\mathcal{A}. \tag{3.221}$$

The first example on the second line, $USp(4)_1 \cong SU(2)_{10}/\mathcal{A}$, is a known example that has been studied in the literature mainly with the aim of testing and understanding the formalism of non-abelian anyon condensation (see for example [37, 51, 106–108]). The last example in this list $(E_6)_1 \cong (G_2)_3/\mathcal{A}$ can be verified very easily by a non-abelian anyon condensation computation, which we outline in Section 3.6.2.

Three-State Potts Model Maverick Coset from Level-Rank Duality

In this subsection we show the simplest duality implied by the Maverick cosets, Eqn. (3.75), but instead of doing the calculation directly, we will first use our knowledge of the conformal embeddings to simplify the calculation. To understand the three-state Potts Model, we make

use of the first of the embeddings in (3.206), and write

$$SU(2)_3 \cong (G_2)_1 \times SU(2)_{-1}. \tag{3.222}$$

It is also straightforward to check the duality $U(1)_6 \cong SU(3)_1 \times SU(2)_{-1}$, so that we have

$$SU(2)_3 \times U(1)_{-6} \cong SU(3)_{-1} \times (G_2)_1 \times SU(2)_{-1} \times SU(2)_1. \tag{3.223}$$

Now we can use the first embedding on the second line of (3.206), and use our knowledge of non-abelian anyon condensation to isolate $(G_2)_1$, obtaining:

$$(G_2)_1 \cong \frac{(F_4)_1 \times SO(3)_{-4}}{\mathcal{Z}(\mathbf{Fib})}. \tag{3.224}$$

This duality may be obtained from the arguments outlined previously, but it is simple and sufficiently interesting that we verify it by a direct non-abelian anyon condensation on the next subsection.

We also use the third embedding on the first line of (3.206) to claim

$$SU(3)_2 \cong (F_4)_1 \times SU(3)_{-1}. \tag{3.225}$$

These expressions allows us to introduce the first $SU(3)_{-1}$ factor on the right-hand side of (3.223) into the quotient given by (3.224), with the $\mathcal{Z}(\mathbf{Fib})$ denominator acting trivially on such $SU(3)_{-1}$ factor, and write

$$SU(2)_3 \times U(1)_{-6} \cong \frac{SU(3)_2 \times SO(3)_{-4}}{\mathcal{Z}(\mathbf{Fib})} \times SU(2)_{-1} \times SU(2)_1. \tag{3.226}$$

$SO(3)_4$		
Line label	Quantum Dimension	Conformal Weight
0	$d_0 = 1$	$h_0 = 0$
$2 \cong (4,0)$	$d_2 = (3+\sqrt{5})/2$	$h_2 = 1/5$
$4_1 \cong (2,4)$	$d_{4_1} = (1+\sqrt{5})/2$	$h_{4_1} = 3/5$
$4_2 \cong (3,3)$	$d_{4_2} = (1+\sqrt{5})/2$	$h_{4_2} = 3/5$

Table 3.11: $SO(3)_4$ data.

Finally, gauging the $\mathbb{Z}_2$ Drinfeld center $SU(2)_1 \times SU(2)_{-1}$ we obtain

$$\frac{SU(2)_3 \times U(1)_{-6}}{\mathbb{Z}_2} \cong \frac{SU(3)_2 \times SO(3)_{-4}}{\mathcal{Z}(\mathbf{Fib})}, \cong \frac{SU(3)_2 \times SU(2)_{-8}}{\mathcal{A}}, \tag{3.227}$$

which is indeed what we have obtained above using Maverick coset considerations instead of several conformal embeddings/exceptional level-rank duality manipulations. On the last line we have used that by definition $SO(3)_4 \cong SU(2)_8/\mathbb{Z}_2$.

Checking the $(G_2)_1 \cong \big((F_4)_1 \times SO(3)_{-4}\big)/\mathcal{Z}(\mathbf{Fib})$ Duality

This calculation arises when we prove the duality suggested by the simplest Maverick coset (3.75) using exceptional conformal embeddings. See the previous subsection. The spectrum of $(F_4)_1$ is that of $(G_2)_1$, but with the only non-trivial line having spin 3/5 instead of 2/5. We call ϕ the only non-trivial anyon of $(F_4)_1$, which obeys Fibonacci fusion rules. The spectrum of $SO(3)_4$ is shown in Table 3.11, and its non-trivial fusion rules are

$$\begin{aligned} &2 \times 2 = 0 + 2 + 4_1 + 4_2, \quad 2 \times 4_1 = 2 + 4_2, \quad 2 \times 4_2 = 2 + 4_1, \\ &4_1 \times 4_1 = 0 + 4_1, \quad 4_1 \times 4_2 = 2, \quad 4_2 \times 4_2 = 0 + 4_2. \end{aligned} \tag{3.228}$$

We first need to determine the bosons that condense. It is easy to verify that the only bosons in the product $(F_4)_1 \times SO(3)_{-4}$ are $(\phi, 4_1)$ and $(\phi, 4_2)$, which are non-abelian. From

the fusions

$$(\phi, 4_1) \times (\phi, 4_1) = (0,0) + (0,4_1) + (\phi,0) + (\phi,4_1), \tag{3.229}$$

$$(\phi, 4_1) \times (\phi, 4_2) = (0,2) + (\phi,2), \tag{3.230}$$

$$(\phi, 4_2) \times (\phi, 4_2) = (0,0) + (0,4_2) + (\phi,0) + (\phi,4_2), \tag{3.231}$$

it is clear that $(\phi, 4_1)$ and $(\phi, 4_2)$ cannot simultaneously condense, so me must make a choice. However, lines 4_1 and 4_2 are symmetric in $SO(3)_4$, so the choice is actually immaterial. We choose $(\phi, 4_1)$ to condense:

$$(\phi, 4_1) \longrightarrow 0 + (\phi, 4_1)_2. \tag{3.232}$$

The quantum dimension of $(\phi, 4_1)_2$ is $d_{(\phi,4_1)_2} = (1+\sqrt{5})/2$, so there is no further splitting allowed by conservation of the quantum dimension. Since $(\phi, 4_2)$ does not condense, we can also see from the above fusion rules that it does not split and $d_{(\phi,4_2)} = (3+\sqrt{5})/2$.

The quantum dimensions do not allow $(0, 4_1)$ and $(0, 4_2)$ to split, but in principle they allow for $(0, 2)$ to split. This is not the case, which can be verified from

$$(0,2) \times (0,2) = (0,0) + (0,2) + (0,4_1) + (0,4_2) \tag{3.233}$$

since no non-trivial bosons appear on the right-hand side. Since none of these anyons split, the fusion

$$(\phi, 4_1) \times (0, 4_1) = (\phi, 0) + (\phi, 4_1) \longrightarrow 0 + \ldots, \tag{3.234}$$

implies the identification $(\phi, 4_1)_2 \cong (0, 4_1)$, which in turn implies the confinement of such excitations.

We now consider the rest of the (ϕ, i) anyons that are not bosons. Start noticing that

$$(\phi, 2) \times (\phi, 2) = (0, 0) + (\phi, 4_1) + \ldots, \longrightarrow 0 + 0 + \ldots, \tag{3.235}$$

implies that $(\phi, 2)$ splits: $(\phi, 2) \to (\phi, 2)_1 + (\phi, 2)_2$. To assign quantum dimensions we can consider the fusion

$$(\phi, 2) \times (0, 2) = (\phi, 4_1) + \ldots \longrightarrow 0 + \ldots, \tag{3.236}$$

so $(0, 2)$ belongs to the restriction of $(\phi, 2)$. Let $(\phi, 2)_2$ be by definition the component that identifies with $(0, 2)$. The quantum dimensions must then be $d_{(\phi,2)_1} = (1 + \sqrt{5})/2$, and $d_{(\phi,2)_2} = (3 + \sqrt{5})/2$. With this knowledge it is now straightforward to take the fusions $(\phi, 2) \times (0, 4_2)$ and $(\phi, 2) \times (\phi, 4_2)$ and deduce the identifications $(\phi, 2)_1 \cong (0, 4_2)$ and $(\phi, 2)_2 \cong (\phi, 4_2)$ using the by-now usual arguments.

Finally, $(\phi, 0)$ is self-conjugate and cannot split. Moreover, the fusion

$$(\phi, 0) \times (0, 4_1) = (\phi, 4_1) + \ldots \to 0 + \ldots \tag{3.237}$$

implies the identification $(\phi, 0) \cong (0, 4_1)$, which in turn shows the confinement of such excitations.

To summarize, we have the following condensation pattern:

$$(0, 0) \to 0, \quad (0, 2) \to (0, 2), \quad (0, 4_1) \to (0, 4_1), \quad (0, 4_2) \to (0, 4_2), \tag{3.238}$$

$$(\phi, 0) \to (0, 4_1), \quad (\phi, 2) \to (0, 4_2) + (0, 2), \quad (\phi, 4_1) \to 0 + (0, 4_1), \quad (\phi, 4_2) \to (0, 2). \tag{3.239}$$

Studying the lifts implied by the previous restrictions to the anyons in the parent theory, we can check that the unconfined excitations are the vacuum and $(0, 4_2)$. These have indeed the correct quantum dimensions, fusion rules and spin to recognize the result as $(G_2)_1$.

3.6 Additional Comments and Results

3.6.1 Mathematical Results on Gauging, Cosets and Dualities

In this section we summarize some mathematical nomenclature and results from [24] that were claimed in Section 3.3.1 and allow a better understanding of it.

Local Algebra Modules and Cosets

Throughout the text we have given a rather physical picture of the ideas at play. Here we focus on a few more mathematical statements that are the basis for many claimed statements, mainly in Section 3.3. See below Chapter 4 for many of the definitions used here.

In the following, we have to recall that the TQFT obtained by the gauging of a one-form symmetry in a 3D TQFT described by some MTC $\mathcal{C}$, is given by the category $\mathcal{C}_{\mathcal{A}}^{\text{loc}}$ of local $\mathcal{A}$-modules for some special symmetric commutative Frobenius algebra object $\mathcal{A}$ over $\mathcal{C}$. The category $\mathcal{C}_{\mathcal{A}}^{\text{loc}}$ is again an MTC, so it appropriately describes a new 3D TQFT descending from the parent one described by $\mathcal{C}$. We stress that from the physics viewpoint the previous result does not necessarily restrict to the notion of gauging by some group-like symmetry, so the construction generically involves gauging by a non-invertible symmetry.

The primary focus of this section is to state and discuss the main result of [24] in our context. This result states that when a MTC $\mathcal{M}$ is written as the category of local $\mathcal{A}$-modules for some commutative symmetric special Frobenius algebra $\mathcal{A}$ in the direct product of two MTCs $\mathcal{C}$ and $\mathcal{M}'$:

$$\mathcal{M} \cong (\mathcal{C} \boxtimes \mathcal{M}')_{\mathcal{A}}^{\text{loc}}, \tag{3.240}$$

and if we require the algebra $\mathcal{A}$ in $\mathcal{C} \boxtimes \mathcal{M}'$ to be such that the only subobject of $\mathcal{A}$ of the form $a \times \mathbf{1}$ is $\mathbf{1} \times \mathbf{1}$, where $\mathbf{1}$ is the tensor unit, then there exists a commutative symmetric special Frobenius algebra $\mathcal{B}$ in the direct product $\mathcal{M} \boxtimes \overline{\mathcal{M}'}$, such that if we take the corresponding

category of local modules, we obtain

$$\mathcal{C} \cong (\mathcal{M} \boxtimes \overline{\mathcal{M}'})^{\mathrm{loc}}_{\mathcal{B}}. \tag{3.241}$$

The algebra $\mathcal{B}$ can in principle be computed from the categories $\mathcal{M}$ and $\mathcal{M}'$, and the modularity of $\mathcal{C}$ can actually be derived from that of $\mathcal{M}$ and $\mathcal{M}'$. In practice, it is often found to be more useful to inspect for a Frobenius algebra object (a set of condensing bosons), and carry the non-abelian anyon condensation procedure.

The previous is often sufficient for most practical applications, but it is important to point out that if we do not require $\mathcal{A}$ to fulfill the condition below Eqn. (3.240), then a version of the previous theorem still holds. Namely, there exist certain algebras $\mathcal{T}_1$ and $\mathcal{T}_2$ such that if we take local modules:

$$\mathcal{C}^{\mathrm{loc}}_{\mathcal{T}_1} \cong (\mathcal{M} \boxtimes \overline{\mathcal{M}'})^{\mathrm{loc}}_{\mathcal{T}_2}. \tag{3.242}$$

Essentially, what the requirement over $\mathcal{A}$ below (3.240) does is to trivialize the gauging on the left-hand side.

The previous mathematical results have a clear interpretation in physics. In the standard coset construction, Eqn. (3.240) is the statement that an affine lie algebra embeds in another one, with the corresponding TQFTs described by the MTCs $\mathcal{M}'$ and $\mathcal{M}$ respectively. The coset theory, whose construction we reviewed in the CFT context in Section 3.2, is then described in the corresponding TQFT setup by the MTC $\mathcal{C}$ whose content is in principle determined by the data of $\mathcal{M}$ and $\mathcal{M}'$ via (3.241). Notice however that the previous theorem in some sense generalizes the standard GKO coset construction since nowhere above it was needed that $\mathcal{M}$ or $\mathcal{M}'$ were MTCs associated with those of an affine Lie algebra. They may be arbitrary MTCs (see [114] for some work on generalizing the coset construction to higher spin currents in the context of 2D CFT). More importantly, a second point of generalization,

stressed above, is that $\mathcal{B}$ in (3.241) does not necessarily have to correspond to some abelian gauging. As seen in the previous section, one instance where this phenomenon takes place would be the Maverick cosets [35–37, 87, 105].

One form of the statement that a duality exists follows from this mathematical perspective when the same MTC $\mathcal{C}$, not (necessarily) having a path-integral or gauge theory description, appears "connecting" two different pairs of MTCs $(\mathcal{M}_1, \mathcal{M}_1')$ and $(\mathcal{M}_2, \mathcal{M}_2')$ having such a description. That is:

$$\mathcal{M}_1 \cong (\mathcal{C} \boxtimes \mathcal{M}_1')^{\mathrm{loc}}_{\mathcal{A}_1}, \quad \text{and} \quad \mathcal{M}_2 \cong (\mathcal{C} \boxtimes \mathcal{M}_2')^{\mathrm{loc}}_{\mathcal{A}_2}, \tag{3.243}$$

for some Frobenius algebras $\mathcal{A}_1$ and $\mathcal{A}_2$. By the theorem above we can isolate $\mathcal{C}$ in two different ways, and write

$$(\mathcal{M}_1 \boxtimes \overline{\mathcal{M}_1'})^{\mathrm{loc}}_{\mathcal{B}_1} \cong (\mathcal{M}_2 \boxtimes \overline{\mathcal{M}_2'})^{\mathrm{loc}}_{\mathcal{B}_2} \tag{3.244}$$

for some Frobenius algebras $\mathcal{B}_1$ and $\mathcal{B}_2$. For instance, these could correspond to two different descriptions of the parafermions. One of them could be a Maverick coset description, as in Section 3.3.2, and the other could be the standard coset description $SU(2)_k \times U(1)_{-2k}/\mathbb{Z}_2$ [5]. This is essentially the path we followed for the first infinite family of Maverick dualities studied in Section 3.3.2. It could also be that $\mathcal{C}$ itself admits a field theory description, in which case (3.241) allows us to express such a description in terms of a different one based on $\mathcal{M}$ and $\mathcal{M}'$. The latter is what happens with the conformal embedding $SU(N)_k \times SU(k)_N \hookrightarrow SU(Nk)_1$ reviewed at the end of Section 3.2. Here we can take a standard Chern-Simons description for $SU(k)_N$, but we can take an alternative one given by the right-hand side of (3.241). The latter is nothing but the $SU(Nk)_1 \times SU(N)_{-k}/\mathbb{Z}_N$ expression of the same theory, which is essentially the content of the duality (3.43).

The form (3.242) of the theorem is sometimes useful. To illustrate this [24], we can

consider in the contexts of the conformal embeddings:

$$\frac{(E_8)_1}{SU(3)_6 \times SU(2)_{16}}, \tag{3.245}$$

which implies that $(E_8)_1$ can be written as in (3.240) with $\mathcal{C} = SU(3)_6$ and $\mathcal{M}' = SU(2)_{16}$. In this case we need to use (3.242), and fortunately the gaugings are abelian so we can easily verify that

$$SU(3)_6/\mathbb{Z}_3 \cong (E_8)_1 \times SU(2)_{-16}/\mathbb{Z}_2. \tag{3.246}$$

That is, both sides involve a non-trivial gauging, which is the main point of the theorem in the form (3.242).

3.6.2 Further Examples on Non-Abelian Anyon Condensation

In this section we present in detail various check example computations of non-invertible anyon condensation that pertain to the global subject of the chapter but for the sake of organization we have summarized here instead. The reader may want to first look at the beginning of Section 3.4 where we outline the rules that we use below to verify such examples on non-invertible anyon condensation.

$(G_2)_1 \times (G_2)_{-1} \longrightarrow \mathbb{1}$

This is a rather trivial example of condensation by a non-abelian anyon that condenses the theory to the trivial theory. The example is trivial in the sense that the theory is of the form $G_k \times G_{-k}$, which is known to condense to the vacuum [47, 50, 80]. Equivalently, a gapped boundary exists that separates the trivial theory from $G_k \times G_{-k}$, which hosts topological degrees of freedom described by the G_k/G_k topological coset. For completeness, we write here the condensation computation explicitly, since this particular example is easy and it appears twice in this work, both in our example in Section 3.1.1 and in the derivation of the

three-state Potts model Maverick duality from exceptional conformal embeddings.

The spectrum of $(G_2)_1$ is shown in Table 3.1. The lines in the double are denoted $(0,0)$, $(\phi,0)$, $(0,\phi)$, and (ϕ,ϕ). Here we have abused notation and called ϕ to the non-trivial entry in both $(G_2)_1$ and $(G_2)_{-1}$, but where there is no ambiguity as we can tell them apart by their position in the ordered pair.

Assume that the unique non-trivial boson (ϕ,ϕ) condenses. That is:

$$(\phi,\phi) \longrightarrow 0 + (\phi,\phi)_2, \tag{3.247}$$

or in mathematical terms, the algebra that we condense is

$$\mathcal{A} = (0,0) + (\phi,\phi), \tag{3.248}$$

which is nothing but the Lagrangian algebra given by the diagonal anyons that always exists in a theory of the form $\mathcal{C} \times \overline{\mathcal{C}}$, with $\mathcal{C} = (G_2)_1$ here.

By conservation of the quantum dimension $d_{(\phi,\phi)_2} = \frac{1+\sqrt{5}}{2}$, implying that (ϕ,ϕ) can only split into two lines. Further, since (ϕ,ϕ) and 0 are self-conjugate, it follows that $(\phi,\phi)_2$ also is self-conjugate. It is easy to check that the other lines $(\phi,0)$ and $(0,\phi)$ cannot split and are also self-conjugate.

Since (ϕ,ϕ) condenses, the fusion rules

$$(\phi,\phi) \times (0,\phi) = (\phi,0) + (\phi,\phi) \longrightarrow 0 + \ldots, \tag{3.249}$$

$$(\phi,\phi) \times (\phi,0) = (0,\phi) + (\phi,\phi) \longrightarrow 0 + \ldots \tag{3.250}$$

imply that (ϕ,ϕ) contains in its restriction the conjugates of $(0,\phi)$ and $(\phi,0)$, which are however self-conjugate. Since their quantum dimensions are $d_{(0,\phi)} = d_{(\phi,0)} = (1+\sqrt{5})/2$ they cannot be identified to the vacuum, and must be identified with $(\phi,\phi)_2$. In other words,

we have the identification

$$(0,\phi) \cong (\phi,0) \cong (\phi,\phi)_2. \tag{3.251}$$

These labels therefore lift to lines in the parent theory with different topological spins, and so it follows that all such excitations confine. The only non-trivial line in the gauged theory is thus the vacuum, obtaining the expected result.

$Spin(9)_1 \cong \big(Spin(3)_3 \times Spin(3)_3\big)/\mathcal{A}$

In this subsection we consider an example in the infinite family of conformal embeddings corresponding to spin groups:

$$\frac{Spin(Nk)_1}{Spin(N)_k \times Spin(k)_N}, \text{ for } \quad k, N \text{ odd.} \tag{3.252}$$

This family of embeddings is intimately related to level-rank dualities for orthogonal groups (see [8,9,32]), and furthermore conformal embeddings with spin groups in the numerator have the very important property of describing the low-energy dynamics of 2D QCD [1,90,115].[18][19] For the specific case $N = k = \nu$ the previous conformal embeddings are also intrinsically related to anomalous theories for time-reversal symmetry that realize a value ν for such anomaly [32, 116] (once we add fermionic invertible factors).

We will consider the example $N = k = 3$ as this gives rise to the simplest example where the numerator ($Spin(9)_1$) has interesting non-abelian fusion rules; namely, Ising fusion rules. In this case, there exists the exceptional isomorphism of chiral algebras $Spin(3)_3 \cong SU(2)_6$. So the task consists of condensing some (non-abelian) boson(s) in $SU(2)_6 \times SU(2)_6$, and matching the unconfined lines of the condensed theory with those of $Spin(9)_1$. The spectrum

18. More precisely, fermionic conformal embeddings $SO(N)_1/H_{\tilde{k}}$ describe the low-energy dynamics of 2D QCD with gauge group H and $\tilde{k}$ the index of the embedding, which in this case corresponds to the Dynkin index of the representation in which the fermions transform.

19. Rigorously speaking this result is conjectural, but supported by highly non-trivial evidence on its support like the matching of anomalies.

$SU(2)_6$		
Line label	Quantum Dimension	Conformal Weight
0	$d_0 = 1$	$h_0 = 0$
1	$d_1 = \sqrt{2+\sqrt{2}}$	$h_1 = 3/32$
2	$d_2 = 1+\sqrt{2}$	$h_2 = 1/4$
3	$d_3 = \sqrt{2(2+\sqrt{2})}$	$h_3 = 15/32$
4	$d_4 = 1+\sqrt{2}$	$h_4 = 3/4$
5	$d_5 = \sqrt{2+\sqrt{2}}$	$h_5 = 35/32$
6	$d_6 = 1$	$h_6 = 3/2$

Table 3.12: $SU(2)_6$ data.

of $SU(2)_6$ is shown in Table 3.12, and the fusion rules can be read from (3.92). The lines in the product theory are denoted as (i, j), where $i, j = 0, \ldots, 6$ is the label of a single factor.

There are four bosons in the product theory $SU(2)_6 \times SU(2)_6$: $(0,0)$, $(2,4)$, $(4,2)$, and $(6,6)$. The latter is the "common center" of the product, which is abelian. The remaining two non-trivial bosons are non-abelian. Merely condensing the common center in $Spin(4)_6 \cong SU(2)_6 \times SU(2)_6$ leads to the well-known answer $SO(4)_6$. Then, as expected, one needs to take at least one of the non-abelian bosons to condense in order to obtain $Spin(9)_1$.

Assume that $(2,4)$ condenses; that is:

$$(2,4) \longrightarrow 0 + \ldots \tag{3.253}$$

It is easy to see that since

$$(0,a) \times (0,a) = (0,0) + \sum_i (0,a_i), \tag{3.254}$$

the lines $(0,a)$ and $(a,0)$ do not split and are self-conjugate. With this observation, consider the fusion

$$(0,2) \times (2,4) = (2,2) + (2,4) + (2,6) \longrightarrow 0 + \ldots, \tag{3.255}$$

which implies that $(0,2)$ belongs to the restriction of $(2,4)$. This means that $(2,4)$ restricts

as

$$(2,4) \longrightarrow 0 + (2,4)_2 + (2,4)_3, \tag{3.256}$$

with $(2,4)_2 \cong (0,2)$, and since $d_{(0,2)} = 1+\sqrt{2}$ by conservation of the quantum dimension we must have that $d_{(2,4)_3} = 1 + \sqrt{2}$. Notice that a priori the quantum dimension is sufficiently large to allow $(2,4)$ to split into four lines, but this is ruled out by the fusion

$$(2,4) \times (2,4) = (0,0) + (2,4) + (4,2) + \ldots, \tag{3.257}$$

since there are not enough bosons on the right side that could potentially condense to accommodate four vacua. Furthermore, we also see from this fusion rule that $(2,4)$ can split as (3.256) only if $(4,2)$ also condenses. Thus we have deduced that if $(2,4)$ condenses, $(4,2)$ also condenses.

By a similar argument, $(2,0)$ also belongs to the restriction of $(2,4)$. However, $(0,2)$ and $(2,0)$ cannot be identified with each other. To see this, consider the fusion with $(0,6)$ which has unit quantum dimension:

$$(0,6) \times (2,4) = (2,2) = (0,2) \times (2,0) \stackrel{!}{=} (0,2) \times (0,2) = (0,0) + (0,2) + (0,4) \tag{3.258}$$

$$= (0,6) + \ldots, \tag{3.259}$$

where in the third equality in the first row we have (wrongly) assumed that $(0,2)$ and $(2,0)$ identify, and in the second row we have first restricted $(2,4)$ on the left-hand side and isolated the trivial fusion between the vacuum and $(0,6)$. Since both rows must agree, $(0,6)$ must identify with some line in the last equality of the first row, but only one line has unit quantum dimension; namely, the vacuum. This identification, however, is equivalent to the statement that $(0,6)$ condenses, which is not possible since it does not have the correct topological spin to do so. We thus reach the conclusion that $(0,2)$ and $(2,0)$ cannot be identified with each

other.

Gathering this knowledge, we find the restrictions of $(2,4)$ and $(4,2)$ (the latter follows from the same arguments, once we know it condenses as we have shown above):

$$(2,4) \longrightarrow 0 + (0,2) + (2,0), \tag{3.260}$$

$$(4,2) \longrightarrow 0 + (0,2) + (2,0). \tag{3.261}$$

We now deduce a few more identifications. First:

$$(2,4) \times (6,6) = (4,2) \Longrightarrow (6,6) + \ldots = 0 + \ldots, \tag{3.262}$$

where we have used the restrictions of $(2,4)$ and $(4,2)$, and then isolated the fusion of $(6,6)$ with the vacuum on the left-hand side. Only the vacuum on the right-hand side has unit quantum dimension that can match that of $(6,6)$. Thus, we have deduced that $(6,6)$ condenses: $(6,6) \to 0$.

In passing, notice that what we have just found is that the condensing algebra is

$$\mathcal{A} = (0,0) + (2,4) + (4,2) + (6,6), \tag{3.263}$$

and in these terms what we want to show is that

$$Spin(9)_1 \cong \frac{Spin(3)_3 \times Spin(3)_3}{\mathcal{A}}, \tag{3.264}$$

for the algebra object $\mathcal{A}$ in (3.263) above.

Now $(4,0) \times (0,2) = (4,2) \to 0 + \ldots$, but $(0,a)$ and $(a,0)$ are self-conjugate for any a, and thus we must have the identifications $(2,0) \cong (0,4)$, $(0,2) \cong (4,0)$. Similarly, $(2,6) \times (6,6) = (4,0)$, but $(6,6)$ restricts only to the vacuum, and thus we have the identification

$(2,6) \cong (0,4)$. By similar arguments, we find, overall: $(2,6) \cong (4,0) \cong (0,2) \cong (6,4)$, and $(6,2) \cong (0,4) \cong (2,0) \cong (4,6)$. It is straightforward to check from these identifications that the corresponding labels confine on the child theory.

The simple currents $(0,6)$ and $(6,0)$ identify with each other since $(0,6) = (6,6) \times (6,0)$ and $(6,6)$ condenses. Using that $(4,4) = (6,6) \times (2,2)$ we obtain $(2,2) \cong (4,4)$, and using that $(2,2) = (0,6) \times (2,4)$ we obtain the restriction:

$$(2,2) \longrightarrow (0,6) + (2,0) + (0,2). \tag{3.265}$$

Notice that $(0,6)$ always lifts to anyons in the parent theory that share the same topological spin, and thus it does not confine.

We now study lines (a,b) that have a and b odd integers. First, notice that since

$$(1,1) \times (1,1) = (0,0) + (0,2) + (2,0) + (2,2), \tag{3.266}$$

(1,1) cannot split. A similar argument shows that $(1,5)$ also does not split. Since $(1,1) \times (6,6) = (5,5)$ and $(1,5) \times (6,6) = (5,1)$ and $(6,6)$ condenses, we find the identifications $(1,1) \cong (5,5)$ and $(1,5) \cong (5,1)$. Furthermore:

$$(1,1) \times (1,5) = (2,4) + \ldots \longrightarrow 0 + \ldots, \tag{3.267}$$

which means $(1,5)$ is conjugate to $(1,1)$ in the child theory, but $(1,1)$ is self-conjugate, which implies the further identifications $(1,1) \cong (1,5) \cong (5,1) \cong (5,5)$.

To make progress, study now the fusion rules

$$(3,3) \times (3,3) = (0,0) + (2,4) + (4,2) + (6,6) + \ldots \longrightarrow 0 + 0 + 0 + 0 + \ldots \tag{3.268}$$

$$(1,1) \times (3,3) = (2,2) + (2,4) + (4,2) + (4,4) \longrightarrow 0 + 0 + \ldots \tag{3.269}$$

The first fusion rule allows two possibilities: either $(3,3)$ splits into four distinct labels or one label with multiplicity two. The first possibility is however not consistent with (3.269), so it follows that $(3,3)$ restricts as $(3,3) \to 2(1,1)$ for consistency in between both (3.268) and (3.269). This restriction also shows that $(1,1)$ confines, as it lifts to anyons in the parent theory with different topological spins.

Consider now the rest of the lines with two odd entries. In particular, let us consider the fusion rule

$$(1,1) \times (1,3) = (0,2) + (0,4) + (2,2) + (2,4) \longrightarrow 0 + \ldots, \tag{3.270}$$

which implies that $(1,1)$ belongs in the restriction of $(1,3)$ (a similar statement holds for $(3,1)$). In turn, by conservation of the quantum dimension, this implies that $(1,3)$ has a restriction of the form:

$$(1,3) \longrightarrow (1,3)_1 + (1,1), \tag{3.271}$$

with $d_{(1,3)_1} = \sqrt{2}$. Clearly, there is no sufficient quantum dimension for further splitting.

Using the standard arguments: $(1,3)\times(6,6) = (5,3) \Rightarrow (1,3) \cong (5,3)$ and $(3,1)\times(6,6) = (3,5) \Rightarrow (3,1) \cong (3,5)$, meaning the restrictions we have to consider are

$$(1,3) \longrightarrow (1,3)_1 + (1,1), \tag{3.272}$$

and

$$(3,1) \longrightarrow (3,1)_1 + (1,1). \tag{3.273}$$

It is straightforward to check that the three fusion rules $(1,3) \times (1,3)$, $(1,3) \times (3,1)$, and $(3,1) \times (3,1)$ contain two vacua after restriction. Since we know $(1,1)$ is self-conjugate, this means that $(1,3)_1$ and $(3,1)_1$ must both be self-conjugate, but conjugate to each other as well. We have to then identify $(1,3)_1 \cong (3,1)_1$. Clearly, the previous identifications do not lead to confinement of $(1,3)_1$.

$Spin(9)_1$		
Line label	Quantum Dimension	Conformal Weight
0	$d_0 = 1$	$h_0 = 0$
1	$d_1 = 1$	$h_1 = 1/2$
2	$d_2 = \sqrt{2}$	$h_2 = 9/16$

Table 3.13: $Spin(9)_1$ data.

Finally, the lines in $SU(2)_6 \times SU(2)_6$ of the form $(2m, 2n+1)$ with m, n integer confine. For example, $(0,1) \times (6,6) = (6,5)$, and since $(6,6)$, condenses we have to identify $(0,1) \cong (6,5)$. However, these expressions lift to anyons of different topological spins and thus confine. The same argument holds for the rest of such lines.

All in all, the spectrum of unconfined lines that we have found is given by $(0,0)$, $(6,0)$, and $(1,3)_1$ with topological spins and quantum dimensions that match those of $Spin(9)_1$, in accordance with the conformal embedding $Spin(3)_3 \times Spin(3)_3 \hookrightarrow Spin(9)_1$. The previous can be readily verified by looking at the spectrum of $Spin(9)_1$, presented in Table 3.13.

In the current example the child theory has interesting fusion rules (Ising fusion rules), and the condensation procedure is also sufficiently straightforward to deduce them explicitly from the parent theory. We turn to do this next.

First, $(0,0)$ and $(6,0)$ descend trivially from the parent theory so they maintain $\mathbb{Z}_2$ fusion rules:

$$(0,6) \times (0,6) = (0,0). \tag{3.274}$$

To deduce the fusion rule $(0,6) \times (1,3)_1$ we fuse $(0,6)$ with $(1,3)$:

$$\begin{aligned}(0,6) \times (1,3) = (1,3) &= (1,3)_1 + (1,1) \\ &= (0,6) \times (1,3)_1 + (0,6) \times (1,1) = (0,6) \times (1,3)_1 + (1,5) \cong (0,6) \times (1,3)_1 + (1,1),\end{aligned} \tag{3.275}$$

where in the first row we have performed the fusion in the parent theory and restricted the

result, while in the second row we have first restricted on the left-hand side, then performed the fusions from the lines that descend trivially from the parent, and then used the identification $(1,5) \cong (1,1)$. Since both rows must match, we have the fusion rule in the child theory:

$$(0,6) \times (1,3)_1 = (1,3)_1. \tag{3.276}$$

Deducing $(1,3)_1 \times (1,3)_1$ is slightly more complicated. We consider the fusion $(1,3) \times (1,3)$ in the parent theory:

$$(1,3) \times (1,3) = (0,0) + (0,2) + (0,4) + (0,6) + (2,0) + (2,2) + (2,4) + (2,6) \tag{3.277}$$

$$= (1,3)_1 \times (1,3)_1 + (1,3)_1 \times (1,1) + (1,1) \times (1,3)_1 + (1,1) \times (1,1), \tag{3.278}$$

where in the first row we have performed the fusion in the parent theory, while in the second row we have restricted the left-hand side first.

The matching of (3.277) with (3.278) is simplified if we use the explicit fusion in Eqn. (3.266), finding:

$$(0,4) + (0,6) + (2,4) + (2,6) = (1,3)_1 \times (1,3)_1 + (1,3)_1 \times (1,1) + (1,1) \times (1,3)_1. \tag{3.279}$$

We use now that if a genuine line operator fuses with another genuine line operator it must give genuine line operators, while if a genuine line operator fuses with a confining/non-genuine line operator, it must give confining/non-genuine line operators. Since $(1,1)$ confines and $(1,3)_1$ does not, the previous means that we can extract the fusion $(1,3)_1 \times (1,3)_1$ by inspecting the unconfined excitations on the left hand side of (3.279) after restriction. Doing this we obtain:

$$(1,3)_1 \times (1,3)_1 = 0 + (0,6). \tag{3.280}$$

As promised, the fusion rules (3.274), (3.276), and (3.280) are indeed those of Ising.

$SU(4)_1$		
Line label	Quantum Dimension	Conformal Weight
$\mathbf{1}$	$d_{\mathbf{1}} = 1$	$h_{\mathbf{1}} = 0$
$\mathbf{4}$	$d_{\mathbf{4}} = 1$	$h_{\mathbf{4}} = 3/8$
$\mathbf{6}$	$d_{\mathbf{6}} = 1$	$h_{\mathbf{6}} = 1/2$
$\bar{\mathbf{4}}$	$d_{\bar{\mathbf{4}}} = 1$	$h_{\bar{\mathbf{4}}} = 3/8$

Table 3.14: $SU(4)_1$ data.

$\big(SU(4)_1 \times SU(2)_{-10}\big)/\mathcal{A}$

This is an amusing example that we touched upon in Section 3.3.2 of a Maverick duality expressing the Ising TQFT (or rather any of its many coset descriptions) in terms of $SU(4)_1$ and $SU(2)_{10}$ Chern-Simons gauge theories via non-abelian anyon condensation. The spectrum of $SU(4)_1$ can be found in Table 3.14 and that of $SU(2)_{10}$ can be found in Table 3.15. $SU(4)_1$ follows $\mathbb{Z}_4$ fusion rules, while those of $SU(2)_{10}$ can be obtained from Eqn. (3.92). The product theory has three non-trivial bosons: $(\mathbf{6}, 10), (\mathbf{1}, 6)$, and $(\mathbf{6}, 4)$. The first of these is abelian, while the other two are non-abelian. Condensing just the non-abelian boson $(\mathbf{1}, 6)$ is tantamount to condensing only the anyon 6 in $SU(2)_{10}$, which leads to $SU(2)_{10}/\mathcal{A} \cong USp(4)_1$ where $\mathcal{A} = 0 + 6$. In the product theory, one would then obtain $SU(4)_1 \times USp(4)_{-1}$. This points to the fact that one should instead condense all available bosons to obtain the Ising TQFT:

$$(\mathbf{6}, 10) \longrightarrow 0, \tag{3.281}$$

$$(\mathbf{1}, 6) \longrightarrow 0 + (\mathbf{1}, 6)_2, \tag{3.282}$$

$$(\mathbf{6}, 4) \longrightarrow 0 + (\mathbf{6}, 4)_2, \tag{3.283}$$

where the non-abelian anyons cannot be split further, as it is not allowed by the fusion rules. For example:

$$(\mathbf{1}, 6) \times (\mathbf{1}, 6) = (\mathbf{1}, 0) + (\mathbf{1}, 6) + \ldots \longrightarrow 0 + 0 + \ldots, \tag{3.284}$$

implies that $(\mathbf{1},6)$ can have at most a twofold split. It is also easy to see from $(\mathbf{6},10)\times(\mathbf{1},6) = (\mathbf{6},4)$ that $(\mathbf{1},6)$ and $(\mathbf{6},4)$ must share the same restriction: $(\mathbf{1},6)_2 \cong (\mathbf{6},4)_2$. This finishes the discussion as far as the bosons go.

We focus now on anyons that are fermions, i.e., that have topological spin $\theta = -1$. These are $(\mathbf{6},0)$, $(\mathbf{1},10)$, $(\mathbf{1},4)$, and $(\mathbf{6},6)$. Using similar fusion rule arguments as above we can deduce that the anyons in the parent $(\mathbf{1},4)$ and $(\mathbf{6},6)$ share the same restriction, and moreover:

$$(\mathbf{6},0)\times(\mathbf{1},4) = (\mathbf{6},4) \longrightarrow 0 + \ldots, \tag{3.285}$$

implies $(\mathbf{1},4) \to (\mathbf{6},0) + (\mathbf{1},4)_2$. We can show that the second component $(\mathbf{1},4)_2$ confines by studying the fusion with the boson $(\mathbf{1},6)$:

$$(\mathbf{1},4)\times(\mathbf{1},6) = (\mathbf{1},6) + \ldots \longrightarrow 0 + \ldots \tag{3.286}$$

so $(\mathbf{1},4)$ and $(\mathbf{1},6)$ must have one of their components identified. But $(\mathbf{6},0) \in (\mathbf{1},4)$ cannot

$SU(2)_{10}$		
Line label	Quantum Dimension	Conformal Weight
0	$d_0 = 1$	$h_0 = 0$
1	$d_1 = \sqrt{2+\sqrt{3}}$	$h_1 = 1/16$
2	$d_2 = 1+\sqrt{3}$	$h_2 = 1/6$
3	$d_3 = \sqrt{2}+\sqrt{2+\sqrt{3}}$	$h_3 = 5/16$
4	$d_4 = 2+\sqrt{3}$	$h_4 = 1/2$
5	$d_5 = 2\sqrt{2+\sqrt{3}}$	$h_5 = 35/48$
6	$d_6 = 2+\sqrt{3}$	$h_6 = 1$
7	$d_7 = \sqrt{2}+\sqrt{2+\sqrt{3}}$	$h_7 = 21/16$
8	$d_8 = 1+\sqrt{3}$	$h_8 = 5/3$
9	$d_9 = \sqrt{2+\sqrt{3}}$	$h_9 = 33/16$
10	$d_{10} = 1$	$h_{10} = 5/2$

Table 3.15: $SU(2)_{10}$ data.

condense (i.e., we cannot identify it to the vacuum), so the only consistent identification is

$$(\mathbf{1},4)_2 \cong (\mathbf{1},6)_2, \tag{3.287}$$

from which it is easy to study their lift to anyons in the parent and check that they confine. The remaining fermion is $(\mathbf{1},10)$, which identifies with $(\mathbf{6},0)$ since $(\mathbf{6},10)\times(\mathbf{1},10)=(\mathbf{6},0)$ and $(\mathbf{6},10)\to 0$, so $(\mathbf{1},10)\cong(\mathbf{6},0)$.

At this point the list of unconfined anyons are the trivial one, and one fermion $(\mathbf{6},0)$. Let us focus now on the spectrum of anyons in the parent with topological spin $\theta = e^{2\pi i/16}$. These correspond to $(\mathbf{4},3)$, $(\bar{\mathbf{4}},3)$, $(\mathbf{4},7)$, and $(\bar{\mathbf{4}},7)$. The quantum dimensions of all these anyons in the parent is $d_{(\mathbf{4},3)}=\sqrt{2}+\sqrt{2+\sqrt{3}}$, and fusions of the form

$$(\mathbf{4},3)\times(\bar{\mathbf{4}},3) = (\mathbf{1},0)+(\mathbf{1},2)+(\mathbf{1},4)+(\mathbf{1},6) \longrightarrow 0+0+\ldots, \tag{3.288}$$

allows to conclude that this set of anyons all split in two. Furthermore, because $(\mathbf{6},10)\to 0$, the fusions $(\mathbf{6},10)\times(\mathbf{4},3)=(\bar{\mathbf{4}},7)$ and $(\mathbf{6},10)\times(\bar{\mathbf{4}},3)=(\mathbf{4},7)$ imply that the following pairs of anyons in the parent share their restriction:

$$(\mathbf{4},3)\cong(\bar{\mathbf{4}},7), \quad \text{and} \quad (\mathbf{4},7)\cong(\bar{\mathbf{4}},3) \tag{3.289}$$

To deduce the splitting of the quantum dimensions we will consider the fusion with the anyon $(\bar{\mathbf{4}},9)$. This anyon is such that

$$(\mathbf{4},9)\times(\bar{\mathbf{4}},9) = (\mathbf{1},0)+(\mathbf{1},2) \longrightarrow 0+\ldots, \tag{3.290}$$

so it does not split, and such that

$$(\mathbf{4},9)\times(\mathbf{4},9) = (\mathbf{6},0+2) = (\mathbf{6},0)+(\mathbf{6},2), \tag{3.291}$$

so it is not self-conjugate. That is, $(\bar{\mathbf{4}}, 9)$ corresponds to a different excitation in the child theory. Then:

$$(\bar{\mathbf{4}}, 9) \times (\mathbf{4}, 3) = (\mathbf{1}, 6) + (\mathbf{1}, 8) \longrightarrow 0 + \ldots, \tag{3.292}$$

implies that $(\mathbf{4}, 9) \in (\mathbf{4}, 3)$, so the splitting of the quantum dimensions in $(\mathbf{4}, 3)$ corresponds to $d_{(\mathbf{4},9)} = \sqrt{2+\sqrt{3}}$, and another component with quantum dimension $\sqrt{2}$. From the previous we also conclude that $(\mathbf{4}, 9)$ and $(\bar{\mathbf{4}}, 9)$ confine. Finally, from the fusions

$$(\mathbf{4}, 3) \times (\mathbf{4}, 7) = (\mathbf{6}, 4) + (\mathbf{6}, 6) + (\mathbf{6}, 8) + (\mathbf{6}, 10) \longrightarrow 0 + 0 + \ldots, \tag{3.293}$$

$$(\mathbf{4}, 3) \times (\mathbf{4}, 3) = (\mathbf{6}, 0) + (\mathbf{6}, 2) + (\mathbf{6}, 4) + (\mathbf{6}, 6) \longrightarrow 0 + \ldots, \tag{3.294}$$

we conclude that the restrictions must be

$$(\mathbf{4}, 3) = (\mathbf{4}, 3)_1 + (\mathbf{4}, 9), \tag{3.295}$$

$$(\mathbf{4}, 7) = (\mathbf{4}, 3)_1 + (\bar{\mathbf{4}}, 9), \tag{3.296}$$

with $(\mathbf{4}, 9)$ and $(\bar{\mathbf{4}}, 9)$ confining. $(\mathbf{4}, 3)_1$ is then the anyon that descends to the spin field with topological spin $\theta = e^{2\pi i/16}$ in the Ising model.

It is now straightforward to argue for the confinement of the remaining excitations. For example, $(\mathbf{6}, 10) \times (\mathbf{1}, 3) = (\mathbf{6}, 7) \Longrightarrow (\mathbf{1}, 3) \cong (\mathbf{6}, 7)$. Studying the lift of their spin to the parent, it can readily be checked for the confinement of $(\mathbf{6}, 7)$ and $(\mathbf{1}, 3)$. A similar argument holds for the rest of the anyons, with the exception of $(\mathbf{4}, 5)$. To argue for the confinement of this anyon, notice

$$(\mathbf{4}, 5) \times (\mathbf{4}, 5) = (\mathbf{6}, 4) + (\mathbf{6}, 10) \longrightarrow 0 + 0 + \ldots, \tag{3.297}$$

$(G_2)_3$		
Line label	Quantum Dimension	Conformal Weight
$\mathbf{1}$	$d_{\mathbf{1}} = 1$	$h_{\mathbf{1}} = 0$
$\mathbf{7}$	$d_{\mathbf{7}} = \frac{3+\sqrt{21}}{2}$	$h_{\mathbf{7}} = 2/7$
$\mathbf{27}$	$d_{\mathbf{27}} = \frac{7+\sqrt{21}}{2}$	$h_{\mathbf{27}} = 2/3$
$\mathbf{77}$	$d_{\mathbf{77}} = \frac{3+\sqrt{21}}{2}$	$h_{\mathbf{77}} = 8/7$
$\mathbf{14}$	$d_{\mathbf{14}} = \frac{3+\sqrt{21}}{2}$	$h_{\mathbf{14}} = 4/7$
$\mathbf{64}$	$d_{\mathbf{64}} = \frac{5+\sqrt{21}}{2}$	$h_{\mathbf{64}} = 1$

Table 3.16: $(G_2)_3$ data.

so $(\mathbf{4}, 5)$ splits in two, and

$$(\mathbf{4}, 9) \times (\mathbf{4}, 5) = (\mathbf{6}, 4) + (\mathbf{6}, 6) \longrightarrow 0 + \ldots, \tag{3.298}$$

$$(\bar{\mathbf{4}}, 9) \times (\mathbf{4}, 5) = (\mathbf{1}, 4) + (\mathbf{1}, 6) \longrightarrow 0 + \ldots, \tag{3.299}$$

imply that $(\mathbf{4}, 9), (\bar{\mathbf{4}}, 9) \in (\mathbf{4}, 5)$. As argued above, $(\mathbf{4}, 9)$ and $(\bar{\mathbf{4}}, 9)$ cannot identify with each other, so it must be that $(\mathbf{4}, 5) \longrightarrow (\mathbf{4}, 9) + (\bar{\mathbf{4}}, 9)$, and thus all components of $(\mathbf{4}, 5)$ confine.

Then, the unconfined excitations are 0, $(\mathbf{6}, 0)$ and $(\mathbf{4}, 3)_1$, which as expected, gives the data of the Ising TQFT.

$(E_6)_1 \cong (G_2)_3/\mathcal{A}$

This is an interesting example of a single affine lie algebra embedding into another single one mentioned in Section 3.5.2. The spectrum of $(G_2)_3$ can be found in Table 3.16 while

$(E_6)_1$		
Line label	Quantum Dimension	Conformal Weight
$\mathbf{1}$	$d_{\mathbf{1}} = 1$	$h_{\mathbf{1}} = 0$
$\mathbf{27}$	$d_{\mathbf{27}} = 1$	$h_{\mathbf{27}} = 2/3$
$\overline{\mathbf{27}}$	$d_{\overline{\mathbf{27}}} = 1$	$h_{\overline{\mathbf{27}}} = 2/3$

Table 3.17: $(E_6)_1$ data.

the spectrum of $(E_6)_1$ which is the expect result is presented in Table 3.17. The $(E_6)_1$ Chern-Simons theory has $\mathbb{Z}_3$ fusion rules. Those of $(G_2)_3$ are fairly unwieldy to write down, so instead we just use them as we need them through the calculation.

Our starting theory $(G_2)_3$ has only one non-trivial boson; namely **64**, and it is non-abelian. We assume it condenses, and the fusion rule

$$\mathbf{64} \times \mathbf{64} = \mathbf{1} + \mathbf{7} + \mathbf{27} + \mathbf{77} + \mathbf{14} + \mathbf{64} \longrightarrow 0 + 0 + \ldots \tag{3.300}$$

needs **64** to split in two for consistency with the right-hand side. Thus, $\mathbf{64} \to 0 + \mathbf{64}_2$, with $d_{\mathbf{64}_2} = (3 + \sqrt{21})/2$. We can now use the fusion rules

$$\mathbf{7} \times \mathbf{64} = \mathbf{27} + \mathbf{77} + \mathbf{14} + \mathbf{64} \longrightarrow 0 + \ldots \tag{3.301}$$

$$\mathbf{14} \times \mathbf{64} = \mathbf{7} + \mathbf{27} + \mathbf{77} + \mathbf{64} \longrightarrow 0 + \ldots \tag{3.302}$$

$$\mathbf{77} \times \mathbf{64} = \mathbf{7} + \mathbf{27} + \mathbf{14} + \mathbf{64} \longrightarrow 0 + \ldots \tag{3.303}$$

where we conclude that **7**, **14**, and **77** belong in the restriction of **64**. Clearly, the only possibility is to have the identifications $\mathbf{7} \cong \mathbf{14} \cong \mathbf{77} \cong \mathbf{64}_2$ from which we also deduce the confinement of these excitations.

It only remains to study **27**. Examining the self-fusion

$$\mathbf{27} \times \mathbf{27} = \mathbf{1} + 2(\mathbf{64}) + \ldots \longrightarrow 0 + 0 + 0 + \ldots, \tag{3.304}$$

we see that **27** splits in three: $\mathbf{27} \to \mathbf{27}_1 + \mathbf{27}_2 + \mathbf{27}_3$. To assign quantum dimensions it is sufficient to study the fusion

$$\mathbf{27} \times \mathbf{64} = \mathbf{64} + \ldots \longrightarrow 0 + \ldots, \tag{3.305}$$

$USp(6)_1$		
Line label	Quantum Dimension	Conformal Weight
$\mathbf{1}$	$d_{\mathbf{1}} = 1$	$h_{\mathbf{1}} = 0$
$\mathbf{14'}$	$d_{\mathbf{14'}} = 1$	$h_{\mathbf{14'}} = 3/4$
$\mathbf{14}$	$d_{\mathbf{14}} = \frac{1+\sqrt{5}}{2}$	$h_{\mathbf{14}} = 3/5$
$\mathbf{6}$	$d_{\mathbf{6}} = \frac{1+\sqrt{5}}{2}$	$h_{\mathbf{6}} = 7/20$

Table 3.18: $USp(6)_1$ data.

from which we deduce that one component of $\mathbf{27}$ must belong in the restriction of $\mathbf{64}$. Obviously, $\mathbf{27}$ cannot condense so one of its components, say $\mathbf{27}_3$, must identify with $\mathbf{64}_2$: $\mathbf{27}_3 \cong \mathbf{64}_2$, so $\mathbf{27}_3$ confines, and we must have $d_{\mathbf{27}_1} = d_{\mathbf{27}_2} = 1$ and $d_{\mathbf{27}_3} = (3+\sqrt{21})/2$.

The fusion rules of the remaining non-confined excitations 0, $\mathbf{27}_1$ and $\mathbf{27}_2$ can be deduced from the associativity of the fusion and the fact that all these components are abelian. Then, indeed they have the correct spins, fusion rules, and quantum dimensions to recognize the expected result $(E_6)_1$. So we have indeed found that

$$(G_2)_3/\mathcal{A} = (E_6)_1, \tag{3.306}$$

where $\mathcal{A} = \mathbf{1} + \mathbf{64}$.

$SU(2)_3 \cong \big(USp(6)_1 \times SO(3)_{-4}\big)/\mathcal{A}$

In this subsection we consider an example in the infinite family of conformal embeddings studied in Section 3.5.1:

$$SO(N)_4 \times SU(2)_N \hookrightarrow USp(2N)_1, \tag{3.307}$$

where we attempt to express $SU(2)_N$ in terms of $SO(N)_4$ and $USp(2N)_1$. We consider $N = 3$ which is the simplest case in which non-abelian anyon condensation must be considered.

The spectrum of $USp(6)_1$ and $SO(3)_4$ can be found in Tables 3.18 and 3.11 respectively.

The fusion rules of $USp(6)_1$ are given as follows:

$$\mathbf{14}' \times \mathbf{14}' = \mathbf{1}, \quad \mathbf{14}' \times \mathbf{14} = \mathbf{6}, \quad \mathbf{14}' \times \mathbf{6} = \mathbf{14},$$

$$\mathbf{14} \times \mathbf{14} = \mathbf{1} + \mathbf{14}, \quad \mathbf{14} \times \mathbf{6} = \mathbf{14}' + \mathbf{6}, \quad \mathbf{6} \times \mathbf{6} = \mathbf{1} + \mathbf{14}. \tag{3.308}$$

The fusion rules of $SO(3)_4$ may be found in Eqn. (3.228).

It is easy to see that the product $USp(6)_1 \times SO(3)_{-4}$ has two bosons, both of which are non-abelian: $(\mathbf{14}, 4_1)$ and $(\mathbf{14}, 4_2)$. Running a similar argument as in the beginning of Section 3.5.2 we can see that only one of them can condense, and since 4_1 and 4_2 are symmetric between each other the choice is immaterial. We choose $(\mathbf{14}, 4_1)$ to condense, and thus $(\mathbf{14}, 4_2)$ does not split and has quantum dimension $d_{(\mathbf{14},4_2)} = (3+\sqrt{5})/2$. To study how $(\mathbf{14}, 4_1)$ splits consider the fusion and restriction $(\mathbf{14}, 4_1) \times (\mathbf{1}, 4_1) = (\mathbf{14}, 0) + (\mathbf{14}, 4_1) \to 0$. Then, $(\mathbf{1}, 4_1)$ belongs to the restriction of $(\mathbf{14}, 4_1)$ and therefore confines.

We can study the fate of the boson $(\mathbf{14}, 4_2)$ by computing the fusion with $(\mathbf{14}, 2)$:

$$(\mathbf{14}, 2) \times (\mathbf{14}, 2) = (\mathbf{1}, 0) + (\mathbf{14}, 4_1) + \ldots \longrightarrow 0 + 0 + \ldots, \tag{3.309}$$

$$(\mathbf{14}, 4_2) \times (\mathbf{14}, 2) = (\mathbf{1}, 2) + (\mathbf{1}, 4_1) + (\mathbf{14}, 2) + (\mathbf{14}, 4_1) \longrightarrow 0 + \ldots \tag{3.310}$$

The first fusion says that $(\mathbf{14}, 2)$ splits into two components $(\mathbf{14}, 2) \to (\mathbf{14}, 2)_1 + (\mathbf{14}, 2)_2$, and the second fusion implies the identification $(\mathbf{14}, 4_2) \cong (\mathbf{14}, 2)_1$[20] and corresponding confinement of these excitations. Correspondingly, $d_{(\mathbf{14},2)_1} = (3 + \sqrt{5})/2$ and $d_{(\mathbf{14},2)_2} = (1 + \sqrt{5})/2$. We may now identify the remaining component of $(\mathbf{14}, 2)$ with $(\mathbf{1}, 4_2)$, in accordance with the fusion

$$(\mathbf{1}, 4_2) \times (\mathbf{14}, 2) = (\mathbf{14}, 2) + (\mathbf{14}, 4_1) \longrightarrow 0 + \ldots \tag{3.311}$$

20. Here we have defined $(\mathbf{14}, 2)_1$ to be the component of $(\mathbf{14}, 2)$ that identifies.

and matching of quantum dimensions. So, indeed $(\mathbf{14}, 2)_2 \cong (\mathbf{1}, 4_2)$.

There are two additional identifications that we can deduce, namely

$$(\mathbf{14}, 4_2) \times (\mathbf{1}, 2) = (\mathbf{14}, 2) + (\mathbf{14}, 4_1) \longrightarrow 0 + \ldots \tag{3.312}$$

implies $(\mathbf{1}, 2) \cong (\mathbf{14}, 4_2)$, and so $(\mathbf{1}, 2)$ confines. Also

$$(\mathbf{14}, 0) \times (\mathbf{1}, 4_1) = (\mathbf{14}, 4_1) \longrightarrow 0 + \ldots \tag{3.313}$$

implies $(\mathbf{14}, 0) \cong (\mathbf{1}, 4_1)$, and since $(\mathbf{1}, 4_1)$ confines, so does $(\mathbf{14}, 0)$.

We move-on now to consider anyons of the form $(\mathbf{14'}, a)$ and $(\mathbf{6}, a)$, with a a label in $SO(3)_{-4}$. Studying self-fusions as usual we deduce that $(\mathbf{6}, 2)$ and $(\mathbf{6}, 4_1)$ split into two components, while $(\mathbf{6}, 4_2)$ does not split. The fusion

$$(\mathbf{6}, 4_2) \times (\mathbf{6}, 2) = (\mathbf{14}, 4_1) + \ldots \longrightarrow 0 + \ldots, \tag{3.314}$$

implies that $(\mathbf{6}, 2)$ restricts as $(\mathbf{6}, 2) \to (\mathbf{6}, 4_2) + (\mathbf{6}, 2)_2$, and as such $(\mathbf{6}, 4_2)$ confines. The remaining component is identified with $(\mathbf{14'}, 4_2)$ because of the fusion

$$(\mathbf{14'}, 4_2) \times (\mathbf{6}, 2) = (\mathbf{14}, 2) + (\mathbf{14}, 4_1) \longrightarrow 0 + \ldots \tag{3.315}$$

and the matching of the quantum dimensions, so we obtain the full restriction $(\mathbf{6}, 2) \to (\mathbf{14'}, 4_2) + (\mathbf{6}, 4_2)$.

Similarly, we have the fusions $(\mathbf{14'}, 0) \times (\mathbf{6}, 4_1) = (\mathbf{14}, 4_1) \to 0 + \ldots$ and $(\mathbf{14'}, 4_1) \times (\mathbf{6}, 4_1) = (\mathbf{14}, 0) + (\mathbf{14}, 4_1) \to 0 + \ldots$. From this we find the restriction $(\mathbf{6}, 4_1) \to (\mathbf{14'}, 0) + (\mathbf{14'}, 4_1)$, and in turn we deduce the confinement of $(\mathbf{14'}, 4_1)$.

Finally, from the fusions $(\mathbf{14'}, 2) \times (\mathbf{6}, 4_2)$ and $(\mathbf{6}, 0) \times (\mathbf{14'}, 4_1)$ we may deduce the identifications $(\mathbf{14'}, 2) \cong (\mathbf{6}, 4_2)$ and $(\mathbf{6}, 0) \cong (\mathbf{14'}, 4_1)$ and the corresponding confinement of such

excitations.

All in all, considering identifications we get the unconfined excitations $(\mathbf{14'}, 4_2)$, $(\mathbf{1}, 4_2)$ and $(\mathbf{14'}, 0)$ on top of the vacuum. This correctly reproduces the spectrum of the expect result $SU(2)_3$ (presented in Table 3.2) according to the conformal embedding (3.203).

CHAPTER 4

TOPOLOGICAL COSETS VIA ANYON CONDENSATION AND APPLICATIONS TO GAPPED QCD_2

4.1 Introduction

For the past half-century, the Standard Model of particle physics has been our best description of the dynamics of elementary particles. However, despite its tremendous success, we still lack a clear analytical understanding of the low-energy regime of the QCD sector, where strong interactions take over, and we observe a gapped energy spectrum with no long-range topological degrees of freedom. This enduring mystery is one of the main motivations for developing new general tools to understand strongly coupled dynamics in quantum field theory. Directly addressing these questions is a formidable long-term challenge. Nevertheless, analogs of QCD in lower dimensions are under better technical control and provide a valuable window into the strongly interacting regime of quantum field theory.

In this context, in recent years there has been significant progress in our understanding of the strongly coupled regime of 2D QCD [1, 90, 115, 117–128]. For instance, an elegant explanation for (de)confinement in massless $SU(N)$ adjoint 2D QCD was derived in [1] based on the presence of non-invertible topological line defects [6,11,62,129] in these systems. Meanwhile, [90] established criteria for a 2D QCD theory (with vanishing bare quark masses) to be gapped or gapless at long distances. Specifically, if we take a gauge theory with gauge group F with left-moving fermions in some representation R_ℓ and right-moving fermions in some representation R_r, the corresponding QCD theory is gapped if and only if the following operator equations hold:

$$T_{SO(\dim(R_\ell))_1} - T_{F_{I(R_\ell)}} = 0, \tag{4.1}$$

$$\bar{T}_{SO(\dim(R_r))_1} - \bar{T}_{F_{I(R_r)}} = 0, \tag{4.2}$$

where $I(R)$ is the Dynkin index of the representation R and T_{F_k} ($\bar{T}_{F_k}$) is the holomorphic (antiholomorphic) part of the stress-energy tensor of the WZW theory with symmetry group F and level k (denoted F_k). To simplify the discussion, we will assume from now on that the gauge theory we are working with is non-chiral $R_\ell = R_r = R$, unless otherwise specified. Equivalently, a non-chiral 2D QCD theory is gapped if and only if the coset

$$\frac{SO(\dim(R))_1}{F_{I(R)}} \tag{4.3}$$

is a conformal embedding, i.e. it has vanishing central charge:[1]

$$c_{SO(\dim(R))_1/F_{I(R)}} = c_{SO(\dim(R))_1} - c_{F_{I(R)}} = 0. \tag{4.4}$$

As in [90], we call cosets satisfying this condition *topological cosets*. A complete list of gapped 2D QCD theories can be found in [90], and a list of all conformal embeddings can be found in [50].

An intuitive way to understand this result is to bosonize the fermionic theory and cast 2D QCD as a gauged WZW model with a kinetic term for the gauge fields with coupling $g_{\rm YM}$ (for details on bosonization and fermionization, see Section 4.6.3). Here, the WZW model captures the global symmetry of the free UV fermions and is therefore given by $Spin(\dim(R))_1$. However, the following discussion holds for any conformal embedding. Assuming that the infrared fixed point is obtained upon taking the limit $g_{\rm YM} \to \infty$:

$$\begin{aligned}\lim_{g_{\rm YM}\to\infty} \int \mathcal{D}g\,\mathcal{D}A\, \exp\Big[- S_{\rm WZW}[g,A] + \frac{1}{4g_{\rm YM}^2}\int_\Sigma d^2x\ {\rm Tr}(F^2)\Big] \\ = \int \mathcal{D}g\,\mathcal{D}A\, \exp\Big[- S_{\rm WZW}[g,A]\Big],\end{aligned} \tag{4.5}$$

1. Notice that $SO(\dim(R))_1$ is a fermionic theory. Since the criterion for a mass gap concerns the central charge, it applies to either the fermionic or bosonic version of the coset theory.

the theory is gapless or gapped if and only if the gauged WZW model is gapless or gapped, reproducing the rigorous statement obtained in [90] based on Eqns. (4.1) and (4.2).

It is textbook conformal field theory (CFT) that for a generic coset (i.e., non-zero central charge) there exist standard algebraic methods to characterize the associated coset CFT, meaning (roughly) that we can recover, e.g., the spectrum of local operators and their fusion rules. For an overview, see [5]. In this sense, describing explicitly (4.5) in the gapless case is straightforward. For concrete examples in the context of 2D QCD, see [90, 115]. Not as well known, however, is that historically the standard coset construction has largely ignored the existence of additional topological sectors, with multiple vacua and topological line defects that are important to fully characterize the theory (4.5). This observation is particularly significant in the case that the gauged WZW model is given by a conformal embedding (corresponding to a gapped 2D QCD theory), as in this case the topological sectors are all the information that is contained in (4.5). This is the situation we will be interested in below.

A fruitful way to describe the topological coset (4.5) makes use of a suitable 3D construction. More precisely, the 2D theory can be obtained after interval compactification of the well-known 3D construction of gauged WZW models of [2]. Indeed, in this construction, if

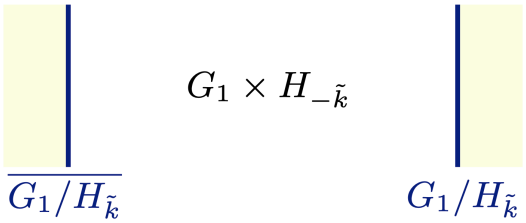

Figure 4.1: Finding the full IR description of gapped 2D QCD is tantamount to describing the topological local operators and topological line operators of the 2D theory obtained upon interval compactification of a $G_1 \times H_{-\tilde{k}}$ topological order with topological coset boundary conditions. The latter boundary conditions exist when $G_1/H_{\tilde{k}}$ is a topological coset, i.e., when the embedding of chiral algebras is conformal.

the topological coset consists of a WZW model ${G_1}^2$ with gauge group H and index of embedding $\tilde{k}$, we can construct the topological coset $G_1/H_{\tilde{k}}$ by starting with the three-dimensional Chern-Simons theory $G_1 \times H_{-\tilde{k}}$ and setting coset boundary conditions describing the embedding of $H_{\tilde{k}}$ into G_1 on the left and right boundaries of the interval. See Figure 4.1 and Section 4.6.1 for additional details.

Thus far, the construction described is not unique to conformal embeddings. The crucial difference between the coset boundary conditions for a conformal embedding and that of a generic coset at non-zero central charge is that in the former case the coset boundary conditions are *topological* (also called *gapped*) boundary conditions.[3] Gapped boundary conditions are special in the sense that, unlike a generic boundary condition, they can always be described by a gauging operation for topological defect lines with non-necessarily-invertible fusion rules known as *non-abelian anyon condensation*, or *non-invertible anyon condensation*. For a collection of references and applications in this subject, see [3, 51, 52, 64, 106–109, 130–132].

Indeed, topological defects in quantum field theory have seen significant applications in recent years. Their interpretation as "non-invertible symmetries" was originally developed in [6, 11, 53, 54, 62, 133–135]. See also [41–46] for earlier pioneering work in the subject. Most relevant to our analysis below, generalized symmetries have proved useful in characterizing phases of general quantum field theories [72, 73, 136, 137], and in signaling phases of 2D gauge theory in particular in [1]. These symmetries can be gauged [3, 62–65, 67, 75] and can constrain strongly coupled RG flows through anomalies [53, 66, 68–71, 133, 138–140]. They have also recently seen applications directly relevant to particle physics in 2D including scattering theory [141, 142], and representation theory of generalized multiplets of particles [143, 144] and operators [56, 61, 145–152].

2. As reviewed in [5], unless $H_{\tilde{k}} = G_k$, conformal embeddings can only occur when the numerator has level $k = 1$, which we assume in the rest of this discussion.

3. Mathematically, this is the statement that conformal embeddings belong to the trivial Witt class [50].

In this chapter, we will use the technology of non-invertible anyon condensation to provide a explicit description of topological cosets –and thus in particular the IR fixed point of (bosonized) gapped 2D QCD– explaining how to obtain the spectrum of line operators and their fusion ring, the spectrum of local operators and their topological OPE, and action of line operators on local operators. For previous work in this direction, see [1, 57, 90, 115]. Below we will concentrate on the bosonic version of the topological cosets, and will leave the study of their fermionic analogs (crucial for a proper description of gapped fermionic 2D QCD) for future investigations, perhaps along the lines of [135, 153, 154].

In mathematical terms, the problem of solving for the line operators has a rather succinct statement. In general, an arbitrary gapped boundary condition for a 3D TQFT always supports a set of topological line defects described by some fusion category $\mathcal{F}$. In turn, full knowledge of the boundary fusion category $\mathcal{F}$ allows us to recover the bulk 3D TQFT (see e.g. [155–157]). Indeed, the corresponding bulk topological order is the Drinfeld center $\mathcal{Z}(\mathcal{F})$ of the fusion category $\mathcal{F}$. Because conformal embeddings always admit a particular gapped boundary describing the embedding of $H_{\tilde{k}}$ into G_1, this means that the Chern-Simons theory $G_1 \times H_{-\tilde{k}}$ is the Drinfeld center $\mathcal{Z}(\mathcal{F}_{G_1/H_{\tilde{k}}})$ of a particular boundary fusion category $\mathcal{F}_{G_1/H_{\tilde{k}}}$ associated to this specific gapped boundary. The problem we must solve then is the inverse of the boundary to bulk correspondence outlined above. Namely, we must determine the boundary fusion category $\mathcal{F}_{G_1/H_{\tilde{k}}}$ given that we know $G_1 \times H_{-\tilde{k}}$ allows for the specific gapped boundary associated to the conformal embedding $H_{\tilde{k}} \hookrightarrow G_1$. As we will describe with more precision in the main text, since we are picking the same boundary condition to the left and right of the interval, this data will fully characterize the 2D theory we are interested in after interval compactification.

This presentation also clarifies the key role of non-invertible symmetry in characterizing the IR of gapped QCD_2. Indeed, the boundary fusion category $\mathcal{F}_{G_1/H_{\tilde{k}}}$ defined above is not the full symmetry of the RG flow, but rather precisely the symmetry along the RG flow that

is spontaneously broken at long distances. See Section 4.6.1. In particular, the vacua of the IR are in one-to-one correspondence with simple objects in $\mathcal{F}_{G_1/H_{\tilde{k}}}$. Due to its importance, we sometimes refer to this symmetry as the *coset zero-form symmetry*. Mathematically, the IR TQFT furnishes a regular module of this coset zero-form symmetry $\mathcal{F}_{G_1/H_{\tilde{k}}}$. This relationship between the bulk 3D TQFT and the boundary symmetry is a particular incidence of the symmetry TQFT construction utilized e.g. in [6, 57–59, 68, 69, 136, 137, 158–166].

A topological coset also consists of a set of local operators. In the context of 2D QCD, these operators are the ones that survive the RG flow and do not decouple at long distances. For works studying the flow of these local operators, see [90, 115]. Below, we will also explain precisely how the gapped boundary conditions in the 3D construction determine the set of local operators, and furthermore, their OPE.[4] See Section 4.3 for more details. In particular, this allows us to go beyond the counting of local operators/vacua, and recover the leading contribution of the OPE of local operators of 2D QCD as we approach the IR fixed point:

$$\phi_1^{UV}(x_1)\phi_2^{UV}(x_2) \to \phi_1^{IR}\phi_2^{IR}. \tag{4.6}$$

In particular, since the IR theory is gapped, the right-hand side above is independent of position and non-singular in the limit $x_1 \to x_2$.

As an example illustrating our results, we will find that in $SU(3)$ gauge theory with a single adjoint fermion, the topological coset $Spin(8)_1/SU(3)_3$ is described by a $\mathbb{Z}_2 \times \mathbb{Z}_2$ triality fusion category:

$\times$	$\mathcal{N}$	$\bar{\mathcal{N}}$	$\mathbf{v}$	$\mathbf{s}$	$\mathbf{c}$
$\mathcal{N}$	$2\bar{\mathcal{N}}$	$0+\mathbf{v}+\mathbf{s}+\mathbf{c}$	$\mathcal{N}$	$\mathcal{N}$	$\mathcal{N}$
$\bar{\mathcal{N}}$	$0+\mathbf{v}+\mathbf{s}+\mathbf{c}$	$2\mathcal{N}$	$\bar{\mathcal{N}}$	$\bar{\mathcal{N}}$	$\bar{\mathcal{N}}$
$\mathbf{v}$	$\mathcal{N}$	$\bar{\mathcal{N}}$	0	$\mathbf{c}$	$\mathbf{s}$
$\mathbf{s}$	$\mathcal{N}$	$\bar{\mathcal{N}}$	$\mathbf{c}$	0	$\mathbf{v}$
$\mathbf{c}$	$\mathcal{N}$	$\bar{\mathcal{N}}$	$\mathbf{s}$	$\mathbf{v}$	0

4. In mathematical terms, the OPE and the sphere one-point functions of the IR local operators furnish a commutative Frobenius algebra [167, 168].

and the local operators, in the basis that diagonalizes the above fusion ring (the one determined by the branching rules of the conformal embedding), satisfy the IR multiplication table:

$$\phi_{(0,\mathbf{10})} \cdot \phi_{(0,\mathbf{10})} = \phi_{(0,\overline{\mathbf{10}})}, \quad \phi_{(0,\overline{\mathbf{10}})} \cdot \phi_{(0,\overline{\mathbf{10}})} = \phi_{(0,\mathbf{10})}, \tag{4.7}$$

$$\phi_{(0,\mathbf{10})} \cdot \phi_{(0,\overline{\mathbf{10}})} = \phi_{(0,\overline{\mathbf{10}})} \cdot \phi_{(0,\mathbf{10})} = \phi_{(0,\mathbf{1})}, \tag{4.8}$$

$$\phi_{(0,\mathbf{10})} \cdot \phi_{(i,\mathbf{8})} = \phi_{(0,\overline{\mathbf{10}})} \cdot \phi_{(i,\mathbf{8})} = \phi_{(i,\mathbf{8})} \cdot \phi_{(0,\mathbf{10})} = \phi_{(i,\mathbf{8})} \cdot \phi_{(0,\overline{\mathbf{10}})} = \phi_{(i,\mathbf{8})}, \tag{4.9}$$

$$\phi_{(\mathbf{v},\mathbf{8})} \cdot \phi_{(\mathbf{s},\mathbf{8})} = \phi_{(\mathbf{s},\mathbf{8})} \cdot \phi_{(\mathbf{v},\mathbf{8})} = 3\phi_{(\mathbf{c},\mathbf{8})}, \tag{4.10}$$

$$\phi_{(\mathbf{s},\mathbf{8})} \cdot \phi_{(\mathbf{c},\mathbf{8})} = \phi_{(\mathbf{c},\mathbf{8})} \cdot \phi_{(\mathbf{s},\mathbf{8})} = 3\phi_{(\mathbf{v},\mathbf{8})}, \tag{4.11}$$

$$\phi_{(\mathbf{c},\mathbf{8})} \cdot \phi_{(\mathbf{v},\mathbf{8})} = \phi_{(\mathbf{v},\mathbf{8})} \cdot \phi_{(\mathbf{c},\mathbf{8})} = 3\phi_{(\mathbf{s},\mathbf{8})}, \tag{4.12}$$

$$\phi_{(\mathbf{v},\mathbf{8})} \cdot \phi_{(\mathbf{v},\mathbf{8})} = \phi_{(\mathbf{s},\mathbf{8})} \cdot \phi_{(\mathbf{s},\mathbf{8})} = \phi_{(\mathbf{c},\mathbf{8})} \cdot \phi_{(\mathbf{c},\mathbf{8})} = 3\phi_{(0,\mathbf{1})} + 3\phi_{(0,\mathbf{10})} + 3\phi_{(0,\overline{\mathbf{10}})}, \tag{4.13}$$

where $i = \mathbf{v}, \mathbf{s}, \mathbf{c}$. See Section 4.4 for details in the notation.

In the spirit of understanding the IR limit of gauge theories like the standard model, it is also interesting to consider the possibility of gapped QCD theories that are trivially gapped, i.e. those where all particle spectra are massive and where there is a unique vacuum state. To see how this possibility is addressed from the 2D-3D correspondence point of view, it is useful to recall the more standard case of counting states of a 2D RCFT $\mathcal{R}$ with a single vacuum from the 3D point of view and how the chiral and antichiral sides of $\mathcal{R}$ are glued together to furnish a full 2D RCFT. [41,169] (see also [1,57]). This will be useful background for Section 4.5 (see also Section 4.6.1). Indeed, if $\mathcal{R}$ is described by some chiral algebra V, then we can construct $\mathcal{R}$ from the 3D perspective by taking a bulk TQFT described by an appropriate MTC $\mathcal{C}$[5] on an interval with canonical boundary conditions respect to such chiral algebra

5. The "appropriate" MTC in this context is the so-called category of V-modules of the chiral algebra V.

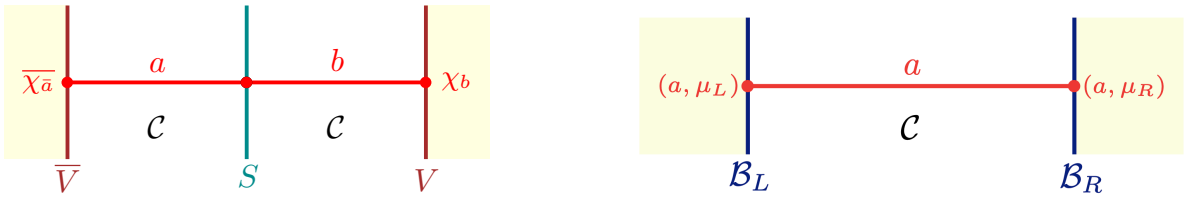

Figure 4.2: On the left: A modular invariant for a chiral algebra V is obtained starting with an appropriate 3D bulk MTC $\mathcal{C}$, possibly with an insertion of a surface operator S, and summing over all the possible junctions of anyons stretching perpendicularly between the left and right boundaries, both with canonical boundary conditions for V. The different modular invariants are given by different choices of bulk surface operators S. On the right: If the bulk MTC $\mathcal{C}$ allows for (several) topological boundary conditions, then the spectrum of topological local operators of the 2D theory obtained after interval compactification is obtained by stretching an anyon between the left and right boundaries. The total partition function is obtained by summing over all such insertions, each with a unit contribution.

(for references on gapless boundaries see the seminal work [4] or more recently [170–172], specially remark 5.4 in [171]). An arbitrary modular invariant giving the partition function for $\mathcal{R}$ is then constructed by studying all the allowed endpoints of anyons of the bulk MTC on the two boundary conditions, possibly with some surface operator inserted in the middle region [169] dictating how the chiral and antichiral sides are glued together, as shown in the left in Figure 4.2. When the surface defect S is invertible the construction leads to a permutation modular invariant, and in the case where the modular invariant is of pure extension type the surface defect S is non-invertible, as in the higher-gauging defects of [65].

The situation when the boundaries are topological is similar, with the difference that characterizing topological boundaries is more subtle technically than the gapless boundaries describing (non-necessarily diagonal) RCFTs with single vacuum, and with the difference that an allowed insertion of an anyon in between two boundaries does not contribute a pair of holomorphic and antiholomorphic characters to the (torus) partition function, but rather just a unit contribution. Allowed insertions of anyons in between topological boundaries then count the number of vacua in the corresponding 2D theory, as shown in the right in Figure 4.2. Thus, if the unique anyon that can be stretched in between two different topological boundaries is the identity anyon, then we have found a trivially gapped IR fixed point.

Indeed, this is the essential idea advocated in [69] to explore anomalies of non-invertible symmetries in two spacetime dimensions. Here, we will take this construction and apply it on our context to argue in Section 4.5 that the chiral $Spin(8)$ QCD_2 with massless fermions in the vectorial and spinorial representations is trivially gapped.

4.2 Lagrangian Algebras and Gapped Boundaries

In this section, we describe the algebraic theory of topological boundaries in terms of non-abelian (non-invertible) anyon condensation and Lagrangian algebras. In the next section we put the theory to use to describe topological cosets. Recall that in Chapter 2 we have reviewed standard material on the algebraic formulation of anyons via MTCs that is useful in the following.

4.2.1 Lagrangian Algebras for Gapped Boundaries

Abelian Case

To understand the general situation, we start by briefly recalling the theory of gapped boundaries for abelian MTCs. These are MTCs whose simple anyons are all abelian, and their fusion rules are always those of some abelian group G. In this case, we can efficiently describe topological boundaries in terms of the gauging of abelian higher-form symmetries [6].

In this setting, we must determine then which objects are gaugable in a bulk region of the 3D spacetime so that the result after gauging is a trivial theory. In the context of abelian MTCs the answer is well-known, and it corresponds to a Lagrangian subgroup L of the given abelian MTC [101–104]. This is a subset of the anyons that fulfills $H \subset G$ fusion rules, and such that all anyons in L are bosons.[6] In particular, notice that this subset of anyons is closed under fusion. Additionally, the following two conditions have to be satisfied:

6. A boson is a simple anyon a with topological spin $\theta_a = 1$. See Chapter 2 for a brief review.

- Any two simple anyons in L have trivial braiding phase (2.16) with each other. This condition can be interpreted as follows: Recall that the braiding phase (2.16) measures the charge of a simple anyon a under the symmetry implemented by an anyon b encircling a. Then, this condition states that the lines generating the gauge symmetry must be gauge-invariant amongst themselves. When we gauge these lines we sum over all possible insertions of them and they become indistinguishable from the identity line in the gauged theory.

- Any simple anyon not in L has non-trivial braiding phase (2.16) with at least one simple anyon belonging to L. This is the statement that the remaining lines are charged under L and thus not gauge-invariant. They are left out of the spectrum of the gauged theory. Overall, after gauging, the result is a completely trivial theory.

Performing this gauging operation on half of spacetime leads then to a gapped boundary, as depicted in the left of Figure 4.3.[7] The order of H is always $|H| = \sqrt{|G|}$. We require anyons in the Lagrangian subgroup to be bosons since otherwise twisting lines into loops gives phases (see (2.14)) that makes the definition of gauging ambiguous [6, 10, 34]. Thus, only bosons can participate in a gaugable symmetry.

As previously stated, lines in the Lagrangian subgroup become indistinguishable from the identity line on the side of the trivial theory. More precisely, the Lagrangian subgroup –seen as a non-simple line of the original theory– becomes the identity line on the side of

7. In practical calculations the gauging of abelian anyons may be implemented along the lines of the three-step gauging rule of [2, 34] (for a more recent review on this topic, see Appendix A.1. in [173]). A gapped boundary is then identified if the outcome of the three-step gauging rule returns the trivial MTC.

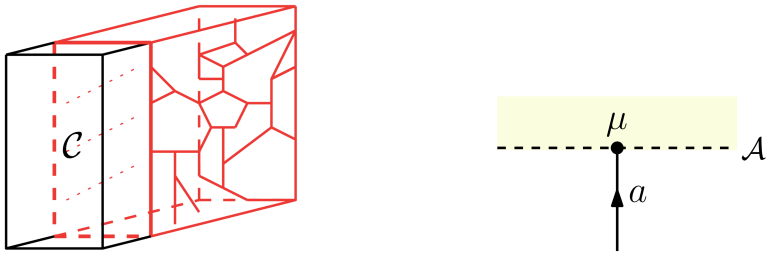

Figure 4.3: On the left: The 3D TQFT described by the MTC $\mathcal{C}$ (in black) exhibits a topological boundary generated by the process of gauging a Lagrangian algebra $\mathcal{A}$ on one half of the spacetime (in red). In the abelian case, the Lagrangian algebra reduces to the notion of a Lagrangian subgroup, and we have $L = \bigoplus_{h\in H} h$ for H a Lagrangian subgroup of G (see main text). On the right: Simple anyons a in the Lagrangian algebra $\mathcal{A}$ are allowed to end perpendicularly at the topological boundary (dashed line) on a set of topological (quasi-)local junctions labeled by μ, a channel in which a embeds into $\mathcal{A}$.

the trivial theory after gauging:

$$\bigoplus_{h\in H} h \to 0_{\text{Trivial}}. \tag{4.14}$$

A simple line in the Lagrangian subgroup is thus mapped by the gapped boundary to the identity line on the side of the trivial theory. When the simple line ends perpendicularly at the gapped boundary, this defines a topological junction for such a simple line at the boundary. See Figure 4.3. Fusion of these junctions follows in the obvious way. Since a Lagrangian subgroup is closed under fusion and fusion of abelian anyons results in a single simple anyon, the fusion of these junctions at the boundary follow the same fusion rules as those of the corresponding Lagrangian subgroup. See Figure 4.4. The special case of Lagrangian subgroups in abelian MTCs will be important in Section 4.5 below.

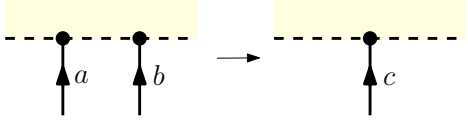

Figure 4.4: Two simple lines ending perpendicularly at a topological boundary always fuse to a single line when the topological boundary is described by a Lagrangian subgroup. In particular, the junctions follow the same fusion rules as those of the corresponding Lagrangian subgroup.

Non-Abelian Case

The general situation for non-abelian MTCs is more delicate, but the general characterization of gapped boundaries is known. In general, any elementary gapped boundary condition of a 3D TQFT is described in terms of a generalization of the concept of a Lagrangian subgroup known as *Lagrangian algebra* (see e.g., [50,52,64,131]). In parallel to the situation of gauging invertible one-form symmetries reviewed above, a gapped boundary is generated by inserting a suitable fine mesh of anyons on half of spacetime and performing a weighted summation over such insertions so that the resulting theory is trivial. (See Figure 4.3)). A Lagrangian algebra is, essentially, the precise description of such a mesh of anyons and their insertions.

In the rest of this subsection, our goal will be to provide a more accurate definition of the concept of Lagrangian algebra. In the subsequent discussion we mainly follow the algebraic definitions of [41]. We follow their interpretation in terms of anyon condensation from [52].

An *algebra* $\mathcal{A}$ in a MTC $\mathcal{C}$ consists, first, of some (non-simple) anyon in $\mathcal{C}$:

$$\mathcal{A} = \bigoplus_{a \in \mathcal{C}} n_a a, \quad n_a \in \mathbb{N}. \tag{4.15}$$

This is the anyon that we will gauge on half of spacetime, so in particular we demand that it becomes indistinguishable from the identity line on the side of the trivial theory. The fact that the anyon $\mathcal{A}$ is (generically) non-simple implies that there exist topological junctions describing the embedding of simple anyons a into $\mathcal{A}$. Generally, there are n_a such junctions, so we label them by Greek letters and draw them as gray arrows:

$\in \mathrm{Hom}(a, \mathcal{A})\,.$ (4.16)

An analogous diagram holds where an algebra is "decomposed" by a topological junction into

its simples.

An algebra is also defined by a "multiplication map" that we denote by m.[8] The multiplication in the algebra corresponds to a trivalent vertex of the algebra object, and may be expressed in terms of the simple lines of the MTC as a collection of complex numbers encoding how the simple lines embed into the algebra object $\mathcal{A}$. Diagrammatically:

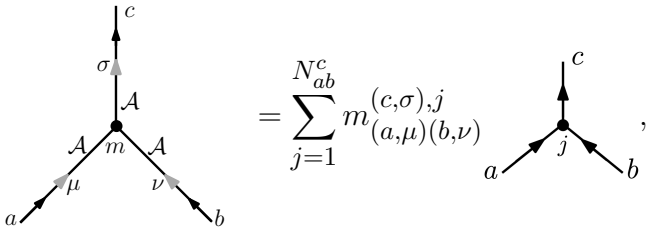

(4.17)

It is important to note that two different algebras may have the same underlying object (4.15) and differ only in their multiplication, so strictly speaking we should write a pair $(\mathcal{A}, m)$ to denote an algebra appropriately. However, as there should be no misunderstanding given context, we will abuse language and use the same notation $\mathcal{A}$ to refer to both the abstract notion of algebra with multiplication, or just the underlying (non-simple) anyon.

A technical point is that a Lagrangian algebra is both an algebra and a *coalgebra*. A coalgebra in a MTC $\mathcal{C}$ is defined similarly by a pair $(\mathcal{A}, m^\vee)$,[9] where now $m^\vee$ is a "comultiplication map", whose diagrammatic expression is similar to (4.17), but where we replace $m \to m^\vee$ and the diagrams now involve splitting spaces instead of fusing spaces. In a unitary theory, there exists a basis where the comultiplication is determined by the multiplication as $m^\vee = m^\dagger$.[10]

Recall that for higher-form symmetries, a gauge transformation corresponds to a rear-

8. Technically, an algebra also requires a unit morphism $u \in \mathrm{Hom}(0, \mathcal{A})$ satisfying a number of properties. In the following we will actually not make use of the unit, and instead refer the reader to [41] for further details.

9. More precisely, by a triple $(\mathcal{A}, m^\vee, u^\vee)$, where $u^\vee$ is a counit morphism $u^\vee \in \mathrm{Hom}(\mathcal{A}, 0)$. As with the unit morphism, the counit will not be needed in the following, so we do not refer to it from now on.

10. Sometimes it is useful to consider the general basis, e.g. when one does not know the F-symbols in unitary basis.

rangement of the trivalent vertices defining the mesh of higher-form symmetry [6]. Similarly, we demand that performing a topological manipulation of our mesh of non-invertible anyons leaves the result invariant. This more general form of gauge invariance implies that the multiplication and comultiplication must satisfy a number of constraints – often expressed diagrammatically – in order to properly trivialize the aforementioned topological manipulations. The first of these are the (co)associativity conditions:[11]

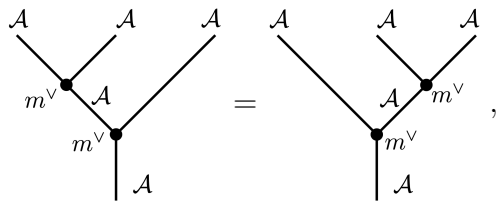

(4.18)

The previous diagrams can be understood as a series of polynomial (quadratic) equations that the multiplication and comultiplication must fulfill, analogous to the pentagon and hexagon equations constraining the F and R-symbols. To be explicit, we can express the coassociativity condition in components:

$$\sum_{\lambda} m^{\vee(d,\phi),k}_{(a,\mu)(f,\lambda)} m^{\vee(f,\lambda),j}_{(b,\nu)(c,\sigma)} = \sum_{(e,\rho),\ell,p} m^{\vee(e,\rho),\ell}_{(a,\mu)(b,\nu)} m^{\vee(d,\phi),p}_{(e,\rho)(c,\sigma)} [F_d^{abc}]_{(e,\ell,p),(f,j,k)} \tag{4.19}$$

Another topological manipulation that must trivialize on the side of the gauged theory corresponds to the braiding of one algebra object around each other. Diagrammatically, one finds the condition:

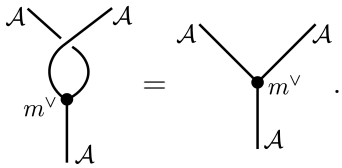

(4.20)

Or in components:

$$m^{\vee(c,\sigma),j}_{(a,\mu)(b,\nu)} = \sum_k m^{\vee(c,\sigma),k}_{(b,\nu)(a,\mu)} [R_c^{ab}]_{kj}. \tag{4.21}$$

11. We could also write the associativity and Frobenius conditions, but since we assume we are working with unitary theories where a basis exist where $m^\vee = m^\dagger$, these are not independent conditions to consider.

We also require that a bubble of the vacuum line on the side of the gauged theory can always be attached or removed to the vacuum line. In terms of the algebra object in the original theory, this leads to the separability condition:[12][13]

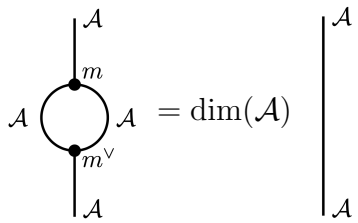

(4.22)

Notice that a choice of multiplication in the Frobenius algebra is unique only up to a "gauge transformation" that replaces $m^{(c,\sigma),j}_{(a,\mu)(b,\nu)} \to \Gamma^a_{\mu\mu'}\Gamma^b_{\nu\nu'} m^{(c,\sigma'),j}_{(a,\mu')(b,\nu')}(\Gamma^c_{\sigma\sigma'})^{-1}$, for a choice of unitary transformations $\Gamma^a_{\mu\mu'}$.

Finally, we demand that a gaugable algebra consists only of bosonic simple anyons. Similarly as with Lagrangian subgroups, this condition arises to avoid ambiguous phases coming from twisting loops (recall (2.14)).

Thus far, the conditions written down define a gaugable algebra in 3D TQFTs along a three-dimensional region. This is, the gauged theory has not been demanded to be trivial. A Lagrangian algebra is furthermore defined by the condition[14]

$$\dim(\mathcal{C}) = \big(\dim(\mathcal{A})\big)^2. \tag{4.23}$$

This finishes the definition of a gapped boundary in 3D TQFTs in terms of Lagrangian

12. In two dimensions, the analogous rearrangement of lines relating different triangulations of a Riemann surface is known as the "bubble move" [41].

13. Notice that the constant on the right-hand side of (4.22) is often set to one. As described in [24, 41], this amounts to a normalization choice of the unit and counit morphisms that we have made to obtain simple-looking expressions in our context. Changing this normalization merely amounts to renormalizing the local operators defined below by a global constant.

14. From the abstract definitions of a gaugable algebra one can deduce that $\dim(\mathcal{D}) = \dim(\mathcal{C})/\big(\dim(\mathcal{A})\big)^2$, where $\dim(\mathcal{D})$ corresponds to the dimension of the MTC $\mathcal{D}$ obtained after gauging the algebra $\mathcal{A}$ in $\mathcal{C}$ (see e.g. [24]). When the result is the trivial theory $\dim(\mathcal{D}) = 1$, and (4.23) follows. Alternatively, one can deduce (4.23) must be fulfilled by a gapped boundary by analyzing the Hopf link between $\mathcal{A}$ and a simple line a as in [64].

algebras.

To give a general example, note that if a MTC is of the form $\mathcal{C} \times \bar{\mathcal{C}}$, then a gapped boundary with Lagrangian algebra object

$$\mathcal{A} = \bigoplus_{a \in \mathcal{I}} (a, a) \tag{4.24}$$

always exists. (Recall that $\mathcal{I}$ labels the simple anyons in $\mathcal{C}$, see Chapter 2.) This is the so-called diagonal Lagrangian algebra. Physically, the existence of this algebra follows from the trivial fact that the identity interface in $\mathcal{C}$ always exists. After folding, the identity interface becomes the topological boundary in $\mathcal{C} \times \bar{\mathcal{C}}$ described by the diagonal Lagrangian algebra. For a mathematical proof that the object (4.24) can always be extended to satisfy the definitions of a Lagrangian algebra above, see e.g. Lemma 6.19 in [24].

As a quick example of a gapped boundary given by the diagonal Lagrangian consider $\mathcal{C} = (G_2)_1$. Then, we have a gapped boundary:

$$\mathcal{A} = (0, 0) \oplus (\tau, \tau), \tag{4.25}$$

where τ is the unique non-trivial anyon in $(G_2)_1$ and the second entry corresponds to the associated anyon in $(G_2)_{-1}$ (For additional details on notation, see the end of Chapter 2). Using the data of the Fibonacci MTC in Section 4.6.5, it is straightforward to check that the associativity, separability, and commutativity conditions just discussed are easily solved by

$$m^{(0,0)}_{(0,0)(0,0)} = m^{(\tau,\tau)}_{(\tau,\tau)(0,0)} = m^{(\tau,\tau)}_{(0,0)(\tau,\tau)} = m^{(0,0)}_{(\tau,\tau)(\tau,\tau)} = m^{(\tau,\tau)}_{(\tau,\tau)(\tau,\tau)} = 1, \tag{4.26}$$

which gives the full algebra for this gapped boundary.

As in the case of abelian gauging discussed above, one can study the behavior of the topological endpoints of anyons at the topological boundary. Here, we highlight the key

differences arising for our more general situation. First, notice that since the Lagrangian algebra behaves as the identity line in the resulting (trivial) gauged theory, a simple object in the Lagrangian algebra is allowed to have as many topological junctions at the topological boundary as the multiplicity with which it appears in the decomposition of the algebra object (4.15) into simple anyons (see Figure 4.3). Secondly, fusion of anyons ending at the boundary is more delicate in the general case of non-invertible anyon condensation since fusion of simple anyons in the Lagrangian algebra is generically not closed. To capture this phenomenon, one introduces the M-symbols (originally introduced in [174]):

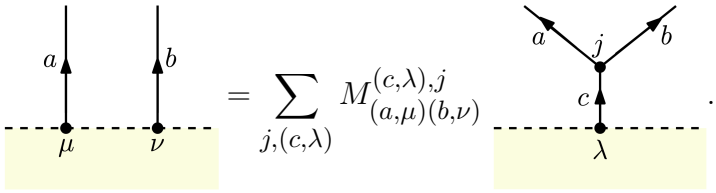

(4.27)

One can easily derive constraints that the M-symbols must satisfy. For instance, since the boundary is topological one must be able to freely move the endpoints of the anyons around each other so we find the commutativity condition:

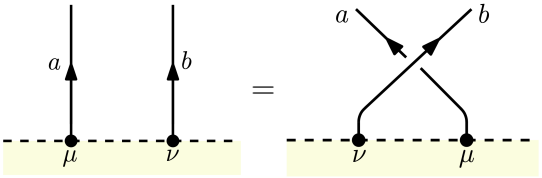

(4.28)

Similarly, one can derive an associativity constraint by manipulating three endpoints at the topological boundary as shown in Figure 4.5.

It is now straightforward to see that the constraints thus obtained on the M-symbol are equivalent to those satisfied by the (co)multiplication of the Lagrangian algebra characterizing the gapped boundary. See Eqns. (4.19) and (4.21). Therefore, the corresponding

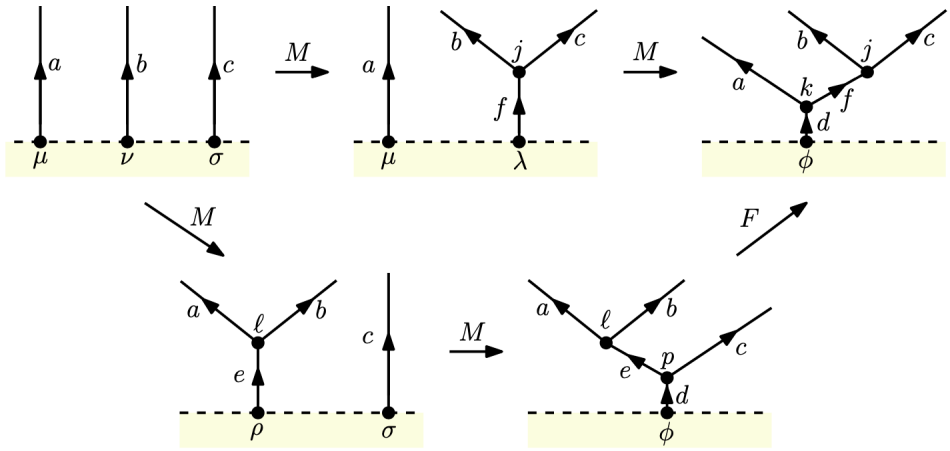

Figure 4.5: An associativity condition for the M-symbols is established by examining the fusion of boundary junctions in varying orders.

Lagrangian algebra necessarily yields a solution for the M-symbols. That is, identifying:

$$M^{(c,\lambda),j}_{(a,\mu)(b,\nu)} \longleftrightarrow m^{\vee(c,\lambda),j}_{\ \ (a,\mu)(b,\nu)}, \tag{4.29}$$

the associativity constraints in Fig. 4.5 and the commutativity constraints (4.28) are automatically fulfilled. Following this identification, below we will refer to the Frobenius algebra multiplication and the M-symbols interchangeably.

4.3 Topological Cosets

Before discussing topological cosets more precisely, let us summarize here the data we seek. Specifically, for a topological coset $G_1/H_{\tilde{k}}$ we look for

- The fusion category of topological line operators living at the boundary of the Chern-Simons theory $G_1 \times H_{-\tilde{k}}$ for the boundary condition describing the embedding of $H_{\tilde{k}}$ into G_1. (We place the same boundary condition in both ends of the interval.)

- The set of local operators, seen as anyons in the 3D theory belonging to the Lagrangian algebra stretching in between both ends of the interval, possibly considering multiplicity, and the OPE between these local operators.

- The linking action of the line operators on the local operators.

Let us clarify the relationship between the OPE and the action of lines on local operators. In any 2D TQFT the set of local operators always admits an idempotent complete basis [55, 167, 175, 176]. Up to normalization, this is the statement that there always exists a basis of topological local operators where the following operator product holds:

$$\mathcal{O}_m \mathcal{O}_n = \frac{\delta_{m,n}}{d_m} \mathcal{O}_m. \tag{4.30}$$

This idempotent complete basis can be obtained by shrinking topological boundary conditions satisfying clustering to a point. See e.g., [143, 176].

Thus, if we do not consider the action of lines on the local operators, the OPE does not contain any information independent of simply the count of the number of local operators. By contrast, when we consider the action of lines, we can find an alternative basis of local operators, which instead diagonalize the action of the lines. It is this latter basis that is obtained, e.g. in the context of 2D QCD, by keeping track of the flow of operators from the UV. In the following, when we present the OPE of local operators, we will therefore work in the basis that diagonalizes the fusion category of line operators, and thus has the interpretation of the leading contribution to the OPE of local operators as they approach the IR fixed point.

In the context of gapped 2D QCD, an important fact about the 3D construction is that it makes manifest that the topological coset zero-form symmetry is present along the whole

RG flow.[15] See Section 4.6.1. Then, the assumption that the IR is given by the topological coset in Figure 4.1 with the same topological coset boundary conditions on the left and on the right means that the topological coset symmetry acts regularly on the vacua of the theory [55,69]. In physical terms, this means that the fusion category symmetry arising from the coset construction is fully spontaneously broken at long distances. Note that this is not, in general, the full symmetry of the flow, but rather a subset that is intrinsically defined by the 3D construction.[16] Hence, the set of vacua, labeled by topological point operators, is in one to one correspondence with the simple lines in coset zero-form symmetry.[17] In practice, this means that the topological lines of the topological coset act over the idempotent complete basis as

$$m(\mathcal{O}_n) = \sum_p \hat{N}_{mn}^p \mathcal{O}_p, \tag{4.31}$$

where $m, n, p, \ldots$ and $\hat{N}_{mn}^p$ above stands for the topological lines and their fusion coefficients in the 2D theory respectively, and d_m stands for the quantum dimension of the m-th line. [18] The notation $m(\mathcal{O}_n)$ stands for the action of the m-th line over the local operators $\mathcal{O}_n$ in the idempotent complete basis. Diagrammatically:

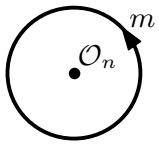

$$= \sum_p \hat{N}_{mn}^p \; \mathcal{O}_p \bullet \qquad . \tag{4.32}$$

We will see many concrete examples of these equations below.

15. Here, we are deliberately not keeping track of possible accidental symmetries which may appear in the strict IR limit but do not extend to the entire RG trajectory.

16. Alternatively, as pointed out in [115], one can also see directly in 2D that the coset chiral algebra is preserved along the flow by analysis of the 2D Hamiltonian [90, 177].

17. Mathematically, if $\mathcal{F}_{G_1/H_{\tilde{k}}}$ is the fusion category describing the topological coset symmetry, then the statement is that the IR is described by a regular $\mathcal{F}_{G_1/H_{\tilde{k}}}$-symmetric 2D TQFT.

18. Here we have specialized the discussion to the case where the 2D theory is obtained upon interval compactification of a 3D TQFT with the same left and right topological boundary conditions, as in our current interest of topological cosets depicted in Figure 4.1, and the expressions are more general when the two topological boundary conditions are different. See [55] for more details.

We now move to a detailed discussion of topological cosets. The coset construction of 2D CFT [85, 86] instructs us that a 2D CFT denoted $G_k/H_{\tilde{k}}$ can be obtained by decomposing the characters of the G_k affine Lie algebra into those of the $H_{\tilde{k}}$ affine Lie algebra:

$$\chi_{\Lambda}^{G_k}(q) = \sum_{\lambda} b_{(\Lambda,\lambda)}(q)\, \chi_{\lambda}^{H_{\tilde{k}}}(q), \tag{4.33}$$

where Λ and λ stand for the integrable representations of G_k and $H_{\tilde{k}}$ respectively, and $q = e^{2\pi i \tau}$ with τ the modular parameter as usual. The quantities $b_{(\Lambda,\lambda)}(q)$ are known as branching functions and describe the spectrum of local operators in the coset 2D CFT. More precisely, the torus partition function for the coset is given by [86, 93, 95, 178, 179]:

$$Z_{G_k/H_{\tilde{k}}}(T^2) = \sum_{\Lambda,\lambda} |b_{\Lambda}^{\lambda}(q)|^2, \tag{4.34}$$

where we assume that the coset theory we are considering corresponds to that of a diagonal modular invariant. The central charge of the coset theory is

$$c_{G_k/H_{\tilde{k}}} = c_{G_k} - c_{H_{\tilde{k}}}. \tag{4.35}$$

The class of cosets we will be interested in arise when the branching rules consist only of non-negative integers, with no non-trivial q-expansion:

$$\chi_{\Lambda}^{G_k}(q) = \sum_{\lambda} b_{(\Lambda,\lambda)}\, \chi_{\lambda}^{H_{\tilde{k}}}(q), \quad b_{(\Lambda,\lambda)} \in \mathbb{N}. \tag{4.36}$$

Then, the coset theory has no excited states and all the states are vacua, or topological local operators of the theory. Following [90], therefore, we refer to this type of coset as *topological coset*. It also follows that the central charge of the coset vanishes $c_{G_k/H_{\tilde{k}}} = 0$, in which case the embedding of affine Lie algebras is known as a conformal embedding. As reviewed in [5],

unless $H_{\tilde{k}} = G_k$, conformal embeddings can only occur when the numerator has level $k = 1$. Our interest in the following will be in the latter case, so we set $k = 1$ from now on.

It is well-known that a conformal embedding $H_{\tilde{k}} \hookrightarrow G_1$ gives rise to an extension of the $H_{\tilde{k}}$ chiral algebra into G_1 [5, 180, 181], and the branching rules express how the integrable representations of G_1 are given from those of $H_{\tilde{k}}$ upon extension. In turn, we know from [113] that the notions of extension of a chiral algebra V and that of gauging an algebra in V[19] are equivalent. In our context, this means that a gaugable algebra $\mathcal{B}$ (in the sense explained in the previous subsection) exists in $H_{\tilde{k}}$ such that

$$H_{\tilde{k}}/\mathcal{B} = G_1, \tag{4.37}$$

and the integrable representations of G_1 are constructed from $H_{\tilde{k}}$ from (4.36). Interpreting this from the 3D TQFT point of view, we see that this observation leads to a topological interface separating $H_{\tilde{k}}$ and G_1 with the line operators connected by a junction(s) at the interface according to (4.36). Upon folding, we conclude that the branching rules induce a Lagrangian algebra object in $G_1 \times H_{-\tilde{k}}$ given by:

$$\mathcal{A} = \bigoplus_{(\Lambda,\lambda)} b_{(\Lambda,\lambda)}(\Lambda, \lambda_{\text{rev}}), \tag{4.38}$$

where λ_{rev} stands for the representation λ in (4.36), but in the theory $H_{-\tilde{k}}$ after orientation-reversal of $H_{\tilde{k}}$. We will see many examples of this Lagrangian algebra below. As a quick check, notice that the anyons $(\Lambda, \lambda_{\text{rev}})$ on the right-hand side are always bosons, since in order for (4.36) to hold, the conformal weights of the primaries on the left and right-hand sides must be equal mod 1. The conclusion then follows from the standard relationship between the topological spins and the conformal weights (see Eqn. (2.14)).

In passing, notice that the partition function (4.34) for a topological coset arises naturally

19. More precisely, gauging an algebra in the category of V-modules.

in terms of the Lagrangian algebra (4.38). Indeed, as recalled in the Introduction, each contribution to the partition function arises from an anyon stretching in between a left and a right boundary. In our construction, each simple anyon $(\Lambda, \lambda_{\text{rev}})$ allows for $b_{(\Lambda,\lambda)}$ topological endpoints at the gapped boundary given by (4.38). Setting the same boundary condition at the left and at the right, we see that the anyon $(\Lambda, \lambda_{\text{rev}})$ contributes $|b_{(\Lambda,\lambda)}|^2$ units to the partition function, thus reproducing the expected result (4.34) overall.

Once we collect all the previous facts, we see that the problem of describing topological cosets is that of determining the boundary theory for the coset 3D topological order $G_1 \times H_{-\tilde{k}}$, which always has a gapped boundary determined by the branching rules of the conformal embedding. Now that we know that topological cosets imply the existence of a Lagrangian algebra, we must move on to describing the spectrum of line and point operators in the 2D theory.

Point Operators

A 2D topological local operator is constructed from the 3D bulk by stretching a boson belonging to the Lagrangian algebra from one boundary to the other, possibly with different junctions at both endpoints, as follows:

$\phi_{(a;\mu_1,\mu_2)} \coloneqq$ 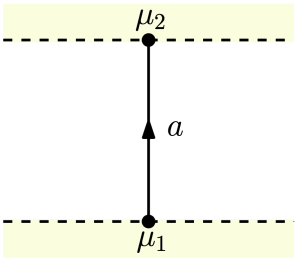

, (4.39)

where in a topological coset, the space of anyons that can end on the boundary are given by the $(\Lambda, \lambda_{\text{rev}})$ in (4.38), with $b_{(\Lambda,\lambda)}$ possible junctions at the boundary. The number of local operators is then $\sum_{\Lambda,\lambda} b^2_{\Lambda,\lambda}$. The OPE coefficients for the topological local operators in the 2D TQFT must be supported by the Lagrangian algebra (co)multiplication/M-symbols,

since one has the following manipulations:

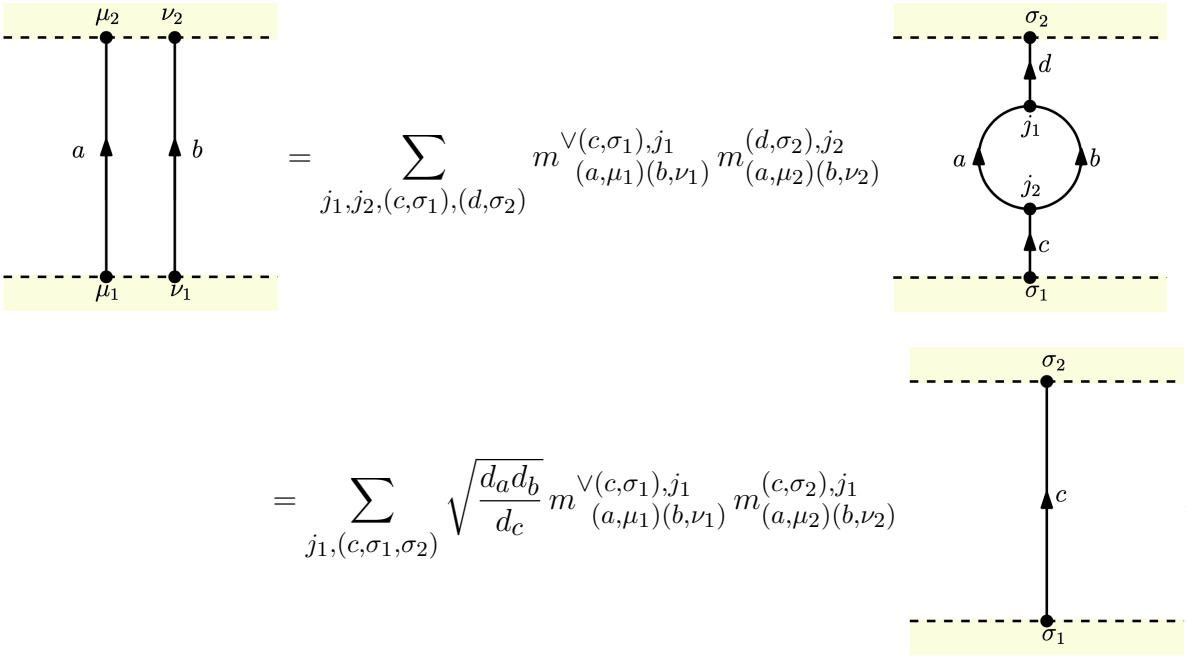

$$= \sum_{j_1,j_2,(c,\sigma_1),(d,\sigma_2)} m^{\vee(c,\sigma_1),j_1}_{(a,\mu_1)(b,\nu_1)}\, m^{(d,\sigma_2),j_2}_{(a,\mu_2)(b,\nu_2)}$$

$$= \sum_{j_1,(c,\sigma_1,\sigma_2)} \sqrt{\frac{d_a d_b}{d_c}}\, m^{\vee(c,\sigma_1),j_1}_{(a,\mu_1)(b,\nu_1)}\, m^{(c,\sigma_2),j_1}_{(a,\mu_2)(b,\nu_2)} \,. \tag{4.40}$$

In particular, notice that the multiplication of the Lagrangian algebra instructs one to consider in the fusion of bulk lines only junctions of the simple anyons belonging to the Lagrangian algebra, as one would have intuitively expected. Thus, one finds:

$$\phi_{(a;\mu_1,\mu_2)} \cdot \phi_{(b;\nu_1,\nu_2)} = \sum_{(c;\sigma_1,\sigma_2)} \mathcal{N}^{(c,\sigma_1,\sigma_2)}_{(a;\mu_1,\mu_2),(b;\nu_1,\nu_2)}\, \phi_{(c;\sigma_1,\sigma_2)}, \tag{4.41}$$

where

$$\mathcal{N}^{(c,\sigma_1,\sigma_2)}_{(a;\mu_1,\mu_2),(b;\nu_1,\nu_2)} := \sqrt{\frac{d_a d_b}{d_c}} \sum_{j_1} m^{\vee(c,\sigma_1),j_1}_{(a,\mu_1)(b,\nu_1)}\, m^{(c,\sigma_2),j_1}_{(a,\mu_2)(b,\nu_2)}. \tag{4.42}$$

In principle, this expression solves the general problem of determining the OPE coefficients $\mathcal{N}$ of the topological local operators (in the basis that diagonalizes the action of the lines) in terms of the data that characterizes the topological boundary.[20] As we saw above, for a

20. Notice the resemblance with the fact that the multiplication in a symmetric commutative special Frobenius algebra $\mathcal{E}$ in a RCFT determines the boundary OPE coefficients of the boundary operators living

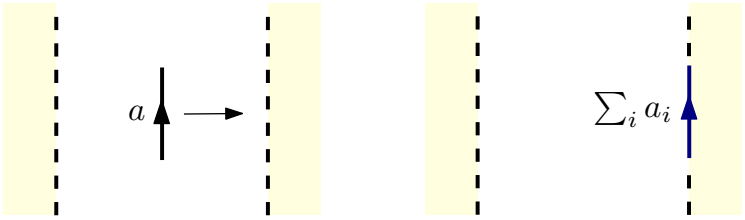

Figure 4.6: A simple line a in bulk generically becomes non-simple when pushed to a topological boundary: $a \to \sum_i a_i$.

topological coset the Lagrangian algebra object and the spectrum of endpoints is moreover determined by the branching rules of the conformal embedding. In particular, notice that the condition (4.22) translates to the fact that the coefficients satisfy

$$\sum_{(a;\mu_1,\mu_2),\,(b;\nu_1,\nu_2)} \mathcal{N}_{(a;\mu_1,\mu_2),(b;\nu_1,\nu_2)}^{(c,\sigma_1,\sigma_2)} = \dim(\mathcal{A}). \tag{4.43}$$

In order to illustrate the general solution, below we will study a couple of examples where the coefficients can be directly obtained from Lagrangian algebra multiplications. Of course, in practice, we may use as many allowed constraints to solve for the OPE coefficients as we wish. Below, we will also see examples where the precise coefficients will be determined from the condition (4.43) along with the constraints of commutativity and associativity of the OPE of local operators.

Line Operators

We move on now to discuss the topological line operators of the topological coset. The fusion category of line operators of the 2D theory can be constructed starting from the line operators in bulk and pushing them to the boundary. See Figure 4.6. Mathematically, the precise way to calculate the result is to construct the category of $\mathcal{A}$-modules, or the Karoubi envelope of the quotient category $\mathcal{C}/\mathcal{A}$ for the bulk MTC $\mathcal{C}$. This construction is rather abstract, so we

in the conformal boundary conditions associated with the $\mathcal{E}$-modular invariant [41].

present the rigorous definitions in Section 4.6.2 and here we content ourselves with outlining the more heuristic approach of [37]. In the following, we denote by $\otimes$ and $\oplus$ the fusion and direct sum of lines in the bulk MTC respectively, while we use $\times$ and $+$ for the fusion and direct sum of topological lines at the boundary respectively.

As stated previously, to find the line operators of the 2D theory we take a simple anyon a in bulk and push it to the boundary. In general, when we do this a simple anyon in bulk becomes non-simple at the boundary. This is, the bulk simple anyon a "splits" in terms of many boundary components:

$$a \longrightarrow \sum_i z_i^a a_i, \quad z_i^a \in \mathbb{N}, \tag{4.44}$$

where the subindex i labels the distinct line operators a_i that arise when a is pushed to the boundary. The integers z_i^a label multiplicities with which the a_i may appear in the decomposition. On the right-hand side of (4.44), it is important to note that the labels a_i that correspond to different simple anyons a in the bulk MTC do not always correspond to different simple line operators of the boundary theory. It generically happens that $a_i = b_j$ for bulk simple anyons $a \neq b$. In other words, not only does there exist a splitting procedure for the bulk anyons at the boundary, but there are also identifications between the boundary labels a_i.

In practice, one can often determine the splittings and identifications by imposing a set of consistency conditions. Firstly, it is important to observe that if one evaluates a loop of a simple anyon a before and after pushing it to the boundary (as depicted in Figure 4.6), one discovers that the quantum dimensions of the bulk lines must be conserved when they are pushed to the boundary:

$$a \longrightarrow \sum_i z_i^a a_i \Longrightarrow d_a = \sum_b z_i^a d_{a_i}. \tag{4.45}$$

Thus, splitting is constrained to preserve quantum dimension.

Secondly, we require that if

$$a \longrightarrow \sum_i z_i^a a_i, \Longrightarrow \bar{a} \longrightarrow \sum_i z_i^a \bar{a_i}. \tag{4.46}$$

Thus, the conjugate of a splits into the conjugates of the split of a.

Thirdly, simple anyons in the Lagrangian algebra $\mathcal{A} = \oplus_a n_a a$ always split into components that contain the identity line of the boundary theory:

$$a \to n_a \, 0 + \cdots . \tag{4.47}$$

In the anyon condensation jargon, these anyons are said to *condense*. As per the discussion in Section 4.2, only bosons can condense.

Finally, one requires consistency between bulk fusion and splitting. This is, when one gauges non-invertible anyons, the resulting boundary theory has a fusion ring satisfying the standard conditions of associativity, existence of a unique identity line, and existence of unique conjugate representations with a unique way to fuse to the identity line. Consistency between bulk fusion and splitting then means that one has that:

$$a \otimes b = \bigoplus_c N_{ab}^c c \Longrightarrow \Big(\sum_i {z_i}^a a_i \Big) \times \Big(\sum_j {z_j}^b b_j \Big) = \sum_{c,k} N_{ab}^c {z_k}^c c_k \, . \tag{4.48}$$

Thus, for instance, one can deduce that an anyon a splits if in the fusion $a \otimes \bar{a}$ more than one identity line appears on the right-hand side after splitting and using (4.47). Similarly, identifications can be found by studying $a \otimes b$ and studying the identity lines that appear after splitting. Once one has found the splitting and identifications of the bulk lines into boundary lines, one can furthermore exploit the previous equation and tightly constrain the fusion ring of the boundary lines. In many concrete cases, like the ones studied later in this

work, this allows one to find the fusion ring exactly.

Once we have obtained the spectrum of line and point operators following the previous discussion we can discuss the interplay of topological line operators with topological local operators on the topological coset. This is straightforward to do by considering a configuration where a loop wraps a line that ends at the boundary. Requiring that we obtain the same result either by calculating the braiding phase (2.16) in bulk first, or by pushing the loop to the boundary first and calculating the action of the boundary lines with the point operators, as in:

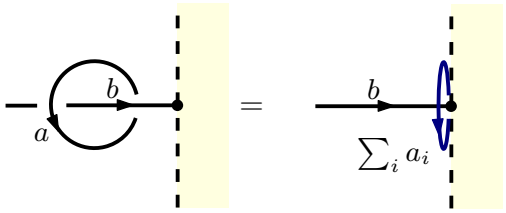

(4.49)

gives a set of equations from which we can readily find the action of the line operators on the point operators in the 2D theory.

4.4 Examples

In previous sections we have outlined the rules to describe a topological coset. In this section we provide concrete examples. One of them is essentially the simplest instance of a topological coset, and can be completely worked out in practice. The other examples are important in that they are (conjecturally) the IR fixed point of a massless 2D QCD theory. Other examples of topological cosets can be found from the table of conformal embeddings in [50].

In the following, we denote by $\otimes$ and $\oplus$ the fusion and direct sum of lines in the bulk MTC respectively, $\times$ and $+$ for the fusion and direct sum of topological lines at the boundary respectively, and by $\cdot$ the product of topological local operators in the diagonal basis (also called bootstrap basis [55]) inherited by the endpoints of the simple anyons in the bulk Lagrangian algebra $\mathcal{A}$. The spectrum and fusion rules of the MTCs used in this section can

be obtained from the KAC software program [111].

4.4.1 A Pedagogical Example

$SU(3)_1/SU(2)_4$

In this subsection we study the topological coset $SU(3)_1/SU(2)_4$. This is arguably the simplest topological coset, so for the sake of illustration we describe it here completely. The branching rules of this conformal embedding are well-known (see [5]) and are given by:

$$\chi_{\mathbf{1}}^{SU(3)_1}(q) = \chi_0^{SU(2)_4}(q) + \chi_4^{SU(2)_4}(q)\,, \tag{4.50}$$

$$\chi_{\mathbf{3}}^{SU(3)_1}(q) = \chi_2^{SU(2)_4}(q)\,, \tag{4.51}$$

$$\chi_{\bar{\mathbf{3}}}^{SU(3)_1}(q) = \chi_2^{SU(2)_4}(q)\,, \tag{4.52}$$

where we label an integrable representation in $SU(3)_1$ by its dimension in boldface and we use the standard indexing $i = 0, 1, \ldots, k$ to label the i-th integrable representation in $SU(2)_k$ (see Section 4.6.5 for a more detailed description of the MTC data of $SU(2)_k$).

Recall from the general discussion above that, as expected from a conformal embedding, all the branching functions are non-negative integers, independent of q. These non-negative integers are interpreted as a contribution to the spectrum of local operators in the coset theory (see e.g., [90]). On the other hand, from the perspective of the bulk-boundary correspondence, these contributions arise from the allowed endpoints of bosons in $SU(3)_1 \times SU(2)_{-4}$ at the topological boundary. That is, the branching rules yield a Lagrangian algebra $\mathcal{A}$ for the MTC $\mathcal{C} = SU(3)_1 \times SU(2)_{-4}$. Explicitly, the algebra object is given by:

$$\mathcal{A} = (\mathbf{1}, 0) \oplus (\mathbf{1}, 4) \oplus (\mathbf{3}, 2) \oplus (\bar{\mathbf{3}}, 2). \tag{4.53}$$

Indeed, it is straightforward to compute the quantum dimensions of the algebra object and the total quantum dimension of $\mathcal{C} = SU(3)_1 \times SU(2)_{-4}$ (recall Eqn. (2.9)) to check that

$$\dim\big(SU(3)_1 \times SU(2)_{-4}\big) = \dim(\mathcal{A})^2,$$

as required by the definition of a Lagrangian algebra in Eqn. (4.23).

Although we do not reproduce the calculation here, it is straightforward to use the setup described in Section 4.2 to check that gauging $\mathcal{A}$ in $SU(3)_1 \times SU(2)_{-4}$ in a bulk region of 3D spacetime results in the trivial MTC, thus generating a topological boundary when gauging on half of spacetime.

We move on now to discuss local operators. In the following, as in Section 4.2, we denote a topological local operator at the end of a bulk line a as ϕ_a.[21] The allowed OPE channels for the topological endpoints of bosons in the Lagrangian algebra may be obtained from the corresponding fusion rules in $SU(3)_1 \times SU(2)_{-4}$ and projecting into the elements of the algebra. Specifically:

$$\begin{aligned}
&(\mathbf{1},4)\otimes(\mathbf{1},4)\longrightarrow(\mathbf{1},0), \quad (\mathbf{1},4)\otimes(\mathbf{3},2)\longrightarrow(\mathbf{3},2), \quad (\mathbf{1},4)\otimes(\bar{\mathbf{3}},2)\longrightarrow(\bar{\mathbf{3}},2),\\
&(\mathbf{3},2)\otimes(\mathbf{3},2)\longrightarrow(\bar{\mathbf{3}},2), \quad (\bar{\mathbf{3}},2)\otimes(\bar{\mathbf{3}},2)\longrightarrow(\mathbf{3},2),\\
&(\mathbf{3},2)\otimes(\bar{\mathbf{3}},2)\longrightarrow(\mathbf{1},0)+(\mathbf{1},4).
\end{aligned} \tag{4.54}$$

In order to obtain a well-defined OPE in between the local operators ϕ_a in the diagonal basis, one must find an associative and commutative product consistent with the bulk Lagrangian algebra and the allowed OPE channels just presented. Indeed, it is straightforward

21. Notice that in Section 4.2, for generality, we kept track of multiple possible junctions in the subindices. In the following, we will suppress such indices since the junctions we will consider below will have single multiplicity.

to check that the fusion product of topological local operators given by

$$\begin{aligned}
&\phi_{(\mathbf{1},0)} \cdot \phi_{(a,b)} = \phi_{(a,b)}, \text{ for } (a,b) \in A, \\
&\phi_{(\mathbf{1},4)} \cdot \phi_{(\mathbf{1},4)} = \phi_{(\mathbf{1},0)}, \quad \phi_{(\mathbf{1},4)} \cdot \phi_{(\mathbf{3},2)} = \phi_{(\mathbf{3},2)}, \quad \phi_{(\mathbf{1},4)} \cdot \phi_{(\bar{\mathbf{3}},2)} = \phi_{(\bar{\mathbf{3}},2)}, \\
&\phi_{(\mathbf{3},2)} \cdot \phi_{(\mathbf{3},2)} = 2\,\phi_{(\bar{\mathbf{3}},2)}, \quad \phi_{(\bar{\mathbf{3}},2)} \cdot \phi_{(\bar{\mathbf{3}},2)} = 2\,\phi_{(\mathbf{3},2)}, \quad \phi_{(\mathbf{3},2)} \cdot \phi_{(\bar{\mathbf{3}},2)} = 2\,\phi_{(\mathbf{1},0)} + 2\phi_{(\mathbf{1},4)}.
\end{aligned} \tag{4.55}$$

is commutative, associative, and that (4.43) holds. As stressed previously, this topological coset can be worked out in detail, and in particular one can see explicitly that the previous OPE coefficients are supported by appropriate Lagrangian algebra multiplications. Specifically:

$$m^{(\mathbf{1},0)}_{(\mathbf{1},0)(\mathbf{1},0)} = m^{(\mathbf{1},4)}_{(\mathbf{1},0)(\mathbf{1},4)} = m^{(\mathbf{3},2)}_{(\mathbf{1},0)(\mathbf{3},2)} = m^{(\bar{\mathbf{3}},2)}_{(\mathbf{1},0)(\bar{\mathbf{3}},2)} = 1, \tag{4.56}$$

$$m^{(\mathbf{1},0)}_{(\mathbf{1},4)(\mathbf{1},4)} = m^{(\mathbf{1},0)}_{(\mathbf{3},2)(\bar{\mathbf{3}},2)} = m^{(\mathbf{1},0)}_{(\bar{\mathbf{3}},2)(\mathbf{3},2)} = 1, \tag{4.57}$$

$$m^{(\mathbf{1},4)}_{(\mathbf{3},2)(\bar{\mathbf{3}},2)} = -m^{(\mathbf{1},4)}_{(\bar{\mathbf{3}},2)(\mathbf{3},2)} = 1, \tag{4.58}$$

$$m^{(\mathbf{3},2)}_{(\mathbf{1},4)(\mathbf{3},2)} = -m^{(\mathbf{3},2)}_{(\mathbf{3},2)(\mathbf{1},4)} = 1, \tag{4.59}$$

$$m^{(\bar{\mathbf{3}},2)}_{(\mathbf{1},4)(\bar{\mathbf{3}},2)} = -m^{(\bar{\mathbf{3}},2)}_{(\bar{\mathbf{3}},2)(\mathbf{1},4)} = -1, \tag{4.60}$$

$$m^{(\bar{\mathbf{3}},2)}_{(\mathbf{3},2)(\mathbf{3},2)} = 2^{1/4}, \tag{4.61}$$

$$m^{(\mathbf{3},2)}_{(\bar{\mathbf{3}},2)(\bar{\mathbf{3}},2)} = -2^{1/4}. \tag{4.62}$$

This can be checked directly by plugging the multiplications into the (co)associativity conditions (4.18), or Eqn. (4.19) in components. Using (4.41) and (4.42), it is then straightforward to reproduce the coefficients in (4.55).

Having discussed the point operators in the theory, we may now proceed to examine the

spectrum of line operators. Given the limited number of objects in this example, it is possible to be particularly explicit about the computation based on Karoubian envelopes discussed in Section 4.6.2. Calculating a few fusions with the Lagrangian algebra object (4.53) will illustrate the procedure. Consider:

$$\mathcal{A} \otimes (\mathbf{1}, 0) = (\mathbf{1}, 0) \oplus (\mathbf{1}, 4) \oplus (\mathbf{3}, 2) \oplus (\bar{\mathbf{3}}, 2), \tag{4.63}$$

$$\mathcal{A} \otimes (\mathbf{1}, 1) = (\mathbf{1}, 1) \oplus (\mathbf{1}, 3) \oplus (\mathbf{3}, 1) \oplus (\mathbf{3}, 3) \oplus (\bar{\mathbf{3}}, 1) \oplus (\bar{\mathbf{3}}, 3), \tag{4.64}$$

$$\mathcal{A} \otimes (\mathbf{1}, 2) = 2(\mathbf{1}, 2) \oplus (\mathbf{3}, 0) \oplus (\mathbf{3}, 2) \oplus (\mathbf{3}, 4) \oplus (\bar{\mathbf{3}}, 0) \oplus (\bar{\mathbf{3}}, 2) \oplus (\bar{\mathbf{3}}, 4), \tag{4.65}$$

$$\mathcal{A} \otimes (\mathbf{3}, 0) = (\mathbf{3}, 0) \oplus (\mathbf{3}, 4) \oplus (\bar{\mathbf{3}}, 2) \oplus (\mathbf{1}, 2), \tag{4.66}$$

$$\mathcal{A} \otimes (\bar{\mathbf{3}}, 0) = (\bar{\mathbf{3}}, 0) \oplus (\bar{\mathbf{3}}, 4) \oplus (\mathbf{3}, 2) \oplus (\mathbf{1}, 2). \tag{4.67}$$

From this we deduce, for example:

$$\mathrm{Hom}((\mathbf{1}, 2), \mathcal{A} \otimes (\mathbf{1}, 2)) = \mathbb{C}^2, \tag{4.68}$$

$$\mathrm{Hom}((\mathbf{1}, 2), \mathcal{A} \otimes (\mathbf{3}, 0)) = \mathbb{C}, \tag{4.69}$$

$$\mathrm{Hom}((\mathbf{1}, 2), \mathcal{A} \otimes (\bar{\mathbf{3}}, 0)) = \mathbb{C}, \tag{4.70}$$

$$\mathrm{Hom}((\mathbf{3}, 0), \mathcal{A} \otimes (\mathbf{3}, 0)) = \mathbb{C}, \tag{4.71}$$

$$\mathrm{Hom}((\bar{\mathbf{3}}, 0), \mathcal{A} \otimes (\bar{\mathbf{3}}, 0)) = \mathbb{C}. \tag{4.72}$$

A few consequences follow from this calculation. For example, $\mathrm{Hom}((\mathbf{1}, 2), \mathcal{A} \otimes (\mathbf{1}, 2)) = \mathbb{C}^2$ implies that $(\mathbf{1}, 2)$ splits into two lines at the boundary. Similarly, $(\mathbf{3}, 0)$ and $(\bar{\mathbf{3}}, 0)$ do not split. The fact that $\mathrm{Hom}((\mathbf{1}, 2), \mathcal{A} \otimes (\mathbf{3}, 0)) = \mathbb{C}$ means that one of the splitting channels of $(\mathbf{1}, 2)$ coincides with the line to which $(\mathbf{3}, 0)$ descends at the boundary. We denote this

$(\mathbf{1},0)$, $(\mathbf{1},4) \to \mathbf{1}$	$(\mathbf{1},2) \to \mathbf{3}+\bar{\mathbf{3}}$
$(\mathbf{3},0)$, $(\mathbf{3},4) \to \mathbf{3}$	$(\mathbf{3},2) \to \mathbf{1}+\bar{\mathbf{3}}$
$(\bar{\mathbf{3}},0)$, $(\bar{\mathbf{3}},4) \to \bar{\mathbf{3}}$	$(\bar{\mathbf{3}},2) \to \mathbf{1}+\mathbf{3}$
$(\mathbf{1},1)$, $(\mathbf{3},1)$, $(\bar{\mathbf{3}},1)$, $(\mathbf{1},3)$, $(\mathbf{3},3)$, $(\bar{\mathbf{3}},3) \to \mathcal{N}$	

Table 4.1: Descent of the bulk topological lines of $SU(3)_1 \times SU(2)_{-4}$ (left of the arrows) to the topological boundary. The resulting lines (right of the arrows) describe the topological line operators in the $SU(3)_1/SU(2)_4$ topological coset.

common line at the boundary $\mathbf{3}$. A similar statement holds for $(\bar{\mathbf{3}},0)$, whose boundary line is denoted as $\bar{\mathbf{3}}$. However, from (4.66) and (4.67), we deduce that $(\mathbf{3},0)$ and $(\bar{\mathbf{3}},0)$ share no common channel at the boundary, so they descend into different boundary lines: $\bar{\mathbf{3}} \neq \mathbf{3}$. A similar procedure can be performed for the rest of the lines, revealing that there is only one further additional line at the boundary, denoted $\mathcal{N}$. The overall result for all the lines and what they descend to at the boundary is presented in Table 4.1.

The fusion rules of the lines at the boundary can be found from the discussion around Eqn. (4.48). Indeed, from the spectrum already found, we see that the only consistent fusion ring is given by

$$\mathbf{3} \times \mathbf{3} = \bar{\mathbf{3}}, \quad \mathbf{3} \times \bar{\mathbf{3}} = \bar{\mathbf{3}} \times \mathbf{3} = \mathbf{1}, \quad \bar{\mathbf{3}} \times \bar{\mathbf{3}} = \mathbf{3}, \tag{4.73}$$

$$\mathbf{3} \times \mathcal{N} = \mathcal{N} \times \mathbf{3} = \mathcal{N}, \quad \bar{\mathbf{3}} \times \mathcal{N} = \mathcal{N} \times \bar{\mathbf{3}} = \mathcal{N}, \quad \mathcal{N} \times \mathcal{N} = \mathbf{1} + \mathbf{3} + \bar{\mathbf{3}}, \tag{4.74}$$

which we recognize as the fusion ring of $\mathbb{Z}_3$ Tambara-Yamagami. Actually, from the simplicity of the topological coset we can further identify the full fusion category as the $\mathbb{Z}_3$ Tambara-Yamagami fusion category with non-trivial bicharacter and non-trivial Frobenius-Schur indicator. See, for instance [182], where it is easy to identify that the Drinfeld center of the fusion category just mentioned indeed coincides with $SU(3)_1 \times SU(2)_{-4}$.

Finally, to check that everything is in order we can check the existence of an idempotent complete basis where the line operators act according to (4.31). This can be straightforwardly

be checked to be correct, with:

$$\mathcal{O}_0 = \frac{1}{6}(\phi_{(\mathbf{1},0)} + \phi_{(\mathbf{1},4)} + \phi_{(\mathbf{3},2)} + \phi_{(\bar{\mathbf{3}},2)}), \tag{4.75}$$

$$\mathcal{O}_{\mathbf{3}} = \frac{1}{6}(\phi_{(\mathbf{1},0)} + \phi_{(\mathbf{1},4)} + \omega\phi_{(\mathbf{3},2)} + \omega^2\phi_{(\bar{\mathbf{3}},2)}), \tag{4.76}$$

$$\mathcal{O}_{\bar{\mathbf{3}}} = \frac{1}{6}(\phi_{(\mathbf{1},0)} + \phi_{(\mathbf{1},4)} + \omega^2\phi_{(\mathbf{3},2)} + \omega\phi_{(\bar{\mathbf{3}},2)}), \tag{4.77}$$

$$\mathcal{O}_{\mathcal{N}} = \frac{1}{6}(\sqrt{3}\phi_{(\mathbf{1},0)} - \sqrt{3}\phi_{(\mathbf{1},4)}). \tag{4.78}$$

In upcoming examples the calculations are essentially equivalent to those displayed in this example, but more complicated to showcase explicitly because of the higher number of objects involved. Thus, we will present results without presenting detailed calculations, leaving implicit that they proceed in the same way as presented in Section 4.2 and this example.

4.4.2 QCD-like Examples

$Spin(5)_1/SU(2)_{10}$

We now move on to describe a topological coset describing the IR fixed point of a 2D QCD theory. Specifically, we study the $Spin(5)_1/SU(2)_{10}$ topological coset, describing the IR fixed point of (bosonized) $SU(2)$ Yang-Mills theory with fermions in the spin 2 representation. The branching rules of the conformal embedding are given by:

$$\chi_0^{Spin(5)_1}(q) = \chi_0^{SU(2)_{10}}(q) + \chi_6^{SU(2)_{10}}(q)\,, \tag{4.79}$$

$$\chi_v^{Spin(5)_1}(q) = \chi_4^{SU(2)_{10}}(q) + \chi_{10}^{SU(2)_{10}}(q)\,, \tag{4.80}$$

$$\chi_\sigma^{Spin(5)_1}(q) = \chi_3^{SU(2)_{10}}(q) + \chi_7^{SU(2)_{10}}(q)\,. \tag{4.81}$$

As before, interpreting the non-negative integers in the branching functions as the allowed topological endpoints of bosons at the gapped boundaries leads us to a Lagrangian algebra for the MTC $\mathcal{C} = Spin(5)_1 \times SU(2)_{-10}$. Explicitly, the algebra object is:

$$\mathcal{A} = (0,0) \oplus (v,10) \oplus (0,6) \oplus (v,4) \oplus (\sigma,3) \oplus (\sigma,7), \tag{4.82}$$

where clearly all the entries are bosons, and using the MTC data summarized in Section 4.6.5, it is straightforward to check that Eqn. (4.23) defining a Lagrangian algebra is fulfilled.

From the MTC data we can also obtain the allowed OPE channels between topological endpoints in the Lagrangian algebra, from which following the discussion in Section 4.2 we can derive the following set of OPE coefficients:

$$\phi_{(0,0)} \cdot \phi_{(a,b)} = \phi_{(a,b)}, \text{ for } (a,b) \in \mathcal{A}, \tag{4.83}$$

$$\phi_{(v,10)} \cdot \phi_{(v,10)} = \phi_{(0,0)}, \quad \phi_{(v,10)} \cdot \phi_{(0,6)} = \phi_{(v,4)}, \quad \phi_{(v,10)} \cdot \phi_{(\sigma,3)} = \phi_{(\sigma,7)}, \tag{4.84}$$

$(0,0) \to 0$	$(v,0) \to v$	$(\sigma,0) \to \sigma$
$(0,1) \to 1$	$(v,1) \to 9$	$(\sigma,1) \to 2$
$(0,2) \to 2$	$(v,2) \to 2$	$(\sigma,2) \to 1+9$
$(0,3) \to 9+\sigma$	$(v,3) \to 1+\sigma$	$(\sigma,3) \to 0+2+v$
$(0,4) \to 2+v$	$(v,4) \to 0+2$	$(\sigma,4) \to 1+9+\sigma$
$(0,5) \to 1+9$	$(v,5) \to 1+9$	$(\sigma,5) \to 2(2)$
$(0,6) \to 0+2$	$(v,6) \to 2+v$	$(\sigma,6) \to 1+9+\sigma$
$(0,7) \to 1+\sigma$	$(v,7) \to 9+\sigma$	$(\sigma,7) \to 0+2+v$
$(0,8) \to 2$	$(v,8) \to 2$	$(\sigma,8) \to 1+9$
$(0,9) \to 9$	$(v,9) \to 1$	$(\sigma,9) \to 2$
$(0,10) \to v$	$(v,10) \to 0$	$(\sigma,10) \to \sigma$

Table 4.2: Splitting of the bulk topological lines of $Spin(5)_1 \times SU(2)_{-10}$ (left of the arrows) to the topological boundary. The resulting lines (right of the arrows) describe the topological line operators in the $Spin(5)_1/SU(2)_{10}$ topological coset.

$\times$	v	1	2	9	σ
v	0	9	2	1	σ
1	9	$0+2$	$1+9+\sigma$	$2+v$	2
2	2	$1+9+\sigma$	$0+v+2(2)$	$1+9+\sigma$	$1+9$
9	1	$2+v$	$1+9+\sigma$	$0+2$	2
σ	σ	2	$1+9$	2	$0+v$

Table 4.3: Fusion ring of the topological defect lines in the $Spin(5)_1/SU(2)_{10}$ topological coset. The line labeled as 0 corresponds to the identity line.

$$\phi_{(0,6)} \cdot \phi_{(0,6)} = \phi_{(v,4)} \cdot \phi_{(v,4)} = (2+\sqrt{3})\phi_{(0,0)} + (1+\sqrt{3})\,\phi_{(0,6)}, \tag{4.85}$$

$$\phi_{(0,6)} \cdot \phi_{(v,4)} = (2+\sqrt{3})\phi_{(v,10)} + (1+\sqrt{3})\,\phi_{(v,4)}, \tag{4.86}$$

$$\phi_{(0,6)} \cdot \phi_{(\sigma,3)} = \phi_{(v,4)} \cdot \phi_{(\sigma,7)} = \frac{1}{2}(1+\sqrt{3})\phi_{(\sigma,3)} + \frac{1}{2}(3+\sqrt{3})\phi_{(\sigma,7)}, \tag{4.87}$$

$$\phi_{(0,6)} \cdot \phi_{(\sigma,7)} = \phi_{(v,4)} \cdot \phi_{(\sigma,3)} = \frac{1}{2}(3+\sqrt{3})\phi_{(\sigma,3)} + \frac{1}{2}(1+\sqrt{3})\phi_{(\sigma,7)}, \tag{4.88}$$

$$\phi_{(\sigma,3)} \cdot \phi_{(\sigma,3)} = (3+\sqrt{3})\phi_{(0,0)} + \sqrt{3}\phi_{(0,6)} + 3\phi_{(v,4)}, \tag{4.89}$$

$$\phi_{(\sigma,3)} \cdot \phi_{(\sigma,7)} = (3+\sqrt{3})\phi_{(v,10)} + 3\phi_{(0,6)} + \sqrt{3}\phi_{(v,4)}, \tag{4.90}$$

$$\phi_{(\sigma,7)} \cdot \phi_{(\sigma,7)} = (3+\sqrt{3})\phi_{(0,0)} + \sqrt{3}\phi_{(0,6)} + 3\phi_{(v,4)}. \tag{4.91}$$

This result is exact in the extreme IR limit, and the OPE coefficients along the RG flow must tend towards these expressions as one approaches the IR fixed point. Notice that associativity alone does not completely fix the coefficients above, but the special Frobenius condition (4.43) derived from consistency with the Lagrangian algebra multiplication adds an additional equation that readily fixes their values.

Similar to the previous example, it is possible to verify that the previous coefficients are supported by suitable Lagrangian algebra multiplications (see Eqn. (4.42)). The specific values are presented in Section 4.6.4, however, since there are too many entries to present here in a streamlined manner. As explained in Section 4.2, the multiplications are derived

using the (co)associativity conditions (4.18) and the specific input obtained from the MTC data in Section 4.6.5.

Now that we have discussed the point operators in the theory, we move on to obtain the spectrum of line operators and their fusion ring. To find the topological lines operators of the topological coset, we have to compute the spectrum of topological lines at the boundary. Either if we use Karoubi completions, or using the consistency conditions of splitting discussed in Section 4.2 directly, we find the spectrum of boundary lines presented in Table 4.2 with the fusion ring presented in Table 4.3.

To check the consistency of the data obtained one may check the existence of the idempotent complete basis (4.30). The specific transformation in this case is given by:

$$
\begin{aligned}
\mathcal{O}_0 &= \frac{1}{4(3+\sqrt{3})}(\phi_{(0,0)} + \phi_{(0,6)} + \phi_{(v,10)} + \phi_{(v,4)} + \phi_{(\sigma,3)} + \phi_{(\sigma,7)}),\\
\mathcal{O}_v &= \frac{1}{4(3+\sqrt{3})}(\phi_{(0,0)} + \phi_{(0,6)} + \phi_{(v,10)} + \phi_{(v,4)} - \phi_{(\sigma,3)} - \phi_{(\sigma,7)}),\\
\mathcal{O}_2 &= \frac{1}{4(3+\sqrt{3})}((1+\sqrt{3})\phi_{(0,0)} + (1-\sqrt{3})\phi_{(0,6)} + (1+\sqrt{3})\phi_{(v,10)} + (1-\sqrt{3})\phi_{(v,4)}),\\
\mathcal{O}_\sigma &= \frac{1}{4(3+\sqrt{3})}(\sqrt{2}\phi_{(0,0)} + \sqrt{2}\phi_{(0,6)} - \sqrt{2}\phi_{(v,10)} - \sqrt{2}\phi_{(v,4)}),\\
\mathcal{O}_1 &= \frac{1}{4(3+\sqrt{3})}(\sqrt{2+\sqrt{3}}\phi_{(0,0)} - \sqrt{2-\sqrt{3}}\phi_{(0,6)} - \sqrt{2+\sqrt{3}}\phi_{(v,10)}\\
&\qquad + \sqrt{2-\sqrt{3}}\phi_{(v,4)} + \phi_{(\sigma,3)} - \phi_{(\sigma,7)}),\\
\mathcal{O}_9 &= \frac{1}{4(3+\sqrt{3})}(\sqrt{2+\sqrt{3}}\phi_{(0,0)} - \sqrt{2-\sqrt{3}}\phi_{(0,6)} - \sqrt{2+\sqrt{3}}\phi_{(v,10)}),\\
&\qquad + \sqrt{2-\sqrt{3}}\phi_{(v,4)} - \phi_{(\sigma,3)} + \phi_{(\sigma,7)}).
\end{aligned}
\tag{4.92}
$$

$Spin(8)_1/SU(3)_3$

In this subsection we work out the topological coset $Spin(8)_1/SU(3)_3$, which describes the IR fixed point of (bosonized) 2D QCD with gauge group $SU(3)$ and fermions in the adjoint representation. The branching rules for this coset are well-known and are given by:

$$\chi_0^{Spin(8)_1}(q) = \chi_{\mathbf{1}}^{SU(3)_3}(q) + \chi_{\mathbf{10}}^{SU(3)_3}(q) + \chi_{\overline{\mathbf{10}}}^{SU(3)_3}(q), \tag{4.93}$$

$$\chi_{\mathbf{v}}^{Spin(8)_1}(q) = \chi_{\mathbf{8}}^{SU(3)_3}(q), \tag{4.94}$$

$$\chi_{\mathbf{s}}^{Spin(8)_1}(q) = \chi_{\mathbf{8}}^{SU(3)_3}(q), \tag{4.95}$$

$$\chi_{\mathbf{c}}^{Spin(8)_1}(q) = \chi_{\mathbf{8}}^{SU(3)_3}(q). \tag{4.96}$$

Correspondingly, we can construct the following Lagrangian algebra object:

$$\mathcal{A} = (0,\mathbf{1}) \oplus (0,\mathbf{10}) \oplus (0,\overline{\mathbf{10}}) \oplus (\mathbf{v},\mathbf{8}) \oplus (\mathbf{s},\mathbf{8}) \oplus (\mathbf{c},\mathbf{8}), \tag{4.97}$$

where it is easy to check, for instance, the constraint on the quantum dimensions (4.23) demanded by the definition of a Lagrangian algebra. Working out the spectrum of topological local operators in the diagonal basis and their OPE along the lines of Section 4.2 (see also previous examples), we find the OPE coefficients:

$$\phi_{(0,\mathbf{10})} \cdot \phi_{(0,\mathbf{10})} = \phi_{(0,\overline{\mathbf{10}})}, \quad \phi_{(0,\overline{\mathbf{10}})} \cdot \phi_{(0,\overline{\mathbf{10}})} = \phi_{(0,\mathbf{10})}, \tag{4.98}$$

$$\phi_{(0,\mathbf{10})} \cdot \phi_{(0,\overline{\mathbf{10}})} = \phi_{(0,\overline{\mathbf{10}})} \cdot \phi_{(0,\mathbf{10})} = \phi_{(0,\mathbf{1})}, \tag{4.99}$$

$$\phi_{(0,\mathbf{10})} \cdot \phi_{(i,\mathbf{8})} = \phi_{(0,\overline{\mathbf{10}})} \cdot \phi_{(i,\mathbf{8})} = \phi_{(i,\mathbf{8})} \cdot \phi_{(0,\mathbf{10})} = \phi_{(i,\mathbf{8})} \cdot \phi_{(0,\overline{\mathbf{10}})} = \phi_{(i,\mathbf{8})}, \tag{4.100}$$

$$\phi_{(\mathbf{v},\mathbf{8})} \cdot \phi_{(\mathbf{s},\mathbf{8})} = \phi_{(\mathbf{s},\mathbf{8})} \cdot \phi_{(\mathbf{v},\mathbf{8})} = 3\phi_{(\mathbf{c},\mathbf{8})}, \tag{4.101}$$

$$\phi_{(\mathbf{s},\mathbf{8})} \cdot \phi_{(\mathbf{c},\mathbf{8})} = \phi_{(\mathbf{c},\mathbf{8})} \cdot \phi_{(\mathbf{s},\mathbf{8})} = 3\phi_{(\mathbf{v},\mathbf{8})}, \tag{4.102}$$

$$\phi_{(\mathbf{c},\mathbf{8})} \cdot \phi_{(\mathbf{v},\mathbf{8})} = \phi_{(\mathbf{v},\mathbf{8})} \cdot \phi_{(\mathbf{c},\mathbf{8})} = 3\phi_{(\mathbf{s},\mathbf{8})}, \tag{4.103}$$

$$\phi_{(\mathbf{v},\mathbf{8})} \cdot \phi_{(\mathbf{v},\mathbf{8})} = \phi_{(\mathbf{s},\mathbf{8})} \cdot \phi_{(\mathbf{s},\mathbf{8})} = \phi_{(\mathbf{c},\mathbf{8})} \cdot \phi_{(\mathbf{c},\mathbf{8})} = 3\phi_{(0,\mathbf{1})} + 3\phi_{(0,\mathbf{10})} + 3\phi_{(0,\overline{\mathbf{10}})}, \tag{4.104}$$

where obviously $\phi_{(0,\mathbf{1})} \cdot \phi_a = \phi_a$ for any $a \in \mathcal{A}$. It is straightforward to check that the product above is commutative, associative, and that the special Frobenius condition (4.22) is fulfilled. This result is exact in the extreme IR limit, and of course approximate along the RG flow slightly above the IR fixed point. Notice that associativity alone does not completely fix the coefficients above, but the special Frobenius condition (4.43) adds an additional equation that readily fixes their values.

Similarly, we can study the topological line operators of the topological coset. The bulk line operators descend to line operators at the boundary according to the splitting and identifications shown in Table 4.4. It is straightforward to calculate the fusion ring of the line defects, and the result is shown in Table 4.5.

$(0,0) \to 0$	$(v,0) \to \mathbf{v}$	$(s,0) \to \mathbf{s}$	$(c,0) \to \mathbf{c}$
$(0,\mathbf{10}) \to 0$	$(v,\mathbf{10}) \to \mathbf{v}$	$(s,\mathbf{10}) \to \mathbf{s}$	$(c,\mathbf{10}) \to \mathbf{c}$
$(0,\bar{\mathbf{10}}) \to 0$	$(v,\bar{\mathbf{10}}) \to \mathbf{v}$	$(s,\bar{\mathbf{10}}) \to \mathbf{s}$	$(c,\bar{\mathbf{10}}) \to \mathbf{c}$
$(0,\mathbf{3}) \to \mathcal{N}$	$(v,\mathbf{3}) \to \mathcal{N}$	$(s,\mathbf{3}) \to \mathcal{N}$	$(c,\mathbf{3}) \to \mathcal{N}$
$(0,\mathbf{15}) \to \mathcal{N}$	$(v,\mathbf{15}) \to \mathcal{N}$	$(s,\mathbf{15}) \to \mathcal{N}$	$(c,\mathbf{15}) \to \mathcal{N}$
$(0,\bar{\mathbf{6}}) \to \mathcal{N}$	$(v,\bar{\mathbf{6}}) \to \mathcal{N}$	$(s,\bar{\mathbf{6}}) \to \mathcal{N}$	$(c,\bar{\mathbf{6}}) \to \mathcal{N}$
$(0,\mathbf{6}) \to \bar{\mathcal{N}}$	$(v,\mathbf{6}) \to \bar{\mathcal{N}}$	$(s,\mathbf{6}) \to \bar{\mathcal{N}}$	$(c,\mathbf{6}) \to \bar{\mathcal{N}}$
$(0,\bar{\mathbf{15}}) \to \bar{\mathcal{N}}$	$(v,\bar{\mathbf{15}}) \to \bar{\mathcal{N}}$	$(s,\bar{\mathbf{15}}) \to \bar{\mathcal{N}}$	$(c,\bar{\mathbf{15}}) \to \bar{\mathcal{N}}$
$(0,\bar{\mathbf{3}}) \to \bar{\mathcal{N}}$	$(v,\bar{\mathbf{3}}) \to \bar{\mathcal{N}}$	$(s,\bar{\mathbf{3}}) \to \bar{\mathcal{N}}$	$(c,\bar{\mathbf{3}}) \to \bar{\mathcal{N}}$
$(0,\mathbf{8}) \to \mathbf{v}+\mathbf{s}+\mathbf{c}$	$(v,\mathbf{8}) \to 0+\mathbf{s}+\mathbf{c}$	$(s,\mathbf{8}) \to 0+\mathbf{v}+\mathbf{c}$	$(c,\mathbf{8}) \to 0+\mathbf{v}+\mathbf{s}$

Table 4.4: Descent of the bulk topological lines of $Spin(8)_1 \times SU(3)_{-3}$ (left of the arrows) to the topological boundary. The resulting lines (right of the arrows) describe the topological line operators in the $Spin(8)_1/SU(3)_3$ topological coset.

$\times$	$\mathcal{N}$	$\bar{\mathcal{N}}$	$\mathbf{v}$	$\mathbf{s}$	$\mathbf{c}$
$\mathcal{N}$	$2\bar{\mathcal{N}}$	$0+\mathbf{v}+\mathbf{s}+\mathbf{c}$	$\mathcal{N}$	$\mathcal{N}$	$\mathcal{N}$
$\bar{\mathcal{N}}$	$0+\mathbf{v}+\mathbf{s}+\mathbf{c}$	$2\mathcal{N}$	$\bar{\mathcal{N}}$	$\bar{\mathcal{N}}$	$\bar{\mathcal{N}}$
$\mathbf{v}$	$\mathcal{N}$	$\bar{\mathcal{N}}$	0	$\mathbf{c}$	$\mathbf{s}$
$\mathbf{s}$	$\mathcal{N}$	$\bar{\mathcal{N}}$	$\mathbf{c}$	0	$\mathbf{v}$
$\mathbf{c}$	$\mathcal{N}$	$\bar{\mathcal{N}}$	$\mathbf{s}$	$\mathbf{v}$	0

Table 4.5: Fusion ring of the topological defect lines in the $Spin(8)_1/SU(3)_3$ topological coset. The line labeled as 0 corresponds to the identity line.

As a check of the formalism, we can transform the topological local operators to the idempotent complete basis. The transformation is given by:

$$\mathcal{O}_0 = \frac{1}{12}(\phi_{(0,0)} + \phi_{(0,\mathbf{10})} + \phi_{(0,\bar{\mathbf{10}})} + \phi_{(\mathbf{v},\mathbf{8})} + \phi_{(\mathbf{s},\mathbf{8})} + \phi_{(\mathbf{c},\mathbf{8})}), \tag{4.105}$$

$$\mathcal{O}_{\mathbf{v}} = \frac{1}{12}(\phi_{(0,0)} + \phi_{(0,\mathbf{10})} + \phi_{(0,\bar{\mathbf{10}})} + \phi_{(\mathbf{v},\mathbf{8})} - \phi_{(\mathbf{s},\mathbf{8})} - \phi_{(\mathbf{c},\mathbf{8})}), \tag{4.106}$$

$$\mathcal{O}_{\mathbf{s}} = \frac{1}{12}(\phi_{(0,0)} + \phi_{(0,\mathbf{10})} + \phi_{(0,\bar{\mathbf{10}})} - \phi_{(\mathbf{v},\mathbf{8})} + \phi_{(\mathbf{s},\mathbf{8})} - \phi_{(\mathbf{c},\mathbf{8})}), \tag{4.107}$$

$$\mathcal{O}_{\mathbf{c}} = \frac{1}{12}(\phi_{(0,0)} + \phi_{(0,\mathbf{10})} + \phi_{(0,\bar{\mathbf{10}})} - \phi_{(\mathbf{v},\mathbf{8})} - \phi_{(\mathbf{s},\mathbf{8})} + \phi_{(\mathbf{c},\mathbf{8})}), \tag{4.108}$$

$$\mathcal{O}_{\mathcal{N}} = \frac{1}{12}(2\phi_{(0,0)} + 2\omega\phi_{(0,\mathbf{10})} + 2\omega^2\phi_{(0,\bar{\mathbf{10}})}), \tag{4.109}$$

$$\mathcal{O}_{\bar{\mathcal{N}}} = \frac{1}{12}(2\phi_{(0,0)} + 2\omega^2\phi_{(0,\mathbf{10})} + 2\omega\phi_{(0,\bar{\mathbf{10}})}). \tag{4.110}$$

Indeed, it is straightforward to check that the lines in the 2D theory act according to (4.31) for any of the line operators in Table 4.4 and the fusion rules in the fusion ring displayed in Table 4.5.

$Spin(16)_1/Spin(9)_2$

In this subsection we work out the topological coset $Spin(16)_1/Spin(9)_2$, which describes the IR fixed point of (bosonized) 2D QCD with gauge group $Spin(9)$ with fermions in the

$(0,\mathbf{1}) \to 0$	$(\mathbf{v},\mathbf{1}) \to \mathbf{v}$	$(\mathbf{s},\mathbf{1}) \to \mathbf{s}$	$(\mathbf{c},\mathbf{1}) \to \mathbf{c}$
$(0,\mathbf{44}) \to \mathbf{s}$	$(\mathbf{v},\mathbf{44}) \to \mathbf{c}$	$(\mathbf{s},\mathbf{44}) \to 0$	$(\mathbf{c},\mathbf{44}) \to \mathbf{v}$
$(0,\mathbf{16}) \to \mathbf{v}+B$	$(\mathbf{v},\mathbf{16}) \to 0+A$	$(\mathbf{s},\mathbf{16}) \to \mathbf{c}+B$	$(\mathbf{c},\mathbf{16}) \to \mathbf{s}+A$
$(0,\mathbf{128}) \to \mathbf{c}+B$	$(\mathbf{v},\mathbf{128}) \to \mathbf{s}+A$	$(\mathbf{s},\mathbf{128}) \to \mathbf{v}+B$	$(\mathbf{c},\mathbf{128}) \to 0+A$
$(0,\mathbf{126}) \to A$	$(\mathbf{v},\mathbf{126}) \to B$	$(\mathbf{s},\mathbf{126}) \to A$	$(\mathbf{c},\mathbf{126}) \to B$
$(0,\mathbf{84}) \to 0+\mathbf{s}$	$(\mathbf{v},\mathbf{84}) \to \mathbf{v}+\mathbf{c}$	$(\mathbf{s},\mathbf{84}) \to 0+\mathbf{s}$	$(\mathbf{c},\mathbf{84}) \to \mathbf{v}+\mathbf{c}$
$(0,\mathbf{36}) \to A$	$(\mathbf{v},\mathbf{36}) \to B$	$(\mathbf{s},\mathbf{36}) \to A$	$(\mathbf{c},\mathbf{36}) \to B$
$(0,\mathbf{9}) \to A$	$(\mathbf{v},\mathbf{9}) \to B$	$(\mathbf{s},\mathbf{9}) \to A$	$(\mathbf{c},\mathbf{9}) \to B$

Table 4.6: Descent of the bulk topological lines of $Spin(16)_1 \times Spin(9)_{-2}$ (left of the arrows) to the topological boundary. The resulting lines (right of the arrows) describe the topological line operators in the $Spin(16)_1/Spin(9)_2$ topological coset.

spinorial representation. We borrow the branching rules from [90]:

$$\chi_0^{Spin(16)_1}(q) = \chi_{\mathbf{1}}^{Spin(9)_2}(q) + \chi_{\mathbf{84}}^{Spin(9)_2}(q), \tag{4.111}$$

$$\chi_{\mathbf{v}}^{Spin(16)_1}(q) = \chi_{\mathbf{16}}^{Spin(9)_2}(q), \tag{4.112}$$

$$\chi_{\mathbf{s}}^{Spin(16)_1}(q) = \chi_{\mathbf{44}}^{Spin(9)_2}(q) + \chi_{\mathbf{84}}^{Spin(9)_2}(q), \tag{4.113}$$

$$\chi_{\mathbf{c}}^{Spin(16)_1}(q) = \chi_{\mathbf{128}}^{Spin(9)_2}(q). \tag{4.114}$$

The associated Lagrangian algebra object is:

$$\mathcal{A} = (0,\mathbf{1}) \oplus (0,\mathbf{84}) \oplus (\mathbf{v},\mathbf{16}) \oplus (\mathbf{s},\mathbf{44}) \oplus (\mathbf{s},\mathbf{84}) \oplus (\mathbf{c},\mathbf{128}). \tag{4.115}$$

Again, it is straightforward to check the constraint on the quantum dimensions: $\dim(\mathcal{A})^2 = \dim(Spin(16)_1 \times Spin(9)_{-2})$. Working out the spectrum of topological local operators and their OPE along the lines of Section 4.2, we find the following OPE coefficients:

$$\phi_{(\mathbf{s},\mathbf{44})} \cdot \phi_{(\mathbf{s},\mathbf{44})} = \phi_{(0,\mathbf{1})}, \tag{4.116}$$

$$\phi_{(\mathbf{s},\mathbf{44})} \cdot \phi_{(\mathbf{v},\mathbf{16})} = \phi_{(\mathbf{v},\mathbf{16})} \cdot \phi_{(\mathbf{s},\mathbf{44})} = \phi_{(\mathbf{c},\mathbf{128})}, \tag{4.117}$$

$$\phi_{(\mathbf{s},\mathbf{44})} \cdot \phi_{(0,\mathbf{84})} = \phi_{(0,\mathbf{84})} \cdot \phi_{(\mathbf{s},\mathbf{44})} = \phi_{(\mathbf{s},\mathbf{84})}, \tag{4.118}$$

$$\phi_{(\mathbf{v},\mathbf{16})} \cdot \phi_{(0,\mathbf{84})} = \phi_{(0,\mathbf{84})} \cdot \phi_{(\mathbf{v},\mathbf{16})} = 2\phi_{(\mathbf{v},\mathbf{16})}, \tag{4.119}$$

$$\phi_{(\mathbf{v},\mathbf{16})} \cdot \phi_{(\mathbf{v},\mathbf{16})} = \phi_{(\mathbf{c},\mathbf{128})} \cdot \phi_{(\mathbf{c},\mathbf{128})} = 3\phi_{(0,\mathbf{1})} + 3\phi_{(0,\mathbf{84})} \tag{4.120}$$

$$\phi_{(0,\mathbf{84})} \cdot \phi_{(0,\mathbf{84})} = \phi_{(\mathbf{s},\mathbf{84})} \cdot \phi_{(\mathbf{s},\mathbf{84})} = 2\phi_{(0,\mathbf{1})} + \phi_{(0,\mathbf{84})}, \tag{4.121}$$

where the rest of the coefficients may be found by associativity. It is also straightforward to check that the special Frobenius condition (4.22) is fulfilled.

Meanwhile, the spectrum of line operators of the topological coset can be obtained from the splitting and identifications shown in Table 4.6. It is straightforward to calculate the fusion ring of the resulting line defects, and the result is shown in Table 4.7. The obtained fusion ring can be recognized as that of $\mathbb{Z}_2 \times \mathrm{Rep}(S_3)$. As before, we can transform to the idempotent complete basis to check that everything is in order. The transformation is given by:

$$\mathcal{O}_0 = \frac{1}{12}(\phi_{(0,\mathbf{1})} + \phi_{(0,\mathbf{84})} + \phi_{(\mathbf{s},\mathbf{44})} + \phi_{(\mathbf{v},\mathbf{16})} + \phi_{(\mathbf{c},\mathbf{128})} + \phi_{(\mathbf{s},\mathbf{84})}), \tag{4.122}$$

$$\mathcal{O}_\mathbf{s} = \frac{1}{12}(\phi_{(0,\mathbf{1})} + \phi_{(0,\mathbf{84})} + \phi_{(\mathbf{s},\mathbf{44})} - \phi_{(\mathbf{v},\mathbf{16})} - \phi_{(\mathbf{c},\mathbf{128})} + \phi_{(\mathbf{s},\mathbf{84})}), \tag{4.123}$$

$$\mathcal{O}_\mathbf{v} = \frac{1}{12}(\phi_{(0,\mathbf{1})} + \phi_{(0,\mathbf{84})} - \phi_{(\mathbf{s},\mathbf{44})} + \phi_{(\mathbf{v},\mathbf{16})} - \phi_{(\mathbf{c},\mathbf{128})} - \phi_{(\mathbf{s},\mathbf{84})}), \tag{4.124}$$

$$\mathcal{O}_\mathbf{c} = \frac{1}{12}(\phi_{(0,\mathbf{1})} + \phi_{(0,\mathbf{84})} - \phi_{(\mathbf{s},\mathbf{44})} - \phi_{(\mathbf{v},\mathbf{16})} + \phi_{(\mathbf{c},\mathbf{128})} - \phi_{(\mathbf{s},\mathbf{84})}), \tag{4.125}$$

$$\mathcal{O}_A = \frac{1}{12}(2\phi_{(0,\mathbf{1})} - \phi_{(0,\mathbf{84})} + 2\phi_{(\mathbf{s},\mathbf{44})} - \phi_{(\mathbf{s},\mathbf{84})}), \tag{4.126}$$

$$\mathcal{O}_B = \frac{1}{12}(2\phi_{(0,\mathbf{1})} - \phi_{(0,\mathbf{84})} - 2\phi_{(\mathbf{s},\mathbf{44})} + \phi_{(\mathbf{s},\mathbf{84})}), \tag{4.127}$$

$\times$	$\mathbf{s}$	$\mathbf{v}$	$\mathbf{c}$	A	B
$\mathbf{s}$	0	$\mathbf{c}$	$\mathbf{v}$	A	B
$\mathbf{v}$	$\mathbf{c}$	0	$\mathbf{s}$	B	A
$\mathbf{c}$	$\mathbf{v}$	$\mathbf{s}$	0	B	A
A	A	B	B	$0+\mathbf{s}+A$	$\mathbf{v}+\mathbf{c}+B$
B	B	A	A	$\mathbf{v}+\mathbf{c}+B$	$0+\mathbf{s}+A$

Table 4.7: Fusion ring of topological defect lines in the $Spin(16)_1/Spin(9)_2$ topological coset. The line labeled as 0 corresponds to the identity line.

and it is straightforward to check that the operators so defined are acted on by the lines according to (4.31).

4.5 A Trivially Gapped Chiral QCD$_2$ Theory

As reviewed above, it was shown in [90] that the criterion for a massless 2D QCD theory to be gapped is that the coset CFT

$$Spin(\dim(R))_1/G_{I(R)} \tag{4.128}$$

is actually a topological theory.[22] That is, if the coset is a conformal embedding, the corresponding QCD theory is gapped. Remarkably, [90] also found that there exist *chiral* QCD theories that are gapped. One mechanism to construct such chiral theories is given as follows: Starting from a vector-like theory (G, R, R) which is gapped, the chiral theory (G, R_ℓ, R_r) is also gapped, where $(R_\ell, R_r) = (\sigma_\ell \cdot R, \sigma_r \cdot R)$ and σ_ℓ and σ_r are outer automorphisms of the Lie algebra of G. A concrete example is given by $Spin(8)$ gauge theory coupled to massless fermions in the vectorial and spinorial representations, where the automorphism σ is given by the triality of $Spin(8)$:

$$(Spin(8), \mathbf{8_v}, \mathbf{8_c}). \tag{4.129}$$

22. More precisely, the authors of [90] consider $SO(\dim(R))_1/G_{I(R)}$, where $SO(\dim(R))_1$ corresponds to the fermionization of $Spin(\dim(R))_1$. Since the statement concerns the central charge, we can take the criterion to hold either in the fermionic or bosonic version of the theory.

In the following, we will argue that this theory is in fact trivially gapped. For this, we will make use of some details regarding fermionic 2D CFTs and bosonization, for which we provide a quick summary in Section 4.6.3. To understand how the chiral theory is different from its vector-like counterpart, notice that if the right-moving fermions transform in the spinorial $\mathbf{c}$ representation, we may regard the branching rules of the fermionic characters in the UV theory as given by

$$d_{\mathrm{NS,NS}}(q) = \chi_{\mathbf{1}}(q) + \chi_{\mathbf{v}}(q), \quad \tilde{d}_{\mathrm{NS,NS}}(\bar{q}) = \tilde{\chi}_{\mathbf{1}}(\bar{q}) + \tilde{\chi}_{\mathbf{c}}(\bar{q}), \tag{4.130}$$

$$d_{\mathrm{NS,R}}(q) = \chi_{\mathbf{1}}(q) - \chi_{\mathbf{v}}(q), \quad \tilde{d}_{\mathrm{NS,R}}(\bar{q}) = \tilde{\chi}_{\mathbf{1}}(\bar{q}) - \tilde{\chi}_{\mathbf{c}}(\bar{q}), \tag{4.131}$$

$$d_{\mathrm{R,NS}}(q) = \chi_{\mathbf{s}}(q) + \chi_{\mathbf{c}}(q), \quad \tilde{d}_{\mathrm{R,NS}}(\bar{q}) = \tilde{\chi}_{\mathbf{s}}(\bar{q}) + \tilde{\chi}_{\mathbf{v}}(\bar{q}), \tag{4.132}$$

$$d_{\mathrm{R,R}}(q) = \chi_{\mathbf{s}}(q) - \chi_{\mathbf{c}}(q), \quad \tilde{d}_{\mathrm{R,R}}(\bar{q}) = \tilde{\chi}_{\mathbf{s}}(\bar{q}) - \tilde{\chi}_{\mathbf{v}}(\bar{q}), \tag{4.133}$$

where $d_{\mathrm{X,Y}}$ stands for the characters of the fermionic theory with a choice of $\mathrm{X}, \mathrm{Y} = \mathrm{NS}, \mathrm{R}$ boundary conditions along the cycles of the torus. Both sides differ by a triality transformation exchanging $\mathbf{v}$ and $\mathbf{c}$, in accordance with (4.129). Bosonizing, we obtain the following modular invariant capturing the action of triality in the bosonic version of the UV (ungauged) theory:

$$Z_1 = \tilde{\chi}_{\mathbf{1}}\chi_{\mathbf{1}} + \tilde{\chi}_{\mathbf{c}}\chi_{\mathbf{v}} + \tilde{\chi}_{\mathbf{v}}\chi_{\mathbf{s}} + \tilde{\chi}_{\mathbf{s}}\chi_{\mathbf{c}}. \tag{4.134}$$

It is well-known that bosonization is not unique. Instead, we can redefine the original fermionic chiral QCD theory by stacking with a 2D spin SPT and bosonize (see Section 4.6.3 for more details), obtaining

$$Z_2 = \tilde{\chi}_{\mathbf{1}}\chi_{\mathbf{1}} + \tilde{\chi}_{\mathbf{c}}\chi_{\mathbf{v}} + \tilde{\chi}_{\mathbf{v}}\chi_{\mathbf{c}} + \tilde{\chi}_{\mathbf{s}}\chi_{\mathbf{s}}, \tag{4.135}$$

We will consider both these cases in the following.

Recall that in the bulk-boundary correspondence, as reviewed in the Introduction, for any modular invariant of a chiral algebra, there exists a topological surface operator in the 3D bulk dictating the gluing of holomorphic and antiholomorphic modes [1, 41, 57, 169]. Recall the left side in Figure 4.2. In more modern terms, the existence of such a topological surface can be understood via higher-gauging of the abelian one-form symmetries generated by the anyons of the bulk [65]. More specifically for our purposes, the modular invariant (4.135) can straightforwardly be constructed by the higher-gauging of the $\mathbb{Z}_2$ symmetry generated by the $\mathbf{s}$ anyon along a surface, while (4.134) arises from the higher-gauging of the $\mathbb{Z}_2 \times \mathbb{Z}_2$ symmetry generated by $\mathbf{s}$ and $\mathbf{c}$ along a surface.[23] We call the latter topological surface $S_{\mathbf{sc}}$. The specifics of higher-gauging will not be necessary in the following, other than to point out the existence of the $S_{\mathbf{sc}}$ topological surface and the fact that it acts over the anyons of the theory according to the coupling of antiholomorphic and holomorphic modes in the corresponding modular invariant. For example:

$$S_{\mathbf{sc}}[\mathbf{1}] = \mathbf{1}, \quad S_{\mathbf{sc}}[\mathbf{v}] = \mathbf{s}, \quad S_{\mathbf{sc}}[\mathbf{s}] = \mathbf{c}, \quad S_{\mathbf{sc}}[\mathbf{c}] = \mathbf{v}, \tag{4.136}$$

and thus $S_{\mathbf{sc}}$ implements the triality action in bulk.

From the previous discussion, it follows that the 3D realization of the bosonized 2D QCD theory we wish to consider in the UV corresponds to the top picture in Figure 4.7, as this reproduces the modular invariant (4.134). Along the RG flow, we can run a similar picture as the 3D construction of the non-chiral case reviewed in Section 4.6.1. This gives rise to a similar picture, but with the topological surface $S_{\mathbf{sc}}$ inserted. Notice that along the flow we have two $Spin(8)$ factors in the bulk TQFT, as shown in the bottom picture in Figure 4.7. One of these is associated with the UV fermions, which we have written as $Spin(8)^{\psi}$, while the other is associated with the gauge group, which we have written as $Spin(8)^{G}$.

23. Higher-gauging with discrete torsion gives rise to the other triality modular invariant $Z_3 = \tilde{\chi}_{\mathbf{1}}\chi_{\mathbf{1}} + \tilde{\chi}_{\mathbf{s}}\chi_{\mathbf{v}} + \tilde{\chi}_{\mathbf{c}}\chi_{\mathbf{s}} + \tilde{\chi}_{\mathbf{v}}\chi_{\mathbf{c}}$.

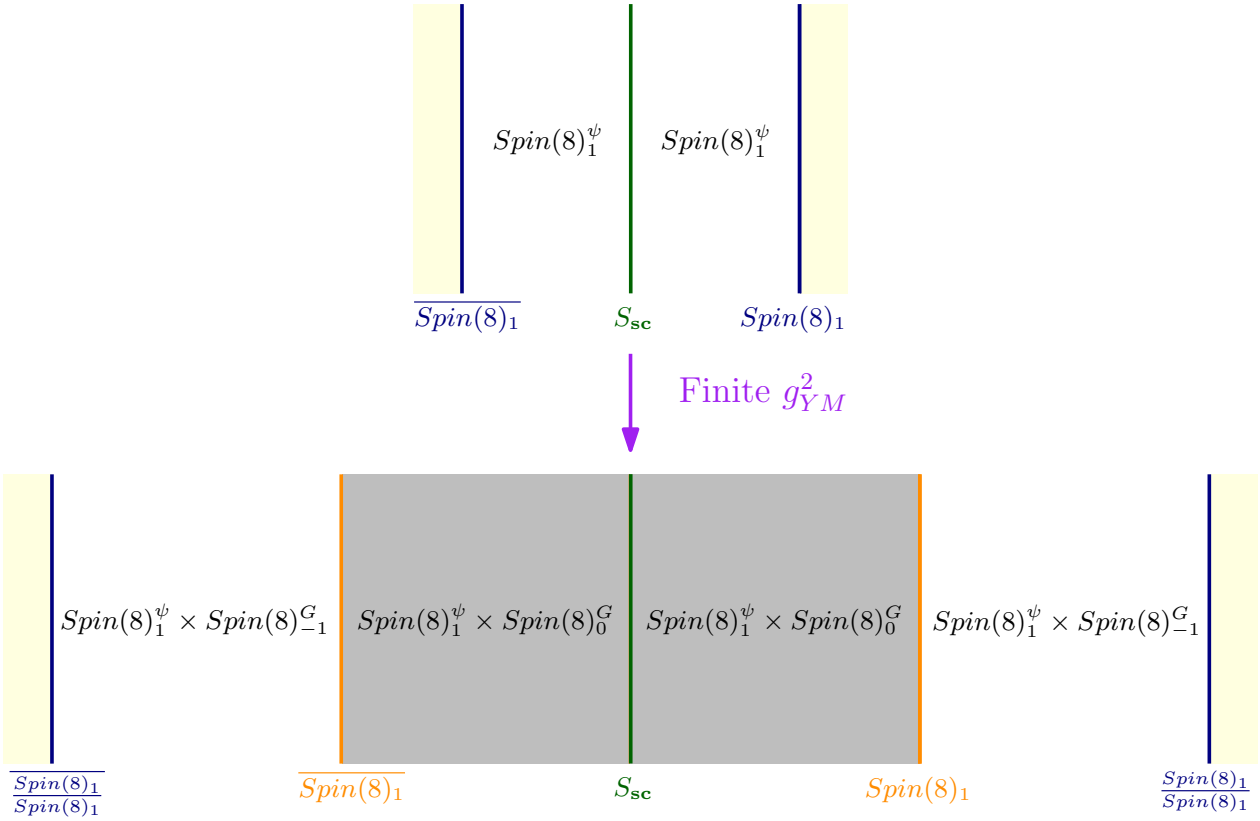

Figure 4.7: Three-dimensional construction of chiral $Spin(8)$ 2D QCD coupled to massless fermions in the vectorial and spinorial representations. The top picture represents the UV theory at zero coupling. The chirality of the theory is implied by the surface $S_{\mathbf{sc}}$ permuting bulk anyons by triality. Notice that at a finite value of g_{YM}^2 the topological surface $S_{\mathbf{sc}}$ can be positioned anywhere and not necessarily in the middle region, as the middle interfaces are transparent respect to the $Spin(8)_1^{\psi}$ factor, from which we are constructing the surface $S_{\mathbf{sc}}$.

Importantly, it is immaterial where the surface $S_{\mathbf{sc}}$ is inserted in bulk since it has been constructed from the $Spin(8)_1^{\psi}$ factor (via higher-gauging), while the three regions differ by $Spin(8)^G$ factors.

In the extreme infrared limit, the region containing the pure Yang-Mills kinetic term collapses to an interface. This is analogous to what happens in the non-chiral case that we review in Section 4.6.1, where the assumption that this interface reduces to the trivial interface is equivalent to the assumption that the IR is given by the topological coset in Figure 4.1. Notice that the collapse of the bulk region to an interface is a local operation,

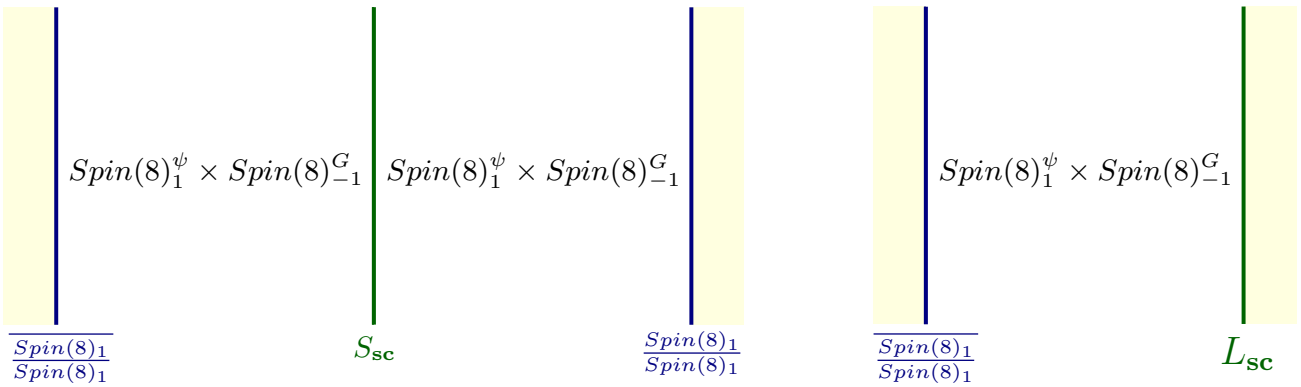

Figure 4.8: On the left: Configuration at the infrared fixed point $g_{YM}^2 \to \infty$. The collapse of the region with the Yang-Mills kinetic term in Fig. 4.7 (grey region) gives the identity interface, and what remains in bulk is the surface $S_{\mathbf{sc}}$ that implemented the permutation modular invariant in the UV. On the right: Final configuration of the system after we push the topological interface $S_{\mathbf{sc}}$ to the right boundary. This consists of a bulk 3D TQFT $Spin(8)_1 \times Spin(8)_{-1}$ with two different topological boundary conditions on the left and on the right, characterized by the Lagrangian subgroups (4.137) and (4.138) respectively.

in the sense that the resulting collapsed interface is not sensitive to the boundary conditions to the left or to the right or to the insertions of any other topological surfaces inserted to its left or right in the bulk. Thus, the assumption in the non-chiral case that the collapsed interface gives the trivial interface can be applied again in the chiral case, and we obtain the configuration shown at the left side of Figure 4.8.

Recall that the coset boundary conditions appearing at the left and right boundaries in the left side of Figure 4.8 are the same thus far as in the non-chiral theory and are characterized by the diagonal Lagrangian subgroup:

$$L_D = (0,0) \oplus (\mathbf{v},\mathbf{v}) \oplus (\mathbf{s},\mathbf{s}) \oplus (\mathbf{c},\mathbf{c}), \tag{4.137}$$

which tells us the anyons that end perpendicularly at such topological boundary, as discussed in Section 4.2. The chirality of the full theory is taken into account by the middle interface $S_{\mathbf{sc}}$, as explained above.

Now, we can push the higher-gauging surface $S_{\mathbf{sc}}$ to the right boundary. Clearly, this

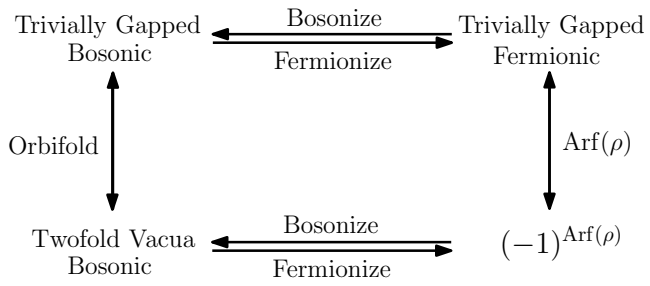

Figure 4.9: Commutative diagram showing the interplay between bosonizations and fermionizations of the trivially gapped IR fixed points found in the strongly coupled regime of chiral $Spin(8)$ 2D QCD with massless fermions in the vectorial and spinorial representations.

changes the boundary condition, since the anyons that end on the boundary are permuted according to triality. For instance:

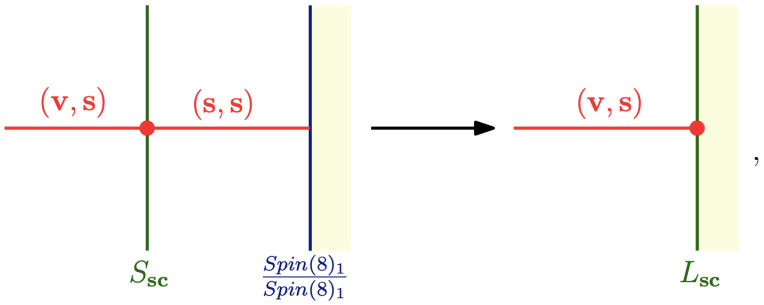

and similarly for other anyon permutations. The final configuration is shown at the right of Figure 4.8, where the new right topological boundary is characterized by the Lagrangian subgroup $L_{\mathbf{sc}}$:

$$L_{\mathbf{sc}} = (0,0) \oplus (\mathbf{v},\mathbf{s}) \oplus (\mathbf{s},\mathbf{c}) \oplus (\mathbf{c},\mathbf{v}), \tag{4.138}$$

which is easy to derive from the diagonal Lagrangian subgroup, and the action of triality.

Now that we know the final configuration, all that remains is to study the 2D TQFT arising under compactification to obtain the IR fixed point of $Spin(8)$ chiral 2D QCD. However, this final configuration is rather simple, since the two Lagrangian subgroups (4.137) and (4.138) characterizing the topological boundaries have no anyons in common other than the identity anyon. As a result, following [69], no topological local operator (vacua) arises under compactification, and the system must be trivially gapped.

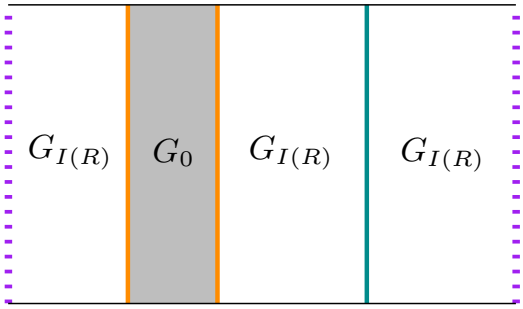

Figure 4.10: Circle compactification construction of 2D QCD [1]. The purple dotted lines are identified to form a circle geometry. The topological order $G_{I(R)}$ is glued along the circle by a G_0 Yang-Mills term. A topological surface in the $G_{I(R)}$ topological order (in green) is inserted to induce the embedding $G_{I(R)} \hookrightarrow Spin(\dim(R))_1$ capturing the free fermions in the UV.

We may now go back to the original fermionic theory by inverting the bosonization map (as summarized in Section 4.6.3), where we find a trivial fermionic theory, with a single trivial state in both the Neveu-Schwarz and Ramond sectors.

It is interesting to ask what happens if instead we consider the modular invariant (4.135), corresponding to bosonizing the original chiral fermionic theory after we stack it with an Arf invariant. Following the same arguments given in this section, it is straightforward to derive that now the IR has two vacua. Then, inverting the bosonization map we find that, unlike in the previous case, the corresponding fermionic theory has one state in the Neveu-Schwarz sector and one state in the Ramond sector, with the latter charged under $(-1)^F$. As expected, both fermionic endpoints just discussed differ by the Arf invariant. Indeed, all the bosonic and fermionic IR endpoints can be seen to fit into Figure 4.9 in Section 4.6.3, which summarizes the relations between different bosonizations/fermionizations and topological manipulations on bosonic and fermionic CFTs.

4.6 Additional Comments and Results

4.6.1 Circle and Interval Constructions of Massless $\mathbf{QCD_2}$

In this section, we show how the 3D circle compactification construction of (bosonic) 2D QCD from [1] (see also [57]) is equivalent to the interval compactification described in Appendix A of [115]. We make sure to keep track of all appropriate bulk topological orders, which is important to set boundary conditions.

To start, notice that a way to construct a surface in a MTC $\mathcal{C}$ consists in performing non-abelian anyon condensation along a volume enclosing a MTC $\mathcal{C}/\mathcal{A}$ and collapsing the volume into a surface. Importantly, for non-abelian condensation to take place in a region, the Frobenius algebra $\mathcal{A}$ must be commutative (see Section 4.2 for precise definitions). This implies that if we start with the operator generated by $\mathcal{A}$ along a surface, we can braid the algebra element outside of the locus of the surface and proliferate the surface into a volume that encloses $\mathcal{C}/\mathcal{A}$, as shown in Fig. 4.13. (For a related discussion of these type of defects, see Section 5.2 of [183].)

Next, we take the circle compactification construction of 2D QCD [1], reproduced here in Fig. 4.10. In this construction, the information that the gauge group can be embedded into the free fermions in the UV is encoded in the existence of a topological interface between $G_{I(R)}$ and $G_{I(R)}$ that gives rise to the modular invariant associated with the conformal

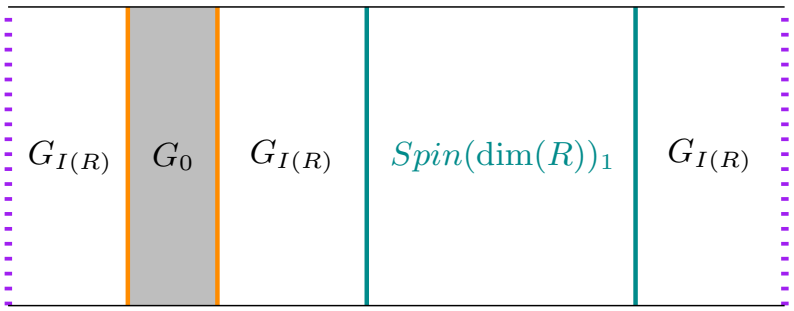

Figure 4.11: We expand the topological surface into a non-trivial volume enclosing the $Spin(\dim(R))_1$ topological order.

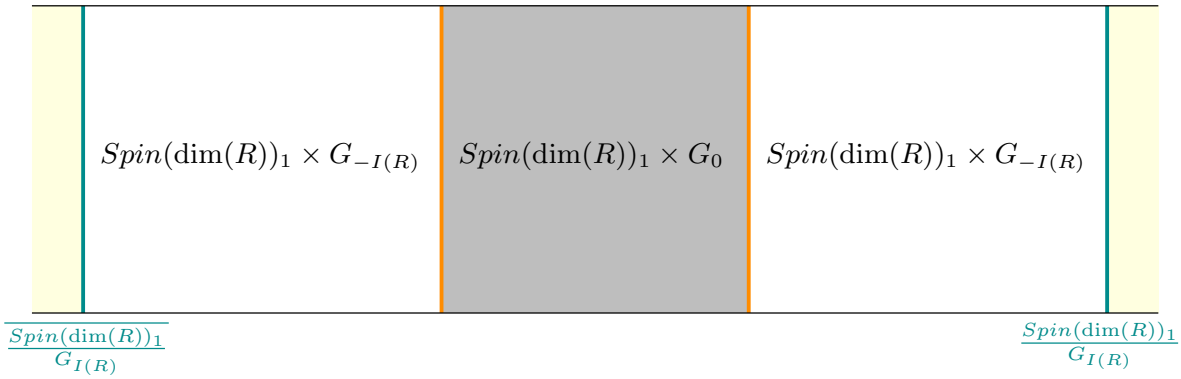

Figure 4.12: After using the folding trick we obtain the interval compactification construction of 2D QCD. Both the topological boundary conditions at the ends of this figure, and the topological interfaces connecting $G_{I(R)}$ with $Spin(\dim(R))_1$ in Fig. 4.11 are due to a non-abelian anyon condensation $G_{I(R)}/\mathcal{A} = Spin(\dim(R))_1$. The interval compactification is more general, however, since it allows for the coset boundary conditions to be non-topological at the ends.

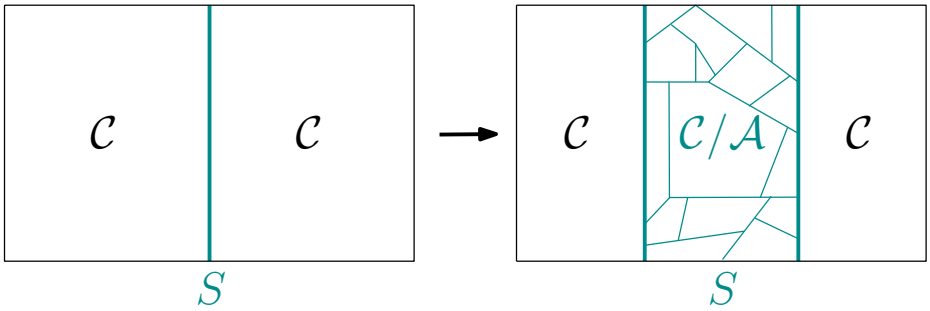

Figure 4.13: When the surface S in a MTC $\mathcal{C}$ is generated by a commutative Frobenius algebra $\mathcal{A}$ along a surface, we can think of the surface as a small sliver of volume with topological interfaces enclosing the topological order $\mathcal{C}/\mathcal{A}$.

embedding $G_{I(R)} \hookrightarrow Spin(\dim(R))_1$. The important point is that conformal embeddings are always implied by some non-abelian anyon condensation, or equivalently by gauging some commutative Frobenius algebra [50, 113]. In our case:

$$G_{I(R)}/\mathcal{A} \cong Spin(\dim(R))_1. \tag{4.139}$$

Using this fact, we can turn the surface into a volume containing $Spin(\dim(R))_1$, as shown in Fig. 4.11. We can now use the folding trick along the topological interfaces

joining $G_{I(R)}$ with $Spin(\dim(R))_1$ to turn the circle compactification into an interval with topological boundary conditions at both ends. The result is shown in Fig. 4.12, which is essentially the interval compactification of [115], but where we have kept track of the $Spin(\dim(R))_1$ topological order to ensure appropriate coset boundary conditions at the ends. (See [3] for a discussion on coset boundary conditions with a modern emphasis on anyon condensation.) Finally, notice that the interval compactification smoothly connects the gapless and gapped theories of [90], as well as their criteria for a QCD theory to be gapped: If the coset boundary conditions support gapless degrees of freedom, the corresponding theory is gapless. On the other hand, if the coset boundary conditions are topological (in the case of the conformal embeddings), the corresponding theory is gapped. In the latter case, the construction also shows that the topological coset symmetry is present along the whole flow since the topological coset symmetry is localized at the boundary, while the flow is local in the bulk. See e.g. [90, 115, 177] for previous observations on this fact. All in all, from the 3D interval construction, the flow looks as in Fig. 4.14.

4.6.2 Bulk-to-Boundary Map, Quotient Category and Karoubi Envelope

In Section 4.3, the spectrum of lines in a topological coset and how such a spectrum of lines is obtained from the bulk MTC were discussed. However, in order to streamline the discussion, instead of providing a set of rigorous definitions and theorems to characterize the fusion category of line operators in the two-dimensional theory, we summarized a set of practical rules that allow one to study the spectrum of lines in a simplified manner. We provide a set of more rigorous results in this section. As an application of the formalism, we briefly outline an example of how to use this method to find the topological lines in a particularly pedagogical example in Section 4.4.1.

As discussed in the subject of anyon condensation (see e.g. [52]), the fusion category of line defects at the boundary is usually characterized in terms of $\mathcal{A}$-module categories. An

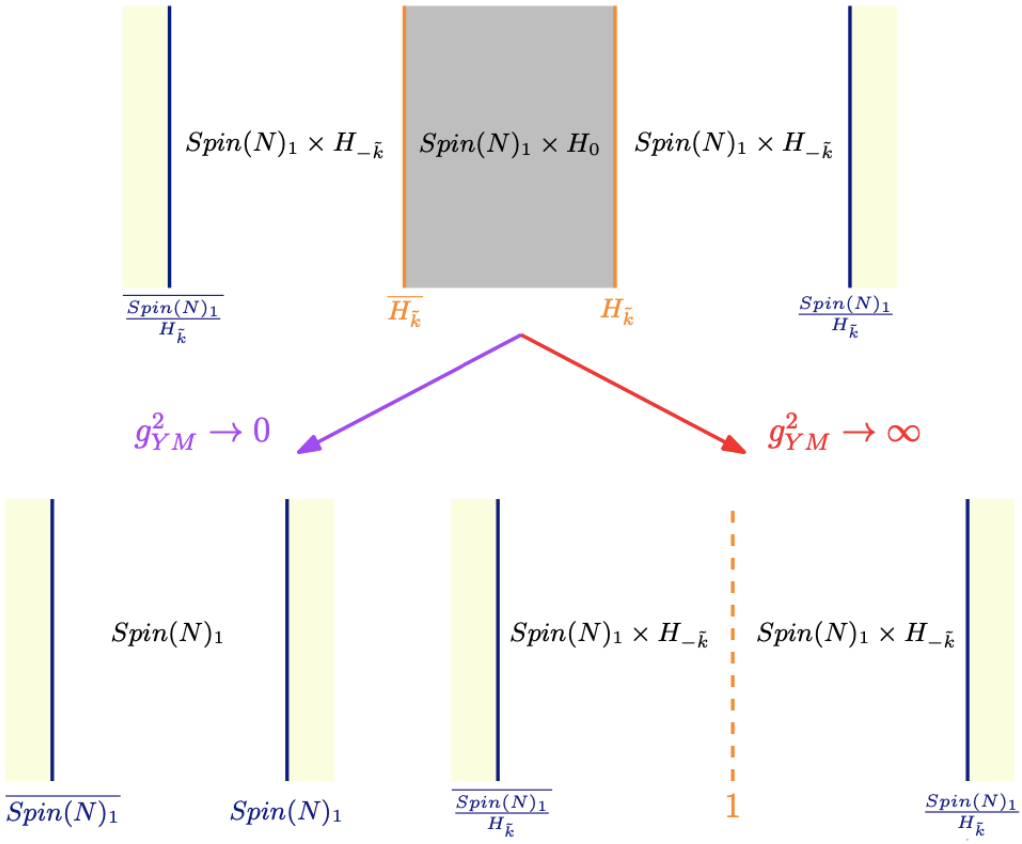

Figure 4.14: Three-dimensional construction of 2D QCD upon interval compactification. We gauge the fermions and couple them to H gauge fields according to the 3D realization of the coset construction, developing accordingly coset boundary conditions on the left and on the right (in blue) [2, 3]. Meanwhile, in bulk we generate interfaces (in orange) by setting $A_0 = 0$ boundary conditions for the $H_{\tilde{k}}$ gauge fields in the left and right regions of the bulk, which generates the standard H_k chiral algebra boundary conditions on them [4]. We glue the interfaces via H_0 gauge fields carrying the 2D Yang-Mills kinetic term (grey region). The interfaces so generated are chosen to have transparent junction conditions for the $Spin(N)_1$ gauge fields. Clearly, in the UV as $g^2_{YM} \to 0$ we recover the expected standard 3D construction of the $Spin(N)_1$ theory (the bosonization of N Majorana fermions), while in the IR the interfaces collapse to a defect in the $Spin(N)_1 \times H_{-\tilde{k}}$ topological order. The statement that the infrared fixed point of massless 2D QCD is given by the topological coset is the statement that the defect so generated corresponds to the identity defect.

alternative viewpoint, a bit more practical for our purposes, makes use of quotient categories and Karoubi envelopes. Specifically, we have the definitions:

Definition 1 (Quotient Category $\mathcal{C}/\mathcal{A}$) Let $\mathcal{C}$ be a MTC,[24] and let $\mathcal{A}$ be a special

24. More generally, a braided fusion category.

Frobenius algebra in $\mathcal{C}$. The quotient category $\mathcal{C}/\mathcal{A}$ consists of the category such that

- The objects in $\mathcal{C}/\mathcal{A}$ are the same as the objects in $\mathcal{C}$.
- The morphisms of $\mathcal{C}/\mathcal{A}$ are given by

$$\mathrm{Hom}_{\mathcal{C}/\mathcal{A}}(a,b) = \mathrm{Hom}_{\mathcal{C}}(a, \mathcal{A}\otimes b). \tag{4.140}$$

One may add now definitions of composition and tensor product, but since we will not make use of these we refer the reader to [184] for details on the definition.

The quotient category is guaranteed to be a tensor category when $\mathcal{A}$ is special Frobenius, but it is not guaranteed to be semisimple since $\mathrm{Hom}_{\mathcal{C}/\mathcal{A}}(a,a)$ could have dimension higher than one for an object a that is simple in $\mathcal{C}$. In this case we make use of the following definition:

Definition 2 (Idempotent Completion or Karoubi envelope) For the quotient category $\tilde{Q} = \mathcal{C}/\mathcal{A}$, we construct the canonical idempotent completion Q (or Karoubi envelope) of $\tilde{Q}$ as follows:

- The objects of Q are pairs (a,p), where $a \in \mathrm{Obj}(\tilde{Q})$, and $p = p^2 \in \mathrm{End}_{\tilde{Q}}(a)$.
- The morphisms of Q are given by

$$\mathrm{Hom}_{Q}\big((a,p),(b,q)\big) = \{f \in \mathrm{Hom}_{\tilde{Q}}(a,b) | f\circ p = q\circ f\}, \tag{4.141}$$

  and other structures in Q are inherited from $\mathcal{C}/\mathcal{A}$.

The category Q so constructed is a semisimple tensor category. It is a result of Müger that the construction mentioned above based on modules categories on the one side and quotient categories and Karoubi envelopes on the other side agree (see specifically Props. 2.11, 2.15, and 2.16 in [184]).

The advantage of the formulation based on quotient categories and Karoubi envelopes is that it offers some computational organization without having to explicitly analyze the equations determining the modules (see e.g., eqn. (4.65) in [41] and the corresponding discussion). In Section 4.4.1 we illustrate this fact in a simple example, and it can of course be used in other examples (for a collection of calculations on non-invertible anyon condensation based on idempotents see for instance [108, 174], or Appendix D in [140] for a calculation based on idempotents applied to Haagerup fusion categories). Conceptually, it also allows for generalizations to higher dimensions [63].

Following the discussion in Section 4.3, the physical content of the idempotent completion construction is that some simple lines in the bulk become non-simple when pushed to the boundary, which happens whenever $\mathrm{Hom}_{\mathcal{C}/\mathcal{A}}(a,a)$ is of dimension greater than one. Then, the objects in Definition 2 are simply the splittings of such bulk lines into the simple lines of the boundary theory. Furthermore, (4.140) tells us that some lines in the bulk can descend into the same simple objects at the boundary. Thus, some of the previous splittings must be identified as the same simple lines of the boundary theory, in accordance with the common Hom-spaces as calculated from (4.140).

In principle, one could compute the fusion ring (and F-symbols) of the boundary fusion category using the abstract definitions above. However, in practice, once one has found the splitting and identification of the bulk lines into boundary lines, one can constrain the fusion ring by asking for consistency between bulk fusion rules and splitting, as explained in Section 4.3 [37, 106]. This allows one to find the fusion ring exactly in many concrete cases.

4.6.3 Fermionization and Bosonization of CFTs

In this section, we summarize a few facts about fermionization and bosonization of CFTs. We follow [54]. Recall that a CFT is said to be *fermionic* if it depends on the choice of spin structure of the spacetime manifold. If not, the theory is said to be *bosonic*. Let us take for

instance the two-torus T^2, which has four possible choices of spin structure. If fermions are periodic along a cycle, we say we have a Ramond (R) boundary condition, and if they are antiperiodic, we say we have a Neveu-Schwarz (NS) boundary condition. We also use the notation R $= +$ and NS $= -$ to refer to these different choices of boundary conditions. The characters in a fermionic CFT depend on spin structure, and we define them as follows:

$$d^{\lambda}_{\text{NS-NS}}(\tau) \coloneqq \text{Tr}_{\mathcal{H}_{\text{NS},\lambda}}\big(q^{L_0-c/24}\big), \tag{4.142}$$

$$d^{\lambda}_{\text{NS-R}}(\tau) \coloneqq \text{Tr}_{\mathcal{H}_{\text{NS},\lambda}}\big((-1)^{F_L}q^{L_0-c/24}\big), \tag{4.143}$$

$$d^{\lambda}_{\text{R-NS}}(\tau) \coloneqq \text{Tr}_{\mathcal{H}_{\text{R},\lambda}}\big(q^{L_0-c/24}\big), \tag{4.144}$$

$$d^{\lambda}_{\text{R-R}}(\tau) \coloneqq \text{Tr}_{\mathcal{H}_{\text{R},\lambda}}\big((-1)^{F_L}q^{L_0-c/24}\big), \tag{4.145}$$

where $(-1)^{F_L}$ is the holomorphic fermion parity operator, $q = e^{2\pi i\tau}$ with τ the modular parameter as usual, and $\mathcal{H}_{\text{NS}}$ and $\mathcal{H}_{\text{R}}$ are the Hilbert spaces when we have anti-periodic and periodic boundary conditions on the circle, respectively.

As in bosonic CFTs, the torus partition function decomposes into characters labeled by the primaries of the theory:

$$\mathcal{Z}_{\pm,\pm}(\tau,\overline{\tau}) = \sum_{\lambda,\overline{\lambda}} \mathcal{M}^{\pm}_{\lambda\overline{\lambda}}\, d^{\lambda}_{\pm\pm}(\tau)\, \overline{d}^{\overline{\lambda}}_{\pm\pm}(\overline{\tau}) \tag{4.146}$$

Notice that, unlike bosonic CFTs, the torus partition function now depends on spin structure, and it is not modular invariant but rather modular covariant. The rules for how the different spin structures are exchanged under modular transformations in a fermionic CFTs are easy to find keeping track of the boundary conditions for fermionic fields (the explicit exchanges may be found in [90]). As in the bosonic case, the mass matrix $\mathcal{M}^{\pm}_{\lambda\overline{\lambda}}$ is not arbitrary but is constrained to make the torus partition function modular covariant.

Recall that given a bosonic theory B with a $\mathbb{Z}_2$ symmetry defined on a compact surface

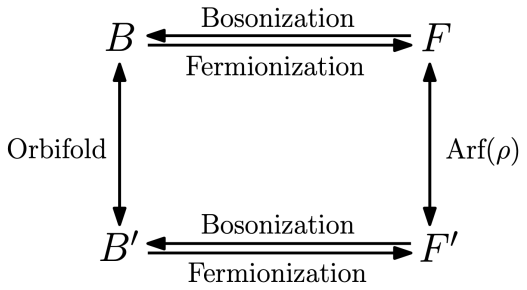

Figure 4.15: Commutative diagram relating two bosonic theories B and B' related by a $\mathbb{Z}_2$ orbifold, and their corresponding fermionization differing by stacking $\text{Arf}(\rho)$. The $\mathbb{Z}_2$ symmetry that we use to orbifold in the bosonic theories is the same $\mathbb{Z}_2$ symmetry used to fermionize.

Σ with genus g, it is possible to fermionize it and obtain a fermionic CFT with partition function

$$\mathcal{Z}_F(\rho) = \frac{1}{2^g} \sum_{\alpha \in H^1(\Sigma, \mathbb{Z}_2)} (-1)^{\text{Arf}[\alpha+\rho]} \mathcal{Z}_B(\alpha), \tag{4.147}$$

where ρ denotes a choice of spin structure, α denotes the $\mathbb{Z}_2$ gauge field for the $\mathbb{Z}_2$ symmetry in B that we use to fermionize the theory, and $\text{Arf}(\rho)$ denotes the Arf invariant, where $(-1)^{\text{Arf}(\rho)} = 1$ for even spin structure and $(-1)^{\text{Arf}(\rho)} = -1$ for odd spin structure. This map is invertible, and from a fermionic theory we can obtain a bosonic CFT by summing over spin structures:

$$\mathcal{Z}_B(\alpha) = \frac{1}{2^g} \sum_{\rho} (-1)^{\text{Arf}[\alpha+\rho]} \mathcal{Z}_F(\rho). \tag{4.148}$$

Indeed, it is straightforward to check that plugging (4.147) into (4.148) we obtain an identity.

It is well-known that bosonization is not unique, as we can always stack a 2D Spin SPT –the Arf invariant– and find a generically different bosonic theory with partition function:

$$\mathcal{Z}_{B'}(\alpha) = \frac{1}{2^g} \sum_{\rho} (-1)^{\text{Arf}[\alpha+\rho]+\text{Arf}[\rho]} \mathcal{Z}_F(\rho). \tag{4.149}$$

Alternatively, we can think of B' as the first defined bosonization (4.148), but starting from a different fermionic theory which differs from the original one by stacking with the Arf

invariant:

$$\mathcal{Z}_{F'}(\rho) = \mathcal{Z}_F(\rho)(-1)^{\mathrm{Arf}[\rho]} \tag{4.150}$$

Then, the bosonic theories B and B' differ by a $\mathbb{Z}_2$ orbifold by the same $\mathbb{Z}_2$ symmetry that we have used to fermionize the theories.

All these properties can be summarized in a commutative diagram, shown in Fig. 4.15.

4.6.4 Lagrangian Algebra Multiplications for $Spin(5)_1/SU(2)_{10}$

In order to verify the formalism as described in Section 4.2, this section provides a summary of the specific Lagrangian algebra multiplications for the example $Spin(5)_1/SU(2)_{10}$. Specifically, one may readily check that the coefficients presented in (4.83)-(4.91) are obtained via the Lagrangian algebra multiplications using Eqn. (4.42). The data here can be obtained directly from the MTC data provided in Section 4.6.5.

$$m^{(a,b)}_{(0,0)(a,b)} = m^{(0,0)}_{(a,b)(a,b)} = 1, \text{ for } (a,b) \in \mathcal{A} \tag{4.151}$$

$$m^{(0,6)}_{(0,6)(0,6)} = 2^{1/4} i, \tag{4.152}$$

$$m^{(v,4)}_{(0,6)(v,4)} = m^{(v,4)}_{(v,4)(0,6)} = -2^{1/4} i, \tag{4.153}$$

$$m^{(v,10)}_{(0,6)(v,4)} = -m^{(v,10)}_{(v,4)(0,6)} = -i, \tag{4.154}$$

$$m^{(v,4)}_{(0,6)(v,10)} = -m^{(v,4)}_{(v,10)(0,6)} = i, \tag{4.155}$$

$$m^{(\sigma,3)}_{(0,6)(\sigma,3)} = m^{(\sigma,3)}_{(\sigma,3)(0,6)} = i/2^{1/4}, \tag{4.156}$$

$$m^{(\sigma,7)}_{(0,6)(\sigma,3)} = -m^{(\sigma,7)}_{(\sigma,3)(0,6)} = (3/2)^{1/4}, \tag{4.157}$$

$$m^{(\sigma,3)}_{(\sigma,7)(0,6)} = -m^{(\sigma,3)}_{(0,6)(\sigma,7)} = (3/2)^{1/4}, \tag{4.158}$$

$$m^{(\sigma,7)}_{(0,6)(\sigma,7)} = m^{(\sigma,7)}_{(\sigma,7)(0,6)} = -i/2^{1/4}, \tag{4.159}$$

$$m^{(\sigma,7)}_{(v,10)(\sigma,3)} = m^{(\sigma,7)}_{(\sigma,3)(v,10)} = i, \tag{4.160}$$

$$m^{(\sigma,3)}_{(v,10)(\sigma,7)} = m^{(\sigma,3)}_{(\sigma,7)(v,10)} = i, \tag{4.161}$$

$$m^{(0,6)}_{(v,4)(v,4)} = -2^{1/4}i, \tag{4.162}$$

$$m^{(0,6)}_{(v,4)(v,10)} = -m^{(0,6)}_{(v,10)(v,4)} = -i, \tag{4.163}$$

$$m^{(\sigma,3)}_{(v,4)(\sigma,3)} = m^{(\sigma,3)}_{(\sigma,3)(v,4)} = (3/2)^{1/4}, \tag{4.164}$$

$$m^{(\sigma,7)}_{(v,4)(\sigma,3)} = -m^{(\sigma,7)}_{(\sigma,3)(v,4)} = i/2^{1/4}, \tag{4.165}$$

$$m^{(\sigma,3)}_{(v,4)(\sigma,7)} = -m^{(\sigma,3)}_{(\sigma,7)(v,4)} = -i/2^{1/4}, \tag{4.166}$$

$$m^{(\sigma,7)}_{(v,4)(\sigma,7)} = m^{(\sigma,7)}_{(\sigma,7)(v,4)} = -(3/2)^{1/4}, \tag{4.167}$$

$$m^{(0,6)}_{(\sigma,3)(\sigma,3)} = i/2^{1/4}, \tag{4.168}$$

$$m^{(0,6)}_{(\sigma,7)(\sigma,7)} = -i/2^{1/4}, \tag{4.169}$$

$$m^{(4,v)}_{(\sigma,3)(\sigma,3)} = +(3/2)^{1/4}, \tag{4.170}$$

$$m^{(4,v)}_{(\sigma,7)(\sigma,7)} = -(3/2)^{1/4}, \tag{4.171}$$

$$m^{(v,10)}_{(\sigma,3)(\sigma,7)} = m^{(v,10)}_{(\sigma,7)(\sigma,3)} = i, \tag{4.172}$$

$$m^{(v,4)}_{(\sigma,3)(\sigma,7)} = -m^{(v,4)}_{(\sigma,7)(\sigma,3)} = +i/2^{1/4}, \tag{4.173}$$

$$m^{(0,6)}_{(\sigma,3)(\sigma,7)} = -m^{(0,6)}_{(\sigma,7)(\sigma,3)} = +(3/2)^{1/4}, \tag{4.174}$$

4.6.5 Explicit MTC Data

For self-containment, in this section we summarize the MTC data of $Spin(\nu)_1$ for ν odd and $SU(2)_k$ for integer k, which are cases of interest in this work.

Fibonacci

This MTC has two simple lines called 0 and τ with topological spins $\theta_0 = 1$, $\theta_\tau = e^{is\frac{4\pi}{5}}$ and quantum dimensions $d_0 = 1$, $d_\tau = \phi$. The only non-trivial fusion rule is

$$\tau \times \tau = 0 + \tau. \tag{4.175}$$

The non-trivial F-symbols are given by

$$[F_\tau^{\tau\tau\tau}]_{ef} = \begin{bmatrix} \phi^{-1} & \phi^{-1/2} \\ \phi^{-1/2} & -\phi^{-1} \end{bmatrix}_{ef}, \tag{4.176}$$

while the non-trivial R-symbols are given by

$$R_0^{\tau\tau} = e^{-is\frac{4\pi}{5}}, \quad R_\tau^{\tau\tau} = e^{is\frac{3\pi}{5}}. \tag{4.177}$$

Above, ϕ is the golden ratio and $s = \pm 1$ corresponds to the chirality of the two MTCs with this data and central charges $c_- = 14s/5 \bmod 8$. For instance, the $(G_2)_1$ and $(F_4)_1$ Chern-Simons theories are described by this MTC data with $s = +1$ and $s = -1$ respectively.

$Spin(\nu)_1$

We take ν an odd integer. In this case the MTC has three simple lines labeled 0, v and σ with fusion rules

$$v \times v = 0, \quad \sigma \times v = \sigma, \quad \sigma \times \sigma = 0 + v. \tag{4.178}$$

The topological spins are $\theta_0 = 1$, $\theta_v = -1$, $\theta_\sigma = e^{2\pi i\nu/16}$, and the modular S-matrix is that of Ising:

$$S = \frac{1}{2}\begin{pmatrix} 1 & 1 & \sqrt{2} \\ 1 & 1 & -\sqrt{2} \\ \sqrt{2} & -\sqrt{2} & 0 \end{pmatrix}. \tag{4.179}$$

The quantum dimensions are $d_0 = d_v = 1$, $d_\sigma = \sqrt{2}$. Meanwhile, the non-trivial F-symbols are given by

$$F_\sigma^{v\sigma v} = F_v^{\sigma v\sigma} = -1, \quad [F_\sigma^{\sigma\sigma\sigma}]_{ef} = \frac{\kappa_\sigma}{\sqrt{2}}\begin{bmatrix} 1 & 1 \\ 1 & -1 \end{bmatrix}_{ef}, \tag{4.180}$$

where κ_σ is the Frobenius-Schur indicator $\kappa_\sigma = (-1)^{(\nu^2-1)/8}$, while the R-symbols are

$$R_0^{vv} = -1, \quad R_\sigma^{v\sigma} = R_\sigma^{\sigma v} = (-i)^\nu, \quad R_0^{\sigma\sigma} = \kappa_\sigma e^{-i\frac{\pi}{8}\nu}, \quad R_v^{\sigma\sigma} = \kappa_\sigma e^{i\frac{3\pi}{8}\nu}. \tag{4.181}$$

$SU(2)_k$

The MTC $SU(2)_k$ with integer k consists of $k+1$ simple lines labeled from 0 to k, with fusion rules

$$\Lambda_1 \times \Lambda_2 = \sum_{\Lambda=|\Lambda_1-\Lambda_2|}^{\min(\Lambda_1+\Lambda_2, 2k-\Lambda_1-\Lambda_2)} \Lambda\ , \tag{4.182}$$

where the sum is restricted such that $\Lambda_1 + \Lambda_2 - \Lambda$ is even.

The topological spins are given by $\theta_j = \exp\left(2\pi i \frac{j(j+2)}{4(k+2)}\right)$ with $j = 0, 1, \ldots, k$, while the modular S-matrix is:

$$S_{j_1 j_2} = \sqrt{\frac{2}{k+2}} \sin\left(\frac{\pi(j_1+1)(j_2+1)}{(k+2)}\right), \quad j_1, j_2 = 0, 1, \ldots, k, \tag{4.183}$$

from which we obtain the quantum dimensions $d_j = \sin\left(\frac{(j+1)\pi}{k+2}\right) / \sin\left(\frac{\pi}{k+2}\right)$.

In the following $q = e^{2\pi i/(k+2)}$. Then, the F-symbols have entries

$$[F_d^{abc}]_{ef} = i^{a+b+c+d}\sqrt{[e+1]_q[f+1]_q}\begin{Bmatrix} a & b & e \\ c & d & f \end{Bmatrix}, \tag{4.184}$$

where

$$\begin{Bmatrix} a & b & e \\ c & d & f \end{Bmatrix} = \Delta(a,b,e)\Delta(e,c,d)\Delta(b,c,f)\Delta(a,f,d)$$

$$\times \sum_z \left[\frac{(-1)^z [z+1]_q!}{[z-\frac{a+b+e}{2}]_q![z-\frac{e+c+d}{2}]_q![z-\frac{b+c+f}{2}]_q!} \frac{1}{[z-\frac{a+f+d}{2}]_q![\frac{a+b+c+d}{2}-z]_q!} \right.$$

$$\left. \times \frac{1}{[\frac{a+e+c+f}{2}-z]_q![\frac{b+e+d+f}{2}-z]_q!} \right] \tag{4.185}$$

with

$$\Delta(a,b,c) = \sqrt{\frac{[\frac{-a+b+c}{2}]_q![\frac{a-b+c}{2}]_q![\frac{a+b-c}{2}]_q!}{[\frac{a+b+c}{2}+1]_q!}} \tag{4.186}$$

and

$$[n]_q! = \prod_{m=1}^{n} [m]_q, \quad [n]_q = \frac{q^{n/2}-q^{-n/2}}{q^{1/2}-q^{-1/2}}. \tag{4.187}$$

Finally, the R-symbols are given by:

$$R_c^{ab} = i^{c-a-b} q^{\frac{1}{8}[c(c+2)-a(a+2)-b(b+2)]}. \tag{4.188}$$

CHAPTER 5

PARTICLE-SOLITON DEGENERACY IN 2D QUANTUM CHROMODYNAMICS

Gauge theory is a central paradigm in particle physics. Among its most fascinating properties is its strongly coupled nature: ultraviolet (UV) degrees of freedom consisting of manifest quarks and gauge fields give way in the infrared (IR) to a surprising particle spectrum of mesons and baryons. Analytically understanding this phenomenon has served as a driving goal of theoretical physics for the past half-century.

Two-dimensional (2D) theories have long served as a playground for testing new techniques to attack strongly-coupled physics. In particular, in quantum chromodynamics (QCD_2) 't Hooft famously solved the theory in the large number of colors limit [185]. More recently, novel non-invertible symmetries have been applied to understand confinement [1], and to characterize the vacuum structure of QCD_2 where the distinct states are parameterized by expectation values of gauge-invariant composite operators [12, 90, 115]. (See Section 5.5.2 below for explicit examples in QCD_2.)

In this work, we continue this line of development building on the recent results [143,144]. Focusing on the case of gapped QCD_2, we aim to directly characterize the spectrum. We realize QCD_2 via an interval compactification from a three-dimensional (3D) topological quantum field theory (TQFT) and following [12] identify the fusion category $\mathcal{C}$ which describes the mathematical structure of the non-invertible symmetry [11,46,62,129]. Physically, such symmetries are realized by topological line operators that commute with the Hamiltonian [6], but are not in general represented by unitary operators acting on the Hilbert space. Moreover, as noted in [12], the fusion category $\mathcal{C}$ is fully spontaneously broken in the IR and hence characterizes the vacua of the gauge theory.

We harness the representation theory of this fusion category to determine the allowed multiplets of particles, excitations above a single vacua, and solitons interpolating between

distinct vacua. Strikingly, we find that the fusion category symmetry $\mathcal{C}$ often implies that particle and solitons are in the same representation and hence necessarily have equal masses. This feature is unique to spontaneously broken non-invertible symmetries and illustrates the intrinsically quantum (strongly-coupled) nature of these symmetries.

We exhibit our results in several explicit gauge theories below. The implied degeneracies are elegantly encoded in a quiver diagram where the nodes are vacua and the arrows are excited particle and soliton states. Such diagrams echo those discussed in many contexts such as the lattice integrable models of [186], the relation between graphs, non-diagonal modular invariants, and conformal boundary conditions of [187, 188] (see also [49, 51] for the relationship between anyon condensation and generalized ADE diagrams), and in the direct analysis of supersymmetric solitons [189].

5.1 Background on QCD_2

We are interested in QCD in two spacetime dimensions with massless fermions. The gauge group is denoted by G, and the fermions transform in a representation $\mathbf{R}$ of G. We take the fermions to have vanishing bare mass. The action is:

$$S_f(g_{\mathrm{YM}}) = \int_\Sigma d^2x \Big[\mathrm{Tr}(\Psi^T i \not{D}_\rho \Psi) - \frac{1}{4g_{\mathrm{YM}}^2} \mathrm{Tr}(F^2) \Big]. \tag{5.1}$$

For simplicity in the following, we consider only vector-like theories where the left-moving and right-moving fermions transform in the same representation $\mathbf{R}$ of the gauge group G, and further restrict to the case where $\mathbf{R}$ is irreducible.

As defined above, QCD_2 is a fermionic theory, i.e. there are fermionic local operators and the partition functions depend on a choice of spacetime spin structure. To simplify our discussion, we can bosonize the fermions [190], and recast these degrees of freedom as a theory of currents, a WZW model $\mathrm{Spin}(\dim(\mathbf{R}))_1$. Coupling to G gauge fields then results

in a bosonic version of QCD_2 as a gauged WZW model with a G gauge field kinetic term:

$$S_b(g_{\mathrm{YM}}) = S_{\mathrm{WZW}}[g, A] - \frac{1}{4g_{\mathrm{YM}}^2}\int_\Sigma d^2x\ \mathrm{Tr}(F^2). \tag{5.2}$$

We present our results below for this bosonized theory. Since bosonization/fermionization is an invertible operation [54, 191], this involves no loss in generality.

Our goal is to constrain particle and soliton states. This is cleanest when the theory in question has a mass gap so that we can separate the spectrum from any residual gapless modes. In QCD_2, there is a simple criterion that controls the gap [90]. Denote by $I(\mathbf{R})$ the Dynkin index of the representation $\mathbf{R}$ and by c_{G_k} the central charge of the WZW model based on a Lie group G at level k. Then, the theory is gapped if and only if the coset

$$\frac{\mathrm{Spin}(\dim(\mathbf{R}))_1}{G_{I(\mathbf{R})}}, \tag{5.3}$$

has vanishing central charge:

$$c_{\mathrm{Spin}(\dim(\mathbf{R}))_1/G_{I(\mathbf{R})}} = c_{\mathrm{Spin}(\dim(\mathbf{R}))_1} - c_{G_{I(\mathbf{R})}} = 0. \tag{5.4}$$

When this is the case, we refer to (5.3) as a *topological coset*. This condition for a gap is valid irrespective of the global form of the gauge group G, provided that $\mathbf{R}$ is an allowed representation of G.

Next we turn to the effective infrared (IR) description of the QCD_2 theory (5.2). A natural candidate arises if we examine (5.2), and assume that the IR is described by the corresponding $g_{\mathrm{YM}} \to \infty$ limit:

$$S_b(g_{\mathrm{YM}}) \xrightarrow[g_{\mathrm{YM}}\to\infty]{} S_{\mathrm{WZW}}[g, A]. \tag{5.5}$$

We find that the IR is described by the aforementioned gauged WZW model consisting of

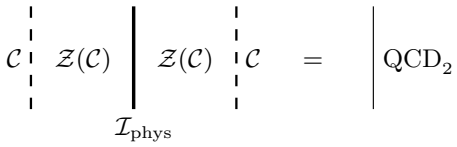

Figure 5.1: Three-dimensional construction of QCD_2.

$\mathrm{Spin}(\dim(\mathbf{R}))_1$ matter content coupled to G gauge fields. We assume this description below. Algebraically, this corresponds to the quotient of chiral algebras in (5.3) however, one must carefully keep track of all topological sectors i.e. distinct vacua. (See e.g. [3, 12, 90].)

One potential source of vacua of the theory can be seen directly in the ultraviolet from the presence of topological local operators, or equivalently exact (in contrast to emergent) one-form symmetries. Such symmetries arise in particular from the subgroup of the center of the gauge group G which acts trivially on the matter representation $\mathbf{R}$. As discussed in [1], exact one-form symmetries split the theory into distinct *universes*, with no finite energy configurations interpolating between them. A given universe contains, however, its own set of vacua, and it remains meaningful to discuss finite-energy configurations in between such vacua. For simplicity below, we will avoid this phenomenon by focusing on examples with trivial one-form symmetry whose unique exact topological local operator is the identity.

Next, we discuss how to characterize the zero-form symmetries of gapped QCD_2. These symmetries play a crucial role in our treatment of particle-soliton degeneracy. An insightful approach is to construct QCD_2 via compactification from three spacetime dimensions on a transverse interval [1, 12, 115, 127]. In this viewpoint, QCD_2 with simply-connected gauge group can be constructed by taking a Chern-Simons theory in bulk:

$$\mathcal{Z}(\mathcal{C}) \coloneqq \mathrm{Spin}(\dim(\mathbf{R}))_1 \times G_{-I(\mathbf{R})} \ , \tag{5.6}$$

and setting coset boundary conditions on the left and on the right of the interval. Notice that since we are considering the gapped case, these are *topological boundary conditions* for $\mathcal{Z}(\mathcal{C})$. See Fig. 5.1. An interface $\mathcal{I}_{\mathrm{phys}}$ controlling the RG flow at finite values of the coupling is

set in the middle of the interval. The assumption that the IR is described by the topological coset (5.5) is then equivalent to the statement that in the far IR the surface $\mathcal{I}_{\text{phys}}$ becomes the transparent identity interface in $\mathcal{Z}(\mathcal{C})$.

The construction of QCD_2 sketched above manifests the symmetries. Indeed, given any 3D TQFT, a fusion category $\mathcal{C}$ of line operators is always supported at any topological boundary [192]. Viewed purely from two dimensions, $\mathcal{C}$ are topological lines and hence yield the desired symmetries. Moreover, the 3D construction of QCD_2 implies that such a fusion category of line operators persists along the whole RG flow and hence can be used to analyze the spectrum.[1] In the IR, the surface $\mathcal{I}_{\text{phys}}$ becomes transparent and this symmetry is fully spontaneously broken:

$$\mathcal{C} \longrightarrow \mathbf{1}. \tag{5.7}$$

In particular, the vacua are in one-to-one correspondence with simple objects in $\mathcal{C}$ [12]. Finally, we remark that, in general, $\mathcal{C}$ may not be the complete finite symmetry of a given (bosonized) gapped QCD_2. However, because of its manifest nature from 3D, $\mathcal{C}$ can be readily determined in practice and hence its implications for spectra are especially computable.[2]

5.2 Anyon Condensation and Topological Cosets

Our previous analysis has indicated the central importance of $\mathcal{C}$, the fusion category of lines at a topological boundary of a 3D TQFT. To determine $\mathcal{C}$ directly, we use anyon condensation. We refer to [192] for a detailed presentation, and in the following provide a simplified presentation sufficient for our examples. For an introduction to the algebraic theory of anyons, see [15, 16]. Our conventions follow [12].

In general, an arbitrary topological boundary condition of a 3D TQFT $\mathcal{T}$ can be described

1. One can also see that the quotient of chiral algebras is preserved along the whole RG directly in 2D [90, 115, 177].

2. We also remark that, following [12], our methods are in principle generalizable to any gauged WZW model described by a conformal embedding in (5.2) with IR description (5.5).

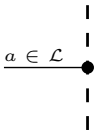

Figure 5.2: An anyon $a \in \mathcal{L}$ can end at a topological junction at the topological boundary defined by $\mathcal{L}$.

in terms of a non-simple anyon called a *Lagrangian algebra* [64, 192]:

$$\mathcal{L} = \bigoplus_{a \in \mathcal{T}} n_a \, a, \quad n_a \in \mathbb{N}, \tag{5.8}$$

where a are simple anyons, and n_a positive integers. For simplicity, we will consider the multiplicity-free case $n_a = 0, 1$. A useful interpretation of the Lagrangian algebra is that it dictates the anyons that are allowed to end perpendicularly in a topological junction at the topological boundary described by $\mathcal{L}$. See Fig. 5.2. Lagrangian algebras can only be composed of bosons. This is, if the topological spin $\theta_a \neq 1 \Rightarrow n_a = 0$. Moreover, Lagrangian algebras satisfy the quantum dimension constraints $\dim(\mathcal{T}) = \big(\dim(\mathcal{L})\big)^2$, where $\dim(\mathcal{T}) = \sum_{a \in \mathcal{T}} d_a^2$ and $\dim(\mathcal{L}) = \sum_{a \in \mathcal{T}} n_a d_a$. In general, it is a non-trivial requirement for a 3D TQFT to have a set of anyons fulfilling these properties, so this already provides a non-trivial tool to characterize topological boundaries. For a complete characterization of Lagrangian algebras, we refer to the aforementioned references.

The line operators at the topological boundary can be found by taking a simple anyon a of the bulk TQFT and moving it to the boundary. Generically, such a simple anyon becomes a non-simple line operator at the boundary. This is encapsulated in the following "splitting" rule:

$$a = \sum_{\alpha} z_a^{\alpha} \, \alpha, \quad z_a^{\alpha} \in \mathbb{N}, \tag{5.9}$$

where α stands for the distinct simple line operators of the boundary fusion category. Generically, a simple line operator α may appear with multiplicity in the splitting rule, a fact that is encoded in the non-negative integers z_a^{α}. Simple anyons in the Lagrangian algebra

$\mathcal{L} = \oplus_a n_a a$ always have a component of the identity line of the boundary theory: $a \to 1 + \cdots$.

The boundary fusion category $\mathcal{C}$ is constrained to satisfy the following set of consistency conditions:

- $a = \sum_\alpha z_a^\alpha \, \alpha \Longrightarrow d_a = \sum_b z_a^\alpha \, d_\alpha$.
- $a = \sum_\alpha z_a^\alpha \, \alpha \Longrightarrow \bar{a} = \sum_\alpha z_a^\alpha \, \bar{\alpha}$.
- $a \otimes b = \bigoplus_c N_{a,b}^c \, c \Longrightarrow \left(\sum_\alpha z_a^\alpha \, \alpha \right) \times \left(\sum_\beta z_b^\beta \, \beta \right) = \sum_{c,\gamma} N_{a,b}^c \, z_c^\gamma \, \gamma$.

The boundary fusion category must also satisfy the standard conditions of associativity, existence of a unique identity line, and existence of unique conjugates with a unique way to fuse to the identity line. Often, one can exploit the previous constrains and find the fusion ring of the fusion category exactly. This will be our main practical tool below.

The relation between topological cosets and topological boundary conditions has recently been studied in detail in [12]. In short, when we have an embedding of chiral algebras $G_k \hookrightarrow \mathcal{Q}_1$ with associated gauged WZW model with vanishing central charge and simply-connected G, then the Chern-Simons theory $\mathcal{Q}_1 \times G_{-k}$ admits a topological boundary. (This is the statement that topological cosets belong to the trivial Witt class [50].) More specifically, the branching rules of the conformal embedding

$$\chi_\Lambda^{\mathcal{Q}_1}(q) = \sum_\lambda b_{(\Lambda,\lambda)} \, \chi_\lambda^{G_k}(q), \quad b_{(\Lambda,\lambda)} \in \mathbb{N}, \tag{5.10}$$

with q the modular parameter, induce the existence of a Lagrangian algebra $\mathcal{L} = \bigoplus_{(\Lambda,\lambda)} b_{(\Lambda,\lambda)} (\Lambda, \lambda^{\mathrm{op}})$ defining the corresponding topological boundary of $\mathcal{Q}_1 \times G_{-k}$. Thus, we can in particular apply this observation to the topological cosets (5.3) pertinent to QCD_2 and apply the rules of anyon condensation to obtain the fusion categories that are present throughout the RG flow.

As discussed above, in order to avoid the phenomenon of universe splitting in QCD_2, we may consider global forms of the gauge group that have trivial center. To address this in

the 3D construction, we follow [2,3,193] and gauge the "common center" one-form symmetry in $\text{Spin}(\dim(\mathbf{R}))_1 \times G_{-I(\mathbf{R})}$. After this is done, no exact one-form symmetry given by the center of the gauge group remains, and all the topological local operators in the IR correspond to vacua of a single universe. Notice that a gapped boundary for the gauged theory $(\text{Spin}(\dim(\mathbf{R}))_1 \times G_{-I(\mathbf{R})})/Z$ (with Z the "common center") is guaranteed to exist given the gapped boundary determined by (5.10), since the gauging by Z is just a topological manipulation. In practice, a Lagrangian algebra in $(\text{Spin}(\dim(\mathbf{R}))_1 \times G_{-I(\mathbf{R})})/Z$ is easily found by direct examination of the TQFT.

Anyon condensation also allows us to make statements regarding the expectation values in the different vacua of the local operators that do not decouple in the IR fixed point. Indeed, local operators in the 2D theory in the IR are constructed from stretching anyons between the two ends of the interval:

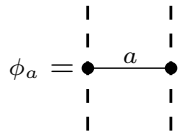

(5.11)

Thus, Lagrangian algebras determine the set of topological local operators, or vacua in the IR of QCD_2. Below, the topological OPE of these local operators can be obtained exploiting commutativity, associativity, consistency of the OPE with the local operators allowed by the Lagrangian algebra, and existence of an idempotent complete basis $\{\mathbf{v}_i\}$ of local operators that are in one-to-one correspondence with the clustering vacua of the theory. In turn, determining the ϕ_a in terms of the idempotent complete basis allows us to calculate the vacuum expectation value of each local operator ϕ_a.

5.3 Representation Theory

Having identified a collection of finite non-invertible symmetry in gapped QCD_2 theories, we now consider their implications for particle spectra. Recent work [143, 144] has shown

that non-invertible symmetry in a QFT can enforce mass degeneracies. An especially novel feature of such degeneracies is they can be between stable particle and soliton excitations. In this section we briefly review the representation theory that governs such degeneracies, following and deferring detailed discussion to [144].

We first consider a general 2D bosonic QFT before returning to the specific context of QCD_2. In general, the finite symmetry is described by a fusion category $\mathcal{C}$ [11, 62, 129, 194] and the phase of the symmetry is described by a $\mathcal{C}$-module category $\mathcal{M}$ [53, 55, 62]. In a gapped theory quantized on $\mathbb{R}$, the simple objects of $\mathcal{M}$ correspond to the clustering grounding states of the theory [1, 143].

In a gapped 2D QFT quantized on $\mathbb{R}$, the action of the finite non-invertible symmetry on the state space is through an algebra called the "strip algebra". This algebra depends both on the symmetry ($\mathcal{C}$) and its phase ($\mathcal{M}$) and is denoted $\mathbf{Str}_{\mathcal{C}}(\mathcal{M})$. It is the representation theory of the strip algebra that governs symmetry enforced degeneracies of the theory. $\mathbf{Str}_{\mathcal{C}}(\mathcal{M})$ is a C^*-weak Hopf algebra, which means that its representations can act on multi-particle states (tensor products), have charge conjugates (duals), and are compatible with the unitary structure on the Hilbert space of states. The representation theory of such algebras is well studied and admits techniques for analysis similar to those used in the unitary representation theory of finite groups. In fact, in the special case of a symmetry described by a finite group H in its unbroken phase, $\mathbf{Str}_{\mathcal{C}}(\mathcal{M}) = \mathbb{C}[H]$, the group algebra of H, and hence recovers the familiar representation theory of finite groups.

In analyzing the degeneracies of gapped QCD_2 theories, one can leverage that the representation category $\mathbf{Rep}(\mathbf{Str}_{\mathcal{C}}(\mathcal{M}))$ also admits a more abstract description,

$$\mathbf{Rep}(\mathbf{Str}_{\mathcal{C}}(\mathcal{M})) \simeq \mathcal{C}^*_{\mathcal{M}}. \tag{5.12}$$

Here $\mathcal{C}^*_{\mathcal{M}}$ is called the "dual category" of $\mathcal{C}$ with respect to $\mathcal{M}$ and is physically the dual symmetry obtained by performing a generalized gauging of $\mathcal{C}$ associated to $\mathcal{M}$ [62, 75]. This

category naturally acts on $\mathcal{M}$. Taking α to be a simple line, its corresponding irreducible representation is the boundary junction vector space

$$V_\alpha = \bigoplus_{m,n} \mathrm{Hom}(m \otimes \alpha, n), \tag{5.13}$$

where m, n are the clustering ground states of the theory. This presentation of the representation is especially useful since it makes clear how many particles (solitons) there are above (between) each vacuum in it.

To compute the action of $\mathbf{Str}_{\mathcal{C}}(\mathcal{M})$ on V_α in this approach, it is necessary to know the complete ($\mathcal{C}$-$\mathcal{C}^*_{\mathcal{M}}$)-bimodule category structure on $\mathcal{M}$. This data is generically difficult to compute. Fortunately, equation (5.13) contains a significant amount of information about the representation and is determined by far less data. The dimensions of each summand is given by the module category fusion coefficients

$$m \otimes \alpha = \bigoplus_n \tilde{N}^n_{m,\alpha} n, \quad \tilde{N}^n_{m,\alpha} \in \mathbb{N}. \tag{5.14}$$

The fusion coefficients can be conveniently encoded in a quiver (i.e. a directed graph):

- For each clustering ground state $m \in \mathcal{M}$ draw a node of the quiver.
- Add $\tilde{N}^n_{m,\alpha}$ directed arrows from node m to node n.

This provides a convenient graphical presentation of the module fusion coefficients.

We can apply this discussion to analyze symmetry-enforced degeneracies of gapped QCD_2 theories. As discussed in Section 5.1, the relevant fusion category symmetry is the category of lines of the coset boundary condition of the 3D coset TQFT, $\mathcal{C}$. The assumed symmetry breaking pattern (5.7), implies that the phase of the symmetry is given by $\mathcal{M} = \mathcal{C}$ viewed as

a $\mathcal{C}$-module category. Therefore, we must compute $\mathcal{C}_{\mathcal{C}}^*$, which is just the category itself [195],

$$\mathcal{C}_{\mathcal{C}}^* \simeq \mathcal{C}. \tag{5.15}$$

To compute the quivers describing the allowed symmetry enforced degeneracies one therefore only needs to know the fusion rules for $\mathcal{C}$

$$\tilde{N} = N, \quad \alpha \otimes \beta = \bigoplus_{\gamma} N_{\alpha,\beta}^{\gamma} \gamma. \tag{5.16}$$

Before continuing to examples, a comment regarding one-form symmetry is in order. The mixing of particle and soliton states by non-invertible symmetry is particularly powerful because it can require the existence of particle states in a theory. This is unlike the case of group-like symmetry where the realization of a particular representation is a dynamical rather than kinematic question. This follows from the fact that a theory has no non-trivial one-form symmetry if and only if the quiver describing the complete collection of stable solitons is connected. As will be demonstrated in the following examples, this additional information is often enough to require the existence of some stable particles or solitons from purely kinematic considerations.

5.4 Examples of Particle-Soliton Degeneracy

We now consider examples of this analysis in gapped QCD_2 theories. In doing so we demonstrate the necessary existence of a collection of stable particle and/or soliton states in each theory. Details of the computations are included in Section 5.5.1, including the data of the boundary condensation maps and allowed quivers for each of the following theories.

$\boldsymbol{SO(3) + \psi_5}$: Our first example is $SO(3)$ gauge theory with Majorana fermions in the five.

The bosonized theory has the 3D coset TQFT

$$\frac{Spin(5)_1 \times SU(2)_{-10}}{\mathbb{Z}_2} = \mathcal{Z}(\mathcal{C}). \tag{5.17}$$

Its coset boundary condition has 3 lines $\{1, v, A\}$ with the non-trivial fusions

$\times$	v	A
v	1	A
A	A	$1 + v + 2A$

. (5.18)

The QCD_2 theory therefore has 3 vacua and 3 possible irreducible multiplets. Because the theory has no one-form symmetry along the flow, the stable solitons and particles must realize a representation furnishing a connected quiver. All such quivers contain

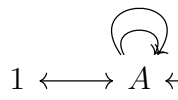

, (5.19)

as a sub-quiver. It follows that this theory must contain at least two stable particles over the $|\Omega_A\rangle$ vacuum and two soliton-anti-soliton pairs. Furthermore, this quiver is realized by an irreducible representation of the strip algebra and therefore the excitations all have equal mass.

***Spin*(9) + ψ_σ**: Our next example is $Spin(9)$ gauge theory with Majorana fermions in the spinorial. The bosonized theory has the 3D coset TQFT

$$Spin(16)_1 \times Spin(9)_{-2} = \mathcal{Z}(\mathcal{C}). \tag{5.20}$$

The coset boundary condition has 6 lines $\{1, s, v, c, A, B\}$ with non-trivial fusions

$\times$	s	v	c	A	B
s	1	c	v	A	B
v	c	1	s	B	A
c	v	s	1	B	A
A	A	B	B	$1+s+A$	$v+c+B$
B	B	A	A	$v+c+B$	$1+s+A$

. (5.21)

The theory therefore has 6 vacua and 6 possible irreducible representations. This theory also does not have one-form symmetry along the flow and so its stable excitations must realize representations assembling into a connected quiver. All such quivers contain

$$\begin{array}{ccccc} & & v & & 1 \\ & & & & \\ c & & A & \longleftrightarrow & B \qquad\qquad s \end{array} \quad , \tag{5.22}$$

as a sub-quiver. Therefore this theory must contain a soliton-anti-soliton pair of equal mass. Moreover, this pair necessarily exists as a member of one of three possible minimal connected sub-quivers[3]

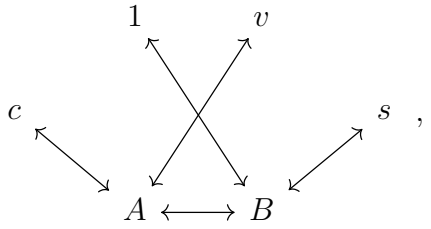

, (5.23)

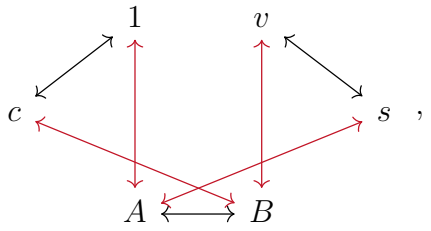

, (5.24)

3. Meaning that every connected quiver of stable solitons must contain one of these as a sub-quiver.

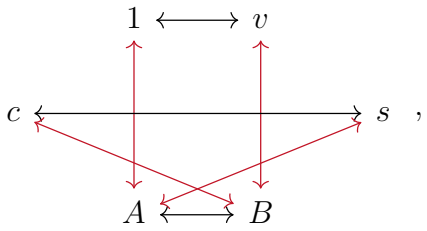

(5.25)

where colors are used to distinguish the sub-quivers of irreducible representations comprising a reducible representation. One such quiver must be realized, but symmetry considerations alone do not determine which. This instead is a question of dynamics. Note that in the later two cases, since the representations are reducible, not all solitons are required to have degenerate masses. Rather, this allows for two multiplets of stable solitons, each having a different mass.

$\boldsymbol{PSU(4)+\psi_{15}}$: Our final example is $PSU(4)$ gauge theory with Majorana fermions in the fifteen. The bosonized theory has the 3D coset TQFT

$$\frac{Spin(15)_1 \times SU(4)_{-4}}{\mathbb{Z}_4} = \mathcal{Z}(\mathcal{C}). \tag{5.26}$$

The coset boundary condition has 4 lines $\{1, v, A, B\}$ with non-trivial fusions

$\times$	v	A	B
v	1	B	A
A	B	$1+A+B$	$v+A+B$
B	A	$v+A+B$	$1+A+B$

. (5.27)

The theory therefore has 4 vacua and 4 possible irreducible multiplets. As in the prior examples, this theory has no one-form symmetry along the flow and so its stable particles and solitons must furnish representations that combine to give a connected quiver. All such quivers contain

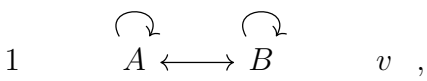

(5.28)

as a sub-quiver. Therefore the theory contains at least two stable particles, one above $|\Omega_A\rangle$ and the other above $|\Omega_B\rangle$, and a soliton-anti-soliton pair between these vacua.

These excitations are necessarily members of one of two possible minimal connected sub-quivers,

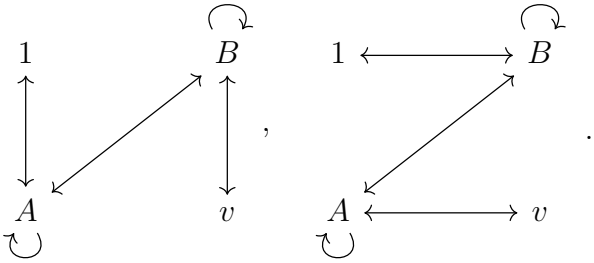

(5.29)

Again, which sub-quiver is realized by the theory is not determined by symmetry, but by dynamics. Both quivers correspond to irreducible representations and therefore all stable particles and solitons labeled by them will have degenerate mass.

5.5 Additional Comments and Results

5.5.1 Quiver Calculations

In this section, we show how to calculate the quivers of the gapped QCD_2 theories discussed in the main text. Recall we are interested in topological cosets where for simply-connected gauge group the bulk 3D TQFT is given by

$$\mathrm{Spin}(\dim(\mathbf{R}))_1 \times G_{-I(\mathbf{R})}. \tag{5.30}$$

The line operators in this 3D TQFT will be labeled as (Λ, λ), with Λ an integrable representation of $\mathrm{Spin}(\dim(\mathbf{R}))_1$ and λ an integrable representation of $G_{I(\mathbf{R})}$, with the negative level implicit in the notation. When $\dim(\mathbf{R})$ is even, we denote the four integrable representation of $\mathrm{Spin}(\dim(\mathbf{R}))_1$ as $\{\mathbf{1}, \mathbf{v}, \mathbf{s}, \mathbf{c}\}$ with $\mathbf{1}$ labeling the identity, $\mathbf{v}$ the vectorial, and $\mathbf{s}$ and $\mathbf{c}$ the spinorials. When $\dim(\mathbf{R})$ is odd, we denote the three integrable representations of

$\mathrm{Spin}(\dim(\mathbf{R}))_1$ as $\{\mathbf{1}, \mathbf{v}, \mathbf{s}\}$ with $\mathbf{v}, \mathbf{s}$ the vectorial and spinorial representations respectively. When the gauge group is not simply-connected, we denote the lines of the bulk TQFT $(\mathrm{Spin}(\dim(\mathbf{R}))_1 \times G_{-I(\mathbf{R})})/Z$ with Z the "common center" in terms of their representatives in the simply-connected case before gauging Z.

$\boldsymbol{SO(3) + \psi_5}$. For the bosonized theory, the 3D coset TQFT is

$$\frac{Spin(5)_1 \times SU(2)_{-10}}{\mathbb{Z}_2} = \mathcal{Z}(\mathcal{C}). \tag{5.17}$$

This theory has 10 lines while its coset boundary condition has 3, $\{1, v, A\}$. The condensation maps from the 3D theory to the coset boundary are

a	$p(a)$
$(\mathbf{1}, \mathbf{1})$	1
$(\mathbf{1}, \mathbf{11})$	v
$(\mathbf{1}, \mathbf{3})$	A
$(\mathbf{1}, \mathbf{9})$	A
$(\mathbf{1}, \mathbf{5})$	$v + A$

a	$p(a)$
$(\mathbf{1}, \mathbf{7})$	$1 + A$
$(\mathbf{s}, \mathbf{2})$	A
$(\mathbf{s}, \mathbf{4})$	$1 + v + A$
$(\mathbf{s}, \mathbf{6})_1$	A
$(\mathbf{s}, \mathbf{6})_2$	A

. (5.31)

The boundary lines have non-trivial fusions

$\times$	v	A
v	1	A
A	A	$1 + v + 2A$

. (5.18)

Because the coset boundary has 3 lines, there are therefore 3 irreducible representations of the strip algebra, with one labeled by each line.

Recall from the main text that the module category fusion coefficients are simply the

fusion coefficients which are computed from (5.18),

$$\begin{aligned} N_{1,1}^{1} = N_{v,1}^{v} = N_{A,1}^{A} = 1, \\ N_{1,v}^{v} = N_{v,v}^{1} = N_{A,v}^{A} = 1, \\ N_{1,A}^{A} = N_{v,A}^{A} = N_{A,A}^{1} = N_{A,A}^{v} = 1,\ N_{A,A}^{A} = 2. \end{aligned} \tag{5.32}$$

Therefore the quivers realized by 1, v, and A are

1 : 

, (5.33)

v : 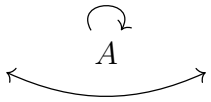

, (5.34)

A : 
. (5.35)

The single minimal connected sub-quiver[4] is clearly (5.35). Therefore this must be realized as a sub-quiver in the QCD_2 theory, requiring the particle-soliton degeneracies discussed in the bulk text.

A : 
. (5.36)

v : 
, (5.37)

A : 
. (5.38)

4. See footnote 3.

$$A: \quad \bullet \longleftrightarrow \bullet \longleftrightarrow \bullet \longleftrightarrow \bullet \quad . \tag{5.39}$$

$\boldsymbol{Spin(9)} + \psi_\sigma$. For the bosonized theory, the 3D coset TQFT is

$$Spin(16)_1 \times Spin(9)_{-2} = \mathcal{Z}(\mathcal{C}). \tag{5.20}$$

This theory has 32 lines while its coset boundary condition has 6 lines, $\{1, s, v, c, A, B\}$. The

condensation maps from the 3D theory to the coset boundary are:

a	$p(a)$
$(\mathbf{1},\mathbf{1})$	1
$(\mathbf{1},\mathbf{44})$	s
$(\mathbf{1},\mathbf{16})$	$v+B$
$(\mathbf{1},\mathbf{128})$	$c+B$
$(\mathbf{1},\mathbf{126})$	A
$(\mathbf{1},\mathbf{84})$	$1+s$
$(\mathbf{1},\mathbf{36})$	A
$(\mathbf{1},\mathbf{9})$	A

a	$p(a)$
$(\mathbf{v},\mathbf{1})$	v
$(\mathbf{v},\mathbf{44})$	c
$(\mathbf{v},\mathbf{16})$	$1+A$
$(\mathbf{v},\mathbf{128})$	$s+A$
$(\mathbf{v},\mathbf{126})$	B
$(\mathbf{v},\mathbf{84})$	$v+c$
$(\mathbf{v},\mathbf{36})$	B
$(\mathbf{v},\mathbf{9})$	B

a	$p(a)$
$(\mathbf{s},\mathbf{1})$	s
$(\mathbf{s},\mathbf{44})$	1
$(\mathbf{s},\mathbf{16})$	$c+B$
$(\mathbf{s},\mathbf{128})$	$v+B$
$(\mathbf{s},\mathbf{126})$	A
$(\mathbf{s},\mathbf{84})$	$1+s$
$(\mathbf{s},\mathbf{36})$	A
$(\mathbf{s},\mathbf{9})$	A

a	$p(a)$
$(\mathbf{c},\mathbf{1})$	c
$(\mathbf{c},\mathbf{44})$	v
$(\mathbf{c},\mathbf{16})$	$s+A$
$(\mathbf{c},\mathbf{128})$	$1+A$
$(\mathbf{c},\mathbf{126})$	B
$(\mathbf{c},\mathbf{84})$	$v+c$
$(\mathbf{c},\mathbf{36})$	B
$(\mathbf{c},\mathbf{9})$	B

. (5.40)

The boundary lines have non-trivial fusions

$\times$	s	v	c	A	B
s	1	c	v	A	B
v	c	1	s	B	A
c	v	s	1	B	A
A	A	B	B	$1+s+A$	$v+c+B$
B	B	A	A	$v+c+B$	$1+s+A$

. (5.21)

There are therefore 6 distinct irreducible representations of the strip algebra, labeled by each boundary line in $\mathcal{C}$. The module fusion coefficients (and hence quivers) again follow from (5.21).

For example, consider the line A. The relevant non-zero fusion coefficients in $\mathcal{C}$ are

$$\begin{aligned} N_{1,A}^{A} = N_{v,A}^{B} = N_{c,A}^{B} = N_{s,A}^{A} = 1, \\ N_{A,A}^{1} = N_{A,A}^{s} = N_{A,A}^{A} = 1, \\ N_{B,A}^{v} = N_{B,A}^{c} = N_{B,A}^{B} = 1. \end{aligned} \tag{5.41}$$

These realize the quiver

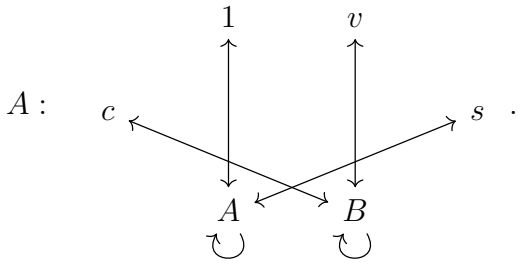

. (5.42)

The remaining quivers are

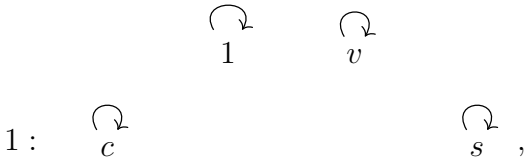

(5.43)

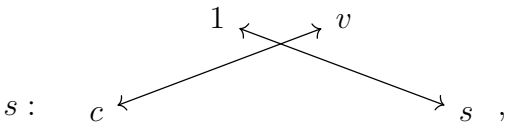

(5.44)

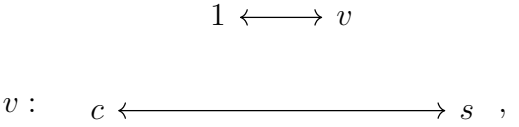

(5.45)

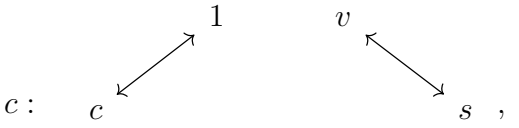

(5.46)

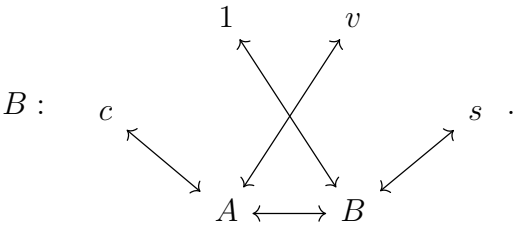

(5.47)

We would now like to find the minimal connected sub-quivers. Since the quiver labeled by B is connected it is clearly one. By analyzing sums of quivers directly, one finds that there are two more minimal connected subquivers corresponding to reducible representations:

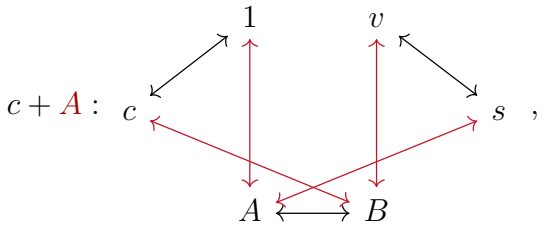

(5.48)

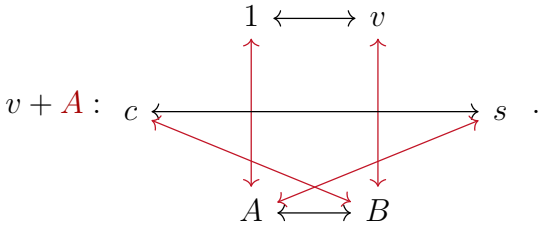

(5.49)

Here the coloring distinguishes the sub-quiver corresponding each subrepresentation. By inspection, the common sub-quiver of all minimal connected sub-quivers

$$\begin{array}{ccccc} & & v & & 1 \\ & & & & \\ c & & A & \longleftrightarrow & B & & s \end{array} \quad , \tag{5.22}$$

producing the required particle-soliton degeneracies discussed in the text.

$\boldsymbol{PSU(4) + \psi_{15}}$. For the bosonized theory, the 3D coset TQFT is

$$\frac{Spin(15)_1 \times SU(4)_{-4}}{\mathbb{Z}_4} = \mathcal{Z}(\mathcal{C}). \tag{5.26}$$

This theory has 14 lines while its coset boundary condition has 4, $\{1, v, A, B\}$. The conden-

sation maps from the 3D theory to the coset boundary are:

a	$p(a)$
$(\mathbf{1},\mathbf{1})$	1
$(\mathbf{1},\mathbf{35})$	v
$(\mathbf{1},\mathbf{45})$	$1+A+B$
$(\mathbf{1},\mathbf{15})$	$v+A+B$
$(\mathbf{1},\mathbf{20'})_1$	A
$(\mathbf{1},\mathbf{20'})_2$	B
$(\mathbf{1},\mathbf{84})_1$	B

a	$p(a)$
$(\mathbf{1},\mathbf{84})_2$	A
$(\mathbf{s},\mathbf{10})$	$A+B$
$(\mathbf{s},\mathbf{6})$	$A+B$
$(\mathbf{s},\mathbf{64})_1$	$1+B$
$(\mathbf{s},\mathbf{64})_2$	$1+A$
$(\mathbf{s},\mathbf{64})_3$	$v+A$
$(\mathbf{s},\mathbf{64})_4$	$v+B$

. (5.50)

The boundary lines have non-trivial fusions

$\times$	v	A	B
v	1	B	A
A	B	$1+A+B$	$v+A+B$
B	A	$v+A+B$	$1+A+B$

. (5.27)

There are therefore 4 distinct irreducible representations of the strip algebra. Following the prior two examples, the module fusion coefficients are determined by (5.27).

As a final example, consider the line A. From (5.27), the non-zero fusion coefficients we need are

$$\begin{aligned} N_{1,A}^{A} = N_{v,A}^{B} = 1, \\ N_{A,A}^{1} = N_{A,A}^{A} = N_{A,A}^{B} = 1, \\ N_{B,A}^{v} = N_{B,A}^{A} = N_{B,A}^{B} = 1. \end{aligned} \tag{5.51}$$

This defines the quiver

A : 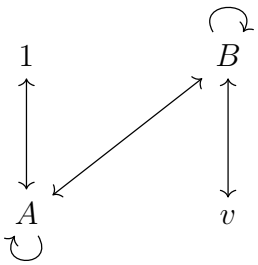 . (5.52)

Continuing in the same way, the remaining quivers are

1 : , (5.53)

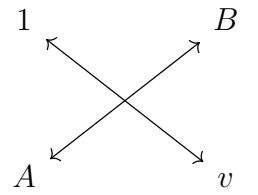

v : , (5.54)

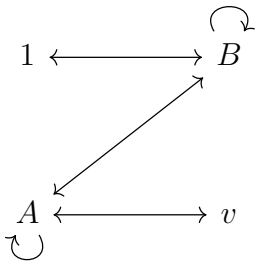

B : . (5.55)

The minimal connected sub-quivers are easily seen to only be (5.52) and (5.55). Their common connected sub-quiver is

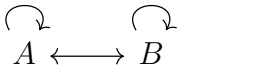

, (5.28)

implying the existence of degenerate particles and solitons as discussed in the main text.

5.5.2 Vacuum Condensates

In this section, we briefly discuss the characterization of the different vacua by the expectation values of the local operators that do not decouple in the IR. In the context of QCD_2, the flow of local operators has been studied e.g. in [90, 115] (see also [12]). As discussed in the main text, the topological local operators ϕ_a (in the basis diagonalized by the zero-form symmetry throughout the flow) can be obtained via anyon condensation by studying the endpoints of anyons at the topological boundaries. See (5.11). In particular, we are interested in topological cosets where for simply-connected gauge group the Lagrangian algebra is determined by the branching rules

$$\chi_{\Lambda}^{\mathcal{Q}_1}(q) = \sum_{\lambda} b_{(\Lambda,\lambda)}\, \chi_{\lambda}^{G_k}(q), \quad b_{(\Lambda,\lambda)} \in \mathbb{N}. \tag{5.56}$$

Specifically, $\mathcal{L} = \bigoplus_{(\Lambda,\lambda)} b_{(\Lambda,\lambda)}(\Lambda, \lambda^{\mathrm{op}})$. Thus, in the local operators ϕ_a the label a runs through all the representations (Λ, λ) such that $b_{(\Lambda,\lambda)} = 1$, since these would be the allowed endpoints in (5.11). [5] As in Section 5.5.1, when the gauge group is not simply-connected, we denote the labels a in the Lagrangian algebra of $(\mathcal{Q}_1 \times G_{-k})/Z$ with Z the "common center" in terms of their representatives in the simply-connected case before gauging Z.

We aim to diagnose the different vacua by the expectation value (condensates) of the operators ϕ_a in the presence of boundary conditions i. This can be done in terms of boundary states $|\mathbf{v}_i\rangle$:

$$\langle \phi_a \rangle_i = \langle \mathbf{v}_i | \phi_a | \mathbf{v}_i \rangle. \tag{5.57}$$

The overlap can be found using commutativity of the topological OPE of the ϕ_a, associativity, consistency of the OPE with the junctions allowed by the Lagrangian algebra, and the well-

5. Recall that in this work, for simplicity, we assume single multiplicity in the Lagrangian algebra. For higher multiplicity $b_{(\Lambda,\lambda)} \in \mathbb{Z}_+$, we must keep track of the multiple topological junctions at each boundary, and how these junctions can couple to each other in between the two boundaries of (5.11) in order to properly label local operators. See e.g. [12] for a more detailed discussion on this issue.

known result that topological local operators always allow for an idempotent complete basis $\mathbf{v}_i$:

$$\mathbf{v}_i\mathbf{v}_j = \delta_{ij}\mathbf{v}_i. \tag{5.58}$$

The idempotent complete basis of local operators corresponds, actually, by the operator-state correspondence to the clustering boundary states $|\mathbf{v}_i\rangle$. The overlap is thus straightforwardly calculated using this result, and the expectation value of the order parameters can be encapsulated in a matrix

$$\mathrm{B}_{ai} \coloneqq \langle \mathbf{v}_i|\phi_a|\mathbf{v}_i\rangle, \tag{5.59}$$

providing the expectation value of the order parameter ϕ_a in the clustering vacuum state $|\mathbf{v}_i\rangle$.

$\boldsymbol{SO(3)} + \psi_{\mathbf{5}}$. Using the condensation data above for this example, we find that the idempotent complete basis is given as

$$\mathbf{v}_1 = \frac{1}{2(3+\sqrt{3})}\big(\phi_{(\mathbf{1},\mathbf{1})} + \phi_{(\mathbf{1},\mathbf{7})} + \phi_{(\mathbf{s},\mathbf{4})}\big), \tag{5.60}$$

$$\mathbf{v}_v = \frac{1}{2(3+\sqrt{3})}\big(\phi_{(\mathbf{1},\mathbf{1})} + \phi_{(\mathbf{1},\mathbf{7})} - \phi_{(\mathbf{s},\mathbf{4})}\big), \tag{5.61}$$

$$\mathbf{v}_A = \frac{1}{2\sqrt{3}}\Big((1+\sqrt{3})\phi_{(\mathbf{1},\mathbf{1})} + (1-\sqrt{3})\phi_{(\mathbf{1},\mathbf{7})}\Big). \tag{5.62}$$

Inverting (5.60)-(5.62), we obtain the matrix of condensates:

$$\mathrm{B} = \begin{pmatrix} 1 & 1 & 1 \\ 2+\sqrt{3} & 2+\sqrt{3} & -1 \\ 3+\sqrt{3} & -3-\sqrt{3} & 0 \end{pmatrix}. \tag{5.63}$$

$\boldsymbol{Spin(9)} + \psi_\sigma$. Using the condensation data above for this example, we find that the

idempotent complete basis is given as

$$\mathbf{v}_1 = \frac{1}{12}\big(\phi_{(\mathbf{1},\mathbf{1})} + \phi_{(\mathbf{s},\mathbf{44})} + \phi_{(0,\mathbf{84})} + \phi_{(\mathbf{s},\mathbf{84})} + \phi_{(\mathbf{v},\mathbf{16})} + \phi_{(\mathbf{c},\mathbf{128})}\big), \tag{5.64}$$

$$\mathbf{v}_s = \frac{1}{12}\big(\phi_{(\mathbf{1},\mathbf{1})} + \phi_{(\mathbf{s},\mathbf{44})} + \phi_{(0,\mathbf{84})} + \phi_{(\mathbf{s},\mathbf{84})} - \phi_{(\mathbf{v},\mathbf{16})} - \phi_{(\mathbf{c},\mathbf{128})}\big), \tag{5.65}$$

$$\mathbf{v}_v = \frac{1}{12}\big(\phi_{(\mathbf{1},\mathbf{1})} - \phi_{(\mathbf{s},\mathbf{44})} + \phi_{(0,\mathbf{84})} - \phi_{(\mathbf{s},\mathbf{84})} + \phi_{(\mathbf{v},\mathbf{16})} - \phi_{(\mathbf{c},\mathbf{128})}\big), \tag{5.66}$$

$$\mathbf{v}_c = \frac{1}{12}\big(\phi_{(\mathbf{1},\mathbf{1})} - \phi_{(\mathbf{s},\mathbf{44})} + \phi_{(0,\mathbf{84})} - \phi_{(\mathbf{s},\mathbf{84})} - \phi_{(\mathbf{v},\mathbf{16})} + \phi_{(\mathbf{c},\mathbf{128})}\big), \tag{5.67}$$

$$\mathbf{v}_A = \frac{1}{6}\big(2\phi_{(\mathbf{1},\mathbf{1})} + 2\phi_{(\mathbf{s},\mathbf{44})} - \phi_{(0,\mathbf{84})} - \phi_{(\mathbf{s},\mathbf{84})}\big), \tag{5.68}$$

$$\mathbf{v}_B = \frac{1}{6}\big(2\phi_{(\mathbf{1},\mathbf{1})} - 2\phi_{(\mathbf{s},\mathbf{44})} - \phi_{(0,\mathbf{84})} + \phi_{(\mathbf{s},\mathbf{84})}\big). \tag{5.69}$$

Inverting (5.64)-(5.69), we obtain the matrix of condensates:

$$\mathrm{B} = \begin{pmatrix} 1 & 1 & 1 & 1 & 1 & 1 \\ 1 & 1 & -1 & -1 & 1 & -1 \\ 2 & 2 & 2 & 2 & -1 & -1 \\ 2 & 2 & -2 & -2 & -1 & 1 \\ 3 & -3 & 3 & -3 & 0 & 0 \\ 3 & -3 & -3 & 3 & 0 & 0 \end{pmatrix}. \tag{5.70}$$

$\boldsymbol{PSU(4)} + \psi_{\mathbf{15}}$. Using the condensation data above for this example, we find that the

idempotent complete basis is given as

$$\mathbf{v}_1 = \frac{1}{4(2+\sqrt{2})}\big(\phi_{(\mathbf{1},\mathbf{1})} + \phi_{(\mathbf{1},\mathbf{45})} + \phi_{(\mathbf{s},\mathbf{64})_1} + \phi_{(\mathbf{s},\mathbf{64})_2}\big), \tag{5.71}$$

$$\mathbf{v}_v = \frac{1}{4(2+\sqrt{2})}\big(\phi_{(\mathbf{1},\mathbf{1})} + \phi_{(\mathbf{1},\mathbf{45})} - \phi_{(\mathbf{s},\mathbf{64})_1} - \phi_{(\mathbf{s},\mathbf{64})_2}\big), \tag{5.72}$$

$$\mathbf{v}_A = \Big((1+\sqrt{2})\phi_{(\mathbf{1},\mathbf{1})} - (\sqrt{2}-1)\phi_{(\mathbf{1},\mathbf{45})} - \phi_{(\mathbf{s},\mathbf{64})_1} + \phi_{(\mathbf{s},\mathbf{64})_2}\Big)/4\sqrt{2}, \tag{5.73}$$

$$\mathbf{v}_B = \Big((1+\sqrt{2})\phi_{(\mathbf{1},\mathbf{1})} - (\sqrt{2}-1)\phi_{(\mathbf{1},\mathbf{45})} + \phi_{(\mathbf{s},\mathbf{64})_1} - \phi_{(\mathbf{s},\mathbf{64})_2}\Big)/4\sqrt{2}. \tag{5.74}$$

Inverting (5.71)-(5.74), we obtain the matrix of condensates:

$$\mathrm{B} = \begin{pmatrix} 1 & 1 & 1 & 1 \\ 3+2\sqrt{2} & 3+2\sqrt{2} & -1 & -1 \\ 2+\sqrt{2} & -2-\sqrt{2} & -\sqrt{2} & \sqrt{2} \\ 2+\sqrt{2} & -2-\sqrt{2} & \sqrt{2} & -\sqrt{2} \end{pmatrix}. \tag{5.75}$$

CHAPTER 6

HIGGSING TRANSITIONS FROM TOPOLOGICAL FIELD THEORY & NON-INVERTIBLE SYMMETRY IN CHERN-SIMONS MATTER THEORIES

6.1 Introduction

Gapped phases in (2+1) dimensions are characterized by a spectrum of massive anyons and patterns of non-abelian statistics. In the continuum limit, these systems are described by topological quantum field theory (TQFT), a paradigm for mathematically organizing the resulting long-range correlations and quantum entanglement. While the system remains gapped, the long-distance physics is robust. However, when the gap closes the system may transition from one topological phase to another. Such transitions may be either first order, or more interestingly, gapless, and characterized by a conformal fixed point which is in general strongly coupled.

One rich source of such transitions are Chern-Simons matter gauge theories. In these models the transition is driven by a charged scalar field ϕ which is massive on one side of the transition and condensed on the other. Such Chern-Simons matter theories have been intensively investigated and can serve as continuum models for deconfined quantum criticality [196]. (See [197] for a review). They are also a fruitful playground to explore dualities where the fixed point is described in two complementary fashions using distinct ultraviolet degrees of freedom [7, 198–201].

One of our main goals in this work is to elucidate aspects of these transitions between topological phases from the vantage point of the infrared topological field theories that they connect. To carry this out, we introduce a mesoscopic model of the transition built from a network of domain walls separating the two infrared phases. The network is shaped as a lattice permeating spacetime (or space in a related Hamiltonian model). Along each domain

wall there are gapless (1+1)d chiral degrees of freedom, defined by a coset conformal field theory / gauged WZW model [5,179,202,203]. As we cross the domain wall, the potential for the scalar field ϕ changes shape: on one side ϕ is massive, and on the other side it develops a vacuum expectation value. The (1+1)d fields on the domain walls may thus be viewed as edge modes confined to loci where the ϕ has vanishing mass.

As parameters of the domain wall network are changed, our model transitions between the given topological phases and plausibly has a phase transition in the same universality class as the desired Chern-Simons matter fixed point. As described, our model is conceptually similar to the coupled wire constructions of [204] and related models [205–207]. However, our approach is distinctly rooted in continuum field theory and does not, for instance, provide a microscopic lattice description of either the topological phases or the gapless domain wall modes. Related constructions based on continuum field theory ideas have also appeared in [208].

6.1.1 Topological Lines at Critical Points

From the vantage point of the microscopic Chern-Simons gauge theory many symmetries of the fixed point are emergent, meaning they are valid only at the infrared universality class characterizing the transition. This is a well-studied phenomenon for ordinary (zero-form) global symmetries where key examples of duality are characterized by emergent time reversal, or non-abelian global symmetry [32, 201, 209, 210]. By contrast, the possibility of emergent one-form symmetries is much less explored. A one-form symmetry is by definition, an extended line operator whose correlation functions depend only topologically on the support of the line [6]. Such a line is an emergent symmetry when this topological dependence is a property only of the correlation functions of the fixed-point universality class, but not the microscopic gauge theory Lagrangian. Note that while topological lines are ubiquitous in the gapped topological phases discussed above, their appearance at a gapless transition

is more striking.

The simplest possible notion of a one-form global symmetry is an abelian symmetry group. For instance, these are common in abelian gauge theory and often occur as center symmetries of non-abelian gauge theory with suitable non-minimal matter [6]. In gapped phases, these abelian one-form symmetries are described by abelian anyons with characteristic fusion rules. Notice that such symmetries always act on Hilbert space by invertible (unitary) operators. More exotic, and the focus of much of our discussion below, is the possibility of non-invertible one-form symmetry at a fixed point. These operators form a braided fusion category and, while they commute with the Hamiltonian, they do not act by invertible (unitary) operators on Hilbert space. One of the main results of our analysis is to provide qualitatively new examples of Chern-Simons matter fixed points with precisely this form of novel emergent symmetry. Again we emphasize that while non-invertible one-form symmetries are characteristic in topological phases, described by the non-abelian anyons of the theory, their appearance in a gapless phase is a new phenomenon.

To explain more precisely what is new about the examples to follow, it is helpful to recall that given any (2+1)-dimensional theory with a finite non-anomalous zero-form global symmetry K, gauging K produces a new theory with one-form symmetry given by the fusion category $\mathrm{Rep}(K)$. Moreover, if K is non-abelian, the fusion ring of $\mathrm{Rep}(K)$ is not described by any abelian group. Thus, any such example gives a simple construction of non-invertible one-form symmetry. In a sense then, examples of non-invertible one-form symmetries abound and indeed examples based on finite, or more generally, disconnected gauge groups have been discussed in the literature. See e.g. [134, 211–216]. However, unfortunately one-form symmetries manufactured by this construction do not provide any significant dynamical insight. Indeed, gauging the finite subgroup K is a topological operation on a field theory and hence commutes with the renormalization group flow. Therefore, the presence of the $\mathrm{Rep}(K)$ symmetry is simply an avatar K symmetry of the related "ungauged" theory. In contrast with

the above, the examples we discuss below will have non-invertible one-form symmetry but *connected* gauge groups. In these models the presence of non-invertible one-form symmetry is a fundamentally new constraint on the dynamics at the fixed point. (A gapless example in (3+1)d with a connected gauge group and non-invertible one-form symmetry is a model of axions [217].)

6.1.2 Condensation, Higgsing, and Hierarchies

To argue for the presence of these new symmetries we make use of the mesoscopic model described above. Indeed, one of the key advantages of this model is that it manifestly possess the non-invertible symmetries throughout its phase diagram. Therefore, the bulk of our technical analysis is to understand the precise one-form symmetries of the mesoscopic model. As we explain, the key idea is to ask how an anyon worldline in one topological phase can penetrate the gapless domain wall and continue as a new worldline in a different gapped phase. This in turn is a question of how to describe the Higgsed phase of the gauge theory (ϕ condensed) in terms of the anyons of the massive phase of the gauge theory (ϕ not condensed).

We achieve such a description by modifying the vacuum of the massive phase to include loops of the ϕ field viewed as anyons in the topological phase. This procedure is complicated by two important physical effects:

- The anyons described by ϕ quanta in general carry spin. Hence, on their own, they cannot be consistently summed.
- When these anyons collide, they produce new anyons which must also be summed by consistency.

Both of these problems are solved in the mesoscopic model. In that case, gapless degrees of freedom on the domain wall can be viewed as an edge state for a gapped bulk known as

the coset TQFT. By pairing with degrees of freedom from the coset TQFT, the ϕ quanta become effectively bosonic and may then condense. This is technically achieved using anyon condensation [2, 24, 37, 131, 192, 218] which also explains how to consistently incorporate the fusion products. Thus in our model, the Chern-Simons matter transition driven by the Higgs mechanism, itself a form of "condensation," modifies the vacuum via anyon condensation in a product TQFT modeling both the massive phase and the coset.

We remark that analogous considerations have been applied in the context of hierarchy constructions of fractional Hall states [219, 220] (See [221] for a review). In particular in [222] a transition from one fractional Hall state to another is modeled as anyon condensation in a product theory, which includes the initial state as well a new topological degrees of freedom. Applying the logic of our mesoscopic construction, we anticipate that these additional topological degrees of freedom have as an edge mode, the chiral gapless fields that appear as the magnetic field is modulated. One can then envision a mesoscopic domain wall network model of fractional Hall state transitions directly analogous to our construction below for Higgsing transitions.

6.1.3 Implications of Higher Symmetry

As one of our main results is the appearance of non-invertible one-form symmetries in Chern-Simons matter fixed points, we summarize here several of their key physical consequences. Some of these features are common to any one-form symmetry, while others depend particularly on the fact that the symmetries are non-invertible.

- The non-invertible symmetry does not act on local operators in the fixed point theory [6]. Therefore, it cannot be explicitly broken by any relevant deformation of the fixed point and must be present in all resulting phases. In our examples this symmetry will be spontaneously broken in the gapped phases that resulted from the fixed point by relevant deformation.

- The non-invertible one-form symmetry may form a modular invariant full TQFT on its own, in which case it plausibly decouples from the rest of the theory. Alternatively, it may be non-modular in which case it cannot decouple from the fixed-point dynamics [34, 223–225]. In the latter case, we deduce that the fixed point, if gapless, must support conformally invariant line-defects that are charged under this non-invertible one-form symmetry.[1] Upon relevant deformation to a gapped phase, these conformally invariant defects flow to the additional anyons needed to make the braiding matrix non-degenerate.

- The braiding of non-invertible one-form symmetries is an anomaly that must be reproduced in any phase resulting from the fixed point [6, 226]. When the fusion rules of the symmetry are not those of the representation ring of a finite group, the braiding must be non-trivial [227, 228]. Hence, such a symmetry is always anomalous and obstructs a trivially gapped phase.

- Beyond its action on the vacuum, the one-form symmetry will organize the non-zero energy states into multiplets. For instance, the spectrum of the theory with periodic boundary conditions is constrained by the presence of a one-form symmetry. When this symmetry is non-invertible the multiplets will be representations of algebras, not groups. See [56, 61, 144, 146–148, 150] for related discussion.

We hope to explore many of these features in future work.

6.2 The Higgsing Transition

In this section, we motivate our study of Chern-Simons matter theories. Our goal is to analyze the Higgsing transition using tools of topological quantum field theory and (1+1)d

1. Here by line defect we mean an extended operator whose total dimension in spacetime is one. Such an object may act as an operator at a fixed time, or alternatively may define a point-like defect in space for all time.

conformal field theory. We introduce a mesoscopic model for this transition based on domain wall networks. Using this model we provide a framework to find the topological lines, in general non-invertible, that exist at these fixed points.

6.2.1 Chern-Simons Matter Flows

We consider a (2+1)d Chern-Simons theory coupled to charged scalar matter. The defining data of such a field theory are given as follows:

- A gauge group G, and a Chern-Simons level $k \in \mathbb{Z}$. We denote this pair as G_k. (Below we take G to be a connected compact Lie group.)
- A scalar field in a representation $\mathbf{R}$ of G. (Below, we take $\mathbf{R}$ to be irreducible for simplicity.) In general, the representation, and hence scalar is complex unless otherwise noted. We denote the scalar as $\phi_{\mathbf{R}}$.
- An interaction potential $V(\phi_{\mathbf{R}})$. Typically, this potential includes a quadratic term, as well a cubic, quartic, etc. interactions among the scalars. We denote the coefficient of the quadratic term as m^2 :

$$V(\phi_{\mathbf{R}}) = m^2 |\phi_{\mathbf{R}}|^2 + \cdots \ . \tag{6.1}$$

Given this data, our focus is the critical point defined by tuning the scalars to be massless $m^2 \to 0$. In general, such a system is a gapless conformal field theory. It is also possible that the resulting system is first-order.

One way to understand the $G_k + \phi_{\mathbf{R}}$ fixed point described above, is that it provides a transition between two topological phases. These are achieved by activating the quadratic term in the potential and flowing to the infrared. The result of these flows can be deduced by examining the initial gauge theory description of the fixed point:

- $m^2 > 0$: The scalar field $\phi_{\mathbf{R}}$ is massive and is integrated out. At long distances, this results in the G_k topological Chern-Simons theory.

- $m^2 < 0$: The scalar field $\phi_{\mathbf{R}}$ condenses and Higgses the gauge group from G to a subgroup H stabilizing the expectation value. At long distances, this results in a $H_{\tilde{k}}$ topological Chern-Simons theory. Here, the level $\tilde{k}$ of H is given by $\tilde{k} = nk$ where $n \in \mathbb{N}$ is the index of embedding of H in G.[2]

These two flows are shown below:

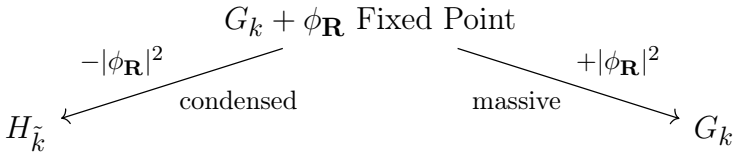

(6.2)

To make this discussion more precise, note that we should in fact view the potential deformations described above as relevant deformations of the Chern-Simons matter fixed point. Thus, our discussion assumes that these deformations remain relevant at this fixed point and further that we can analyze their effects using the microscopic gauge theory Lagrangian. In other words, we assume throughout that the flow to the fixed point and the potential flows commute. Additionally, since our analysis is concerned primarily with the nature of this fixed point, in the following we will describe energy scales relative to the flow diagram (6.2). Therefore, the ultraviolet will generally refer to the fixed point (not the weakly coupled gauge theory), and the infrared to the topological phases G_k and $H_{\tilde{k}}$.

2. The index n of the embedding $H \hookrightarrow G$ can be computed by taking any representation R_G of G, decomposing it into an H-representation R_H, and evaluating the ratio of Dynkin indices: $n = I_H/I_G$.

The Non-Relativistic Approximation

The massive flow, $m^2 > 0$, to G_k provides a starting point to analyze the transition. At long distances, the scalar field $\phi_{\mathbf{R}}$ may be viewed as an anyon $a_{\mathbf{R}}$ in this topological field theory:

$$\phi_{\mathbf{R}} \to a_{\mathbf{R}} \ . \tag{6.3}$$

More precisely, in the strict infrared, quanta of $\phi_{\mathbf{R}}$ have a parametrically large mass and therefore the number of them in any process is conserved. Amplitudes with N scalar particles may then be approximated in the TQFT as correlation functions involving N anyon worldlines $a_{\mathbf{R}}$.

We may reverse this idea to obtain a non-relativistic approximation to the massive flow valid at non-zero energies, which are small compared to the mass of $\phi_{\mathbf{R}}$. Indeed, in this limit, the field $\phi_{\mathbf{R}}$ fluctuates and costs only finite (but large) energy to activate. Thus, the vacuum should be viewed as containing a sum over virtual loops of scalar quanta, or equivalently loops of the anyon $a_{\mathbf{R}}$. It follows that we may approximate the partition function of the Chern-Simons matter fixed-point theory, Z_{CSM}, as a sum over insertions of loops of $a_{\mathbf{R}}$. Schematically:

$$\begin{aligned} Z_{\text{CSM}}(m) \approx Z_{G_k} + \int \mathcal{D}L \; e^{-m|L_i|} Z_{G_k}(a_{\mathbf{R}}(L)) \\ + \int \mathcal{D}L_1 \mathcal{D}L_2 \; e^{-\sum_i m|L_i|} Z_{G_k}(a_{\mathbf{R}}(L_1), a_{\mathbf{R}}(L_2)) + \cdots \ , \end{aligned} \tag{6.4}$$

where L_i is a worldline with length $|L|$ of the i-th anyon, and $\mathcal{D}L_i$ is an appropriate regularized path-integral measure over the space of loops. In this approximation, each integrand $Z_{G_k}(a_{\mathbf{R}}(L_1), \cdots)$ is a correlator in the topological phase G_k.

The non-relativistic approximation, can provide a useful first analysis of the fixed point. For instance, it can be used to analyze scattering matrices and crossing symmetry of anyonic

particles [229–231].

6.2.2 Mesoscopic Models of Higgsing

To analyze the transition in more detail, we now construct a mesoscopic model that interpolates between the same two topological phases appearing in (6.2). This model is Euclidean. A related Hamiltonian model is presented below. To motivate the construction, we consider subjecting our Chern-Simons matter theory to a position (and time)-dependent mass term in the potential:

$$m^2 \to m^2(x) \ . \tag{6.5}$$

In the bulk of spacetime, $m^2(x)$ is assigned a large, positive value, whereas in cylindrical regions that intersect to form a cubical lattice, it takes a large, negative value. See Figure 6.1a. The interface between these two regions is a higher-genus Riemann surface, a domain wall network, where the mass parameter crosses zero. Upon flowing to the infrared, the region exterior to the cylinders is in the topological phase G_k, while the interior region is in the topological phase $H_{\tilde{k}}$. See also Figure 6.2.

Observe that the chiral central charges of G_k and $H_{\tilde{k}}$ in general do not match. Therefore, the domain wall interface between the bulk regions is in general chiral and thus gapless. We claim that this chiral mode is the (1+1)d coset theory $G_k/H_{\tilde{k}}$. This model is the chiral sector of the gauged WZW model based on target space G_k with gauge group $H_{\tilde{k}}$. To see this, consider a Wilson line in the Chern-Simons matter theory in a G-representation, χ, that crosses interface. In the mesoscopic description, in the $H_{\tilde{k}}$ region the G representation χ branches into a direct sum of H representations. Therefore, the domain wall modes should provide a junction (in general non-topological) between the G_k Wilson line χ and the $H_{\tilde{k}}$ Wilson line ψ, as depicted in Fig. 6.3(a) precisely when the branching of χ includes ψ.

The existence of these junctions is exactly the defining property of the chiral coset CFT.

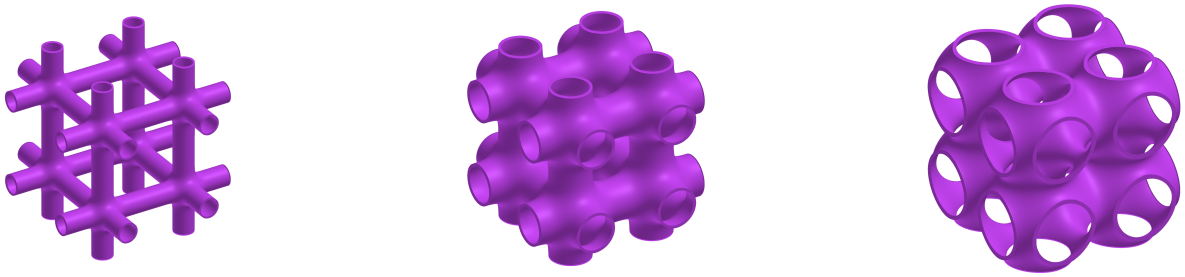

(a) (b) (c)

Figure 6.1: A mesoscopic model of the Higgsing transition (6.2). In (a) we have intersecting cylindrical regions of radius W. The cylinders form a regular lattice as depicted, and the distance between two of the nearest parallel cylinders is L. Outside the cylinders the theory is an a G_k phase, inside it is in an $H_{\tilde{k}}$ phase. At the interface is the coset $G_k/H_{\tilde{k}}$ which is in general gapless and chiral. See also Fig. 6.2 for the definitions of L and W. The width W of the cylindrical regions is a parameter of the model. For $W \to 0$ the theory is in a G_k phase, while as $W \to L$, (c), it is in an $H_{\tilde{k}}$ phase.

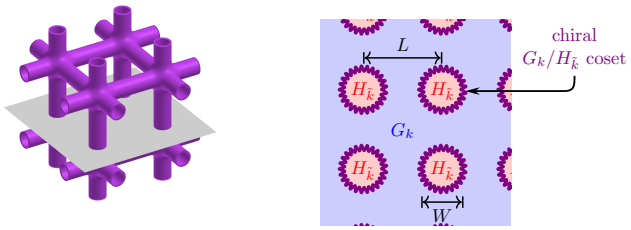

(a) (b)

Figure 6.2: A cross section (b) of the gray plane depicted in (a).

Indeed, the representations (modules) of $G_k/H_{\tilde{k}}$, which we label by ρ, satisfy

$$\chi_\chi^{G_k}(q) = \sum_{\rho,\psi} n_\chi^{\rho\psi}\, \chi_\rho^{G_k/H_{\tilde{k}}}(q)\, \chi_\psi^{H_{\tilde{k}}}(q)\ , \tag{6.6}$$

with q the modular parameter, and where $n_\chi^{\rho\psi} \in \mathbb{Z}^+$ dictates how the representations (modules) ρ of the coset CFT couple to those of the $H_{\tilde{k}}$ WZW theory to yield the representation χ of G_k.[3] This branching rule indicates that a vertex operator in the module V_ρ can connect

3. Notice that several copies of the trivial representation of the coset CFT $G_k/H_{\tilde{k}}$ with single vacuum may appear in the branching decomposition. This signals the possible appearance of additional topological sectors.

χ line in the G_k phase and a ψ line in the $H_{\tilde{k}}$ when $n_\chi^{\rho\psi} \neq 0$.

A Model of the Quantum Field $\phi_R(x)$

We can further motivate the mesoscopic model introduced above by comparing its features to those of the Chern-Simons matter fixed point.

To begin, let us return to the non-relativistic expansion (6.4) of the partition function. In this description, it is clear that degrees of freedom are missing and have been integrated out along the renormalization group trajectory. Most directly we should ask: how can we produce the quantum field $\phi_{\mathbf{R}}(x)$? Of course, the particles created by $\phi_{\mathbf{R}}(x)$ are the anyons modeled by the line operator $a_{\mathbf{R}}$ in G_k. In the IR these particles are infinitely massive and correspondingly, the lines are unbreakable. In the fixed point however, the Wilson line in the representation $\mathbf{R}$ can end on the insertions of the field $\phi_{\mathbf{R}}(x)$. Note that this is compatible with the fact that $\phi_{\mathbf{R}}(x)$ is not gauge invariant: it is not a well-defined local operator but instead lives at the end of a line.

Now consider instead the mesoscopic model. Here, in contrast, we will find a clear analog of the scalar field $\phi_R(x)$. We start again with the Wilson line $a_{\mathbf{R}}$ in the same representation $\mathbf{R}$ as the scalar field. Note that the Higgsed group $H_{\tilde{k}}$ is characterized precisely by the fact that the branching of the G representation $\mathbf{R}$ includes the trivial representation of H:

$$\mathbf{R}|_H \cong \mathbf{1}_H + \cdots \ . \tag{6.7}$$

In terms of the coset character formula (6.6) this means that $n_{\mathbf{R}}^{\rho \mathbf{1}_H} \neq 0$ for some module ρ in the coset CFT. Thus, when the Wilson line $a_{\mathbf{R}}$ crosses the domain wall into the $H_{\tilde{k}}$ phase, it becomes transparent. In other words, the line $a_{\mathbf{R}}$ can end on the interface as depicted in Fig. 6.3(b), where it terminates on an operator $\mathcal{O}_\rho$ in the coset CFT. We regard these ray-shaped operators of $a_{\mathbf{R}}$ terminating on $\mathcal{O}_\rho$ as a proxy of the scalar field $\phi_{\mathbf{R}}(x)$.

Let us also inspect the two-point function of these operators in the limit $L \gg W$. We consider a segment of the line $a_{\mathbf{R}}$ terminating at two points, x_1 and x_2, on the interface. Then, the correlator contains a factor of the two-point function in the coset CFT on the interface surface Σ:

$$\langle \mathcal{O}_\rho(x_1)\mathcal{O}_{\overline{\rho}}(x_2)\rangle_\Sigma \sim e^{-\frac{1}{W}h_\rho|x_1-x_2|} \ , \tag{6.8}$$

where h_ρ is the conformal dimension of the primary $\mathcal{O}_\rho$. Here, this estimate arises because the state on a circle created by $\mathcal{O}_\rho$ has energy h_ρ/W and is propagated the distance $|x_1-x_2|$ before annihilating against the second insertion. On the other hand, we can compare (6.8) to the expected exponential decay of the two-point correlator of the massive field $\phi_R(x)$. From this we can identify the scalar mass as:

$$m \sim \frac{h_\rho}{W} \ . \tag{6.9}$$

Finally, we note that as we increase the width W of the cylinders close to the lattice spacing L, it is no longer reliable to estimate the two-point function using radial quantization. In particular, the exponential falloff in the coset two-point function will transition at short distances to power law behavior, indicating a potential gapless phase transition.

In summary, dialing W from zero to L in the mesoscopic model produces a phase transition between G_k and $H_{\tilde{k}}$. Our basic hypothesis is that this phase transition is in the same universality class as that of the underlying Chern-Simons matter fixed-point theory (6.2). It is also possible that there are multiple intermediate phases as the parameters of the mesoscopic model are varied in which case we assume that one of the intermediate phases coincides with the fixed-point.

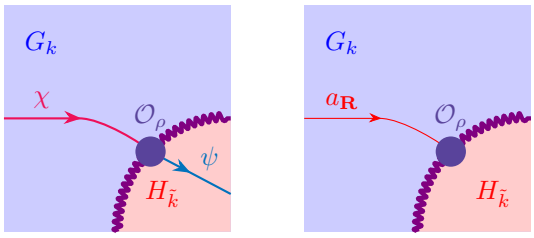

(a) (b)

Figure 6.3: Lines transitioning between phases. In (a) the transition between a general G_k line χ to an $H_{\tilde{k}}$ line ψ through a local operator $\mathcal{O}_\rho$ in the (1+1)d coset $G_k/H_{\tilde{k}}$. In (b), a ray-shaped operator showing that in the mesoscopic model the anyon line $a_{\mathbf{R}}$ can end. These ray-shaped operators model the quantum field $\phi_{\mathbf{R}}$.

Hamiltonian Model

So far, we have described the mesoscopic model in a Euclidean framework with discrete time translation symmetry. Here, we outline the corresponding Hamiltonian formulation with continuous time.

The Hilbert space $\mathcal{H}$ is defined by the configuration in Figure 6.2b. In physical terms this consists of local coset modes from each cylinder-shaped "lattice site" in the model. Additionally, we must take into account the fact that each cylinder appears at long distances to be a (non-simple) line inserted along time in the G_k TQFT exterior. Such lines induce additional states that we include.

To write this more explicitly, let $r, s, \cdots$ be abstract indices labeling the lattice sites in the model. At each site the (1+1)d coset can be decomposed into modules V_{ρ_s} (representations of the relevant chiral algebra). We include in each site Hilbert space those summands which have a junction with the vacuum in $H_{\tilde{k}}$. Physically, this corresponds to the fact that the spatial regions of $H_{\tilde{k}}$ are empty, i.e. they do not contain any non-trivial anyon inserted along time. The full Hilbert space of the model is then a direct sum over all such sectors, indicated by $\{\rho_s\}$, where each local factor is dressed by an appropriate line from the bulk

G_k Chern-Simons theory. Explicitly:

$$\mathcal{H} = \bigoplus_{\{\rho_s\}_s} \left(\mathrm{Hom}_{G_k} \left(\mathbf{1}, \bigotimes_r \chi(\rho_r) \right) \otimes \bigotimes_s V_{\rho_s} \right) , \tag{6.10}$$

where $\mathrm{Hom}_{G_k}(\mathbf{1}, \chi)$ is the Hilbert space of the G_k Chern-Simons theory with an inserted timelike Wilson line χ, and χ_s is:

$$\chi(\rho_s) = \sum_{\chi \in G_k} n_\chi^{\rho_s \mathbf{1}_H} \chi \ . \tag{6.11}$$

(The coefficients $n_\chi^{\rho\psi}$ are defined in (6.6).) To understand (6.11), consider adiabatically shrinking the diameter of an $H_{\tilde{k}}$ cylinder while keeping it extended in the time direction. This results in the insertion of the line defined above at each site.[4]

The "free" part of the Hamiltonian is given by the sum of the coset conformal field theory Hamiltonians acting on each module V_{ρ_s}. Note that this implies that in the strict zero-size limit, the non-vacuum ρ contributions in the Hilbert space (6.10) acquire infinite energy $h_\rho/W \to \infty$ from the coset modes. In particular, in this limit the model reduces to the expected G_k Chern-Simons theory without additional insertions.

Beyond the free Hamiltonian, local interaction terms between neighboring sites mediated by anyon exchanges can be introduced. Schematically, such an interaction is represented as

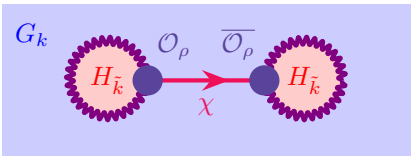

(6.12)

where χ denotes an anyon in G_k and $\mathcal{O}_\rho$ represents an operator in the module V_ρ of the chiral

4. The factor $\mathrm{Hom}_{G_k}(\mathbf{1}, \otimes_s \chi(\rho_s))$ in (6.10) is for when the spatial manifold is S^2. For a general spatial manifold, the factor should be replaced by the result of quantizing the G_k Chern-Simons theory with $\chi(\rho_s)$ inserted at each site and along time and hence depends on the global spatial topology.

coset theory, with $n_\chi^{\rho \mathbf{1}_H} \neq 0$. This can intuitively be understood as an infinitesimal version of one step time translation in the Euclidean model in Figure 6.1a. We expect that such interactions couple the cylinders effectively, thereby realizing the configurations illustrated in panels (b) and (c) of Figure 6.1 as the interaction strength is increased.

Here we note that the above construction cannot be used to realize the exact microscopic free Chern-Simons matter theory in any continuous limit. This is because, the model allows G_k lines χ to have an end only when $n_\chi^{\rho \mathbf{1}_H} \neq 0$ for some ρ in the coset CFT. In the microscopic gauge theory, any G_k line can end on a composite operator as long as it does not have a non-trivial electric one-form symmetry charge. To realize that behavior, we further add the sectors including $H_{\tilde{k}}$ lines at the core of the cylinders. In the Hamiltonian picture, such new sector should be given an energy for each nontrivial line, modeling the massive excitations in the $H_{\tilde{k}}$ cylinder. Our assumption is that such massive degrees of freedom are not important for the nature of phase transition between G_k and $H_{\tilde{k}}$ phases.

We also emphasize that our model does *not* provide a local way of constructing Chern-Simons theory Hilbert spaces; hence, it should not be interpreted as a microscopic model of the G_k Chern-Simons theory. Instead, we assume that the microscopic realization of the G_k theory is given and use it as the basis for constructing a mesoscopic model of the transition to the $H_{\tilde{k}}$ phase. In the extreme case where G_k is trivial and the chiral coset theory is replaced by the corresponding $H_{\tilde{k}}$ WZW model, the total Hilbert space reduces to a direct product of identical infinite-dimensional spaces $V_{\mathbf{1}_H}$. This scenario corresponds to the setup of [208], and we anticipate that an appropriate choice of interaction terms in (6.12) will yield a vacuum adiabatically connected to the state proposed in [208].

6.2.3 Anyon Condensation and Cosets

The coset degrees of freedom on the domain walls provide us with a natural way to compare the lines in the two topological phases G_k and $H_{\tilde{k}}$. Indeed, for the examples that we will study

below the (2+1)d TQFT $H_{\tilde{k}}$ admits the following presentation via anyon condensation:[5]

$$H_{\tilde{k}} \cong \frac{\left[G_k \times \left(\frac{\overline{G_k}}{H_{\tilde{k}}}\right)\right]}{\mathcal{B}} \ . \tag{6.13}$$

Let us elaborate on the meaning of the above:

- Each factor above is a (2+1)d TQFT. In particular, $G_k/H_{\tilde{k}}$ is the coset TQFT which has as its one-sided chiral boundary the (1+1)d coset CFT. The coset TQFT is in turn defined as follows:

  - In simple cases the coset TQFT is a product Chern-Simons theory where the denominator has a time-reversed (negative) level yeilding:

$$\frac{G_k}{H_{\tilde{k}}} \equiv G_k \times H_{-\tilde{k}} \ . \tag{6.14}$$

  - When the gauge groups G and H have a common center subgroup Z we must modify the right-hand side of (6.14) by quotienting by this common center factor.
  - There may also be non-abelian bosons in the product Chern-Simons theory (6.14) which must be condensed to accurately describe the TQFT. In complete generality, the principle defining the coset TQFT is that one should condense (gauge) the maximal braided fusion category which is common to both G_k and $H_{\tilde{k}}$. The case of the center quotient is an example of this principle when the common subfusion category is abelian.

  Examples of coset TQFTs which differ from (6.14) by non-abelian anyon condensation are called *maverick cosets* and play a prominent role below. See [5, 24, 36, 105, 232].

5. More precisely, coset inversion (see [3, 24]) says that, given a coset decomposition as in (6.6), there exists an algebra $\mathcal{C}$ such that $H_{\tilde{k}}/\mathcal{C} = \left[G_k \times \left(\frac{\overline{G_k}}{H_{\tilde{k}}}\right)\right]/\mathcal{B}$. In our context, $\mathcal{C}$ will always be the trivial algebra.

- In (6.13), the barred factor has been time-reversed. For the Chern-Simons factors, this flips the sign of the levels. More generally, this conjugates the spins of all anyons.

- In the denominator, $\mathcal{B}$ is an algebra object of the TQFT. The notation means that certain anyons have been condensed i.e. gauged on the right-hand side. Intuitively, this expression thus means that any line ψ in the $H_{\tilde{k}}$ theory can be viewed as a pair $(\chi, \bar{\rho})$ in $G_k \times \overline{\frac{G_k}{H_{\tilde{k}}}}$ provided that we enforce the selection rules and identifications implied by non-abelian anyon condensation.

In the above, the operation of non-abelian anyon condensation dictated by the object $\mathcal{B}$ is the least familiar. In brief this gauging operation is characterized by a finite formal sum of lines (non-simple anyon) [192] :

$$\mathcal{B} = \sum_i \beta_i \ , \tag{6.15}$$

where in our context, each β_i appearing above is a pair:

$$\beta_i = (\chi_i, \bar{\rho}_i) \in G_k \times \overline{\frac{G_k}{H_{\tilde{k}}}} \ , \tag{6.16}$$

and $\mathcal{B}$ includes the identity line with unit multiplicity in the sum. Additionally, we require that $\mathcal{B}$ admit a fusion channel to itself dictated by a multiplication map μ:

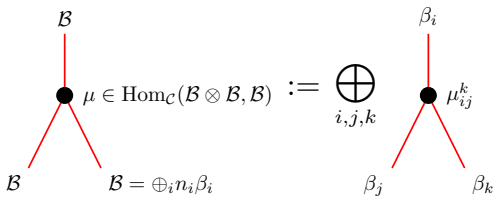

. (6.17)

Moreover, $\mathcal{B}$ must braid trivially with itself through the multiplication map:

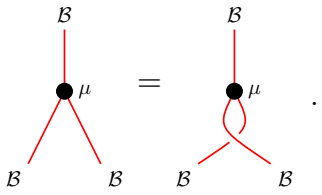

. (6.18)

In particular, this implies that each line in the gauged algebra $\mathcal{B}$ must be a boson, i.e. it must have integral spin.[6]

One consequence of this discussion is a formula for the total quantum dimension before and after gauging. We recall that the total quantum dimension of a TQFT is sum over quantum dimensions squared of its simple lines, $\sum_{\ell\in\mathcal{I}} d_\ell^2$, where the individual quantum dimension of a simple line operator ℓ is defined as the expectation value of a trivial loop of ℓ:

$d_\ell =$ 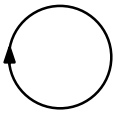 . (6.19)

Defining the quantum dimension of an algebra as

$$\dim(\mathcal{B}) = \sum_i d_{\beta_i} \ , \tag{6.20}$$

we then have the general formula:

$$\dim(H_{\tilde{k}}) = \frac{\dim(\left[G_k \times \left(\frac{\overline{G_k}}{H_{\tilde{k}}}\right)\right])}{\dim(\mathcal{B})^2} \ . \tag{6.21}$$

In practical examples below, we use these constraints to conjecture the existence of various algebras and apply them to analyze the behavior of topological lines across the Higgsing transition.

6.2.4 Symmetries of the Higgsing Transition

We now have the tools to analyze the symmetries of the Chern-Simons matter fixed point using the mesoscopic model framework. We are particularly interested in (non-invertible) one-form symmetries. Note that local operators are blind to such symmetries. Therefore, all

6. Beyond the conditions enumerated here, there are also algebraic identities that are required by the multiplication map μ. We do not make use of these in the following, and refer to [12, 41, 64, 192] for details.

one-form symmetries must be visible in both gapped phases G_k and $H_{\tilde{k}}$ which reside exterior and interior to the domain wall network in Figure 6.1.

To guide intuition, let us return again to the non-relativistic approximation (6.4). Consider any line/anyon b in the theory G_k. Since this theory is fully topological b is of course also topological. However, in general the line b should be viewed as an emergent symmetry: it is topological in the strict IR, but not in the fixed-point theory where the scalar fluctuates. A necessary condition for b to remain topological at the fixed point can be deduced from (6.4). Specifically b must remain topological in the presence of the new vacuum state which contains a sum over insertions of $a_{\mathbf{R}}$. For instance, this implies that loops of the line $a_{\mathbf{R}}$ must be transparent to loops of b. Pictorially this means:

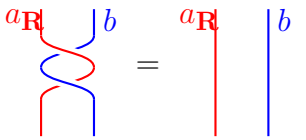

$$\Longrightarrow \frac{S_{a_{\mathbf{R}},b}S_{0,0}}{S_{a_{\mathbf{R}},0}S_{b,0}} = 1 \ , \tag{6.22}$$

where above S is the modular S-matrix of the G_k topological theory. We note that the left-hand side above is a strictly stronger constraint involving the braiding R-matrix of the G_k Chern-Simons theory. We focus on its S-matrix implication (right-hand side) for simplicity of this intuitive discussion. In summary, equation (6.22) thus provides candidate lines b that may, perhaps, remain topological in the Chern-Simons matter fixed point.

Local Modules and Topological Lines

We can obtain more precision using the mesoscopic model of section 6.2.2 above. The key point is that the anyon condensation procedure described above also gives us a complete picture of the lines that survive the gauging of an algebra $\mathcal{B}$. Observe that after condensation, $\mathcal{B}$ becomes transparent and equivalent to the new identity line in the gauged theory ($H_{\tilde{k}}$ above in (6.13)). Technically, the lines that characterize the theory after gauging are the so-called *local modules* with respect to the algebra $\mathcal{B}$ in the original theory [192].

A general $\mathcal{B}$-module, $\mathcal{M}$, is defined diagrammatically as admitting a junction $\tilde{\mu}$ with the algebra $\mathcal{B}$:

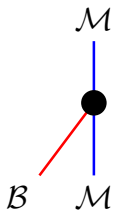

(6.23)

Mathematically, (6.23) dictates how the algebra $\mathcal{B}$ can act on the module $\mathcal{M}$. Physically, $\mathcal{M}$ should be viewed as a candidate line after gauging $\mathcal{B}$. Since $\mathcal{B}$ has become the identity in the gauged theory, it must admit a trivial fusion channel with $\mathcal{M}$.

Furthermore, for a $\mathcal{B}$-module $\mathcal{M}$ to be physically interpreted as a line in the theory after condensation, we require it to be *local*. That is, to satisfy the condition

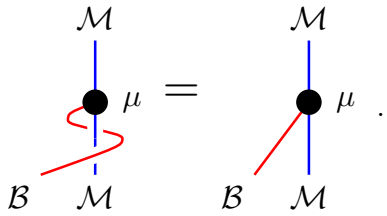

(6.24)

encapsulating the fact that a well-defined line in the theory after condensation must braid trivially with the algebra $\mathcal{B}$ since the latter is now transparent.

Notice in particular the similarity of the diagrams in (6.22) and (6.24), where the putative symmetry b is interpreted as the module $\mathcal{M}$, and $a_{\mathbf{R}}$ a part of the algebra $\mathcal{B}$ that is condensed. This correspondence will be made precise below.

Extracting Topological Lines

Finally, we can now state a sharp proposal to use the mesoscopic model and anyon condensation to identify the lines which remain topological across a Higgsing transition. We proceed as follows:

- Identify a line $b \in G_k$ which braids trivially with the IR matter field line $a_{\mathbf{R}} \in G_k$ as

in (6.22).

- Present the Higgs phase of the Chern-Simons matter theory, i.e. $H_{\tilde{k}}$, via anyon condensation from the product $G_k \times \overline{\frac{G_k}{H_{\tilde{k}}}}$ as in (6.13). Since $a_{\mathbf{R}}$ becomes dynamical, the condensing algebra $\mathcal{B}$ must contain as an element $(a_{\mathbf{R}}, \rho)$ for some ρ in the coset TQFT. This makes precise the discussion below (6.24): only by pairing $a_{\mathbf{R}}$ with coset degrees of freedom can it become bosonic and condense.

- Embed the line b into $G_k \times \overline{\frac{G_k}{H_{\tilde{k}}}}$ by assigning it trivial coset degrees of freedom. In other words, identify $b \in G_k$ with $(b, \mathbf{1}) \in G_k \times \overline{\frac{G_k}{H_{\tilde{k}}}}$.

- Check if b remains a well-defined topological line after condensation so that it can be defined in the Higgsed phase $H_{\tilde{k}}$. Specifically, we examine the fusion:

$$\mathcal{B} \times (b, \mathbf{1}) = (b, \mathbf{1}) + (a_{\mathbf{R}} \times b, \bar{\rho}) + \cdots \ , \tag{6.25}$$

  where above we have extracted several lines known to appear above, but in general there are others in the ellipses. Observe:

  - A necessary condition for $(b, \mathbf{1})$ to survive as a line in $H_{\tilde{k}}$ is that each simple line above that is not projected out by the module map $\tilde{\mu}$ of (6.23) has the same topological spin.
  - A sufficient condition for the above is that all elements on the right-hand side of (6.25) have the same topological spin, neglecting the module map projection. In particular, when this is satisfied the details of the module map are immaterial. (This is the case in our examples below.)

The consistent spin condition discussed above has a simple graphical interpretation. We consider the junction made by b as it crosses the phase boundary from G_k to $H_{\tilde{k}}$. If the line

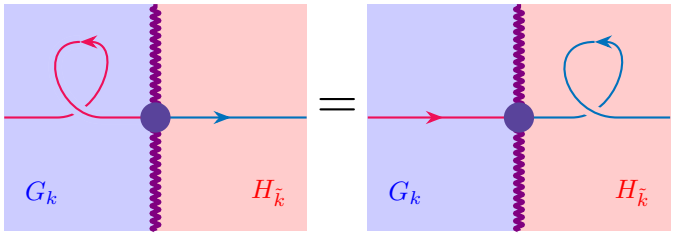

Figure 6.4: A topological line crossing the domain wall network. If the junction is topological it has vanishing spin and hence the topological spins of the G_k and $H_{\tilde{k}}$ lines match.

b is to be topological in both phases of the theory then the junction itself must be topological and hence in particular carry no spin. See Figure 6.4.

The result of the algorithm above are lines that are topological for all values of the parameters L and W in the mesoscopic model. For instance, working in the Hamiltonian model we can see that any line b identified above commutes with the interaction term (6.12). This is because even if b appears to be linked with the χ line in (6.12), it can traverse the coset cylinder without altering the correlation functions, thereby becoming effectively unlinked.

Assuming our basic hypothesis that the mesoscopic model transition is in the same universality class as the Higgsing transition, we are naturally led to conjecture that any such b is topological throughout the Higgsing transition and in particular also at the Chern-Simons matter fixed point. Below we will present a variety of examples of non-trivial one-form symmetries identified in this manner and show that such symmetries can in general be non-abelian.

We emphasize that the argument presented in this section does not suggest that the microscopic G_k Chern-Simons matter theory defined by the short-distance langrangian inherently realizes the one-form symmetry b. Instead, this symmetry is emergent, i.e. present only at the fixed point. Indeed, as remarked below (6.12) modeling the weakly-coupled gauge theory requires the inclusion of $H_{\tilde{k}}$ lines at the center of the cylinders, which generally breaks the non-invertible one-form symmetry.

Inverse Higgsing

Before turning to a discussion of concrete examples, we note that our proposal in fact has a symmetry between the $H_{\tilde{k}}$ and G_k. Indeed, consider a topological line in ψ in $H_{\tilde{k}}$. To test if it remains topological when we transition to the G_k phase, we present the latter TQFT via anyon condensation as:

$$G_k = \frac{H_{\tilde{k}} \times \frac{G_k}{H_{\tilde{k}}}}{\mathcal{A}} \ , \tag{6.26}$$

where as usual $\frac{G_k}{H_{\tilde{k}}}$ is the (2+1)d coset TQFT and $\mathcal{A}$ is a suitable algebra object inducing non-abelian anyon condensation. We embed the line ψ as $(\psi, \mathbf{1}) \in H_{\tilde{k}} \times \frac{G_k}{H_{\tilde{k}}}$, and then run the algorithm above to test whether $(\psi, \mathbf{1})$ remains topological across the phase boundary to G_k. Happily in all our examples below we find perfect agreement between the symmetry algebras identified in this manner starting from either G_k or $H_{\tilde{k}}$.

6.2.5 Higgsing Transitions in Abelian Theories

As a warmup example illustrating some of the ideas above let us consider the Higgsing transition in abelian gauge theory $U(1)_k$ driven by a complex scalar field of charge q, ϕ_q. The flow diagram is then given by:

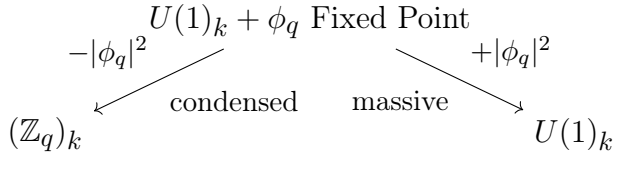

(6.27)

Above, we note that the scalar condensate of charge q Higgses the gauge group $U(1)$ to its $\mathbb{Z}_q$ subgroup that stabilizes the vacuum expectation value (since it does not act on ϕ_q.) Moreover, by the notation $(\mathbb{Z}_q)_k$ we mean the discrete $\mathbb{Z}_q$ gauge theory with a Dijkgraaf-Witten term [33,233] interaction at level k. In practice this system can be efficiently realized

as a $U(1) \times U(1)$ Chern-Simons theory with the level matrix, M, and action:

$$M = \begin{pmatrix} k & q \\ q & 0 \end{pmatrix} \Longrightarrow S = \frac{iq}{2\pi} \int A \wedge dB + \frac{ik}{4\pi} \int A \wedge dA \ . \tag{6.28}$$

In the absence of the term proportional to k above, (6.28) is the standard presentation of a $\mathbb{Z}_q$ gauge theory. The level k term provides the Dijkgraaf-Witten twist. We note that the theory $(\mathbb{Z}_q)_k$ depends periodically on the level k with period $2q$:

$$(\mathbb{Z}_q)_{\ell+2mq} \cong (\mathbb{Z}_q)_\ell \ . \tag{6.29}$$

Below, we take k to be even for simplicity which implies that the theory above is bosonic. Finally, we also recall the spectrum of lines in $(\mathbb{Z}_q)_k$. These may be viewed as Wilson lines of the two gauge fields above with spin h given by:

$$\exp\left(ix \oint A + iy \oint B \right) \ , \quad h = \frac{xy}{q} - \frac{ky^2}{2q^2} \ . \tag{6.30}$$

Here x, y are integers characterizing the charges of the line. They are subject to identifications dictated by the level matrix:

$$(x, y) \sim (x + q, y) \ , \quad (x, y) \sim (x + k, y + q). \tag{6.31}$$

Thus in general, there are q^2 lines. Moreover, we can use the identifications above to determine that the fusion ring formed by the lines is:[7]

$$\mathbb{Z}_{\gcd(k,q)} \times \mathbb{Z}_{q^2/\gcd(k,q)} \ . \tag{6.33}$$

Transitions Without Symmetry: $\gcd(k, q) = 1$

Take k and q coprime with $q < k$. The Chern-Simons level k in the $U(1)_k$ gauge theory truncates the abelian one-form symmetry to $\mathbb{Z}_k$. The charged matter field ϕ_q is described by the anyon of charge q, and hence is a generator of $\mathbb{Z}_k$. In particular, all other non-identity lines braid non-trivially with this anyon. Therefore in the semiclassical analysis of (6.22) there is no candidate symmetry line.

Let us recover this conclusion from the Higgsed phase via coupling to the coset degrees of freedom. We claim that in this case, the coset TQFT is simply:

$$\frac{U(1)_k}{(\mathbb{Z}_q)_k} \cong U(1)_k \times \overline{(\mathbb{Z}_q)_k} \cong U(1)_k \times (\mathbb{Z}_q)_{-k} \ . \tag{6.34}$$

Note per the discussion below (6.13), we expect the coset TQFT to be a product of numerator and denominator (with opposite level) modulo an algebra of condensable common bosons. Thus in (6.34) we are asserting that this algebra of condensable common bosons is trivial. To see this, observe from (6.33) that the total fusion ring in right-hand side of (6.34) is

$$\mathbb{Z}_k \times \mathbb{Z}_{q^2} \ , \tag{6.35}$$

and since k and q are coprime, there is no possible common subgroup in (6.34) to condense.

7. This can be computed for instance, by noting that the Smith normal form of the level matrix M in (6.28) is:

$$\mathrm{SNF}(M) = \begin{pmatrix} \gcd(k,q) & 0 \\ 0 & q^2/\gcd(k,q) \end{pmatrix} \ . \tag{6.32}$$

Physically, since the coset TQFT (6.34) is factorized, we expect its edge modes to also decouple into a chiral boson, the edge of $U(1)_k$, and a gapped sector, the edge of $(\mathbb{Z}_q)_{-k}$.

Now we apply (6.13) to present the Higgsed phase from anyon condensation in the massive phase:

$$\begin{aligned}(\mathbb{Z}_q)_k &\cong \frac{U(1)_k \times \overline{\left(\frac{U(1)_k}{(\mathbb{Z}_q)_k}\right)}}{\mathcal{B}} , \\ &\cong \frac{U(1)_k \times \left(U(1)_{-k} \times (\mathbb{Z}_q)_k\right)}{\mathcal{B}} ,\end{aligned} \tag{6.36}$$

where above, $\mathcal{B}$ is a suitable algebra. However, since all the theories above are abelian $\mathcal{B}$ is simply the sum over elements of a subfusion ring each of which is bosonic. Lines in the numerator of (6.36) can be labeled by quartets (ℓ_1, ℓ_2, x, y) where $\ell_i = 0, \cdots k-1$ indicates a charge in $U(1)_k$ and (x, y) label the Wilson lines in $(\mathbb{Z}_q)_k$ as in (6.30). Adopting this notation it is straightforward to see that:

$$\mathcal{B} = (0,0,0,0) + (1,1,0,0) + \cdots + (k-1, k-1, 0, 0) . \tag{6.37}$$

In particular, we see from this two expected features:

- The condensation includes the anyon corresponding to the scalar field (the term $(q, q, 0, 0)$ above.)

- There are no preserved topological lines in the Higgsed phase. For instance we can apply the uniform spin criterion discussed in (6.25). A candidate line in $\ell \in U(1)_k$ is embedded in the numerator of the right-hand side of (6.36) as $(\ell, 0, 0, 0)$. Fusing with the algebra $\mathcal{B}$ gives:

$$\mathcal{B} \times (\ell, 0, 0, 0) = \sum_{j=0}^{k-1} (\ell + j, j, 0, 0) . \tag{6.38}$$

  We now compare the spin of the left-hand side to the spin of a simple anyon on the

right-hand side. Equality requires for all j:

$$\frac{\ell^2}{2k} = \frac{(\ell+j)^2}{2k} - \frac{j^2}{2k} \mod 1 \ . \tag{6.39}$$

This is clearly false so the symmetry is broken in the Higgsed phase as expected.

Transitions With Symmetry: $k = nq$

Next we consider a Higgsing transition where we expect preserved one-form symmetry. We take $k = nq$ for n a positive integer. In this case the $\mathbb{Z}_k$ one-form symmetry of the Chern-Simons theory $U(1)_k$ should be broken down to the non-trivial subgroup $\mathbb{Z}_q \subseteq \mathbb{Z}_k$.

First, in the non-relativistic approximation of (6.22), we recall that the braiding of lines in $U(1)_k$ with charges ℓ_1, ℓ_2 is:

$$S_{\ell_1,\ell_2} = \exp\left(\frac{2\pi i \ell_1 \ell_2}{k}\right) \ . \tag{6.40}$$

Setting $\ell_1 = q$, corresponding to the charged matter field, and $k = nq$, we see that the above is trivial precisely when ℓ_2 is a multiple of n. These lines generate the expected $\mathbb{Z}_q$ one-from symmetry group.

Now we recover this from the Higgsed phase. In this case, we claim that the coset TQFT is:

$$\frac{U(1)_{nq}}{(\mathbb{Z}_q)_{nq}} \cong U(1)_{nq} \cong U(1)_k \ . \tag{6.41}$$

In other words, the relevant edge modes are simply a chiral boson. To derive this, we first note that in general we expect that the coset TQFT should arise from condensing the maximal common fusion subalgebra of the product Chern-Simons theory. In this case, this results in:

$$\frac{U(1)_{nq}}{(\mathbb{Z}_q)_{nq}} \cong \frac{U(1)_{nq} \times \overline{(\mathbb{Z}_q)_{nq}}}{\mathcal{C}} \ , \tag{6.42}$$

where $\mathcal{C}$ is the abelian algebra corresponding the the $\mathbb{Z}_q$ common fusion algebra above. Hence, equating (6.42) and (6.41) implies the relation:

$$\frac{U(1)_{nq} \times \overline{(\mathbb{Z}_q)_{nq}}}{\mathbb{Z}_q} \cong U(1)_{nq} \ . \tag{6.43}$$

This equivalence was derived in [9] (See Appendix I).[8]

Using the result (6.43), we now proceed to the Higgsed phase of our gauge theory. From the general presentation (6.13) we express:

$$\begin{aligned} (\mathbb{Z}_q)_{qn} &\cong \frac{U(1)_{qn} \times \overline{\left(\frac{U(1)_{qn}}{(\mathbb{Z}_q)_{qn}}\right)}}{\mathcal{B}} \ , \\ &\cong \frac{U(1)_{qn} \times U(1)_{-qn}}{\mathcal{B}} \ , \end{aligned} \tag{6.44}$$

where the appropriate algebra $\mathcal{B}$ is the common $\mathbb{Z}_n$ subgroup above:

$$\mathcal{B} = (0,0) + (q,q) + (2q,2q) + \cdots + ((n-1)q,(n-1)q) \ . \tag{6.45}$$

Notice in particular the condensing algebra $\mathcal{B}$ contains the anyon corresponding to the scalar field in the term (q,q) above.

To verify (6.44) we directly carry out the abelian anyon condensation. The first step in this procedure is to determine which lines are not confined by the condensate $\mathcal{B}$. These are all lines that braid trivially with the generator of $\mathcal{B}$ i.e. (q,q). The braiding of a general line (ℓ_1,ℓ_2) with the condensing anyon (q,q) is trivial if and only if:

$$\frac{\ell_1 q}{nq} - \frac{\ell_2 q}{nq} = 0 \mod 1 \Longrightarrow \ell_1 = \ell_2 \mod n \ . \tag{6.46}$$

8. This equivalence can be directly verified using the abelian anyon condensation techniques illustrated in the examples below.

Thus, after condensation we must restrict the anyons obeying this condition. Next, on this deconfined set, we must identify anyons which differ by fusion with the generator (q, q). Hence:

$$(\ell_1, \ell_2) \sim (\ell_1 + q, \ell_2 + q) \ . \tag{6.47}$$

The solution to the (6.46) modulo the identification imposed by (6.47) leaves precisely q^2 lines which we may parameterize by equivalence classes represented by:

$$(r + sn, r) \ , \quad r, s = 0, \cdots, q-1 \ . \tag{6.48}$$

This completes the condensation procedure.[9] Notice that we have indeed found the correct number of lines to compare to $(\mathbb{Z}_q)_{qn}$. For instance by changing basis, we can verify the spins as follows.

n even: In this case the level periodicity (6.29) implies $(\mathbb{Z}_q)_{qn} \cong (\mathbb{Z}_q)_0$. We express the equivalence classes (6.48) in term of $x, y = 0, 1, \cdots q-1$ as:

$$(r + sn, r) = \left(x + \frac{n}{2}y, x - \frac{n}{2}y\right) \ , \tag{6.49}$$

whose spin is:

$$h = \frac{\left(x + \frac{n}{2}y\right)^2}{2qn} - \frac{\left(x - \frac{n}{2}y\right)^2}{2qn} = \frac{xy}{q} \ , \tag{6.50}$$

exactly matching (6.30).

n odd: Now, (6.29) implies $(\mathbb{Z}_q)_{qn} \cong (\mathbb{Z}_q)_q$. We express the equivalence classes (6.48) in term of $x, y = 0, 1, \cdots q-1$ as:

$$(r + sn, r) = \left(x + \left(\frac{n-1}{2}\right)y, x - \left(\frac{n+1}{2}\right)y\right) \ , \tag{6.51}$$

9. In general, anyon condensation requires a further step, where lines that are fixed under the fusion (6.47) split into distinct species in the theory after condensation [2, 34]. We do not encounter this here but it frequently occurs in more general examples.

whose spins are now:

$$h = \frac{\left(x + \left(\frac{n-1}{2}\right) y\right)^2}{2qn} - \frac{\left(x - \left(\frac{n+1}{2}\right) y\right)^2}{2qn} = \frac{xy}{q} - \frac{y^2}{2q} \ , \tag{6.52}$$

again matching (6.30).

Finally, using the condensation presentation of the Higgsed phase in (6.44), we can see which lines remain topological across the Higgsing transition. These are the lines of the form $(\ell, 0)$ which survive the condensation procedure. Matching with the equivalence classes (6.48) one sees that the charge ℓ is restricted to vanish modulo n (i.e. the variable r must be zero). These anyons generate the expected $\mathbb{Z}_q$ preserved one-form symmetry.

General $\gcd(k, q)$

Let us briefly comment on the more general case when $\gcd(k, q) \neq 1$. The analysis is similar to the example above and we omit derivations.

In this case, the $\mathbb{Z}_k$ one-form symmetry of the pure Chern-Simons theory is screened down to $\mathbb{Z}_{\gcd(k,q)}$ by the dynamical scalar matter. The relevant coset TQFT is now

$$\frac{U(1)_k}{(\mathbb{Z}_q)_k} \cong \frac{U(1)_k \times \overline{(\mathbb{Z}_q)_k}}{\mathbb{Z}_{\gcd(k,q)}} \ . \tag{6.53}$$

Using the above, the presentation of the Higgsed phase via abelian anyon condensation as in (6.13) is:

$$(\mathbb{Z}_q)_k \cong \left[U(1)_k \times \overline{\left(\frac{U(1)_k \times \overline{(\mathbb{Z}_q)_k}}{\mathbb{Z}_{\gcd(k,q)}}\right)}\right] / \mathbb{Z}_{\frac{k}{\gcd(k,q)}} \ . \tag{6.54}$$

In particular, the condensing algebra in the above includes the dynamical charge q matter field in the $U(1)_k$ factor, i.e. $(q, \bar{\ell})$ for some line ℓ in the coset (6.53). Following our algorithm described in Section 6.2.4 then reproduces the expected $\mathbb{Z}_{\gcd(k,q)}$ one-form symmetry.

For completeness, we also note that in this case the analog of (6.26) is

$$U(1)_k \cong \left[(\mathbb{Z}_q)_k \times \left(\frac{U(1)_k \times \overline{(\mathbb{Z}_q)_k}}{\mathbb{Z}_{\gcd(k,q)}}\right)\right]/\mathbb{Z}_{\frac{q^2}{\gcd(k,q)}} \ , \tag{6.55}$$

which can be used to reach the same conclusions about the one-form symmetry of this transition.

6.2.6 Anomalies from Fusion Rules

Here we collect some facts about non-invertible one-form symmetries and their anomalies. As mentioned previously, abstractly a finite one-form non-invertible symmetry in a (2+1)d system is described by topological line operators that form a braided fusion category $\mathcal{C}$. Specifically, it is a fusion category equipped with a braiding isomorphism $\sigma_{a,b}$ that maps $a \times b$ to $b \times a$ for each pair of objects (a, b) in $\mathcal{C}$.

The Hopf link, composed of two simple lines (a, b), defines the braiding S-matrix S_{ab}. When S_{ab} is full-rank, the braided fusion category is called modular. When it is rank-one, or equivalently $\sigma_{ba} = \sigma_{ab}^{-1}$, the category is called symmetric. In a Hopf link, the two lines do not intersect with each other and can remain far apart. Hence, the S-matrix of the topological lines must match along any renormalization group flow. In particular this means that a non-trivial Hopf link of topological lines implies that the vacuum state has long-range entanglement. In other words, an S-matrix with a rank greater than one indicates a non-trivial anomaly, implying that the symmetry $\mathcal{C}$ cannot consistently act on the trivial theory.

When the symmetry is non-anomalous, i.e. the braiding is symmetric, the symmetry category $\mathcal{C}$ in a bosonic system must be equivalent to the representation category $\mathrm{Rep}(K)$ for some finite group K [227].[10] See also [228]. Conversely, if the one-form symmetry $\mathcal{C}$ has

10. For a fermionic theory, the theorem still holds with the group K replaced by a "supergroup", which in this context means a finite group K with an order two element identified as $(-1)^F$, the fermion parity.

fusion rules that cannot be realized as $\mathrm{Rep}(K)$ for any finite group K, then we can conclude that the symmetry $\mathcal{C}$ is necessarily anomalous. This contrasts with the case of an abelian $\mathcal{C}$ (or an invertible symmetry), where the same fusion rule can admit both anomalous and non-anomalous braidings.

Relatedly, let us consider the case where the braided fusion category $\mathcal{C}$ contains a modular subcategory $\mathcal{D}$. Then the full category decomposes into a product [223–225]:

$$\mathcal{C} \cong \mathcal{D} \times \mathcal{D}' \ . \tag{6.56}$$

(The case with abelian $\mathcal{D}$ and modular $\mathcal{C}$ was discussed in [34] from a physical perspective.) Here, $\mathcal{D}'$ is the Müger centralizer of $\mathcal{D}$ in $\mathcal{C}$. In particular, when the system is a TQFT acted on by the symmetry $\mathcal{C}$, a modular subcategory $\mathcal{D}$ indicates that the TQFT contains $\mathcal{D}$ as a decoupled factor. It is natural to expect that this decoupling continues to hold in a non-topological theory with a modular symmetry $\mathcal{D}$.

6.3 Non-Abelian Higgsing & Symmetry

We now turn to examples of Chern-Simons matter theories that conjecturally have non-invertible one-form symmetry. We use the algorithm presented around (6.25) to check these proposals.[11]

6.3.1 Unitary Family: $PSU(2)_{-k}$ Symmetry

Our first model is an $SU(k)$ gauge theory with matter in the symmetric rank two tensor representation.

$$SU(k)_2 + \phi_{\square\square} = SU(k)_2 + \phi_{2\mathbf{w}_1} \ , \tag{6.57}$$

11. The spectrum and fusion rules of the MTCs used in this section can be obtained from the KAC software program [111].

where above, $\mathbf{w}_1$ indicates the weight labeling the fundamental representation of $SU(k)$.

Our basic claim is that this model has topological symmetry lines $PSU(2)_{-k}$. Here, $PSU(2)_k$ means the subset of lines in the Chern-Simons theory $SU(2)_k$ which are neutral under the $\mathbb{Z}_2$ center symmetry. More specifically, the $SU(2)_k$ fusion ring consists of $k+1$ simple lines labeled from 0 to k, with fusion rules

$$j_1 \times j_2 = \sum_{j=|j_1-j_2|}^{\min(j_1+j_2,2k-j_1-j_2)} j \ , \tag{6.58}$$

where $j, j_1, j_2 = 0, 1, \ldots, k$, and the sum is restricted such that $j_1 + j_2 - j$ is even. The topological spins are given by $\theta_j = \exp\left(2\pi i \frac{j(j+2)}{4(k+2)}\right)$. The fusion ring $PSU(2)_k$ is defined as the closed subfusion ring corresponding to lines of even j above. The preserved symmetry $PSU(2)_{-k}$ has spins which are complex conjugates of these. We note that for k odd, $PSU(2)_{-k}$ is a well-defined fully modular-invariant TQFT on its own. Meanwhile, for k even, this symmetry is not modular.

The Chern-Simons matter theory (6.57), has a Higgsing transition given by the following flow diagram:

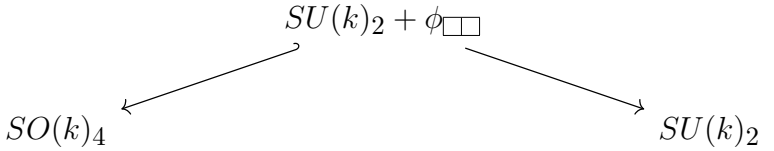

. (6.59)

Here, the Higgsing pattern is achieved by $\phi_{\square\square}$ acquiring an expectation value which is a maximal rank diagonal matrix, and $SO(k) \subset SU(k)$ is the stabilizer subgroup.

To investigate the symmetries, we will make use of the coset:

$$\frac{SU(k)_2}{SO(k)_4} \ , \quad c = \frac{2(k-1)}{k+2} \ , \tag{6.60}$$

where above we have also indicated the chiral central charge c of the (1+1)d edge modes.

This coset is a maverick theory. As reviewed above, this means that when we want to describe the (1+1)d theory using a bulk Chern-Simons theory, we must gauge non-abelian anyons. Let us denote these non-abelian anyons by $\mathcal{C}$. Then, according to [3] we have the following duality of Chern-Simons theories:

$$\frac{SU(k)_2 \times SO(k)_{-4}}{\mathcal{C}} \cong \frac{SU(2)_k \times U(1)_{-2k}}{\mathbb{Z}_2} \equiv \mathrm{PF}_k \ . \tag{6.61}$$

Here PF_k stands for the (2+1)d parafermion TQFT at level k described by the Chern-Simons theories above. Their edge modes are the (1+1)d parafermion coset CFT $SU(2)_k/U(1)$.

When applying our model of the Higgsing transition, we will encounter the following relations between (2+1)d TQFTs (compare with (6.13) and (6.26) above):

$$SO(k)_4 \cong \frac{SU(k)_2 \times \overline{\mathrm{PF}}_k}{\mathbb{Z}_k} \ , \tag{6.62}$$

as well as:

$$SU(k)_2 = \frac{SO(k)_4 \times \mathrm{PF}_k}{\mathcal{A}} \ , \tag{6.63}$$

where $\mathcal{A}$ is a suitable non-abelian algebra specified below.

$k = 3$ and the Three States Potts Model

We begin with the simplest non-trivial case $k = 3$. The flow diagram is:

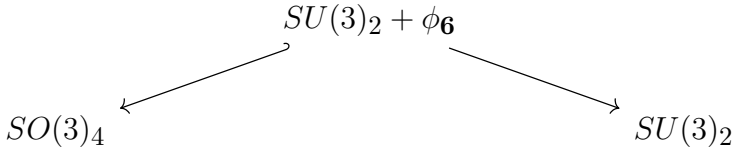

. (6.64)

The data for the $SU(3)_2$ and $SO(3)_4$ Chern-Simons theories are presented in Table 3.9 and Table 3.11 respectively. The coset $SU(3)_2/SO(3)_4$ is known to be the Three State Potts

$SU(3)_2$		
Line label	Quantum Dimension	Conformal Weight
$\mathbf{1}$	$d_{\mathbf{1}} = 1$	$h_{\mathbf{1}} = 0$
$\mathbf{3}$	$d_{\mathbf{3}} = \frac{1+\sqrt{5}}{2}$	$h_{\mathbf{3}} = 4/15$
$\bar{\mathbf{3}}$	$d_{\bar{\mathbf{3}}} = \frac{1+\sqrt{5}}{2}$	$h_{\bar{\mathbf{3}}} = 4/15$
$\mathbf{8}$	$d_{\mathbf{8}} = \frac{1+\sqrt{5}}{2}$	$h_{\mathbf{8}} = 3/5$
$\mathbf{6}$	$d_{\mathbf{6}} = 1$	$h_{\mathbf{6}} = 2/3$
$\bar{\mathbf{6}}$	$d_{\bar{\mathbf{6}}} = 1$	$h_{\bar{\mathbf{6}}} = 2/3$

Table 6.1: $SU(3)_2$ data. The fusion rules of $SU(3)_2$ are those of Fibonacci $\times \mathbb{Z}_3$, with $\mathbf{8}$ the generator of Fibonacci, and the non-trivial elements of the $\mathbb{Z}_3$ factor are $\mathbf{6}$ and $\bar{\mathbf{6}}$.

Model (TSPM) [36], which we present in Table 6.3:

$$\frac{SU(3)_2 \times SO(3)_{-4}}{\mathcal{C}} \cong \frac{SU(2)_3 \times U(1)_{-6}}{\mathbb{Z}_3} \equiv \mathrm{PF}_3 \cong \mathrm{TSPM} \ . \tag{6.65}$$

The explicit anyon condensation relations we must consider are:

$$SO(3)_4 \cong \frac{SU(3)_2 \times \overline{\mathrm{TSPM}}}{\mathbb{Z}_3} \ , \tag{6.66}$$

and

$$SU(3)_2 = \frac{SO(3)_4 \times \mathrm{TSPM}}{\mathcal{A}_3} \ . \tag{6.67}$$

We aim to argue that the fixed point theory has $PSU(2)_{-3}$ symmetry. Note that this symmetry has a unique non-invertible line W (corresponding to the $\mathbf{2}$ of $SU(2)$) with Fibonacci fusion rule:

$$W \times W = \mathbf{1} + W \ . \tag{6.68}$$

As a first check to see the lines preserved along the flow, we employ the non-relativistic analysis and calculate monodromies in $SU(3)_2$ and it is straightforward to check that only $\mathbf{8}$ is preserved by $\mathbf{6}$. Note also that $\mathbf{8}$ has Fibonacci fusion rules.

Next we provide a more detailed check of this symmetry using cosets and anyon conden-

sation. The denominator of (6.66) is abelian, generated by the anyon:

$$\mathcal{B}_3 = (\mathbf{1},\mathbf{1}) + (\mathbf{6},\overline{Z_1}) + (\bar{\mathbf{6}},\overline{Z_2}) \ , \tag{6.69}$$

so we only have to extract the lines that have vanishing charge under the $\mathbb{Z}_3$ in $SU(3)_2$. This is precisely the $\mathbf{8}$ of $SU(3)_2$. Notice that as discussed in Section 6.2.4, the condensation includes the anyon corresponding to the scalar field triggering the Higgsing transition. In this example this is the $\mathbf{6}$.

Next we analyze the condensation (6.67). In this case there are two non-trivial bosons $(4_1,\varepsilon)$, $(4_2,\varepsilon) \in SO(3)_4 \times \text{TSPM}$. To saturate quantum dimension formula (6.21) we must choose only one of them. The choice is immaterial, however, since 4_1 and 4_2 are symmetric in $SO(3)_4$. We choose:

$$\mathcal{A}_3 = (0,\mathbf{1}) + (4_1,\varepsilon) \ . \tag{6.70}$$

We compute the fusions:

$$\begin{aligned}
\mathcal{A}_3 \times (0,\mathbf{1}) &= (0,\mathbf{1}) + (4_1,\varepsilon) \ , \\
\mathcal{A}_3 \times (2,\mathbf{1}) &= (2,\mathbf{1}) + (4_2,\varepsilon) + (2,\varepsilon) \ , \\
\mathcal{A}_3 \times (4_1,\mathbf{1}) &= (4_1,\mathbf{1}) + (0,\varepsilon) + (4_1,\varepsilon) \ , \\
\mathcal{A}_3 \times (4_2,\mathbf{1}) &= (4_2,\mathbf{1}) + (2,\varepsilon) \ .
\end{aligned} \tag{6.71}$$

$SO(3)_4$		
Line label	Quantum Dimension	Conformal Weight
0	$d_0 = 1$	$h_0 = 0$
2	$d_2 = (3+\sqrt{5})/2$	$h_2 = 1/5$
4_1	$d_{4_1} = (1+\sqrt{5})/2$	$h_{4_1} = 3/5$
4_2	$d_{4_2} = (1+\sqrt{5})/2$	$h_{4_2} = 3/5$

Table 6.2: $SO(3)_4$ data. The fusion rules of $SO(3)_4$ are those of two copies of Fibonacci, with the Fibonacci generators being 4_1 and 4_2, and $2 = 4_1 \times 4_2$.

Three-State Potts Model		
Line label	Quantum Dimension	Conformal Weight
$\mathbf{1}$	$d_{\mathbf{1}} = 1$	$h_{\mathbf{1}} = 0$
σ_1	$d_{\sigma_1} = \frac{1+\sqrt{5}}{2}$	$h_{\sigma_1} = 1/15$
σ_2	$d_{\sigma_2} = \frac{1+\sqrt{5}}{2}$	$h_{\sigma_2} = 1/15$
ε	$d_{\varepsilon} = \frac{1+\sqrt{5}}{2}$	$h_{\varepsilon} = 2/5$
Z_1	$d_{Z_1} = 1$	$h_{Z_1} = 2/3$
Z_2	$d_{Z_2} = 1$	$h_{Z_2} = 2/3$

Table 6.3: Three-State Potts Model data. The fusion rules of the TSPM are those of Fibonacci $\times$ $\mathbb{Z}_3$, with ε the generator of Fibonacci, and the non-trivial elements of the $\mathbb{Z}_3$ factor are Z_1 and Z_2.

We observe that the only non-trivial line which satisfies the uniform spin condition discussed in (6.25) is 4_2. This again reproduces the Fibonacci symmetry identified form the massive RG flow.

General k

We now consider the case of general k in (6.59). The analysis is similar and our presentation is brief. The rank 2 symmetric tensor is a generator of the $\mathbb{Z}_k$ center symmetry of $SU(k)_2$.[12] Therefore, in the non-relativistic approximation of (6.22), the candidate lines which are preserved are precisely the lines in $SU(k)_2$ which are neutral under the full $\mathbb{Z}_k$ one-form symmetry. Utilize the level rank duality:

$$SU(k)_2 = \frac{SU(2k)_1 \times SU(2)_{-k}}{\mathbb{Z}_2} \ . \tag{6.72}$$

Upon projecting to the subfusion ring above which is neutral under the $\mathbb{Z}_k$ center of the left-hand side, the right hand side simplifies to $PSU(2)_{-k}$, our claimed general symmetry.

12. To see this, notice that the center of $SU(N)_k$ is isomorphic to the corresponding $\mathbb{Z}_N$ outer automorphism of the affine Dynkin diagram shifting all fundamental weights by the adjacent one. Since the identity, labeled by the extended Dynkin labels $[0, 0, 0, \ldots, 0, k]$, must be in the center, it follows that the elements of the center one-form symmetry are always labeled by extended Dynkin labels with a unique non-zero entry with value k: $[0, 0, \cdots, 0, k, 0, \cdots, 0]$.

Moreover, since the coset (6.62) involves abelian anyon condensation, it simply reproduces this condition.

Now we check this result using the condensation presentation of $SU(k)_2$ as in (6.63). For odd k the full algebra in $SO(k)_4 \times \mathrm{PF}_k$ is given by

$$\mathcal{A}_k = (0,0) + \big((4\mathbf{w}_\sigma)_1, (k-1,0)\big) + \sum_{i=1}^{(k-3)/2} \big((2\mathbf{w}_i)_1, (2i,0)\big) \ . \tag{6.73}$$

In the above, w_σ is the weight of the unique spinor representation, w_i are the non-spinor weights and both are split into two lines (indicated by the subscript) in $SO(k)_4$, and $(2i,0) \in \mathrm{PF}_k = \frac{SU(2)_k \times U(1)_{-2k}}{\mathbb{Z}_k}$ stands for the line with Dynkin label $2i$ in $SU(2)_k$ and trivial charge in the $U(1)$ factor.

The preserved symmetry algebra can now be obtained by finding those lines in $SO(k)_4$ whose decomposition under fusion with $\mathcal{A}_k$ contains only terms of uniform spin as discussed around (6.25). One checks that these lines are precisely[13]:

$$\{0, \quad (4\mathbf{w}_\sigma)_2, \quad (2\mathbf{w}_i)_2\}, \quad i = 1, \ldots, \frac{(k-3)}{2} \ . \tag{6.74}$$

Happily, these again form the fusion algebra $PSU(2)_{-k}$.

Similarly, for even k, the algebra in $SO(k)_4 \times \mathrm{PF}_k$ is given by

$$\begin{aligned} \mathcal{A}_k = (0,0) &+ \sum_{i=1}^{\frac{k}{2}-2} \big((2\mathbf{w}_i)_1, (2i,0)\big) \\ &+ \big((2\mathbf{w}_s + 2\mathbf{w}_c)_1, (k-2,0)\big) + \big((4\mathbf{w}_s), (k,0)\big) \ , \end{aligned} \tag{6.75}$$

where now w_s and w_c are the weights of the two spinor representations, and $(4\mathbf{w}_s) \cong (4\mathbf{w}_c)$. Again checking the uniform spin condition (6.25) we find that the preserved lines in $SO(k)_4$

13. Essentially, this generalizes the fact that for $k = 3$ the line preserved corresponds to the partner of the line that we use in the Frobenius algebra $\mathcal{A}_3$ in the extension (6.63).

are: :

$$\{0, \quad (4\mathbf{w}_s), \quad (2\mathbf{w}_s + 2\mathbf{w}_c)_2, \quad (2\mathbf{w}_i)_2\} \ , \tag{6.76}$$

where $i = 1, \ldots, \frac{k}{2} - 2$. These again define $PSU(2)_{-k}$.

Consistency Check from Conformal Embeddings

Let us provide a general consistency check on the proposed symmetries. Consider the conformal embedding[14]:

$$SU(k)_2 \times SU(2)_k \hookrightarrow SU(2k)_1 \ . \tag{6.77}$$

This implies the existence of an anyon condensation formula:

$$\frac{SU(k)_2 \times SU(2)_k}{\mathcal{D}_k} \cong SU(2k)_1 \ . \tag{6.78}$$

Here, the algebra object $\mathcal{D}_k$ can be understood as follows. Inside $SU(k)_2$ is the previously identified fusion sub-algebra $PSU(2)_{-k}$. Then, $\mathcal{D}_k$ is defined by diagonal subset of lines inside $PSU(2)_{-k} \times PSU(2)_k$ above.[15] Note that since the paired lines have opposite spin, they are condensable bosons. Moreover, we can check the above using the quantum dimension formula (6.21). (See Section 6.4 for an explicit calculation).

Similarly, we have a conformal embedding[16]:

$$SO(k)_4 \times SU(2)_k \hookrightarrow Sp(2k)_1 \ , \tag{6.79}$$

14. The branching rules for the conformal embedding $SU(n)_m \times SU(m)_n \hookrightarrow SU(nm)_1$ have been studied e.g. in [25, 234, 235].

15. Small k examples of this condensation were presented in [3].

16. The branching rules for this conformal embedding have been studied e.g. in [236].

implying the anyon condensation formula:

$$\frac{SO(k)_4 \times SU(2)_k}{\mathcal{D}_k} \cong Sp(2k)_1 \ . \tag{6.80}$$

Here we have abused notation and written the algebra object above also as $\mathcal{D}_k$. The reason is that the object is again composed of the diagonal anyons inside the $PSU(2)_{-k} \times PSU(2)_k$ sub fusion ring on the left-hand side above. More specifically, for odd k:

$$\mathcal{D}_k = (0,0) + \sum_{i=1}^{(k-3)/2} \big((2\mathbf{w}_i)_2, 2i\big) + \big((4\mathbf{w}_\sigma)_2, k-1\big) \ , \tag{6.81}$$

while for even k :

$$\mathcal{D}_k = (0,0) + \sum_{i=1}^{\frac{k}{2}-2} \big((2\mathbf{w}_i)_2, 2i\big) + \big((2\mathbf{w}_s + 2\mathbf{w}_c)_2, k-2\big) + \big((4\mathbf{w}_s), k\big) \ . \tag{6.82}$$

(Compare to equations (6.63), and (6.73) through (6.76)).

Armed with these results, we now take the entire flow diagram (6.59), tensor it with $SU(2)_k$ and condense the algebra object $\mathcal{D}_k$:

$$\begin{array}{ccc} & \frac{SU(k)_2 \times SU(2)_k}{\mathcal{D}_k} + \phi_{\square\square} & \\ \swarrow & & \searrow \\ \frac{SO(k)_4 \times SU(2)_k}{\mathcal{D}_k} & & \frac{SU(k)_2 \times SU(2)_k}{\mathcal{D}_k} \end{array} \ . \tag{6.83}$$

Finally we use the fact that across the duality (6.78) the generators of the $\mathbb{Z}_k$ abelian one-form symmetry must match. Therefore, across the duality the symmetric rank two tensor of $SU(k)_2$ maps to the antisymmetric rank two tensor of $SU(2k)_1$. (See footnote 12.) Hence it

is natural to conjecture that the flow generated by the symmetric rank two tensor of $SU(k)$ maps after gauging to the flow generated by the antisymmetric rank two tensor of $SU(2k)$. Assuming this, and simplifying (6.83) using the condensation formulas (6.78) and (6.80) gives the flow:

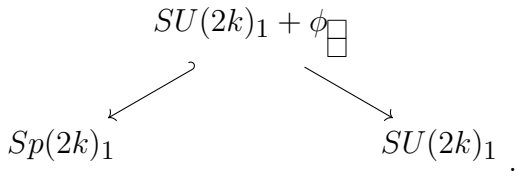

. (6.84)

Strikingly, (6.84) is indeed a consistent Chern-Simons matter flow. The symplectic Higgsing pattern is generated by $\phi_{\square\!\square}$ assuming an expectation value which is a maximal rank antisymmetric tensor (the invariant symbol of $Sp(2k)$).

The fact that we generate consistent RG flows by gauging the conjectured non-invertible symmetry $PSU(2)_{-k}$ in our unitary flows (6.59) provides a strong consistency check on our results.

Interpretation via Symmetry TQFT

The $PSU(2)_{-k}$ symmetry admits a symmetry TQFT description [58, 59]: coupling the $SU(2)_{-k}$ (2+1)d TQFT to a (3+1)d gauge theory with a discrete $\mathbb{Z}_2$ 2-form gauge field B. The bulk (3+1)d TQFT has an exponentiated action

$$\exp\left(\frac{k\pi i}{2}\int_X \mathfrak{P}(B)\right) , \tag{6.85}$$

where X is a four-manifold and $\mathfrak{P}(B)$ is the Pontryagin square:

$$\mathfrak{P}(B) \in H^4(X, \mathbb{Z}_4) . \tag{6.86}$$

The bulk-boundary coupling identifies the $\mathbb{Z}_2$ one-form symmetry line in the $SU(2)_{-k}$ TQFT with the boundary of the Wilson surface of B. We note that all $PSU(2)_{-k}$ lines are confined to the (2+1)d topological boundary, and the bulk theory is invertible when k is odd.

Mathematically, the bulk theory is the Crane-Yetter TQFT [237] for the braided fusion category $PSU(2)_{-k}$, invertible if and only if the category is modular [238].

6.3.2 Spin Family: $PSpin(2N)_2$ Symmetry

Our next class of models are $Spin(2N)$ gauge theories with matter in the symmetric traceless rank two tensor representation.

$$Spin(2N)_2 + \phi_{\square\square} = Spin(2N)_2 + \phi_{2\mathbf{w}_1} \ , \tag{6.87}$$

where above, $\mathbf{w}_1$ indicates the weight labeling the vector representation of $Spin(2N)$. We take the scalars to be real so that the matter content is minimal.

We claim that this Chern-Simons matter fixed point preserves a $PSpin(2N)_2$ fusion algebra. Here, by $PSpin(2N)_2$, we mean the sub-fusion algebra of $Spin(2N)_2$ which is uncharged under the center of $Spin(2N)$. (Recall that for N even, the center of $Spin(2N)$ is $\mathbb{Z}_2 \times \mathbb{Z}_2$ while for N odd, the center is $\mathbb{Z}_4$.) For small N, $PSpin(2N)_2$ coincides, as a fusion ring but not as a braided fusion ring, with the representation ring of the Dihedral group D_N.[17] For instance:

$$PSpin(2N)_2 = \mathrm{Rep}(D_N) \ , \quad N = 3, 4, 5, 6, 7 \ , \tag{6.88}$$

However, for general N, we are unaware of any elementary formula for this fusion ring.[18]

The Higgsing transition of this Chern-Simons matter theory is described by the following

17. In our conventions, D_N is the dihedral group with $2N$ elements.

18. The pattern listed in (6.88) breaks e.g. at $N = 9$ where as a fusion ring $PSpin(18)_2 \cong \mathrm{Rep}(\mathbb{Z}_3 \rtimes D_3)$.

flow diagram:

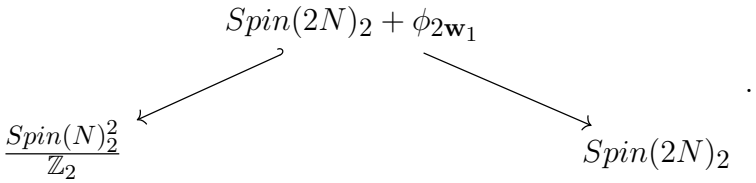

Here, the condensed phase is achieved when $\phi_{\square\square}$ acquires an expectation value which is a maximal rank traceless symmetric tensor with equal eigenvalues on the first $N \times N$ block and the second $N \times N$ block, For instance:

$$\phi_{\square\square} \sim \left(\delta_{ij} - \delta_{i+N,j+N}\right) \ , \quad i,j = 1, \cdots, N \ , \tag{6.89}$$

with $(Spin(N)_2 \times Spin(N)_2)/\mathbb{Z}_2$ the stabilizer of the above. In particular, the $\mathbb{Z}_2$ quotient identifies the $\mathbb{Z}_2$ center subgroups of each $Spin(N)$ factor which measure the vector representation.

To investigate the symmetries, we will make use of the following (1+1)d chiral coset model:

$$\frac{Spin(2N)_2}{\left(Spin(N)_2 \times Spin(N)_2\right)/\mathbb{Z}_2} \ , \quad c = 1 \ , \tag{6.90}$$

where we have also indicated the chiral central charge. It has been observed [3] that this coset is equivalent to a rational point on the orbifold branch of $c = 1$ theories. Specifically:

$$\frac{Spin(2N)_2}{\left(Spin(N)_2 \times Spin(N)_2\right)/\mathbb{Z}_2} \cong U(1)^{\text{orb}}_{2N} \ , \tag{6.91}$$

where above, $U(1)^{\text{orb}}_{2N}$ denotes a $\mathbb{Z}_2$ gauging of $U(1)_{2N}$. The spectrum of this theory is summarized in Table 6.4. Crucial for our analysis below, the orbifold theory $U(1)^{\text{orb}}_{2N}$ has abelian anyons whose fusion mimics the center of $Spin(N)_2$. Specifically, for N odd the

Orbifold Model $U(1)^{\rm orb}_{2N}$		
Line label	Quantum Dimension	Conformal Weight
$\mathbf{1}$	$d_{\mathbf{1}} = 1$	$h_{\mathbf{1}} = 0$
Θ	$d_\Theta = 1$	$h_\Theta = 1$
σ_1, σ_2	$d_\sigma = \sqrt{N}$	$h_{\sigma_1} = h_{\sigma_2} = 1/16$
τ_1, τ_2	$d_\tau = \sqrt{N}$	$h_{\tau_1} = h_{\tau_2} = 9/16$
$\phi_1, \phi_2, \cdots, \phi_{N-1}$	$d_{\phi_i} = 2$	$h_{\phi_i} = i^2/4N$
ϕ_N^1, ϕ_N^2	$d_{\phi_N^1} = d_{\phi_N^2} = 1$	$h_{\phi_N^1} = h_{\phi_N^2} = N/4$

Table 6.4: Data for the orbifold theory $U(1)^{\rm orb}_{2N}$. In the notation of [5], this is Chern-Simons theory with gauge group $O(2)^0_{2N,0}$. The model has a total of $N+7$ simple lines.

abelian fusion ring is $\mathbb{Z}_4$

$$\phi_N^{(i)} \times \phi_N^{(i)} = \Theta \ , \quad \phi_N^{(1)} \times \phi_N^{(2)} = \phi_N^{(2)} \times \phi_N^{(1)} = \mathbf{1} \ , \tag{6.92}$$

while instead for N even the abelian fusion ring is $\mathbb{Z}_2 \times \mathbb{Z}_2$

$$\phi_N^{(i)} \times \phi_N^{(i)} = \mathbf{1} \ , \quad \phi_N^{(1)} \times \phi_N^{(2)} = \phi_N^{(2)} \times \phi_N^{(1)} = \Theta \ . \tag{6.93}$$

When applying our model of the Higgsing transition, we will encounter the following relations between (2+1)d TQFTs. The analog of (6.13) is:

$$\begin{cases} \frac{Spin(N)_2 \times Spin(N)_2}{\mathbb{Z}_2} \cong \frac{Spin(2N)_2 \times U(1)^{\rm Orb}_{-2N}}{\mathbb{Z}_4} \ , & N \text{ odd} \ , \\ \frac{Spin(N)_2 \times Spin(N)_2}{\mathbb{Z}_2} \cong \frac{Spin(2N)_2 \times U(1)^{\rm Orb}_{-2N}}{\mathbb{Z}_2 \times \mathbb{Z}_2} \ , & N \text{ even} \ . \end{cases} \tag{6.94}$$

Similarly, the analog of (6.26) is:

$$Spin(2N)_2 = \frac{\left(\frac{Spin(N)_2 \times Spin(N)_2}{\mathbb{Z}_2} \times U(1)^{\rm Orb}_{2N} \right)}{\mathcal{A}_N} \ , \tag{6.95}$$

where $\mathcal{A}$ is a non-abelian algebra described below.

Abelian Anyons in $Spin(2N)_2$	
Line label	Conformal Weight
$\mathbf{1}$	$h_{\mathbf{1}} = 0$
χ^v	$h_{\chi^v} = 1$
χ^s, χ^c	$h_{\chi^s} = h_{\chi^c} = N/4$

Table 6.5: Abelian anyons in $Spin(2N)_2$. The anyons χ^s and χ^c measure charges of spinor representations, while χ^v measures the vector representation.

Symmetry Analysis

We proceed with the symmetry analysis. First, in the non-relativistic approximation described around (6.22) we note that the symmetric tensor matter in our model is the generator of the $\mathbb{Z}_2$ one-form symmetry which measures the number of vector indices modulo two. (See footnote 12 for related discussion.) Therefore in the notation of Table 6.5, the dynamical matter field flows at long distances to an abelian anyon:

$$\phi_{\square\square} \longrightarrow \chi^v \ . \tag{6.96}$$

The candidate symmetry lines are thus those that are neutral under braiding with χ^v and hence form $Spin(2N)_2/\mathbb{Z}_2$.

To proceed further, we use the anyon condensation argument of section 6.2.4. Specifically, from (6.94) to proceed inside a cylinder of the Higgsed phase, we must condense the whole center of $Spin(2N)_2$. Thus inside $Spin(2N)_2 \times U(1)^{\rm orb}_{-2N}$ we consider the algebra object

$$\mathcal{B} = (\mathbf{1}, \mathbf{1}) + (\chi^s, \overline{\phi^1_N}) + (\chi^c, \overline{\phi^2_N}) + (\chi^v, \overline{\Theta}) \ . \tag{6.97}$$

Note that all spins of the abelian anyons in $Spin(2N)_2$ have paired with anyons in the coset $U(1)^{\rm orb}_{2N}$ to form condensable bosons. For N odd $\mathcal{B}$ is a $\mathbb{Z}_4$ algebra, while for N even it is a $\mathbb{Z}_2 \times \mathbb{Z}_2$ algebra. In summary then condensing $\mathcal{B}$ leads to a fusion algebra of $PSpin(2N)_2$ preserved and faithfully acting in the Higgsed phase.

Analogously, we can investigate the symmetries by transitioning from the Higgsed phase to the massive phase as in (6.26). For odd N, the full algebra object, $\mathcal{A}_N$ in $(Spin(N)_2 \times Spin(N)_2)/\mathbb{Z}_2 \times U(1)^{\text{Orb}}_{2N}$ is:

$$\begin{aligned}\mathcal{A}_N &= (0,\mathbf{1}) + \big((0,2\mathbf{w}_1),\Theta\big) \\ &+ \sum_{i}^{\frac{N-1}{2}-1} \big((\mathbf{w}_i,\mathbf{w}_i)_1,\phi_{2i}\big) + \big((2\mathbf{w}_\sigma,2\mathbf{w}_\sigma)_1,\phi_{N-1}\big)\ .\end{aligned} \tag{6.98}$$

In the above, $\mathbf{w}_\sigma$ is the weight of the unique spinor representation, $\mathbf{w}_i$ are the non-spinor weights and the splitting into two lines is indicated by a subscript. Further, we have the identification $(0,2\mathbf{w}_1) \cong (2\mathbf{w}_1,0)$ in $(Spin(N)_2 \times Spin(N)_2)/\mathbb{Z}_2$ and the notation to label the primaries of $U(1)^{\text{Orb}}_{2N}$ is summarized in Table 6.4.

The lines preserved now correspond to the subset of lines in $(Spin(N)_2 \times Spin(N)_2)/\mathbb{Z}_2$ which obey the uniform spin condition (6.25) upon fusion with $\mathcal{A}_N$. These are precisely:

$$\{(0,0),\quad (0,2\mathbf{w}_1),\quad (2\mathbf{w}_\sigma,2\mathbf{w}_\sigma)_2,\quad (\mathbf{w}_i,\mathbf{w}_i)_2\}\ , \tag{6.99}$$

where $i = 1,\ldots,\frac{(N-3)}{2}$. Again we see that these lines form the algebra $PSpin(2N)_2$.

Analogously for N even, the full algebra $\mathcal{A}_N$ in $\frac{Spin(N)_2\times Spin(N)_2}{\mathbb{Z}_2} \times U(1)^{\text{Orb}}_{2N}$ is:

$$\begin{aligned}\mathcal{A}_N &= (0,\mathbf{1}) + \big((0,2\mathbf{w}_1),\Theta\big) \\ &\quad + \big((2\mathbf{w}_s,2\mathbf{w}_s),\phi_N^{(1)}\big) + \big((2\mathbf{w}_s,2\mathbf{w}_c),\phi_N^{(2)}\big) \\ &\quad + \sum_{i=1}^{\frac{N}{2}-2} \big((\mathbf{w}_i,\mathbf{w}_i)_1,\phi_{2i}\big) \\ &\quad + \big((\mathbf{w}_s+\mathbf{w}_c,\mathbf{w}_s+\mathbf{w}_c)_1,\phi_{N-2}\big)\ ,\end{aligned} \tag{6.100}$$

where now $\mathbf{w}_s, \mathbf{w}_c$ are the two chiral spinor weights and we have the identifications $(0,2\mathbf{w}_1) \cong$

$(2\mathbf{w}_1, 0)$, $(2\mathbf{w}_s, 2\mathbf{w}_s) \cong (2\mathbf{w}_c, 2\mathbf{w}_c)$, and $(2\mathbf{w}_s, 2\mathbf{w}_c) \cong (2\mathbf{w}_c, 2\mathbf{w}_s)$ in $(Spin(N)_2 \times Spin(N)_2)/\mathbb{Z}_2$. The preserved lines are those in $(Spin(N)_2 \times Spin(N)_2)/\mathbb{Z}_2$ obeying the uniform spin condition (6.25):

$$\begin{aligned}\{(0,0), \quad (0,2\mathbf{w}_1), \quad (2\mathbf{w}_s, 2\mathbf{w}_s), \quad (2\mathbf{w}_s, 2\mathbf{w}_c), \\ (\mathbf{w}_s + \mathbf{w}_c, \mathbf{w}_s + \mathbf{w}_c)_2, \quad (\mathbf{w}_i, \mathbf{w}_i)_2\} \ ,\end{aligned} \tag{6.101}$$

where $i = 1, \ldots, \frac{N}{2} - 2$. These again form the fusion algebra $PSpin(2N)_2$.

Interpretation via Symmetry TQFT

The $PSpin(2N)_2$ symmetry admits a symmetry TQFT description [58,59] analogous to that of section 6.3.1. We couple $Spin(2N)_2$ (2+1)d TQFT to a bulk (3+1)d gauge theory based on abelian surfaces whose details depend on the parity of N.

For N odd, the bulk theory is based on a discrete $\mathbb{Z}_4$ 2-form gauge field B. The action for this gauge field is determined by the spin of the abelian anyons corresponding to the center of $Spin(2N)_2$. (See Table 6.5.) Specifically, the exponentiated action is given by

$$\exp\left(\frac{N\pi i}{2}\int_X \mathfrak{P}(B)\right) \ , \tag{6.102}$$

Where X is a four-manifold and $\mathfrak{P}(B)$ is the Pontryagin square:

$$\mathfrak{P}(B) \in H^4(X, \mathbb{Z}_8) \ . \tag{6.103}$$

Similarly, for even N, there are two $\mathbb{Z}_2$ 2-form gauge fields B_1 and B_2. The exponentiated action is:

$$\exp\left(\frac{N\pi i}{4}\int_X \mathfrak{P}(B_1) + \frac{N\pi i}{4}\int_X \mathfrak{P}(B_2)\right) \ , \tag{6.104}$$

$E_{7,2}$		
Line label	Quantum Dimension	Conformal Weight
$0\,(\mathbf{1})$	$d_0 = 1$	$h_0 = 0$
$2\mathbf{w}_6\,(\mathbf{1463})$	$d_{2\mathbf{w}_6} = 1$	$h_{2\mathbf{w}_6} = 3/2$
$\mathbf{w}_7\,(\mathbf{912})$	$d_{\mathbf{w}_7} = \sqrt{2}$	$h_{\mathbf{w}_7} = 21/16$
$\mathbf{w}_6\,(\mathbf{56})$	$d_{\mathbf{w}_6} = (1+\sqrt{5})/\sqrt{2}$	$h_{\mathbf{w}_6} = 57/80$
$\mathbf{w}_5\,(\mathbf{1539})$	$d_{\mathbf{w}_5} = (1+\sqrt{5})/2$	$h_{\mathbf{w}_5} = 7/5$
$\mathbf{w}_1\,(\mathbf{133})$	$d_{\mathbf{w}_1} = (1+\sqrt{5})/2$	$h_{\mathbf{w}_1} = 9/10$

Table 6.6: $E_{7,2}$ data. The fusion ring of $E_{7,2}$ is that of Fib $\times$ TY($\mathbb{Z}_2$), where the Fibonacci element is given by $\mathbf{w}_5$ and those of TY($\mathbb{Z}_2$) by $2\mathbf{w}_6$ and $\mathbf{w}_7$.

where now

$$\mathfrak{P}(B_i) \in H^4(X, \mathbb{Z}_4)\ . \tag{6.105}$$

The bulk-boundary coupling identifies the $\mathbb{Z}_2$ one-form symmetry lines in the $Spin(2N)_2$ TQFT with the boundary of the Wilson surfaces of the bulk 2-form gauge fields.

We observe that the spin of the abelian anyons in $Spin(2N)_2$ is never minimal[19] and correspondingly the theories based on (6.102) and (6.104) are never invertible. Thus, the symmetry lines $PSpin(2N)_2$ cannot decouple since they are not modular.

6.3.3 Exceptional CSM: Ising Symmetry

As a final example, we consider a Chern-Simons matter model with an exceptional gauge group E_7. We recall that the fundamental representation of E_7 is the **56** and for our matter we choose a scalar field in the antisymmetric rank two tensor representation **1539**.

$$E_{7,2} + \phi_{\mathbf{1539}} = E_{7,2} + \phi_{\mathbf{w}_5}\ . \tag{6.106}$$

This theory has a Higgsing transition described by the following flow diagram:

19. For $\mathbb{Z}_N$ anyons with N even, the minimal spin is $1/2N$.

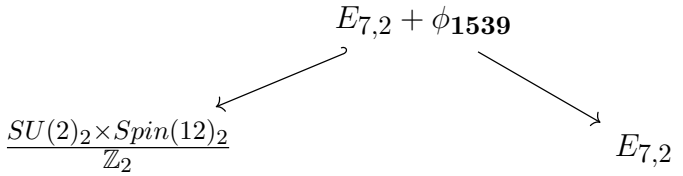

. (6.107)

Our basic claim is that this model has Ising fusion category symmetry, where the spins match those in $Spin(5)_1$.

To clarify the group theory of the Higgsed phase, note that the embedding of $(SU(2)_2 \times Spin(12)_2)\mathbb{Z}_2$ in E_7 is characterized by the branching rule:

$$\mathbf{56} \longrightarrow (\mathbf{2}, \mathbf{12}) + (\mathbf{1}, \mathbf{32}) \ . \tag{6.108}$$

Therefore, denoting by A in index in the **56**, there is a channel above where this decomposes to a product $A \to \alpha i$ where α is doublet index in $SU(2)$ and i a vector index in $Spin(12)$. Thus the antisymmetric tensor **1539** can acquire an expectation value

$$\phi_{AB} \sim \varepsilon_{\alpha\beta} \ \delta_{ij} \ , \tag{6.109}$$

which is a singlet in $(SU(2)_2 \times Spin(12)_2)/\mathbb{Z}_2$. From now on, we assume that the scalar potential is tuned to achieve this Higgsing. The spectrum of the massive phase $E_{7,2}$ is summarized in Table 6.6, while the spectrum in the Higgsed phase $(SU(2)_2 \times Spin(12)_2)/\mathbb{Z}_2$ is summarized in Table 6.8.

To investigate this flow we will analyze the coset

$$\frac{(E_7)_2}{(SU(2)_2 \times Spin(12)_2)/\mathbb{Z}_2} \ , \quad c = 8/10 \ , \tag{6.110}$$

Tetracritical Ising Model		
Line label	Quantum Dimension	Conformal Weight
(1,1)	$d_{(1,1)} = 1$	$h_{(1,1)} = 0$
(4,1)	$d_{(4,1)} = 1$	$h_{(4,1)} = 3$
(4,2)	$d_{(4,2)} = \sqrt{3}$	$h_{(4,2)} = 13/8$
(4,4)	$d_{(4,4)} = \sqrt{3}$	$h_{(4,4)} = 1/8$
(4,3)	$d_{(4,3)} = 2$	$h_{(4,3)} = 2/3$
(3,1)	$d_{(3,1)} = \phi$	$h_{(3,1)} = 7/5$
(2,1)	$d_{(2,1)} = \phi$	$h_{(2,1)} = 2/5$
(2,2)	$d_{(2,2)} = \phi\sqrt{3}$	$h_{(2,2)} = 1/40$
(3,2)	$d_{(3,2)} = \phi\sqrt{3}$	$h_{(3,2)} = 21/40$
(3,3)	$d_{(3,3)} = 2\phi$	$h_{(3,3)} = 1/15$

Table 6.7: Tetracritical Ising Model data. The operator labels follow the Kac labels notation convention [5].

The result of the coset (6.110) is the Tetracritical Ising model [105],

$$\frac{(E_7)_2}{(SU(2)_2 \times Spin(12)_2)/\mathbb{Z}_2} \cong \text{TetraIsing} \ , \tag{6.111}$$

whose spectrum is summarized in Table 6.7. Our symmetry analysis is then based on the anyon condensation patterns (compare to (6.13) and (6.26)):

$$\frac{SU(2)_2 \times Spin(12)_2}{\mathbb{Z}_2} = \frac{E_{7,2} \times \overline{\text{TetraIsing}}}{\mathcal{B}} \ , \tag{6.112}$$

as well as:

$$E_{7,2} = \frac{\frac{SU(2)_2 \times Spin(12)_2}{\mathbb{Z}_2} \times \text{TetraIsing}}{\mathcal{A}} \ , \tag{6.113}$$

where $\mathcal{A}$ and $\mathcal{B}$ are algebras specified below.

Symmetry Analysis

We begin with our analysis of the preserved topological lines using the condensation formula (6.13). By analyzing the quantum dimension formula (6.21) it is easy to see that the only

$(SU(2)_2 \times Spin(12)_2)/\mathbb{Z}_2$		
Line label	Quantum Dimension	Conformal Weight
$(0,0)$	$d_{(0,0)} = 1$	$h_{(0,0)} = 0$
$(0, 2\mathbf{w}_1)$	$d_{(0,2\mathbf{w}_1)} = 1$	$h_{(0,2\mathbf{w}_1)} = 1$
$(0, 2\mathbf{w}_s)$	$d_{(0,2\mathbf{w}_s)} = 1$	$h_{(0,2\mathbf{w}_s)} = 3/2$
$(2,0)$	$d_{(2,0)} = 1$	$h_{(2,0)} = 1/2$
$(0, \mathbf{w}_s)$	$d_{(0,\mathbf{w}_s)} = \sqrt{6}$	$h_{(0,\mathbf{w}_s)} = 11/16$
$(0, \mathbf{w}_1 + \mathbf{w}_c)$	$d_{(0,\mathbf{w}_1+\mathbf{w}_c)} = \sqrt{6}$	$h_{(0,\mathbf{w}_1+\mathbf{w}_c)} = 19/16$
$(0, \mathbf{w}_4)$	$d_{(0,\mathbf{w}_4)} = 2$	$h_{(0,\mathbf{w}_4)} = 4/3$
$(0, \mathbf{w}_2)$	$d_{(0,\mathbf{w}_2)} = 2$	$h_{(0,\mathbf{w}_2)} = 5/6$
$(1, \mathbf{w}_c)_1$	$d_{(1,\mathbf{w}_c)_1} = \sqrt{3}$	$h_{(1,\mathbf{w}_c)_1} = 7/8$
$(1, \mathbf{w}_c)_2$	$d_{(1,\mathbf{w}_c)_2} = \sqrt{3}$	$h_{(1,\mathbf{w}_c)_2} = 7/8$
$(1, \mathbf{w}_1 + \mathbf{w}_s)_1$	$d_{(1,\mathbf{w}_1+\mathbf{w}_s)_1} = \sqrt{3}$	$h_{(1,\mathbf{w}_1+\mathbf{w}_s)_1} = 11/8$
$(1, \mathbf{w}_1 + \mathbf{w}_s)_2$	$d_{(1,\mathbf{w}_1+\mathbf{w}_s)_2} = \sqrt{3}$	$h_{(1,\mathbf{w}_1+\mathbf{w}_s)_2} = 11/8$
$(1, \mathbf{w}_1)$	$d_{(1,\mathbf{w}_1)} = 2\sqrt{2}$	$h_{(1,\mathbf{w}_1)} = 31/48$
$(1, \mathbf{w}_3)_1$	$d_{(1,\mathbf{w}_3)_1} = \sqrt{2}$	$h_{(1,\mathbf{w}_3)_1} = 21/16$
$(1, \mathbf{w}_3)_2$	$d_{(1,\mathbf{w}_3)_2} = \sqrt{2}$	$h_{(1,\mathbf{w}_3)_2} = 21/16$

Table 6.8: $(SU(2)_2 \times Spin(12)_2)/\mathbb{Z}_2$ data.

interesting candidate for $\mathcal{B}$ is[20]

$$\mathcal{B} = (0, \overline{(1,1)}) + (\mathbf{w}_5, \overline{(3,1)}) \ . \tag{6.114}$$

The line $\mathbf{w}_5 = \mathbf{1539}$ in $E_{7,2}$ (the IR limit of the matter field) is a Fibonacci line. Notice that this line corresponds to the anyon in the same representation as that of the scalar field triggering the Higgsing transition, as expected from the discussion in Section 6.2.4.

We can see which lines in $E_{7,2}$ remain topological using the uniform spin condition (6.25) leading to the topological spectrum $0, 2\mathbf{w}_6, \mathbf{w}_7$. Indeed, from:

$$\mathcal{B} \times (2\mathbf{w}_6, \overline{(1,1)}) = (2\mathbf{w}_6, \overline{(1,1)}) + (\mathbf{w}_1, \overline{(3,1)}) \ , \tag{6.115}$$

$$\mathcal{B} \times (\mathbf{w}_7, \overline{(1,1)}) = (\mathbf{w}_7, \overline{(1,1)}) + (\mathbf{w}_6, \overline{(3,1)}) \ , \tag{6.116}$$

20. The algebra $\mathcal{B}' = (0, \overline{(1,1)}) + (\mathbf{w}_5, \overline{(2,1)})$ also saturates quantum dimension, but it is related by the $\mathbb{Z}_2$ symmetry of the Tricritical Ising Model to $\mathcal{B}$, and leads to no new conclusions.

we see that each element on the right-hand side has the same spin. These lines generate an Ising fusion category symmetry:

$$2\mathbf{w}_6 \times 2\mathbf{w}_6 = 0 \ , \quad 2\mathbf{w}_6 \times \mathbf{w}_7 = \mathbf{w}_7 \ , \quad \mathbf{w}_7 \times \mathbf{w}_7 = 0 + 2\mathbf{w}_6 \ . \tag{6.117}$$

More precisely, keeping track of the spins of the lines, the symmetry is $Spin(5)_1$.

Now we make use of (6.113) to check this conclusion. First, we must deduce the algebra $\mathcal{A}$. There are three candidates that are consistent with the fusion rules and that saturate the quantum dimension condition (6.88) which reads:

$$\dim(E_{7,2}) = \frac{\dim(\frac{(SU(2)_2 \times Spin(12)_2}{\mathbb{Z}_2} \times \text{TetraIsing})}{\dim(\mathcal{A})^2} \ . \tag{6.118}$$

Namely:

$$\begin{aligned} \mathcal{A} = &((0,0),(1,1)) + ((0,2\mathbf{w}_1),(4,1)) + ((0,\mathbf{w}_4),(4,3)) \\ &+ ((1,\mathbf{w}_1+\mathbf{w}_s)_2,(4,2)) + ((1,\mathbf{w}_c)_1,(4,4)) \ , \end{aligned} \tag{6.119}$$

$$\begin{aligned} \mathcal{A}' = &((0,0),(1,1)) + ((0,2\mathbf{w}_1),(4,1)) + ((0,\mathbf{w}_4),(4,3)) \\ &+ ((1,\mathbf{w}_1+\mathbf{w}_s)_1,(4,2)) + ((1,\mathbf{w}_c)_2,(4,4)) \ , \end{aligned} \tag{6.120}$$

and

$$\begin{aligned} \mathcal{A}'' = &((0,0),(1,1)) + ((0,0),(4,1)) + ((0,2\mathbf{w}_1),(1,1)) \\ &+ ((0,2\mathbf{w}_1),(4,1)) + 2((0,\mathbf{w}_4),(4,3)) \ . \end{aligned} \tag{6.121}$$

To resolve this ambiguity, we recall from (6.13) that we seek to present the Higgsed phase $H_{\tilde{k}}$ without the additional condensation $\mathcal{C}$ described in footnote 5. According to [3, 24] this requires that the only anyon in the algebra $\mathcal{A}$ of (6.26) of the form $(x, 1)$ has $x = 1$. Inspecting $\mathcal{A}''$ in (6.121) we see the component $((0, 2\mathbf{w}_1), (1, 1))$ in $\mathcal{A}''$ violating this condition. Thus, we do not consider gauging $\mathcal{A}''$.

Meanwhile, the difference between $\mathcal{A}$ and $\mathcal{A}'$ is immaterial since they differ only in which choice of split lines in $(SU(2)_2 \times Spin(12)_2)/\mathbb{Z}_2$ appear in the algebra. We therefore proceed with the algebra object $\mathcal{A}$.

In this case, we claim that the result of the condensation again produces topological lines which form an Ising fusion category. Indeed, the non-trivial lines in $(SU(2)_2 \times Spin(12)_2)/\mathbb{Z}_2$ that remain topological are $(0, 2\mathbf{w}_s)$ and $(1, \mathbf{w}_3)_2$. As a check, we can calculate the fusion with the algebra and see that the uniform spin condition (6.25) is fulfilled:

$$\begin{aligned} \mathcal{A} \times ((0, 2\mathbf{w}_s), (1, 1)) &= ((0, 2\mathbf{w}_s), (1, 1)) + ((2, 0), (4, 1)) \\ &+ ((0, \mathbf{w}_2), (4, 3)) + ((1, \mathbf{w}_c)_2, (4, 2)) \\ &+ ((1, \mathbf{w}_1 + \mathbf{w}_s)_1, (4, 4)) \ , \end{aligned} \tag{6.122}$$

and

$$\begin{aligned} \mathcal{A} \times ((1, \mathbf{w}_3)_2, (1, 1)) &= ((1, \mathbf{w}_3)_2, (1, 1)) + ((1, \mathbf{w}_3)_1, (4, 1)) \\ &+ ((1, \mathbf{w}_1), (4, 3)) + ((0, \mathbf{w}_s), (4, 2)) \\ &+ ((0, \mathbf{w}_1 + \mathbf{w}_c), (4, 4)) \ . \end{aligned} \tag{6.123}$$

The fusions of these lines are:

$$(0, 2\mathbf{w}_s) \times (0, 2\mathbf{w}_s) = (0, 0) \ , \quad (0, 2\mathbf{w}_s) \times (1, \mathbf{w}_3)_2 = (1, \mathbf{w}_3)_2 \ , \tag{6.124}$$

as well as:

$$(1, \mathbf{w}_3)_2 \times (1, \mathbf{w}_3)_2 = (0, 0) + (0, 2\mathbf{w}_s) \ , \tag{6.125}$$

which again define an Ising fusion ring $Spin(5)_1$.

6.4 A Quantum Dimension Check

In this section we briefly check that the quantum dimension constraint on the algebra $\mathcal{D}_k$ mentioned in Section 6.3.1 is indeed fulfilled. Recall that we wish to check that the algebra is such that

$$\frac{\dim(SU(k)_2 \times SU(2)_k)}{\dim(\mathcal{D}_k)^2} = \dim(SU(2k)_1) \ , \tag{6.126}$$

where

$$\dim(SU(k)_2) = \frac{k(k+2)}{4\sin\left(\frac{\pi}{k+2}\right)^2} \ , \tag{6.127}$$

$$\dim(SU(2)_k) = \frac{(k+2)}{2\sin\left(\frac{\pi}{k+2}\right)^2} \ , \tag{6.128}$$

and

$$\dim(SU(2k)_1) = 2k \ . \tag{6.129}$$

Indeed, recall that the quantum dimensions of the $SU(2)_k$ fusion ring are

$$d_j^{SU(2)_k} = \frac{\sin\left(\frac{(j+1)\pi}{k+2}\right)}{\sin\left(\frac{\pi}{k+2}\right)} \ , \tag{6.130}$$

where $j = 0, 1, \ldots, k-1$. Recall as well that the algebra is composed by the diagonal subset of lines inside the $PSU(2)_{-k} \times PSU(2)_k$ subfusion ring of $SU(k)_2 \times SU(2)_k$. Then, the dimension of the algebra is

$$\dim(\mathcal{D}_k) = \sum_{j \text{ even}} (d_j^{SU(2)_k})^2 \ . \tag{6.131}$$

This is easily calculated, and indeed (6.126) is obeyed.

CHAPTER 7

BIBLIOGRAPHY

[1] Z. Komargodski, K. Ohmori, K. Roumpedakis, and S. Seifnashri, *Symmetries and strings of adjoint QCD_2*, *JHEP* **03** (2021) 103, [arXiv:2008.07567].

[2] G. W. Moore and N. Seiberg, *Taming the Conformal Zoo*, *Phys. Lett. B* **220** (1989) 422–430.

[3] C. Córdova and D. García-Sepúlveda, *Non-Invertible Anyon Condensation and Level-Rank Dualities*, [arXiv:2312.16317].

[4] S. Elitzur, G. W. Moore, A. Schwimmer, and N. Seiberg, *Remarks on the Canonical Quantization of the Chern-Simons-Witten Theory*, *Nucl. Phys. B* **326** (1989) 108–134.

[5] P. Di Francesco, P. Mathieu, and D. Senechal, *Conformal Field Theory*. Graduate Texts in Contemporary Physics. Springer-Verlag, New York, 1997.

[6] D. Gaiotto, A. Kapustin, N. Seiberg, and B. Willett, *Generalized Global Symmetries*, *JHEP* **02** (2015) 172, [arXiv:1412.5148].

[7] P.-S. Hsin and N. Seiberg, *Level/rank Duality and Chern-Simons-Matter Theories*, *JHEP* **09** (2016) 095, [arXiv:1607.07457].

[8] O. Aharony, F. Benini, P.-S. Hsin, and N. Seiberg, *Chern-Simons-matter dualities with SO and USp gauge groups*, *JHEP* **02** (2017) 072, [arXiv:1611.07874].

[9] C. Cordova, P.-S. Hsin, and N. Seiberg, *Global Symmetries, Counterterms, and Duality in Chern-Simons Matter Theories with Orthogonal Gauge Groups*, *SciPost Phys.* **4** (2018), no. 4 021, [arXiv:1711.10008].

[10] J. Gomis, Z. Komargodski, and N. Seiberg, *Phases Of Adjoint QCD_3 And Dualities*, *SciPost Phys.* **5** (2018), no. 1 007, [arXiv:1710.03258].

[11] C.-M. Chang, Y.-H. Lin, S.-H. Shao, Y. Wang, and X. Yin, *Topological Defect Lines and Renormalization Group Flows in Two Dimensions*, *JHEP* **01** (2019) 026, [arXiv:1802.04445].

[12] C. Córdova and D. García-Sepúlveda, *Topological Cosets via Anyon Condensation and Applications to Gapped* $\mathbf{QCD_2}$, [arXiv:2412.01877].

[13] C. Córdova, D. García-Sepúlveda, and N. Holfester, *Particle-Soliton Degeneracy in 2D Quantum Chromodynamics*, arXiv:2412.21153.

[14] C. Cordova, D. García-Sepúlveda, and K. Ohmori, *Higgsing Transitions from Topological Field Theory & Non-Invertible Symmetry in Chern-Simons Matter Theories*, [arXiv:2504.03614].

[15] A. Kitaev, *Anyons in an exactly solved model and beyond*, *Annals Phys.* **321** (2006), no. 1 2–111, [cond-mat/0506438].

[16] F. Benini, C. Córdova, and P.-S. Hsin, *On 2-Group Global Symmetries and their Anomalies*, *JHEP* **03** (2019) 118, [arXiv:1803.09336].

[17] S.-S. Chern and J. Simons, *Characteristic forms and geometric invariants*, *Annals Math.* **99** (1974) 48–69.

[18] E. Witten, *Quantum Field Theory and the Jones Polynomial*, *Commun. Math. Phys.* **121** (1989) 351–399.

[19] C. Galindo, *On braided and ribbon unitary fusion categories*, *Canadian Mathematical Bulletin* **57** (2014), no. 3 506–510.

[20] G. W. Moore and N. Seiberg, *Polynomial Equations for Rational Conformal Field Theories*, *Phys. Lett. B* **212** (1988) 451–460.

[21] G. W. Moore and N. Seiberg, *Classical and Quantum Conformal Field Theory*, *Commun. Math. Phys.* **123** (1989) 177.

[22] G. Anderson and G. W. Moore, *Rationality in Conformal Field Theory*, *Commun. Math. Phys.* **117** (1988) 441.

[23] C. Vafa, *Toward classification of conformal theories*, *Physics Letters B* **206** (1988), no. 3 421–426.

[24] J. Frohlich, J. Fuchs, I. Runkel, and C. Schweigert, *Correspondences of ribbon categories*, *Adv. Math.* **199** (2006) 192–329, [math/0309465].

[25] T. Nakanishi and A. Tsuchiya, *Level rank duality of WZW models in conformal field theory*, *Commun. Math. Phys.* **144** (1992) 351–372.

[26] S. G. Naculich, H. A. Riggs, and H. J. Schnitzer, *Group Level Duality in WZW Models and Chern-Simons Theory*, *Phys. Lett. B* **246** (1990) 417–422.

[27] E. J. Mlawer, S. G. Naculich, H. A. Riggs, and H. J. Schnitzer, *Group level duality of WZW fusion coefficients and Chern-Simons link observables*, *Nucl. Phys. B* **352** (1991) 863–896.

[28] E. Witten, *The Verlinde algebra and the cohomology of the Grassmannian*, [hep-th/9312104].

[29] M. R. Douglas, *Chern-Simons-Witten theory as a topological Fermi liquid*, [hep-th/9403119].

[30] S. G. Naculich and H. J. Schnitzer, *Level-rank duality of the U(N) WZW model, Chern-Simons theory, and 2-D qYM theory*, *JHEP* **06** (2007) 023, [hep-th/0703089].

[31] C. Córdova, P.-S. Hsin, and K. Ohmori, *Exceptional Chern-Simons-Matter Dualities*, *SciPost Phys.* **7** (2019), no. 4 056, [arXiv:1812.11705].

[32] C. Córdova, P.-S. Hsin, and N. Seiberg, *Time-Reversal Symmetry, Anomalies, and Dualities in (2+1)d*, *SciPost Phys.* **5** (2018), no. 1 006, [arXiv:1712.08639].

[33] A. Kapustin and N. Seiberg, *Coupling a QFT to a TQFT and Duality*, *JHEP* **04** (2014) 001, [arXiv:1401.0740].

[34] P.-S. Hsin, H. T. Lam, and N. Seiberg, *Comments on One-Form Global Symmetries and Their Gauging in 3d and 4d*, *SciPost Phys.* **6** (2019), no. 3 039, [arXiv:1812.04716].

[35] D. C. Dunbar and K. G. Joshi, *Characters for coset conformal field theories*, *Int. J. Mod. Phys. A* **8** (1993) 4103–4122, [hep-th/9210122].

[36] D. C. Dunbar and K. G. Joshi, *Maverick examples of coset conformal field theories*, *Mod. Phys. Lett. A* **8** (1993) 2803–2814, [hep-th/9309093].

[37] F. A. Bais and J. K. Slingerland, *Condensate induced transitions between topologically ordered phases*, *Phys. Rev. B* **79** (2009) 045316, [arXiv:0808.0627].

[38] C. Cordova, T. T. Dumitrescu, K. Intriligator, and S.-H. Shao, *Snowmass White Paper: Generalized Symmetries in Quantum Field Theory and Beyond*, in *Snowmass 2021*, 5, 2022. arXiv:2205.09545.

[39] S. Schafer-Nameki, *ICTP Lectures on (Non-)Invertible Generalized Symmetries*, [arXiv:2305.18296].

[40] S.-H. Shao, *What's Done Cannot Be Undone: TASI Lectures on Non-Invertible Symmetry*, [arXiv:2308.00747].

[41] J. Fuchs, I. Runkel, and C. Schweigert, *TFT construction of RCFT correlators 1. Partition functions*, *Nucl. Phys. B* **646** (2002) 353–497, [hep-th/0204148].

[42] J. Fuchs, I. Runkel, and C. Schweigert, *TFT construction of RCFT correlators. 2. Unoriented world sheets*, *Nucl. Phys. B* **678** (2004) 511–637, [hep-th/0306164].

[43] J. Fuchs, I. Runkel, and C. Schweigert, *TFT construction of RCFT correlators. 3. Simple currents*, *Nucl. Phys. B* **694** (2004) 277–353, [hep-th/0403157].

[44] J. Fuchs, I. Runkel, and C. Schweigert, *TFT construction of RCFT correlators IV: Structure constants and correlation functions*, *Nucl. Phys. B* **715** (2005) 539–638, [hep-th/0412290].

[45] J. Frohlich, J. Fuchs, I. Runkel, and C. Schweigert, *Kramers-Wannier duality from conformal defects*, *Phys. Rev. Lett.* **93** (2004) 070601, [cond-mat/0404051].

[46] J. Frohlich, J. Fuchs, I. Runkel, and C. Schweigert, *Duality and defects in rational conformal field theory*, *Nucl. Phys. B* **763** (2007) 354–430, [hep-th/0607247].

[47] M. Müger, *From subfactors to categories and topology ii. the quantum double of tensor categories and subfactors*, *arXiv preprint math/0111205* (2001).

[48] M. MÃ¼ger, *Galois theory for braided tensor categories and the modular closure*, *Advances in Mathematics* **150** (2000), no. 2 151–201.

[49] A. Kirillov Jr and V. Ostrik, *On a q-analogue of the mckay correspondence and the ade classification of sl2 conformal field theories*, *Advances in Mathematics* **171** (2002), no. 2 183–227.

[50] A. Davydov, M. Müger, D. Nikshych, and V. Ostrik, *The witt group of non-degenerate braided fusion categories*, *Journal für die reine und angewandte Mathematik (Crelles Journal)* **2013** (2013), no. 677 135–177.

[51] L.-Y. Hung and Y. Wan, *Generalized ADE classification of topological boundaries and anyon condensation*, *JHEP* **07** (2015) 120, [arXiv:1502.02026].

[52] L. Kong, *Anyon condensation and tensor categories*, *Nuclear Physics B* **886** (2014) 436–482.

[53] R. Thorngren and Y. Wang, *Fusion Category Symmetry I: Anomaly In-Flow and Gapped Phases*, [arXiv:1912.02817].

[54] R. Thorngren and Y. Wang, *Fusion Category Symmetry II: Categoriosities at $c = 1$ and Beyond*, [arXiv:2106.12577].

[55] T.-C. Huang, Y.-H. Lin, and S. Seifnashri, *Construction of two-dimensional topological field theories with non-invertible symmetries*, *JHEP* **12** (2021) 028, [arXiv:2110.02958].

[56] Y.-H. Lin, M. Okada, S. Seifnashri, and Y. Tachikawa, *Asymptotic density of states in 2d CFTs with non-invertible symmetries*, *JHEP* **03** (2023) 094, [arXiv:2208.05495].

[57] D. Gaiotto and J. Kulp, *Orbifold groupoids*, *JHEP* **02** (2021) 132, [arXiv:2008.05960].

[58] D. S. Freed, G. W. Moore, and C. Teleman, *Topological symmetry in quantum field theory*, [arXiv:2209.07471].

[59] J. Kaidi, K. Ohmori, and Y. Zheng, *Symmetry TFTs for Non-invertible Defects*, *Commun. Math. Phys.* **404** (2023), no. 2 1021–1124, [arXiv:2209.11062].

[60] D. S. Freed, *Introduction to topological symmetry in QFT*, [arXiv:2212.00195].

[61] L. Bhardwaj and S. Schafer-Nameki, *Generalized Charges, Part II: Non-Invertible Symmetries and the Symmetry TFT*, [arXiv:2305.17159].

[62] L. Bhardwaj and Y. Tachikawa, *On finite symmetries and their gauging in two dimensions*, *JHEP* **03** (2018) 189, [arXiv:1704.02330].

[63] D. Gaiotto and T. Johnson-Freyd, *Condensations in higher categories*, [arXiv:1905.09566].

[64] J. Kaidi, Z. Komargodski, K. Ohmori, S. Seifnashri, and S.-H. Shao, *Higher central charges and topological boundaries in 2+1-dimensional TQFTs*, *SciPost Phys.* **13** (2022), no. 3 067, [arXiv:2107.13091].

[65] K. Roumpedakis, S. Seifnashri, and S.-H. Shao, *Higher Gauging and Non-invertible Condensation Defects*, *Commun. Math. Phys.* **401** (2023), no. 3 3043–3107, [arXiv:2204.02407].

[66] Y. Choi, B. C. Rayhaun, Y. Sanghavi, and S.-H. Shao, *Remarks on boundaries, anomalies, and noninvertible symmetries*, *Phys. Rev. D* **108** (2023), no. 12 125005, [arXiv:2305.09713].

[67] A. Perez-Lona, D. Robbins, E. Sharpe, T. Vandermeulen, and X. Yu, *Notes on gauging noninvertible symmetries, part 1: Multiplicity-free cases*, [arXiv:2311.16230].

[68] J. Kaidi, E. Nardoni, G. Zafrir, and Y. Zheng, *Symmetry TFTs and anomalies of non-invertible symmetries*, *JHEP* **10** (2023) 053, [arXiv:2301.07112].

[69] C. Zhang and C. Córdova, *Anomalies of* $(1+1)D$ *categorical symmetries*, [arXiv:2304.01262].

[70] C. Cordova, P.-S. Hsin, and C. Zhang, *Anomalies of Non-Invertible Symmetries in (3+1)d*, [arXiv:2308.11706].

[71] A. Antinucci, F. Benini, C. Copetti, G. Galati, and G. Rizi, *Anomalies of non-invertible self-duality symmetries: fractionalization and gauging*, [arXiv:2308.11707].

[72] L. Bhardwaj, L. E. Bottini, D. Pajer, and S. Schafer-Nameki, *Gapped Phases with Non-Invertible Symmetries: (1+1)d*, [arXiv:2310.03784].

[73] L. Bhardwaj, L. E. Bottini, D. Pajer, and S. Schafer-Nameki, *Categorical Landau Paradigm for Gapped Phases*, [arXiv:2310.03786].

[74] Y. Choi, D.-C. Lu, and Z. Sun, *Self-duality under gauging a non-invertible symmetry*, [arXiv:2310.19867].

[75] O. Diatlyk, C. Luo, Y. Wang, and Q. Weller, *Gauging Non-Invertible Symmetries: Topological Interfaces and Generalized Orbifold Groupoid in 2d QFT*, [arXiv:2311.17044].

[76] A. N. Schellekens and N. P. Warner, *Conformal subalgebras of kac-moody algebras*, *Phys. Rev. D* **34** (Nov, 1986) 3092–3096.

[77] V. G. Ka and M. N. Sanielevici, *Decompositions of representations of exceptional affine algebras with respect to conformal subalgebras*, *Phys. Rev. D* **37** (Apr, 1988) 2231–2237.

[78] A. Boysal and C. Pauly, *Strange duality for verlinde spaces of exceptional groups at level one*, *International Mathematics Research Notices* **2010** (2010), no. 4 595–618.

[79] V. G. Kac, P. M. Frajria, P. Papi, and F. Xu, *Conformal embeddings and simple current extensions*, *International Mathematics Research Notices* **2015** (2015), no. 14 5229–5288.

[80] A. Davydov and T. Booker, *Commutative Algebras in Fibonacci Categories*, [arXiv:1103.3537].

[81] V. A. Fateev and A. B. Zamolodchikov, *Parafermionic Currents in the Two-Dimensional Conformal Quantum Field Theory and Selfdual Critical Points in Z(n) Invariant Statistical Systems*, *Sov. Phys. JETP* **62** (1985) 215–225.

[82] S. Mukhi and B. C. Rayhaun, *Classification of Unitary RCFTs with Two Primaries and Central Charge Less Than 25*, *Commun. Math. Phys.* **401** (2023), no. 2 1899–1949, [arXiv:2208.05486].

[83] B. C. Rayhaun, *Bosonic Rational Conformal Field Theories in Small Genera, Chiral Fermionization, and Symmetry/Subalgebra Duality*, [arXiv:2303.16921].

[84] A. N. Schellekens, *Meromorphic C = 24 conformal field theories*, *Commun. Math. Phys.* **153** (1993) 159–186, [hep-th/9205072].

[85] P. Goddard, A. Kent, and D. I. Olive, *Virasoro Algebras and Coset Space Models*, *Phys. Lett. B* **152** (1985) 88–92.

[86] P. Goddard, A. Kent, and D. I. Olive, *Unitary Representations of the Virasoro and Supervirasoro Algebras*, *Commun. Math. Phys.* **103** (1986) 105–119.

[87] J. Fuchs, B. Schellekens, and C. Schweigert, *The resolution of field identification fixed points in diagonal coset theories*, *Nucl. Phys. B* **461** (1996) 371–406, [hep-th/9509105].

[88] D. Gepner, *Field Identification in Coset Conformal Field Theories*, *Phys. Lett. B* **222** (1989) 207–212.

[89] A. N. Schellekens and S. Yankielowicz, *Field Identification Fixed Points in the Coset Construction*, *Nucl. Phys. B* **334** (1990) 67–102.

[90] D. Delmastro, J. Gomis, and M. Yu, *Infrared phases of 2d QCD*, *JHEP* **02** (2023) 157, [arXiv:2108.02202].

[91] M. Spiegelglas, *Setting fusion rings in topological landau-ginzburg*, *Physics Letters B* **274** (1992), no. 1 21–26.

[92] M. Spiegelglas and S. Yankielowicz, *G / G topological field theories by cosetting G(k)*, *Nucl. Phys. B* **393** (1993) 301–336, [hep-th/9201036].

[93] E. Witten, *On Holomorphic factorization of WZW and coset models*, *Commun. Math. Phys.* **144** (1992) 189–212.

[94] M. Blau and G. Thompson, *Derivation of the Verlinde formula from Chern-Simons theory and the G/G model*, *Nucl. Phys. B* **408** (1993) 345–390, [hep-th/9305010].

[95] K. Hori, *On global aspects of gauged wess-zumino-witten model. phd thesis*, [hep-th/9402019].

[96] E. Sharpe, *Topological operators, noninvertible symmetries and decomposition*, [arXiv:2108.13423].

[97] E. P. Verlinde, *Fusion Rules and Modular Transformations in 2D Conformal Field Theory*, *Nucl. Phys. B* **300** (1988) 360–376.

[98] V. B. Petkova and J. B. Zuber, *Generalized twisted partition functions*, *Phys. Lett. B* **504** (2001) 157–164, [hep-th/0011021].

[99] N. Drukker, D. Gaiotto, and J. Gomis, *The Virtue of Defects in 4D Gauge Theories and 2D CFTs*, *JHEP* **06** (2011) 025, [arXiv:1003.1112].

[100] D. Gaiotto, *Open Verlinde line operators*, [arXiv:1404.0332].

[101] M. Levin, *Protected edge modes without symmetry*, *Phys. Rev. X* **3** (2013), no. 2 021009, [arXiv:1301.7355].

[102] M. Barkeshli, C.-M. Jian, and X.-L. Qi, *Classification of topological defects in abelian topological states*, *Physical Review B* **88** (dec, 2013).

[103] A. Kapustin and N. Saulina, *Topological boundary conditions in abelian Chern-Simons theory*, *Nucl. Phys. B* **845** (2011) 393–435, [arXiv:1008.0654].

[104] J. Fuchs, C. Schweigert, and A. Valentino, *Bicategories for boundary conditions and for surface defects in 3-d TFT*, *Commun. Math. Phys.* **321** (2013) 543–575, [arXiv:1203.4568].

[105] B. Pedrini, C. Schweigert, and J. Walcher, *New maverick coset theories*, *Phys. Lett. B* **466** (1999) 206–210, [hep-th/9908185].

[106] I. S. Eliëns, J. C. Romers, and F. A. Bais, *Diagrammatics for Bose condensation in anyon theories*, *Phys. Rev. B* **90** (2014), no. 19 195130, [arXiv:1310.6001].

[107] T. Neupert, H. He, C. Von Keyserlingk, G. Sierra, and B. A. Bernevig, *Boson condensation in topologically ordered quantum liquids*, *Physical Review B* **93** (2016), no. 11 115103.

[108] M. Yu, *Gauging Categorical Symmetries in 3d Topological Orders and Bulk Reconstruction*, [arXiv:2111.13697].

[109] F. Burnell, *Anyon condensation and its applications*, *Annual Review of Condensed Matter Physics* **9** (Mar., 2018) 307â327.

[110] O. Aharony, N. Seiberg, and Y. Tachikawa, *Reading between the lines of four-dimensional gauge theories*, *JHEP* **08** (2013) 115, [arXiv:1305.0318].

[111] B. Schellekens, "Kac." https://www.nikhef.nl/~t58/Site/Kac.html, 2006.

[112] Y.-Z. Huang, *Rigidity and modularity of vertex tensor categories*, *Commun. Contemp. Math.* **10** (2008), no. supp01 871–911, [math/0502533].

[113] Y.-Z. Huang, A. Kirillov, and J. Lepowsky, *Braided tensor categories and extensions of vertex operator algebras*, *Commun. Math. Phys.* **337** (2015), no. 3 1143–1159, [arXiv:1406.3420].

[114] F. A. Bais, P. Bouwknegt, M. Surridge, and K. Schoutens, *Coset Construction for Extended Virasoro Algebras*, *Nucl. Phys. B* **304** (1988) 371–391.

[115] D. Delmastro and J. Gomis, *RG flows in 2d QCD*, *JHEP* **09** (2023) 158, [arXiv:2211.09036].

[116] M. Cheng, *Microscopic theory of surface topological order for topological crystalline superconductors*, *Physical Review Letters* **120** (2018), no. 3 036801.

[117] A. Cherman, T. Jacobson, Y. Tanizaki, and M. Ünsal, *Anomalies, a mod 2 index, and dynamics of 2d adjoint QCD*, *SciPost Phys.* **8** (2020), no. 5 072, [arXiv:1908.09858].

[118] R. Dempsey, I. R. Klebanov, and S. S. Pufu, *Exact symmetries and threshold states in two-dimensional models for QCD*, *JHEP* **10** (2021) 096, [arXiv:2101.05432].

[119] N. Anand, A. L. Fitzpatrick, E. Katz, and Y. Xin, *Chiral limit of 2d QCD revisited with lightcone conformal truncation*, *JHEP* **01** (2024) 189, [arXiv:2111.00021].

[120] F. K. Popov, *Supersymmetry in QCD2 coupled to fermions*, *Phys. Rev. D* **105** (2022), no. 7 074005, [arXiv:2202.04017].

[121] R. Dempsey, I. R. Klebanov, L. L. Lin, and S. S. Pufu, *Adjoint Majorana QCD_2 at finite N*, *JHEP* **04** (2023) 107, [arXiv:2210.10895].

[122] R. Dempsey, I. R. Klebanov, S. S. Pufu, and B. T. Søgaard, *Lattice Hamiltonian for adjoint QCD_2*, *JHEP* **08** (2024) 009, [arXiv:2311.09334].

[123] F. Ambrosino and S. Komatsu, *2d QCD and Integrability, Part I: 't Hooft model*, [arXiv:2312.15598].

[124] R. Dempsey, I. R. Klebanov, S. S. Pufu, and B. T. Søgaard, *Small Circle Expansion for Adjoint QCD_2 with Periodic Boundary Conditions*, [arXiv:2406.17079].

[125] F. Ambrosino and S. Komatsu, *2d QCD and Integrability, Part II: Generalized QCD*, [arXiv:2406.11078].

[126] A. Cherman and M. Neuzil, *Beta functions of 2D adjoint QCD*, *Phys. Rev. D* **109** (2024), no. 10 105014, [arXiv:2401.16604].

[127] J. A. Damia, G. Galati, and L. Tizzano, *Symmetries, Universes and Phases of QCD_2 with an Adjoint Dirac Fermion*, [arXiv:2409.17989].

[128] R. Dempsey, S. S. Pufu, B. T. Søgaard, and I. R. Klebanov, *More About the Lattice Hamiltonian for Adjoint QCD_2*, [arXiv:2409.19164].

[129] J. Frohlich, J. Fuchs, I. Runkel, and C. Schweigert, *Defect Lines, Dualities and Generalised Orbifolds*, in *16th International Congress on Mathematical Physics*, pp. 608–613, 2010. arXiv:0909.5013.

[130] T. Lan, J. C. Wang, and X.-G. Wen, *Gapped Domain Walls, Gapped Boundaries and Topological Degeneracy*, *Phys. Rev. Lett.* **114** (2015), no. 7 076402, [arXiv:1408.6514].

[131] I. Cong, M. Cheng, and Z. Wang, *Hamiltonian and Algebraic Theories of Gapped Boundaries in Topological Phases of Matter*, *Commun. Math. Phys.* **355** (2017) 645–689, [arXiv:1707.04564].

[132] C. Zhang, A. Vishwanath, and X.-G. Wen, *Hierarchy construction for non-abelian fractional quantum Hall states via anyon condensation*, [arXiv:2406.12068].

[133] Y. Choi, C. Córdova, P.-S. Hsin, H. T. Lam, and S.-H. Shao, *Noninvertible duality defects in 3+1 dimensions*, *Phys. Rev. D* **105** (2022), no. 12 125016, [arXiv:2111.01139].

[134] J. Kaidi, K. Ohmori, and Y. Zheng, *Kramers-Wannier-like Duality Defects in (3+1)D Gauge Theories*, *Phys. Rev. Lett.* **128** (2022), no. 11 111601, [arXiv:2111.01141].

[135] C.-M. Chang, J. Chen, and F. Xu, *Topological defect lines in two dimensional fermionic CFTs*, *SciPost Phys.* **15** (2023), no. 5 216, [arXiv:2208.02757].

[136] L. Bhardwaj, L. E. Bottini, D. Pajer, and S. Schafer-Nameki, *The Club Sandwich: Gapless Phases and Phase Transitions with Non-Invertible Symmetries*, [arXiv:2312.17322].

[137] L. Bhardwaj, D. Pajer, S. Schafer-Nameki, and A. Warman, *Hasse Diagrams for Gapless SPT and SSB Phases with Non-Invertible Symmetries*, [arXiv:2403.00905].

[138] Y. Choi, C. Córdova, P.-S. Hsin, H. T. Lam, and S.-H. Shao, *Non-invertible Condensation, Duality, and Triality Defects in 3+1 Dimensions*, *Commun. Math. Phys.* **402** (2023), no. 1 489–542, [arXiv:2204.09025].

[139] A. Apte, C. Córdova, and H. T. Lam, *Obstructions to gapped phases from noninvertible symmetries*, *Phys. Rev. B* **108** (2023), no. 4 045134, [arXiv:2212.14605].

[140] P. Putrov and R. Radhakrishnan, *Non-anomalous non-invertible symmetries in 1+1D from gapped boundaries of SymTFTs*, [arXiv:2405.04619].

[141] C. Copetti, L. Córdova, and S. Komatsu, *S-Matrix Bootstrap and Non-Invertible Symmetries*, [arXiv:2408.13132].

[142] C. Copetti, L. Córdova, and S. Komatsu, *Noninvertible Symmetries, Anomalies, and Scattering Amplitudes*, *Phys. Rev. Lett.* **133** (2024), no. 18 181601, [arXiv:2403.04835].

[143] C. Córdova, D. García-Sepúlveda, and N. Holfester, *Particle-Soliton Degeneracies from Spontaneously Broken Non-Invertible Symmetry*, [arXiv:2403.08883].

[144] C. Córdova, N. Holfester, and K. Ohmori, *Representation Theory of Solitons*, [arXiv:2408.11045].

[145] A. Kitaev and L. Kong, *Models for Gapped Boundaries and Domain Walls*, *Commun. Math. Phys.* **313** (2012), no. 2 351–373, [arXiv:1104.5047].

[146] T. Bartsch, M. Bullimore, A. E. V. Ferrari, and J. Pearson, *Non-invertible symmetries and higher representation theory I*, *SciPost Phys.* **17** (2024), no. 1 015, [arXiv:2208.05993].

[147] T. Bartsch, M. Bullimore, A. E. V. Ferrari, and J. Pearson, *Non-invertible symmetries and higher representation theory II*, *SciPost Phys.* **17** (2024), no. 2 067, [arXiv:2212.07393].

[148] T. Bartsch, M. Bullimore, and A. Grigoletto, *Representation theory for categorical symmetries*, [arXiv:2305.17165].

[149] L. Bhardwaj, C. Copetti, D. Pajer, and S. Schafer-Nameki, *Boundary SymTFT*, [arXiv:2409.02166].

[150] Y. Choi, B. C. Rayhaun, and Y. Zheng, *Generalized Tube Algebras, Symmetry-Resolved Partition Functions, and Twisted Boundary States*, [arXiv:2409.02159].

[151] Y. Choi, B. C. Rayhaun, and Y. Zheng, *A Non-Invertible Symmetry-Resolved Affleck-Ludwig-Cardy Formula and Entanglement Entropy from the Boundary Tube Algebra*, [arXiv:2409.02806].

[152] T. Dimofte and W. Niu, *Tannakian QFT: from spark algebras to quantum groups*, [arXiv:2411.04194].

[153] K. Inamura, *Fermionization of fusion category symmetries in 1+1 dimensions*, *JHEP* **10** (2023) 101, [arXiv:2206.13159].

[154] L. Bhardwaj, K. Inamura, and A. Tiwari, *Fermionic Non-Invertible Symmetries in (1+1)d: Gapped and Gapless Phases, Transitions, and Symmetry TFTs*, [arXiv:2405.09754].

[155] M. A. Levin and X.-G. Wen, *String-net condensation: A physical mechanism for topological phases*, *Phys. Rev. B* **71** (Jan, 2005) 045110.

[156] C.-H. Lin, M. Levin, and F. J. Burnell, *Generalized string-net models: A thorough exposition*, *Phys. Rev. B* **103** (May, 2021) 195155.

[157] V. G. Turaev and O. Y. Viro, *State sum invariants of 3 manifolds and quantum 6j symbols*, *Topology* **31** (1992) 865–902.

[158] F. Apruzzi, F. Bonetti, I. n. García Etxebarria, S. S. Hosseini, and S. Schafer-Nameki, *Symmetry TFTs from String Theory*, *Commun. Math. Phys.* **402** (2023), no. 1 895–949, [arXiv:2112.02092].

[159] A. Chatterjee and X.-G. Wen, *Symmetry as a shadow of topological order and a derivation of topological holographic principle*, *Phys. Rev. B* **107** (2023), no. 15 155136, [arXiv:2203.03596].

[160] K. Inamura and X.-G. Wen, *2+1D symmetry-topological-order from local symmetric operators in 1+1D*, [arXiv:2310.05790].

[161] T. D. Brennan and Z. Sun, *A SymTFT for Continuous Symmetries*, [arXiv:2401.06128].

[162] A. Antinucci and F. Benini, *Anomalies and gauging of U(1) symmetries*, [arXiv:2401.10165].

[163] F. Bonetti, M. Del Zotto, and R. Minasian, *SymTFTs for Continuous non-Abelian Symmetries*, [arXiv:2402.12347].

[164] F. Apruzzi, F. Bedogna, and N. Dondi, *SymTh for non-finite symmetries*, [arXiv:2402.14813].

[165] F. Apruzzi, F. Bonetti, D. S. W. Gould, and S. Schafer-Nameki, *Aspects of Categorical Symmetries from Branes: SymTFTs and Generalized Charges*, [arXiv:2306.16405].

[166] M. Del Zotto, S. N. Meynet, and R. Moscrop, *Remarks on Geometric Engineering, Symmetry TFTs and Anomalies*, [arXiv:2402.18646].

[167] S. Sawin, *Direct sum decompositions and indecomposable TQFTs*, *J. Math. Phys.* **36** (1995) 6673–6680, [q-alg/9505026].

[168] L. S. Abrams, *Two-dimensional topological quantum field theories and Frobenius algebras*, *J. Knot Theor. Ramifications* **5** (1996) 569–587.

[169] A. Kapustin and N. Saulina, *Surface operators in 3d Topological Field Theory and 2d Rational Conformal Field Theory*, [arXiv:1012.0911].

[170] L. Kong and H. Zheng, *Gapless edges of 2d topological orders and enriched monoidal categories*, *Nucl. Phys. B* **927** (2018) 140–165, [arXiv:1705.01087].

[171] L. Kong and H. Zheng, *A mathematical theory of gapless edges of 2d topological orders. Part I*, *JHEP* **02** (2020) 150, [arXiv:1905.04924].

[172] L. Kong and H. Zheng, *A mathematical theory of gapless edges of 2d topological orders. Part II*, *Nucl. Phys. B* **966** (2021) 115384, [arXiv:1912.01760].

[173] D. Delmastro, D. Gaiotto, and J. Gomis, *Global anomalies on the Hilbert space*, *JHEP* **11** (2021) 142, [arXiv:2101.02218].

[174] I. Cong, M. Cheng, and Z. Wang, *Topological Quantum Computation with Gapped Boundaries*, [arXiv:1609.02037].

[175] B. Durhuus and T. Jonsson, *Classification and construction of unitary topological field theories in two-dimensions*, *J. Math. Phys.* **35** (1994) 5306–5313, [hep-th/9308043].

[176] G. W. Moore and G. Segal, *D-branes and K-theory in 2D topological field theory*, [hep-th/0609042].

[177] D. Kutasov and A. Schwimmer, *Universality in two-dimensional gauge theory*, *Nucl. Phys. B* **442** (1995) 447–460, [hep-th/9501024].

[178] K. Gawedzki and A. Kupiainen, *Coset Construction from Functional Integrals*, *Nucl. Phys. B* **320** (1989) 625–668.

[179] K. Gawedzki and A. Kupiainen, *G/h Conformal Field Theory from Gauged WZW Model*, *Phys. Lett. B* **215** (1988) 119–123.

[180] P. Bouwknegt and W. Nahm, *Realizations of the exceptional modular invariant a(1)1 partition functions*, *Physics Letters B* **184** (1987), no. 4 359–362.

[181] G. W. Moore and N. Seiberg, *Naturality in Conformal Field Theory*, *Nucl. Phys. B* **313** (1989) 16–40.

[182] C.-H. Lin, M. Levin, and F. J. Burnell, *Generalized string-net models: A thorough exposition*, *Phys. Rev. B* **103** (2021), no. 19 195155, [arXiv:2012.14424].

[183] M. Buican and R. Radhakrishnan, *Invertibility of Condensation Defects and Symmetries of 2 + 1d QFTs*, *Commun. Math. Phys.* **405** (2024), no. 9 217, [arXiv:2309.15181].

[184] M. Müger, *Galois extensions of braided tensor categories and braided crossed g-categories*, *Journal of Algebra* **277** (2004), no. 1 256–281, [math/0209093].

[185] G. 't Hooft, *A Two-Dimensional Model for Mesons*, *Nucl. Phys. B* **75** (1974) 461–470.

[186] P. Di Francesco and J. B. Zuber, *SU(N) Lattice Integrable Models Associated With Graphs*, *Nucl. Phys. B* **338** (1990) 602–646.

[187] V. B. Petkova and J. B. Zuber, *From CFT to graphs*, *Nucl. Phys. B* **463** (1996) 161–193, [hep-th/9510175].

[188] R. E. Behrend, P. A. Pearce, V. B. Petkova, and J.-B. Zuber, *Boundary conditions in rational conformal field theories*, *Nucl. Phys. B* **570** (2000) 525–589, [hep-th/9908036].

[189] S. Cecotti and C. Vafa, *On classification of N=2 supersymmetric theories*, *Commun. Math. Phys.* **158** (1993) 569–644, [hep-th/9211097].

[190] E. Witten, *Nonabelian Bosonization in Two-Dimensions*, *Commun. Math. Phys.* **92** (1984) 455–472.

[191] W. Ji, S.-H. Shao, and X.-G. Wen, *Topological Transition on the Conformal Manifold*, *Phys. Rev. Res.* **2** (2020), no. 3 033317, [arXiv:1909.01425].

[192] L. Kong, *Anyon condensation and tensor categories*, *Nucl. Phys. B* **886** (2014) 436–482, [arXiv:1307.8244].

[193] K. Hori, *Global aspects of gauged Wess-Zumino-Witten models*, *Commun. Math. Phys.* **182** (1996) 1–32, [hep-th/9411134].

[194] N. Carqueville and I. Runkel, *Orbifold completion of defect bicategories*, *Quantum Topol.* **7** (2016), no. 2 203–279, [arXiv:1210.6363].

[195] P. Etingof, S. Gelaki, D. Nikshych, and V. Ostrik, *Tensor Categories: Mathematical Surveys and Monographs. American Mathematical Society.* American Mathematical Society, 2015.

[196] C. Wang, A. Nahum, M. A. Metlitski, C. Xu, and T. Senthil, *Deconfined quantum critical points: symmetries and dualities*, *Phys. Rev. X* **7** (2017), no. 3 031051, [arXiv:1703.02426].

[197] T. Senthil, D. T. Son, C. Wang, and C. Xu, *Duality between* $(2+1)d$ *Quantum Critical Points*, *Phys. Rept.* **827** (2019) 1–48, [arXiv:1810.05174].

[198] S. Giombi, S. Minwalla, S. Prakash, S. P. Trivedi, S. R. Wadia, and X. Yin, *Chern-Simons Theory with Vector Fermion Matter*, *Eur. Phys. J. C* **72** (2012) 2112, [arXiv:1110.4386].

[199] S. Jain, S. Minwalla, and S. Yokoyama, *Chern Simons duality with a fundamental boson and fermion*, *JHEP* **11** (2013) 037, [arXiv:1305.7235].

[200] O. Aharony, *Baryons, monopoles and dualities in Chern-Simons-matter theories*, *JHEP* **02** (2016) 093, [arXiv:1512.00161].

[201] N. Seiberg, T. Senthil, C. Wang, and E. Witten, *A Duality Web in 2+1 Dimensions and Condensed Matter Physics*, *Annals Phys.* **374** (2016) 395–433, [arXiv:1606.01989].

[202] P. Goodard, A. Kent, and D. Olive, *Virasoro algebras and coset space models*, *Physics Letters B* **152** (1985), no. 1 88–92.

[203] D. Karabali, Q.-H. Park, H. J. Schnitzer, and Z. Yang, *A GKO Construction Based on a Path Integral Formulation of Gauged Wess-Zumino-Witten Actions*, *Phys. Lett. B* **216** (1989) 307–312.

[204] C. Kane, R. Mukhopadhyay, and T. Lubensky, *Fractional quantum hall effect in an array of quantum wires*, *Physical review letters* **88** (2002), no. 3 036401.

[205] J. C. Y. Teo and C. L. Kane, *From luttinger liquid to non-abelian quantum hall states*, *Phys. Rev. B* **89** (Feb, 2014) 085101.

[206] R. S. K. Mong, D. J. Clarke, J. Alicea, N. H. Lindner, P. Fendley, C. Nayak, Y. Oreg, A. Stern, E. Berg, K. Shtengel, and M. P. A. Fisher, *Universal topological quantum computation from a superconductor-abelian quantum hall heterostructure*, *Phys. Rev. X* **4** (Mar, 2014) 011036.

[207] Y. Hu and C. L. Kane, *Fibonacci topological superconductor*, *Phys. Rev. Lett.* **120** (Feb, 2018) 066801.

[208] N. Sopenko, *Chiral topologically ordered states on a lattice from vertex operator algebra*, *Adv. Theor. Math. Phys.* **28** (2024), no. 1 1–35, [arXiv:2301.08697].

[209] D. T. Son, *Is the Composite Fermion a Dirac Particle?*, *Phys. Rev. X* **5** (2015), no. 3 031027, [arXiv:1502.03446].

[210] M. A. Metlitski and A. Vishwanath, *Particle-vortex duality of two-dimensional Dirac fermion from electric-magnetic duality of three-dimensional topological insulators*, *Phys. Rev. B* **93** (2016), no. 24 245151, [arXiv:1505.05142].

[211] M. Nguyen, Y. Tanizaki, and M. Ünsal, *Semi-Abelian gauge theories, non-invertible symmetries, and string tensions beyond N-ality*, *JHEP* **03** (2021) 238, [arXiv:2101.02227].

[212] B. Heidenreich, J. McNamara, M. Montero, M. Reece, T. Rudelius, and I. Valenzuela, *Non-invertible global symmetries and completeness of the spectrum*, *JHEP* **09** (2021) 203, [arXiv:2104.07036].

[213] C. Córdova, K. Ohmori, and T. Rudelius, *Generalized symmetry breaking scales and weak gravity conjectures*, *JHEP* **11** (2022) 154, [arXiv:2202.05866].

[214] L. Bhardwaj, L. E. Bottini, S. Schafer-Nameki, and A. Tiwari, *Non-invertible higher-categorical symmetries*, *SciPost Phys.* **14** (2023), no. 1 007, [arXiv:2204.06564].

[215] L. Bhardwaj, S. Schafer-Nameki, and J. Wu, *Universal Non-Invertible Symmetries*, *Fortsch. Phys.* **70** (2022), no. 11 2200143, [arXiv:2208.05973].

[216] L. Bhardwaj, Y. Gai, S.-J. Huang, K. Inamura, S. Schafer-Nameki, A. Tiwari, and A. Warman, *Gapless Phases in (2+1)d with Non-Invertible Symmetries*, arXiv:2503.12699.

[217] Y. Choi, H. T. Lam, and S.-H. Shao, *Non-invertible Gauss law and axions*, *JHEP* **09** (2023) 067, [arXiv:2212.04499].

[218] F. J. Burnell, *Anyon condensation and its applications*, *Ann. Rev. Condensed Matter Phys.* **9** (2018) 307–327, [arXiv:1706.04940].

[219] F. D. M. Haldane, *Fractional quantization of the hall effect: A hierarchy of incompressible quantum fluid states*, *Phys. Rev. Lett.* **51** (Aug, 1983) 605–608.

[220] B. I. Halperin, *Statistics of quasiparticles and the hierarchy of fractional quantized hall states*, *Phys. Rev. Lett.* **52** (Apr, 1984) 1583–1586.

[221] T. H. Hansson, M. Hermanns, S. H. Simon, and S. F. Viefers, *Quantum hall physics: Hierarchies and conformal field theory techniques*, *Rev. Mod. Phys.* **89** (May, 2017) 025005.

[222] C. Zhang, A. Vishwanath, and X.-G. Wen, *Hierarchy construction for non-abelian fractional quantum Hall states via anyon condensation*, 6, 2024.

[223] M. Müger, *On the structure of modular categories*, *Proc. London Math. Soc.* **87** (2003), no. 3 291–308.

[224] M. Müger, *From subfactors to categories and topology. II. the quantum double of tensor categories and subfactors*, *J. Pure Appl. Algebra* **180** (2003), no. 1-2 159–219.

[225] V. Drinfeld, S. Gelaki, D. Nikshych, and V. Ostrik, *On braided fusion categories i*, *Selecta Mathematica* **16** (2010) 1–119.

[226] P. Putrov and R. Radhakrishnan, *Braidings on topological operators, anomaly of higher-form symmetries and the SymTFT*, arXiv:2503.13633.

[227] P. Deligne, *Catégories tensorielles*, *Moscow Mathematical Journal* **2** (2002), no. 2 227–248.

[228] nLab authors, "Deligne's theorem on tensor categories." https://ncatlab.org/nlab/show/Deligne%27s+theorem+on+tensor+categories, Aug., 2024. Revision 85.

[229] S. Jain, M. Mandlik, S. Minwalla, T. Takimi, S. R. Wadia, and S. Yokoyama, *Unitarity, Crossing Symmetry and Duality of the S-matrix in large N Chern-Simons theories with fundamental matter*, *JHEP* **04** (2015) 129, [arXiv:1404.6373].

[230] B. Gabai, J. Sandor, and X. Yin, *Anyon scattering from lightcone Hamiltonian: the singlet channel*, *JHEP* **09** (2022) 145, [arXiv:2205.09144].

[231] U. Mehta, S. Minwalla, C. Patel, S. Prakash, and K. Sharma, *Crossing symmetry in matter Chern–Simons theories at finite N and k*, *Adv. Theor. Math. Phys.* **27** (2023), no. 1 193–310, [arXiv:2210.07272].

[232] J. Frohlich, J. Fuchs, I. Runkel, and C. Schweigert, *Algebras in tensor categories and coset conformal field theories*, *Fortsch. Phys.* **52** (2004) 672–677, [hep-th/0309269].

[233] R. Dijkgraaf and E. Witten, *Topological Gauge Theories and Group Cohomology*, *Commun. Math. Phys.* **129** (1990) 393.

[234] D. Altschuler, M. Bauer, and C. Itzykson, *The Branching Rules of Conformal Embeddings*, *Commun. Math. Phys.* **132** (1990) 349–364.

[235] M. A. Walton, *Conformal Branching Rules and Modular Invariants*, *Nucl. Phys. B* **322** (1989) 775–790.

[236] F. Levstein and J. I. Liberati, *Branching rules for conformal embeddings*, *Communications in Mathematical Physics* **173** (1995), no. 1 1 – 16.

[237] L. Crane, L. H. Kauffman, and D. N. Yetter, *State sum invariants of four manifolds. 1.*, hep-th/9409167.

[238] A. Brochier, D. Jordan, P. Safronov, and N. Snyder, *Invertible braided tensor categories*, *Algebraic & Geometric Topology* **21** (2021), no. 4 2107–2140.